UNIVERSITÉ DU QUÉBEC À CHICOUTIMI

MÉMOIRE PRÉSENTÉ À
L'UNIVERSITÉ DU QUÉBEC À CHICOUTIMI
COMME EXIGENCE PARTIELLE
DE MAÎTRISE EN INGÉNIERIE

PAR

OSSAMA EL SEBAIE

L'EFFET DE L'ADDITION DU « MISCHMETAL », DU TAUX DE REFROIDISSEMENT ET DU TRAITEMENT THERMIQUE SUR LA MICROSTUCTURE ET LA DURETÉ DES ALLIAGES AL-SI DE TYPE 319, 356, ET 413

FÉVRIER 2006

Bibliothèque Paul-Émile-Boulet

UQAC Université du Québec à Chicoutimi

Mise en garde/Advice

Afin de rendre accessible au plus grand nombre le résultat des travaux de recherche menés par ses étudiants gradués et dans l'esprit des règles qui régissent le dépôt et la diffusion des mémoires et thèses produits dans cette Institution, **l'Université du Québec à Chicoutimi (UQAC)** est fière de rendre accessible une version complète et gratuite de cette œuvre.

Motivated by a desire to make the results of its graduate students' research accessible to all, and in accordance with the rules governing the acceptation and diffusion of dissertations and theses in this Institution, the **Université du Québec à Chicoutimi (UQAC)** is proud to make a complete version of this work available at no cost to the reader.

L'auteur conserve néanmoins la propriété du droit d'auteur qui protège ce mémoire ou cette thèse. Ni le mémoire ou la thèse ni des extraits substantiels de ceux-ci ne peuvent être imprimés ou autrement reproduits sans son autorisation.

The author retains ownership of the copyright of this dissertation or thesis. Neither the dissertation or thesis, nor substantial extracts from it, may be printed or otherwise reproduced without the author's permission.

UNIVERSITÉ DU QUÉBEC À CHICOUTIMI

MÉMOIRE PRÉSENTÉ À
L'UNIVERSITÉ DU QUÉBEC À CHICOUTIMI
COMME EXIGENCE PARTIELLE
DE MAÎTRISE EN INGÉNIERIE

PAR

OSSAMA EL SEBAIE

THE EFFECT OF MISCHMETAL, COOLING RATE AND HEAT TREATMENT ON THE MICROSTRUCTURE AND HARDNESS OF 319, 356, AND 413 AL-SI ALLOYS

FEBRUARY 2006

Dedicated to my parents, Hayam and my Kids, Abdo and Salma

☆☆☆☆☆☆

RÉSUMÉ

L'utilisation d'alliages d'aluminium a augmenté énormément dans diverses applications au cours des vingt dernières années. Les demandes faites par l'industrie du transport pour des composants légers (afin de réduire la consommation de carburant) a mené à une plus grande utilisation des alliages d'aluminium dans la production d'une grande variété de bâtis, comprenant certains composants critiques tels que des blocs de moteur et des têtes de cylindre. Parmi ces derniers, les alliages Al-Si, qui sont les alliages commerciaux les plus utilisés pour ces applications, en raison de leur rapport élevé de force / poids, leurs propriétés élevées de tension et de fatigue, et leur excellente résistance à la corrosion. L'addition du silicium fournit une excellente coulabilité et une résistance élevée aux déchirures à chaud. La présence des éléments d'alliage tels que le magnésium et le cuivre offre aux alliages Al-Si des capacités de grande résistance à haute température. Avec ces bonnes propriétés, les alliages Al-Si sont particulièrement utilisés dans l'industrie automobile, l'armement et les industries aéronautique et spatiale.

Les propriétés mécaniques d'un alliage coulé sont contrôlées par sa microstructure qui, elle même, est influencée par la composition chimique de l'alliage, c'est-à-dire par son contenu en silicium, en magnésium et en cuivre, ainsi que par la présence d'impuretés telles que le fer et de défauts du produit coulé (porosité, inclusions, etc.) comme les conditions de solidification (taux de refroidissement) et le traitement thermique appliqué. Dans le cas des alliages Al-Si, ce sont l'espace interdendritique d'α-Al (DAS), la morphologie et la taille des particules eutectiques de silicium, et la quantité d'intermétalliques et / ou d'autres constituants de deuxième phase présents dans la microstructure.

Le taux de refroidissement, en général, commande la finesse de la microstructure : plus le taux de refroidissement est élevé, plus les dendrites d'α-Al et les particules d'autres phases sont fines, et plus l'espace interdendritique est petit.

Dans les alliages Al-Si, il est connu que les caractéristiques eutectiques de particules de silicium (taille, morphologie et distribution) affectent sensiblement les propriétés mécaniques. Dans cet alliage sans traitement thermique le silicium eutectique est observé sous forme de plaquettes aciculaires fragiles qui sont nuisibles aux propriétés de tension et d'impact. Par l'utilisation d'un traitement de modification du métal liquide, la morphologie du silicium eutectique est changée ou modifiée de sa forme aciculaire à une forme fine et fibreuse qui améliore de manière significative la ductilité d'alliage et la résistance mécanique. La modification est effectuée par l'addition d'éléments tels que le Na, le Sr, le Ca ou encore par un mélange de métaux de terre rares (mischmetal).

L'utilisation du Na et du Sr en tant qu'agents de modification pour les alliages Al-Si est bien établie. Récemment, cependant, l'intérêt a été concentré sur l'utilisation du mischmetal comme modificateur pour ces alliages. Le mischmetal est une combinaison de métaux de terre rares (Ce, La, Pr et Nd) et a été rapporté comme modificateur de particules de silicium pour les alliages Al-Si, avec une capacité de surmonter les problèmes d'absorption d'hydrogène, de porosité accrue et d'effacement (fading) liés à l'utilisation du strontium. Le mischmetal a également été rapporté comme ayant une réactivité chimique élevée avec l'Al, le Si, le Cu et le Mg, provoquant la formation des composés intermétalliques durs de point de fusion élevé (Al_4Ce, Al_4La, Al_2Ce, SiCe, etc.) dans les régions de joints de grains, renforçant ces derniers et améliorant de ce fait la résistance mécanique des alliages à température élevée.

Le perfectionnement des caractéristiques eutectiques de particules de silicium peut également être obtenu par l'utilisation d'un procédé proportionné de traitement thermique (traitement thermique de mise en solution, trempe et vieillissement) où, pendant l'étape de traitement thermique de mise en solution, les particules eutectiques de silicium subissent des perturbations dans leur forme et commencent à se casser en plus petits segments (étape de fragmentation), et puis à se sphéroïdiser (étape de sphéroïdisation), acquérant ainsi une forme fibreuse.

Des traitements thermiques sont également appliqués aux alliages Al-Si pour en améliorer la résistance mécanique par la précipitation des précipités fins tels que les Mg_2Si ou Al_2Cu, ce qui renforce la matrice de l'alliage. Les éléments d'alliage Mg et Cu entrent dans la solution pleine pendant l'étape de traitement thermique de mise en solution et précipitent pendant l'étape de vieillissement (précipitation durcissante).

La présente recherche a été effectuée pour étudier l'effet du mischmetal comme modificateur ainsi que les effets du taux de refroidissement et du traitement thermique sur la microstructure et la dureté des alliages de fonderie A319.1, A356.2 et A413.1. Le but principal de cette étude était de déterminer le rôle du mischmetal comme agent de modification ainsi que l'effet combiné du Sr et de la modification par le mischmetal. La microstructure a été analysée au niveau de la taille et de la morphologie des particules eutectiques de silicium et des intermétalliques formés, en particulier des intermétalliques contenant du mischmetal, et corréler ces caractéristiques avec les valeurs de dureté correspondantes des alliages obtenues.

Les coulées ont été préparées à partir des trois alliages cités plus haut, en utilisant une fois une modification en Sr (~ 250 ppm) et l'autre fois sans modification, avec les ajouts de mischmetal de 0, 2, 4 et 6 % en poids. Ayant une forme de L, le moule métallique utilisé pour la coulée a fourni des barres qui ont été employées pour des mesures de dureté. Deux arrangements différents de solidification de moule ont été employés pour fournir des taux bas et haut de refroidissement correspondant respectivement aux valeurs de 40 μm et 120 μm DAS. Les alliages coulés ont été soumis au traitement thermique T6 (comportant le traitement thermique de mise en solution à 495 °C / 8 heures pour les alliages A319.1 et

A413.1, et à 540 °C / 8 heures pour l'alliage A356.2, la trempe à l'eau chaude (60 °C), suivie d'un vieillissement à 155 °C, à 180 °C, à 200 °C, à 220 °C et à 240 °C pour 5 h chacun). Des mesures de dureté ont été effectuées sur les échantillons tels que coulés et sur les alliages ayant subi un traitement thermique en utilisant un appareil de contrôle de dureté Brinell (500 Kgf appliqué pour 30 s, en utilisant une bille en acier de 10 mm de diamètre).

Les caractéristiques des particules de silicium eutectiques (surface, longueur, rapport de la rondeur, rapport longueur / largeur et densité) ont été mesurées en utilisant un microscope optique relié à un analyseur d'image. Pour chaque échantillon d'alliage examiné, les caractéristiques de particules de silicium ont été mesurées sur un total de 50 champs et des caractéristiques moyennes de particules ont été déterminées. La fraction totale de tous les intermétalliques a été obtenue en utilisant la microsonde électronique (EMPA). La spectrométrie des rayons X par longueur d'ondes (WDS) a été employée pour l'identification de tous ces intermétalliques.

Les mesures des particules de silicium eutectiques ont indiqué qu'une modification partielle a été obtenue avec les ajouts de mischmetal, contre la modification complète réalisée avec l'ajout de Sr dans la condition tel que coulé, et ce, aux deux taux de refroidissement. Une interaction entre le Sr et le mischmetal a été observée, celle-ci a affaibli l'efficacité du Sr comme modificateur. Cet effet était particulièrement évident au bas taux de refroidissement.

Pendant le traitement thermique de mise en solution, les particules eutectiques de silicium dans les alliages non modifiés ont subi un grossissement rapide (Ostwald ripening), tandis que dans les alliages modifiés par le Sr, elles ont montré un taux élevé de sphéroïdisation. Le grossissement a été démontré par l'augmentation de l'épaisseur des particules de silicium (clairement observées en alliage A356.2 aux deux taux de refroidissement). Dans les alliages contenant du mischmetal, la présence de ce dernier a réduit la croissance des particules de silicium.

L'analyse EPMA a indiqué que la fraction totale de tous les intermétalliques a augmenté avec l'ajout accru de mischmetal dans tous les alliages. Dans l'alliage A319.1, sans compter l'intermétallique Al_2Cu, un intermétallique de type $Al_{40}MM_2Ti_4CuSi$ a été observé, sous forme de particules grises au taux de refroidissement élevé, avec un rapport élevé de Ce / La (4.1:1). Un autre intermétallique de type Al_5MMCu_2Si a également été observé, sous forme des particules en plaquettes blanches, avec un bas rapport de Ce / La (1.8:1), et ce, aux deux taux de refroidissement. Cette phase intermétallique contenait 0.38 % en poids de Sr dans les alliages modifiés par le Sr, confirmant l'interaction entre le mischmetal et le Sr.

Dans l'alliage A356.2, le mischmetal a formé différents types d'intermétalliques. Au taux de refroidissement élevé, une phase MM-Ti a été observée (Al_4MMTi_2Si à 0.26 % en poids de magnésium) sous forme de particules grises à un rapport élevé de Ce / La (3.4:1). Une autre phase de mischmetal contenant un intermétallique de type Al_2MMSi_2 a été

observée, sous forme de particules arrondies blanches, aux deux taux de refroidissement, contenant 1.4-1.6 % en poids de Sr et 0.35-0.6 % en poids de magnésium, à un bas rapport de Ce / La (1.3:1). Au bas taux de refroidissement, un intermétallique sous forme d'écriture chinoise Al_2MMSi_2 avec 0.25 % de magnésium en poids a également été observé, à un bas rapport de Ce / La (1.5:1). À part les intermétalliques en mischmetal, la phase de Mg_2Si dans ces échantillons d'alliage a été observée, sous forme d'écriture chinoise de couleur noire.

Dans l'alliage A413.1, deux intermétalliques de fer ont été observés, à savoir, (i) la phase α-Fe $Al_{15}(MnFe)_3Si_2$ au bas taux de refroidissement et une autre phase α-Fe contenant un niveau élevé de Ni au taux de refroidissement élevé, avec une formule d'$Al_{11}(MnFeNiCu)_4Si$, sous forme de particules d'écriture chinoise grise, et (ii) la phase β-Fe Al_5FeSi sous forme de particules en plaquettes gris foncé au taux de refroidissement élevé. La basse teneur en cuivre de l'alliage a eu comme conséquence la formation de la phase Al_3NiCu sous forme de blocs gris au taux de refroidissement élevé. Une phase intermétallique mischmetal blanche Al_2MMSi_2 au taux de refroidissement élevé a également été observé, à un bas rapport de Ce / La (1.18:1). Cette phase contenait 2.7 % en poids de Sr, indiquant l'interaction entre le mischmetal et le Sr et un affaiblissement conséquent de l'effet de modification du Sr. Cet intermétallique a encore combiné avec de l'Al, le Si, le Cu et le Ni pour produire une phase intermétallique de type $Al_6MM(CuNi)Si$ en tiges de couleur gris clair, à un rapport modéré de Ce / La de 2:1.

Dans les alliages A413.1 modifiés par le Sr et au bas taux de refroidissement, une phase intermétallique de mischmetal Al_2MMSi_2 sous forme d'écriture chinoise de couleur blanche a également été observée, à un rapport Ce / La de 1.48:1, contenant 0.48 % en poids de Sr, confirmant de nouveau l'interaction Sr - mischmetal. À un rapport légèrement plus élevé de Ce / La de 2.1:1, une autre phase intermétallique en mischmetal était produite, avec une formule d'$Al_5MM(CuNi)Si$, observée dans la microstructure en tant que des particules en plaquettes de couleur gris clair.

Les mesures de dureté ont indiqué que, en général, les valeurs de dureté des alliages tels que coulés étaient plus hautes au taux de refroidissement élevé qu'au bas taux de refroidissement. Les alliages non modifiés ont montré des niveaux légèrement plus élevés de dureté comparés aux alliages modifiés par le Sr, et la dureté a été diminuée par l'ajout de mischmetal, aux deux taux de refroidissement.

Dans l'alliage A319.1 non modifié et après vieillissement aux différentes températures (155 °C – 240 °C / 5 h), deux valeurs maximales de dureté ont été observés (à 200 °C / 5 h et à 240 °C / 5 h) au taux de refroidissement élevé, alors que l'alliage A319.1 modifié par le Sr montrait seulement un maximum (à 200 °C / 5 h). Au bas taux de refroidissement, deux valeurs maximales de dureté ont été observés (à 155 °C / 5 h et à 180 °C / 5 h) dans les alliages non modifiés et dans ceux modifiés par le Sr. En général, les alliages contenant 0 et 2 % en poids de mischmetal ont montré les valeurs de dureté les plus

élevées aux deux taux de refroidissement, et la dureté a diminué avec encore d'autres ajouts de mischmetal.

Dans l'alliage A356.2, après vieillissement aux différentes températures (155 °C - 240 °C / 5 h), la dureté maximale a été obtenue à 180 °C / 5 h dans les alliages non modifiés et les alliages modifiés par le Sr, aux deux taux de refroidissement. Les alliages sans mischmetal ont montré une dureté relativement plus élevée que ceux qui contiennent du mischmetal. La dureté a diminué avec l'augmentation de l'ajout de mischmetal. Au taux de refroidissement élevé, les alliages non modifiés ont montré des valeurs plus élevées de dureté que les alliages modifiés en Sr, alors que la tendance opposée était observée au bas taux de refroidissement.

La diminution en valeurs de dureté peut être attribuée à l'interaction du mischmetal avec les éléments d'alliage Cu et Mg pour former les divers intermétalliques observés. La quantité de la précipitation des phases durcissantes formées dans les alliages A319.1 et A356.2 (Al_2Cu et Mg_2Si) est considérablement réduite, diminuant de ce fait la dureté. L'addition de mischmetal a changé l'ordre de précipitation de la phase Mg_2Si dans l'alliage A356.2. Pour le cas de l'alliage A413.1, pour tous les états du vieillissement température / temps (155 °C – 240 °C / 5 h), la basse teneur en éléments d'alliage a eu comme conséquence une réponse faible de l'alliage au processus de durcissement, et ce, aux deux taux de refroidissement. Ainsi, aucune dureté maximale pour ces alliages n'a été observée.

ABSTRACT

Aluminum cast components have been widely used in many applications for over the past twenty years. The demands made by the transportation industry for light weight components (in order to reduce fuel consumption) has led to an increased use of aluminum alloys in the production of a wide variety of castings including critical components such as engine blocks and cylinderheads. Among these, Al-Si alloys are the most popular commercial alloys used for these applications, due to their high strength-to-weight ratio, high tensile and fatigue properties, and excellent corrosion and wear resistance. The addition of Si provides excellent castability and high resistance to hot-tearing, while the presence of alloying elements such as magnesium and copper offer the ability to heat treat Al-Si castings to high strength levels, which make them suitable for the production of high-stress components for the automotive, aircraft and defense industries.

The mechanical properties of a casting are controlled by its microstructure which, in turn, is influenced by the chemical composition of the alloy, i.e., by its Si, Mg, and Cu content, and by the presence of impurities such as iron, the presence of casting defects (porosity, inclusions, etc.), as well as the solidification conditions (i.e., cooling rate) and heat treatment applied. In the case of Al-Si alloys, this would imply the α-Al dendrite arm spacing (DAS), the morphology and size of the eutectic Si particles, and the amount of intermetallics and/or other second-phase constituents present in the microstructure.

Cooling rate, in general, controls the fineness of the microstructure: the higher the cooling rate, the finer the α-Al dendrites and other phase particles, and the smaller the dendrite arm spacing.

In Al-Si alloys, the eutectic Si particle characteristics (i.e., size, morphology and distribution) are known to appreciably affect the mechanical properties. In the as-cast condition, the eutectic Si is observed in the form of brittle acicular plates that are detrimental to the tensile and impact properties. Through the use of a melt treatment termed "modification", the morphology of the eutectic Si is altered or "modified" from its acicular form to a fine, fibrous form that significantly improves the alloy ductility (and strength). The modification is carried out through the addition of elements such as Na, Sr, Ca, or mischmetal (a mixture of rare earth metals).

The use of Na and Sr as modifying agents for Al-Si alloys is well established. Recently, however, interest has been focused on the use of mischmetal as a modifier for these alloys. Mischmetal is a combination of rare earth metals (Ce, La, Pr and Nd), and has been reported to act as a Si particle modifier in Al-Si alloys, with the capacity to overcome the problems of hydrogen pick-up, increased porosity and fading associated with the use of

strontium. Mischmetal has also been reported to have a high chemical reactivity with Al, Si, Cu and Mg, giving rise to the formation of hard, high melting-point intermetallic compounds (i.e., Al_4Ce, Al_4La, Al_2Ce, SiCe, etc.) in the grain boundary regions, strengthening the latter and thus improving the alloy strength at elevated temperatures.

Enhancement of the eutectic Si particle characteristics can also be obtained through the use of an adequate heat treatment process (solution heat treatment, quenching and aging) where, during the solution heat treatment stage, the eutectic Si particles undergo shape perturbations in which they begin to break into smaller segments (termed the "fragmentation" stage), and then begin to spheroidize ("spherodization" stage), acquiring a fibrous form.

Heat treatments are also applied to Al-Si alloys to ameliorate their strength through the precipitation of fine precipitates such as Mg_2Si or Al_2Cu that strengthen the alloy matrix. The alloying elements Mg and Cu go into solid solution during the solution heat treatment stage and precipitate during the aging stage ("precipitation hardening").

The present study was carried out to investigate the effect of mischmetal as a modifier, as well as the effects of cooling rate and heat treatment on the microstructure and hardness of A319.1, A356.2 and A413.1 Al-Si casting alloys. The main aim of this study was to determine the role of mischmetal as a modifying agent and the combined effect of Sr and mischmetal modification. The microstructure was analyzed in term of the size and morphology of the eutectic Si particles, as well as the intermetallics formed, in particular, mischmetal-containing intermetallics, and correlated with the corresponding alloy hardness values obtained.

Castings were prepared from the three alloys using non-modified and Sr-modified (~ 250 ppm) alloys, with mischmetal additions of 0, 2, 4 and 6 wt%. The L-shaped metallic mold employed for casting provided bars that were used for hardness measurements. Two different mold solidification arrangements were used to provide high and low cooling rates corresponding to 40 μm and 120 μm DAS values, respectively. The castings were subjected to T6 heat treatment (comprising solution heat treatment at 495°C/8h for both A319.1 and A413.1 alloys, and at 540°C/8h for A356.2 alloy, quenching in warm water (60°C), followed by aging at 155°C, 180°C, 200°C, 220°C and 240°C for 5h each). Hardness measurements were carried out on as-cast and heat-treated samples using a Brinell hardness tester (500 Kgf applied for 30s, using a steel ball of 10 mm diameter).

The eutectic Si particle characteristics (area, length, roundness ratio, aspect ratio, and density) were measured using an optical microscope-image analyzer set up. For each alloy sample examined, the Si particle characteristics were measured over an area of 50 fields and the average particle characteristics determined. The total surface fraction of *all* intermetallics was obtained using electron probe microanalysis (EMPA). Wavelength dispersion spectroscopic (WDS) analysis was used for the identification of all intermtallics.

The eutectic Si particle measurements revealed that partial modification was obtained with mischmetal additions versus full modification achieved with Sr addition in the as-cast condition, at the two cooling rates. The interaction between Sr and mischmetal was observed to weaken the effectiveness of Sr as a modifier. This effect was particularly evident at the low cooling rate.

During solution heat treatment, the eutectic Si particles in the non-modified alloys underwent rapid coarsening (Ostwald ripening), whereas those in the Sr-modified alloys exhibited a high spherodization rate. The coarsening was evidenced by the increase in thickness of the Si particles (clearly observed in A356.2 alloy at the two cooling rates). In the mischmetal-containing alloys, the presence of mischmetal reduced the coarsening of the Si particles.

The EPMA analysis revealed that the total surface fraction of all intermetallics increased with increasing mischmetal (MM) addition in all alloys. In the A319.1 alloy, besides the Al_2Cu intermetallic, a MM-Ti intermetallic ($Al_{40}MM_2Ti_4CuSi$) was observed in the form of grey sludge particles at high cooling rate and high Ce/La ratio (4.1:1). Another MM-containing intermetallic Al_5MMCu_2Si was also observed, in the form of white plate-like particles at a low Ce/La ratio (1.8:1), at both cooling rates. This intermetallic phase contained 0.38 wt% Sr in the Sr-modified alloys, confirming the interaction of mischmetal with Sr.

In the A356.2 alloy, the mischmetal formed different types of intermetallics. At high cooling rate, a MM-Ti phase was observed (Al_4MMTi_2Si +0.26 wt% Mg) in the form of grey sludge particles at a high Ce/La ratio (3.4:1). Another mischmetal-containing intermetallic, Al_2MMSi_2, in the form of white rounded particles was observed to form at the two cooling rates, containing 1.4-1.6 wt% Sr and 0.35-0.6 wt% Mg, at a low Ce/La ratio (1.3:1). At the low cooling rate, a white Chinese script-like mischmetal intermetallic (Al_2MMSi_2 + 0.25 wt % Mg) was also observed, at a low Ce/La ratio (1.5:1). Besides the mischmetal intermetallics, Mg_2Si was observed in these alloy samples, in the form of black Chinese script.

In the A413.1 alloy, two Fe-intermetallics were observed: (i) the α-Fe $Al_{15}(MnFe)_3Si_2$ phase at low cooling rate and an α-Fe phase containing a high Ni content at high cooling rate, with a formula of $Al_{11}(MnFeNiCu)_4Si$, in the form of grey Chinese script particles, and (ii) the β-Fe Al_5FeSi phase in the form of dark grey plate-like particles at high cooling rate. The low copper content of the alloy resulted in the formation of the grey block-like phase Al_3NiCu at high cooling rate. A white plate-like mischmetal intermetallic phase Al_2MMSi_2 was also observed at high cooling rate, at a low Ce/la ratio (1.18 :1). This phase contained 2.7 wt% Sr, indicating the interaction between mischmetal and Sr and a consequent weakening of the modification effect of Sr. This intermetallic further combined with Al, Si, Cu and Ni to form a light grey rod-like $Al_6MM(CuNi)Si$ intermetallic phase, at a moderate Ce/La ratio of 2 :1.

At low cooling rate, a white Chinese script mischmetal-containing intermetallic AL_2MMSi_2 was also observed, at a Ce/La ratio of 1.48 :1, and containing 0.48 wt% Sr in the Sr-modified A413.1 alloys, confirming once again the Sr-mischmetal interaction. At a somewhat higher Ce/La ratio of 2.1 :1, another mischmetal intermetallic formed, with a formula of $Al_5MM(CuNI)Si$, observed in the microstructure as medium light grey plate-like particles.

The hardness measurements revealed that, in general, the hardness values of the as-cast alloys were higher at high cooling rate than at low cooling rate. Non-modified alloys displayed slightly higher hardness levels compared to the Sr-modified alloys and the hardness decreased with mischmetal additions at both cooling rates.

In the non-modified A319.1, alloy after aging at different temperatures (155°C - 240°C/5h), two peak hardness values were observed (at 200°C/5h and 240°C/5h) at high cooling rate, while the Sr-modified A319.1 alloy showed only one peak (at 200°C/5h). At low cooling rate, two maximum hardness values were observed (at 155°C/5h and 180°C/5h) in both non-modified and Sr-modified alloys. In general, alloys containing no and 2 wt% mischmetal exhibited the highest hardness values at both cooling rates; the hardness decreased with further mischmetal additions.

In the A356.2 alloy, after aging at different temperatures (155°C - 240°C/5h), peak hardness was observed at 180°C/5h in the non-modified and Sr-modified alloys at both cooling rate conditions. The alloys free of mischmetal exhibited relatively higher levels of hardness than those containing mischmetal. The hardness decreased with increasing mischmetal addition. At the high cooling rate, the non-modified alloys displayed higher hardness values than the Sr-modified alloys, while the opposite trend was observed at the low cooling rate.

The decrease in the hardness values may be attributed to the interaction of the mischmetal with the alloying elements Cu and Mg to form the different intermetallics observed. In tying up these elements, the amount of the precipitation hardening phases formed in the A319.1 and A356.2 alloys (i.e., Al_2Cu and Mg_2Si) is considerably reduced, thereby decreasing the hardness. The addition of mischmetal was also observed to change the precipitation sequence of the Mg_2Si phase in the A356.2 alloy. In the case of the A413.1 alloy, the low content of alloying elements resulted in a weak response of the alloy to the age hardening process at all aging temperature/time conditions (155°C-240°C/5h), at both cooling rates. Thus, no peak hardness was observed in these alloys.

ACKNOWLEDGEMENTS

Finally, I am very glad to get the opportunity to express and convey my great sincere thanks to my supervisors, Professors F. H. Samuel and A. M. Samuel for their help and guidance during different stages of my work to bring it to a successful conclusion.

Financial assistance in the form of a scholarship and in-kind support received from the Natural Science and Engineering Research Council of Canada (NSERC), General Motors Powertrain Group (U.S.A), Corporativo Nemak (Mexico) and the Fondation de l'Uinversité du Québec a Chicoutimi (FUQAC) is thankfully acknowledged.

It gives me much pleasure to thank all my colleagues, in particular, Alain Bérubé and Mathieu Paradis, for their help during the experimental stages of my work. Many thanks to Prof. M. A. Moustafa who encouraged me to join UQAC, and whom I still consider as a continuous source of support and advice.

I would like to convey my deep appreciation to my parents, my wife and my kids. Without their advice and encouragement, I would not have been capable of completing my Master's degree successfully.

TABLE OF CONTENTS

LIST OF TABLES

CHAPTER 2

CHAPTER 3

CHAPTER 4

CHAPTER 5

LIST OF FIGURES

CHAPTER 2

CHAPTER 3

CHAPTER 4

CHAPTER 5

CHAPTER 6

CHAPTER 1

DEFINITION OF THE PROBLEM

CHAPTER I

DEFINITION OF THE PROBLEM

1.1 INTRODUCTION

The use of aluminum components in the automotive industry has increased considerably during the past ten years due to their light weight and reduced fuel energy consumption advantages. Among aluminum alloys, aluminum-silicon (Al-Si) alloys are known for their high fluidity, low shrinkage in casting and good mechanical properties.[1] The mechanical properties attainable in these alloys are strongly influenced by the microstructure which, in turn, is determined by the chemical composition, melt treatment, solidification rate and heat treatment applied to the casting.[2]

Controlling the microstructure that results from the casting process is considered one of the main challenges faced by today's foundry industry. The challenge is to produce metallic components free of defects that demonstrate optimal mechanical properties with the lowest production cost. Fine equiaxed microstructures generally reveal favourable mechanical properties in terms of strength and ductility, with low susceptibility to microporosity and cracks.[3]

The microstructure is characterized by various parameters such as the grain size, the dendrite arm spacing (DAS), the size, shape and distribution of the eutectic silicon

particles, as well as the morphologies and the amounts of intermetallic phases present.[1,4,5] Some of these parameters are changed after heat treatment,[1, 6, 7] which consequently affects the resultant mechanical properties.[1, 8, 9]

One of the main melt treatment processes applied to Al-Si alloys is modification where, by the addition of a controlled amount of sodium (Na) or strontium (Sr), the eutectic Si morphology is 'modified' i.e., changed from acicular or needle-like to a fine, fibrous form (spheroidized), in order to improve the alloy properties. In general, the modified alloy shows an increase in the hardness, tensile strength and ductility.

The use of mischmetal as a beneficial addition to Al-Si alloys in terms of modification has aroused considerable interest in recent years. Mischmetal consists of a combination of rare earth metals like cerium (Ce), lanthanum (La), neodymium (Nd) and praseodymium (Pr). Besides modifying the eutectic silicon, it can form a fine dispersion of coherent intermetallic compounds which strengthen the grain boundaries, increasing the strength of the Al-Si alloys at elevated temperatures.

Modification using rare earth metals was first explained on the basis of the critical growth temperature hypothesis of Kim, and Heine [10] i.e., the modifying element should have a chemical affinity to form compounds with the precipitating silicon phase at a temperature below the normal eutectic temperature, but should also exhibit some ability to form intermetallic compounds with (and have low solubility in) the solvent α-aluminum phase. Lanthanum meets most of these requirements, while cerium and neodymium have a low solubility in α-aluminum. These rare earth metals have been reported to form many compounds with aluminum and silicon (e.g., Al_4Ce, Al_2Ce, SiCe, $SiCe_2$, $SiCe_4$, etc.). [11]

Sharan and his co-workers investigated the modification effect of rare earth additions in hypoeutectic and hypereutectic Al-Si alloys.[12, 13, 14] They found that with up to 0.2% rare earth metal additions to hypoeutectic Al-Si alloys, some refinement in primary α-aluminum and the eutectic structure occurred, leading to an increase in the tensile strength by 36% and the percentage elongation by 2 to 3 times. The role of mischmetal (a mixture of rare earth metals) was first investigated as a modifier, then as a beneficial alloying addition. The modification effect by mischmetal was explained as follows: Ce, La, and Nd react with Al and Si to form intermediate phases like $CeAl_4$, $LaAl_3$, etc. During solidification these intermetallics can act as heterogeneous nuclei for refining the primary Si in hypereutectic alloys.[14]

It was also reported that mischmetal addition in the range of 0.5 to 1% modified the structure significantly in both sand-cast and metal mold-cast conditions and improved the tensile strength and elongation.[15, 16] In the case of hypereutectic Al-Si alloys,[14, 15, 16] mischmetal addition in the range of 1.0 to 1.5% was observed to refine both the primary and eutectic silicon.

Ye *et al.* [11] studied the effect of rare earth addition as modifiers in cast Al-Si alloys. They found that at up to 2% rare earth addition, some primary dendrite refinement became obvious. This was attributed to an alloying effect. They also found that the silicon phase modified by rare earths revealed the same changes in crystallographic structure as that achieved through modification with sodium.

In order to obtain a clear and better understanding of all the factors involved when using mischmetal as a modifier, a study of the effects of mischmetal additions, cooling rate

and heat treatment on the microstructure (Si particle characteristics, and type and surface fraction of intermetallics formed), and hardness behavior of three different commercial grade Al-Si alloys (319, 356 and 413) was carried out. The alloys were investigated in the unmodified and Sr-modified conditions. Microstructural analysis was carried out using optical microscopy, image analysis and electron probe microanalysis, to determine the relation between the microstructure and the corresponding hardness of the alloys.

1.2 OBJECTIVES

The present work aimed to investigate the effect of mischmetal addition, cooling rate and heat treatment on the microstructure and hardness behavior of 319, 356, and 413 Al-Si casting alloys. This was carried out through a study of the following:

I. The role of mischmetal as (a) a modifier, and (b) a beneficial alloying addition.
II. Quantitative measurements of the eutectic Si particles (size, shape, and distribution).
III. Identification of intermetallic phases and the factors affecting their morphologies and surface fractions.
IV. The combined effect of mischmetal and strontium as modifiers.
V. Effect of mischmetal addition on the microstructure and hardness behavior.
VI. Effect of cooling rate and heat treatment on the morphology of the eutectic Si particles.
VII. Effect of heat treatment on the morphology of the intermetallics obtained in the cast alloy and the corresponding change in hardness behavior.

CHAPTER 2

LITERATURE REVIEW

CHAPTER 2

LITERATURE REVIEW

2.1 INTRODUCTION

Among commercial aluminum castings alloys, those with silicon as the major alloying element are the most important, mainly because of their excellent casting characteristics. Addition of silicon to pure aluminum imparts high fluidity, good feeding characteristics, low shrinkage and good hot cracking resistance. The properties of aluminum–silicon (Al-Si) alloys make them very popular in various applications in the automotive, aerospace and defense industries. A high strength-weight ratio is one of their most interesting characteristics. Aluminum has a density of only 2.7 g/cm^3, approximately one third that of steel. As the density of silicon is 2.3 g/cm^3, it is one of the few elements which may be added to aluminum without loss of weight advantage.

For a specific application, the selection of an alloy is determined by its castability, the casting process, the required mechanical and physical properties and the use of the casting. Al-Si alloys may be considered as composite materials. In the soft, ductile, continuous aluminum-rich matrix are found hard silicon particles as well as some intermetallics and inclusions. The higher the silicon content, the harder and stronger the material, but the lower its ductility. Increasing the amount of Si up to the eutectic composition, such as in 413 alloy, results in the formation of a large volume fraction of

eutectic, which improves the alloy fluidity and feeding ability, but decreases the ductility. [17]

Refining the microstructure is an important and effective method for improving the strength and ductility of Al-Si casting alloys. Addition of strontium can cause a transition of the eutectic silicon phase from coarse flakes into fibers, resulting in an improvement of mechanical properties, especially ductility.[18, 19] Investigations suggest that the addition of strontium to near-eutectic Al-Si alloys can promote columnar growth of the α-aluminum dendrites, which are present as fine and slender highly branched columns, and also result in a remarkable increase in the amount of the α-aluminum dendrite phase. [20]

Rare earth metals such as Ce, La, Nd and Pr contained in mischmetal are known to be beneficial modifiers and alloying elements in Al-Si alloys. Besides the modification of the eutectic silicon through a change of the shape and mode of silicon growth, they can react with aluminum, silicon and other alloying elements to form a fine dispersion of coherent intermetallic compounds which strengthens the grain boundaries, thereby increasing the strength and improving the performance of the Al-Si alloys at elevated temperatures.

The mechanical properties of Al-Si alloys are controlled by their chemical composition as well as the quality of their microstructure. [21] Further improvement can be achieved by the addition of other alloying elements, such as magnesium and copper; these elements allow the heat treatment of the alloy and a resultant improvement of the alloy properties. By this means the yield and tensile of an Al-7%Si-0.3%Mg alloy, for example, can almost be increased by a factor of three, whilst the elongation still remains at an acceptable level. The increase in strength during ageing is due to the precipitation of

submicroscopic and metastable phases (Mg_2Si or $CuAl_2$), which provide excellent obstacles for the dislocation movement and hence the precipitation hardening.[22]

2.2 CLASSIFICATION OF ALUMINUM CASTING ALLOYS

Aluminum casting alloys are numbered according to a three-digit (plus decimal) system adopted by the Aluminum Association (AA) in 1954 and approved by the American National Standards Institute in 1957 (ANSI H35.1). [23] The American Society for Testing and Materials (ASTM) specifications for aluminum castings conform to the AA designation system, as shown in Table 2.1 below.

Table 2.1 Classification of aluminum casting alloys [23]

Series	Alloy family
1xx.x	99.0% min Al
2xx.x	Al-Cu
3xx.x	Al-Si-Mg, Al-Si-Cu, Al-Si-Cu-Mg
4xx.x	Al-Si
5xx.x	Al-Mg
6xx.x	Unused
7xx.x	Al-Zn
8xx.x	Al-Sn
9xx.x	Unused

In this system, major alloying elements and certain combinations of elements are indicated by a number series ranging from 1xx.x through 9xx.x. The 6xx.x and 9xx.x series

are not currently in use, but are held open for possible use in the future. The digit following the decimal in each alloy number indicates the form of the product, where

- a "0" (zero) following the decimal indicates the chemistry limits applied to an alloy casting;
- a "1" (one) following the decimal indicates the chemistry limits for ingot used to make the alloy casting;
- a "2" (two) following the decimal also indicates ingot but with somewhat different chemical limits (typically tighter, but still within the limits for ingot).

Generally, the xxx.1 ingot version can be supplied as a secondary product (remelted from scrap, etc.), whereas the xxx.2 ingot version is made from primary aluminum (reduction cell). Some alloy names include a letter. Such letters, which precede an alloy number, distinguish between alloys that differ only slightly in percentages of impurities or minor alloying elements (for example, 356.0, A356.0, B356.0 and F356.0 alloys).

2.3 ALUMINUM–SILICON ALLOY SYSTEM

Aluminum casting alloys with silicon as a major alloying element are by far the most important commercial casting alloys, primarily because of their superior casting characteristics such as high fluidity and low shrinkage, in comparison with other alloys. Al-Si alloys combine the advantage of high corrosion resistance, good weldability, and low specific gravity, [23] which make them very important materials for use in automotive applications.[21] Today, Al-Si alloys have replaced iron and steel in many components,

including transmission cases and intake manifolds, as well as in more critical components such as engine blocks, cylinder heads and wheels. Such applications require that the cast parts exhibit consistent strength-ductility properties throughout the casting.

The Al-Si system is a simple binary eutectic with limited solubility of aluminum in silicon and limited solubility of silicon in aluminum. The solubility of silicon in aluminum reaches a maximum of 1.65 wt% at the eutectic temperature and increases with temperature to 0.016 wt% Si at 1190°C. Figure 2.1 depicts the Al-Si phase diagram. The main reaction in the Al-Si system, besides the melting of pure Al and pure Si, is the eutectic transformation of liquid solution to solid solution Al and nearly pure Si, namely,

$$L \rightarrow Al_{eut} + Si_{eut}$$

It is now established that this eutectic reaction occurs at 577.6° C and 12.6 wt% silicon. [24, 25] According to the amount of silicon, industrial Al-Si alloys are divided into three groups: hypoeutectic alloys with a Si content between 5 and 10 wt%, eutectic alloys with 11-13 wt% Si, and hypereutectic alloys, commonly with a Si content between 14 and 20 wt%.

Binary eutectic alloys, such as 413, 443 and 444 alloys, combine the advantages of high corrosion resistance, good weldability and low specific gravity. Hypoeutectic alloys, such as 319 (Al-6.5%Si-3%Cu) and 356 (Al-7%Si-0.3Mg), offer good castability and corrosion resistance. The 380 (Al-8.5% Si-3.5% Cu) alloy is popularly used in die casting. In this group, the silicon provides good casting properties. The alloys can be strengthened by adding small amounts of Cu, Mg or Ni.

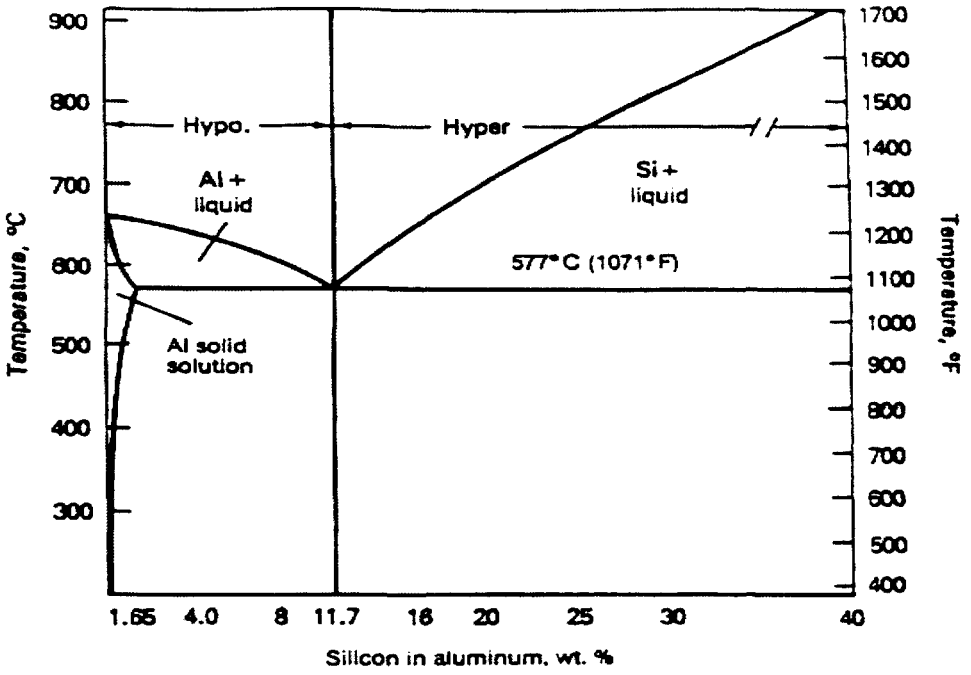

Figure 2.1 Aluminum end of the Al-Si equilibrium diagram.[26]

Hypereutectic alloys, such as 390 alloy, have outstanding wear resistance, a lower thermal expansion coefficient, and very good casting characteristics. There are several commercial alloys of this type, such as A391.0 and B390.0, 392.0 and 393.0. They contain nominal silicon contents of 17%, 19% and 22%, respectively, along with other alloying elements such as copper, magnesium, manganese and nickel. All of these alloys possess great hardness and wear resistance as compared to other aluminum casting alloys.

In general, as the silicon content of hypereutectic alloys increases, wear resistance increase, and the coefficient of thermal expansion decreases. All hypereutectic Al-Si alloys

offer excellent castibility, low coefficient of thermal expansion, good wear resistance and mechanical properties. Ductility, however, is low. [26]

Aluminum-silicon castings constitute 85 to 90% of the total aluminum cast parts produced. The most common aluminum casting alloys are listed in Table 2.2. [27]

Table 2.2 Chemical compositions of common types of Al-Si casting alloys(a) [27]

Alloy		Elements (wt. %)					
	Method(b)	Si	Cu	Mg	Fe	Zn	Others
319.0	S, P	6.0	3.5	<0.10	<1.0	<1.0	
332.0	P	9.5	3.0	1.0	1.2	1.0	
355.0	S, P	5.0	1.25	0.5	<0.06	<0.35	
A356.0	S, P	7.0	<0.20	0.35	<0.2	<0.1	
A357.0	S, P	7.0	<0.20	0.55	<0.2	<0.1	0.05 Be
380.0	D	8.5	3.5	<0.1	<1.3	<3.0	
383.0	D	10.0	2.5	0.10	1.3	3.0	0.15 Sn
384.0	D	11.0	2.0	<0.3	<1.3	<3.0	0.35 Sn
390.0	D	17.0	4.5	0.55	<1.3	<0.1	<0.1 Mg
413.0	D	12.0	<0.1	<0.10	<2.0	-	
443.0	S, P	5.25	<0.3	<0.05	<0.8	<0.5	

(a) Remainder: Aluminum and other impurities
(b) S, Sand Casting; P, Permanent Mold Casting;
D, High Pressure Die Casting

2.3.1 Al-Si-Cu Alloys

Alloys 319.0 and A319.0 have been considered to be the most popular type of Al-Si-Cu alloys used extensively in the automotive industry. In such hypoeutectic alloys, according to Bächerud *et al.* [28] the solidified microstructure forms mainly according to the following sequence:

I. A network of α-aluminum dendrite formed at the start of solidification (at 600°C-610°C).

II. The formation of the eutectic Al-Si structure (eutectic reaction at 550°C-575°C).

III. The precipitation of the hardening $CuAl_2$ phase in the temperature interval 500°C-520°C (post-eutectic reaction).

Depending on the chemical composition of the alloy, conditions of casting, and the type of additives, precipitation of iron-containing intermetallic phases can also occur. The α-iron ($Al_{15}MnFe_3Si_2$) tends to precipitate prior to the formation of the α-aluminum dendrites, in the form of Chinese script particles within the α-Al dendrites, in a pre-eutectic reaction at 650°C. Another type of iron intermetallic that can be formed is the β-iron (Al_5FeSi) phase, which can precipitate in a co-eutectic or post-eutectic reaction. This phase occurs in the form of brittle platelets particles.

It is well known that the addition of Cu makes these types of alloys heat treatable. It is reported that at ~548°C, the amount of Cu in solid solution in Al is about 5.7 wt%. This value decreases as the temperature decreases, reaching 0.1-0.2 wt% at 250°C. [29, 30] Copper combines with Al to form an intermetallic phase that precipitates during solidification at 500°C either as block–like $CuAl_2$ or in eutectic form as ($Al+CuAl_2$). In 319 alloys, the copper intermetallic phase precipitates in these two forms, according to a multicomponent eutectic reaction reported by Mondolfo [29, 31] as:

$$L \rightarrow Al + CuAl_2 + \beta\text{-}Al_5FeSi + Si \qquad \text{at } 525°C$$

Alloys 319.0 and A319.0 exhibit good castability, weldability, pressure toughness and moderate strength and are stable in that their casting and mechanical properties are not affected by fluctuations in the impurity content. Alloys B319.0 and 320.0 show higher strength and hardness than 319.0 and A319.0 alloys, and are generally used for permanent mold casting. Characteristics other than strength and hardness are similar to those of 319.0 and A319.0 alloys. Typical applications of these alloys include internal combustion and diesel engine crankcases, and gasoline and oil tanks - using sand casting, and water-cooled cylinder heads, rear axle housings and engine parts - using permanent mold casting.[32, 33]

2.3.2 Al-Si-Mg Alloys

A very important group of Al-Si alloys is that comprising Al-Si-Mg alloys which are age hardenable due to the presence of magnesium. A uniform distribution of magnesium silicide (Mg_2Si) can be obtained through a solution heat treatment, quenching and aging procedure. The mechanism by which such alloys undergo age or precipitation hardening is described in Section 2.6. The most popular alloy of this family is 356 alloy. [17]

During solidification, the major constituents of the microstructure of Al-Si-Mg alloys precipitate in the following sequence:

I. The formation of the α-aluminum dendrite network.

II. Al-Si eutectic structure (eutetcic reaction).

III. The precipitattion of the hardening Mg_2Si phase (co-eutectic reaction).

In the alloys contain high level of Mg (> 0.2%), it is often expected that the hardening Mg_2Si phase begins to precipitate at a temperature ~ 540°C which is about 30 to 40 degree below the eutectic reaction. [28]

Alloy 356.0 (Al-7%Si-0.4%Mg) has excellent casting chacteristics. Permanent mold castings of this alloy are used in many applications, including machine tool parts, aircraft wheels, hand wheels, pump parts, tank car fittings, valve bodies and bridge railing parts, as well as, fuselage fittings and fuel tank elbows for airplanes and missiles. Automotive applications of permanent mold 356 casting alloy include miscellaneous castings for trucks and trailers, spring brackets, cylinder heads, engine blocks, passenger car wheels and transmission cases. Sand castings of 356.0 include flywheel housings, automotive transmission cases, oil pans, rear axle housings, brackets, water-cooled cylinder blocks, various fittings and pump bodies. The alloy is also used in various marine applications in the T6 condition, where pressure tightness and/or corrosion resistance are major requirements. Alloy A356.0 has greater elongation, higher strength and considerably higher ductility than 356.0 alloy due to the lower amount of impurities in comparison to 356.0 alloy. Typical applications are airframe castings, machine parts, truck chassis parts, aircraft and missile components, and structural parts requiring high strength.[32, 33]

2.4 MICROSTRUCTURE OF CAST AL-SI ALLOYS: ROLE OF COOLING RATE

The microstructure of Al-Si alloys is controlled by the composition, the casting process, and the solidification conditions (*i.e.*, cooling rate). It is well known that a high cooling rate produces a fine eutectic structure, small dendrite cells and arm spacing, and a

reduced grain size. The dendrite arm spacing (DAS) is considered to be the most effective parameter controlling the mechanical properties of an Al-Si alloy. Small DAS values are obtained with rapid cooling rates which are usually associated with finer as-cast grain sizes. Consequently, the mechanical properties are controlled by the DAS, not by the grain size.

Ye *et al.* [11] investigated the influence of cooling rate on the dendrite arm spacing of 356 alloy. They found that with increase in the cooling rate, considerable decrease in the DAS was observed in the non-modified, sodium-modified, and mischmetal modified alloy. A marked decrease in DAS was observed clearly in the alloy modified by 0.2 % mischmetal addition.

It has been established that the Al-Si eutectic can exhibit either of two morphologies: non-modified or modified. Under slow cooling conditions in the non-modified cast alloys, the Si particles appear to be disconnected and exhibit a flake-like structure. At relatively fast cooling rates, such as in chill casting, the eutectic Si particles are much finer, but still exhibit the flake-like structure. In chemically modified alloys, the Si particles have a fibrous morphology, and appear as isolated spherical particles in an optical micrograph.

Haque and Maleque [34] studied the effect of cooling rate on the microstructure of Al-Si piston alloys (Al-12.2Si-0.85Cu-0.86Fe-0.75Mg). They reported that the different cooling rates have a significant effect on the microstructure of both non-modified and Sr-modified castings. The microstructure of sand cast alloys (ie., low cooling rate) is less refined than that obtained from chill casting (i.e., high cooling rate), consisting of α-aluminium dendrites, coarse acicular eutectic silicon particles and primary silicon plates.

As well as affecting the microstructure, the cooling rate also affects the shape and size of the precipitates: as the cooling rate decreases, the size of the precipitates increases. For example, the Al_2Cu phase in A319 alloy was reported to precipitate in the block-like, eutectic-like or both forms them at different cooling rate conditions. [35] As the cooling rate decreased, however, a high proportion of the block-like form of Al_2Cu was observed.

Haque and Maleque [34] also reported that the high cooling rate provided by the chill casting process resulted in a pronounced improvement in the ultimate tensile strength (UTS), percent elongation and hardness values (BHN) of both non-modified and modified alloys, due to the formation of a fine grained structure, while the coarse grained structure obtained from the sand casting process (low cooling rate), led to a reduction in the UTS and percent elongation, as shown in Figure 2.2, taking into consideration the influence of the grain boundary regions.

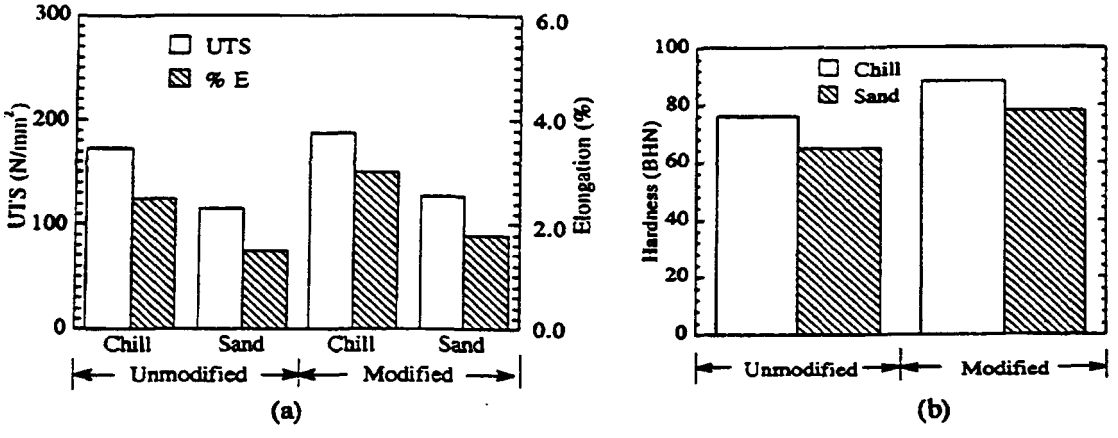

Figure 2.2 Comparsion of (a) tensile properties, and (b) hardness values of unmodified and modified Al-Si piston alloy obtained under chill casting and sand casting conditions. [34]

Ye *et al.* [11] reported the relation between the cooling rate and the hardness values (BHN) of the non-modified and mischmetal modified 356 aluminum alloy. As can be seen in Figure 2.3, the hardness values increase with increasing cooling rate for both non-modified and mischmetal modified castings, where the non-modified castings display somewhat higher hardness values than those modified by mischmetal addition.

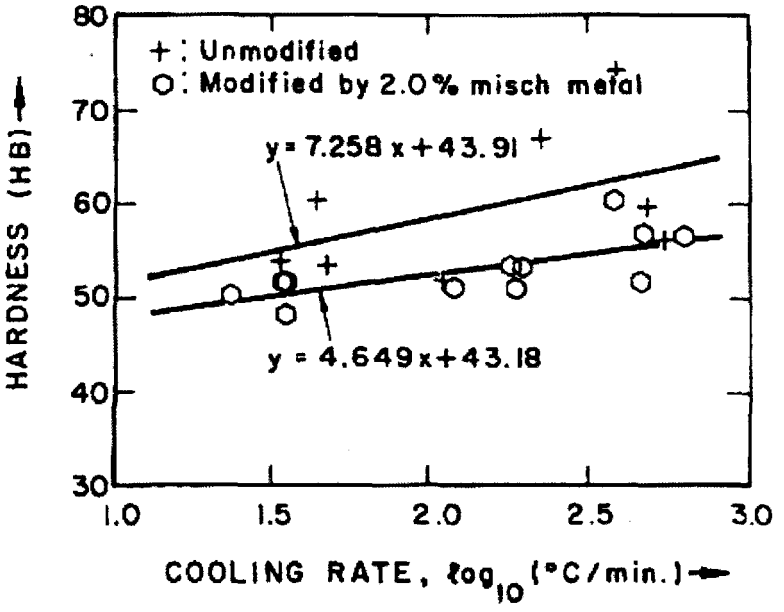

Figure 2.3 Effect of cooling rate on the Brinell hardness of 356 aluminum alloy.[11]

2.5 MODIFICATION OF AL-SI CASTING ALLOYS

The mechanical properties of Al-Si alloys depend strongly on many factors including chemical composition, molten metal processing and casting techniques, heat treatment, and the microstructure, in particular, the morphology of the eutectic silicon. [36] In the normal as-cast condition, the eutectic silicon particles occur as brittle acicular flakes in

the microstructure. Such acicular particles act as crack initiators and provide easy paths for fracture and hence reduce the mechanical properties of the alloy.

The properties can be improved by inducing structural modification of the normally occurring eutectic. Through the addition of "modifiers", the morphology of the eutectic silicon is altered into a fibrous form that allows for significant enhancement in ductility, besides improving the strength to a certain extent. In fact, the commercial application of Al-Si alloys often depends on the successful modification of the eutectic silicon.

The modification is carried out by the addition of chemical modifiers such as sodium (Na), strontium (Sr), antimony (Sb), or rare earth metals. These are normally added to the alloy melt in the form of master alloys in desired quantities, to achieve a well-modified eutectic structure. With modification, the eutectic structure becomes finer and the silicon particles become rounded, which contribute to the higher values of ultimate tensile strength and greatly increased values of ductility.

The amount of each modifier element required to achieve an acceptable level of Si modification depends somewhat on the alloy composition–a higher silicon content requires a larger amount of the modifying agent. For example, sodium is generally used in the range of 0.005-0.1 wt%. Strontium in amounts of 0.02% is sufficient to modify an Al-7% Si alloy such as 356, but up to 0.04% Sr is needed for eutectic alloys such as 413, containing ~12% Si.

In general, the greatest benefits of the modification are achieved in alloys containing from 5 to 13% Si and include the widely used and commercially popular

A332.0, 319.0, 356.0 and 357.0 alloys. The addition of modifiers such as sodium and strontium to hypoeutectic Al-Si alloys containing less than 12% Si is inclined to reduce the interfacial tension between the aluminium and silicon in the eutectic structure. This decrease in the interfacial tension increases the contact angle between aluminum and silicon, permitting the aluminum to envelop and stop the growth of the silicon crystals. [26] Modifier additions are usually accompanied by an increase in hydrogen content. Thus, modification treatment of a melt is followed by inert gas fluxing, in order to obtain acceptable melt hydrogen levels. [37]

As well as modification by the addition of chemical modifiers, Al-Si alloys can also be modified through solution heat treatment or the use of high cooling rates. However, full modification is difficult to achieve by simply increasing the solidification rate of the casting alone.

2.5.1 Chemical Modification

The Group IA and IIA elements are well known to act as effective modifiers in Al-Si alloys [11] where, with the addition of elements like Ca, Na, Sr, and Sb, the morphology of the eutectic silicon particles can be altered to a fine lamellar or fibrous eutectic network. The degree of Si particles modification achieved by the addition of Sr is similar to that obtained by Na and Ca. The change in the eutectic Si morphology may be attributed to the fact that the growth of silicon particles within the eutectic regions is prevented by the addition of such modifiers. [37]

The microstructural change from acicular to fibrous silicon is not a sharp one, and castings with an inadequate amount of either sodium or strontium will exhibit a mixed structure containing regions of fibrous silicon, lamellar silicon and acicular silicon. Modification with strontium is often less uniform than with sodium, while antimony produces only a lamellar, and never a fibrous, structure.

The modification of the eutectic silicon in Al-Si alloys was first reported by Pacz,[34,38] who found that the addition of sodium or its salts to the molten Al-Si alloys, modified the eutectic silicon particles, resulting in an improvement in the strength and ductility.

In spite of the fact that Na modification is very effective, in terms of the fineness and uniformity of the eutectic silicon particles, its action is only short-lived. The addition of sodium produces large numbers of twins in silicon. The normal amount of sodium added is ~ 20 to 150 ppm. Owing to its low melting point (98°C), sodium is easily incorporated into Al-Si melts which are normally treated in the range of 775°C to 800°C. The dissolution of sodium is instantaneous at these temperatures, but its high vapor pressure (0.2 atm. at 730°C) makes it boil off almost immediately. [39] This phenomenon is called "fading" in which the modification action of sodium (Na) diminishes rapidly with time. Figure 2.4 shows the loss or "fading" of Na in a 356 alloy melt with holding time, as indicated by the eutectic undercooling. The amount of undercoooling gives an indication of the level of modification achieved in the alloy melt. It is seen that the modification effect of Na starts to

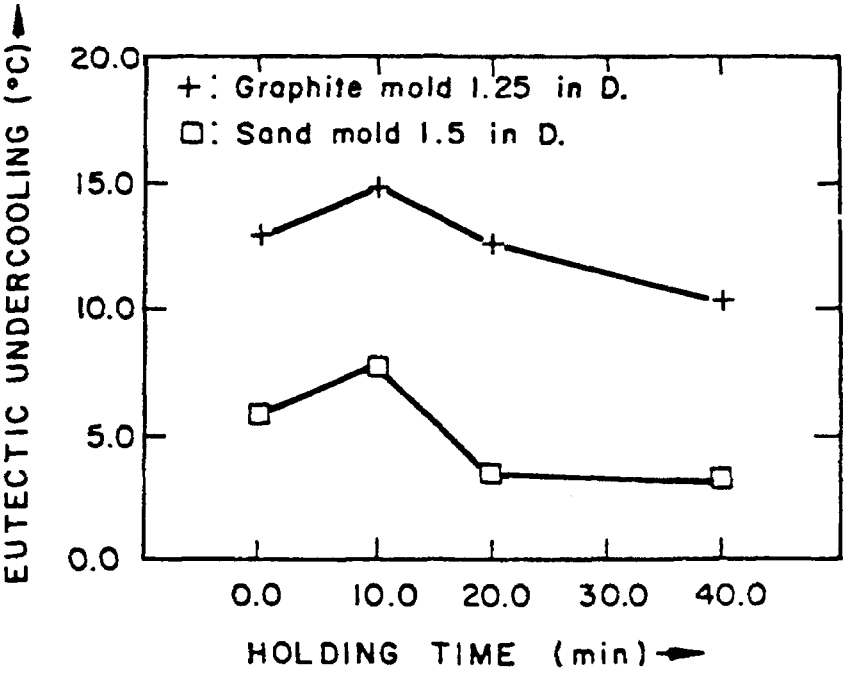

Figure 2.4 Fading effect of sodium in Na-modified 356 aluminum alloy as indicated by eutectic undercooling.[11]

slowly diminish after 10 min and it is more pronounced in the casting obtained from the sand mold. Also it is difficult to retain the modification action of sodium especially when extended holding times are encountered, or where higher temperatures are required. [11] Sodium is also found to be sensitive to porosity and has harmful effects in terms of oxidation and reaction with the mold coating.

Strontium has been widely used as an effective modifier in Al-Si alloys for many years. It is generally added in the form of Al-16%Si-10%Sr master alloy, which is more economic than the use of strontium salts, as its addition overcomes the problem of Sr loss during melting, recovery is high, and there is no fume generation. After the addition of

strontium, there is an incubation period which enhances the modification effect of Sr. Although both Na and Sr exhibit losses during holding, as well as after remelting, Sr is found to retain and improve the modification better than Na, provided enough amount of Sr is added in the original melting process (~ 0.008%) to allow for modification in subsequent meltings. Sr is said to have a greater "staying power" compared to soduim. [40]

Many studies [41, 42] reported in the literature reflected the tendency to replace sodium by Na with Sr in the modification of Al-Si alloys, so that today Sr is the modifier most commonly used for these alloys. The quantity of strontium needed to produce a completely fibrous microstructure depends on the alloy and on the casting conditions, and ranges from 50 to 350 ppm.

Figure 2.5 shows the loss of Sr in a 319.2 alloy melt with time. As can be seen, Sr fades more slowly than Na, and so it is regarded as a semi-permanent modifier. [43]

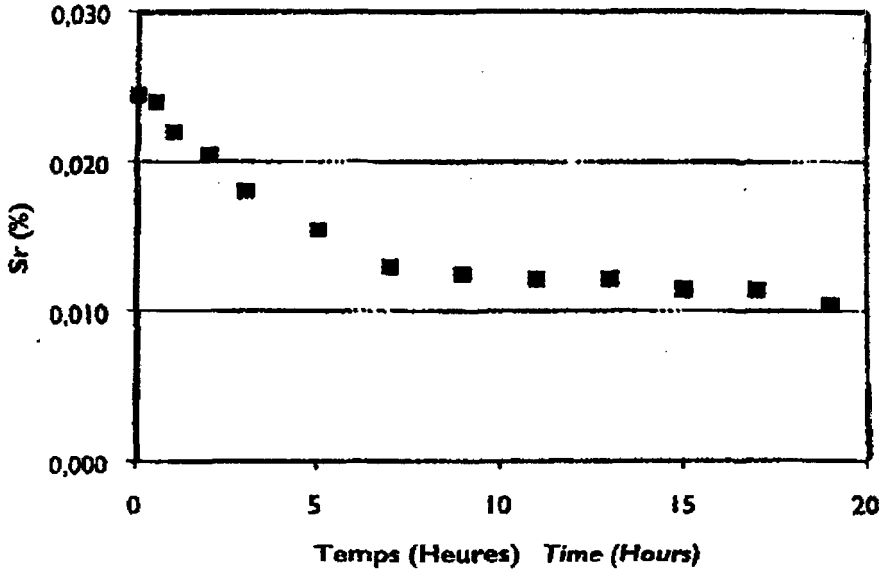

Figure 2.5 Loss of strontium with time.[43]

According to Haque and Maleque, [34] who studied the Sr-modification of Al-Si piston alloys, the extent to which Sr is able to refine the eutectic structure strongly depends on its concentration in the molten alloy before the start of solidification, as well as the cooling rate. The refined structure and the properties reach a maximum at a strontium concentration of about 0.1%, then tend to decrease with further strontium addition beyond this level. Owing to the fact that the microstructure of Sr-modified alloys contains a large amount of rounded silicon particles with no primary silicon crystals, the addition of strontium leads to an increase in the tensile strength and the hardness of the alloys (see Figure 2.2).

In the reviewing the mechanisms of eutectic modification in Al-Si alloys, Makhlouf *et al.* [25] report that many of the hypotheses proposed in the literature assume that (a) the eutectic Si phase nucleates on the primary α-Al dendrites, and that (b) the modifier inhibit the growth of the Si phase, causing the transformation of the Si particle morphology from plate-like to fibrous. However, they are unable to explain the phenomena associated with modification, such as, the large undercooling observed with the addition of modifier, or the occurrence of modification with the use superheat or a high solidification rate instead of a modifier.

2.5.2 Thermal Modification

The modification of the eutectic Si phase can be obtained in the absence of chemical modifiers by subjecting the Al-Si alloy to high temperature solution heat treatment for an extended time. During solution heat treatment, the eutectic Si particles undergo shape

perturbations and began to break down into small particles, which consequently spherodize and then coarsen, depending on the solution treatment temperature, the morphology of the eutectic silicon particles, their initial size, i.e., whether the alloys have a non-modified or modified structure.

During elevated temperature treatments for extended periods (i.e., thermal modification), the changes in the Si particle morphology can occur in several stages. Initially, the Si particles are liable to undergo necking and gradual fragmentation. The fragmentation stage leads to a decrease in the average size of the Si particles and an increase in the average particle density. The fragmented particles then begin to spheroidize and coarsen. As a result of the commencement of the coarsening stage, an increase in the average size of the particles and a decrease in the average number of particles is observed.[44, 45]

Figure 2.6 depicts the behavior of the Si particles in non-modified and modified alloys subjected to solution heat treatment. [46] In the non-modified case, the Si particles are large platelets, which exhibit necking and fragmentation in the early stages of solution treatment. As the solution time increases, the particles begin to spherodize and coarsen, as shown in Figure 2.6(a). In the modified alloys, due to the finer as-cast Si structure, the response of these alloys is different as can be seen from Figure 2.6(b). During the early stage of solution treatment, the Si particles tend to spherodize rapidly owing to the high driving force provided by the finer Si structure.

The spheroidization rate in the modified alloys is higher than that in the non-modified alloys requiring a shorter solution treatment time to reach a fully spheroidized

eutectic Si structure. With further solution treatment, the Si particles begin to coarsen, similar to the case of the non-modified alloy.[46]

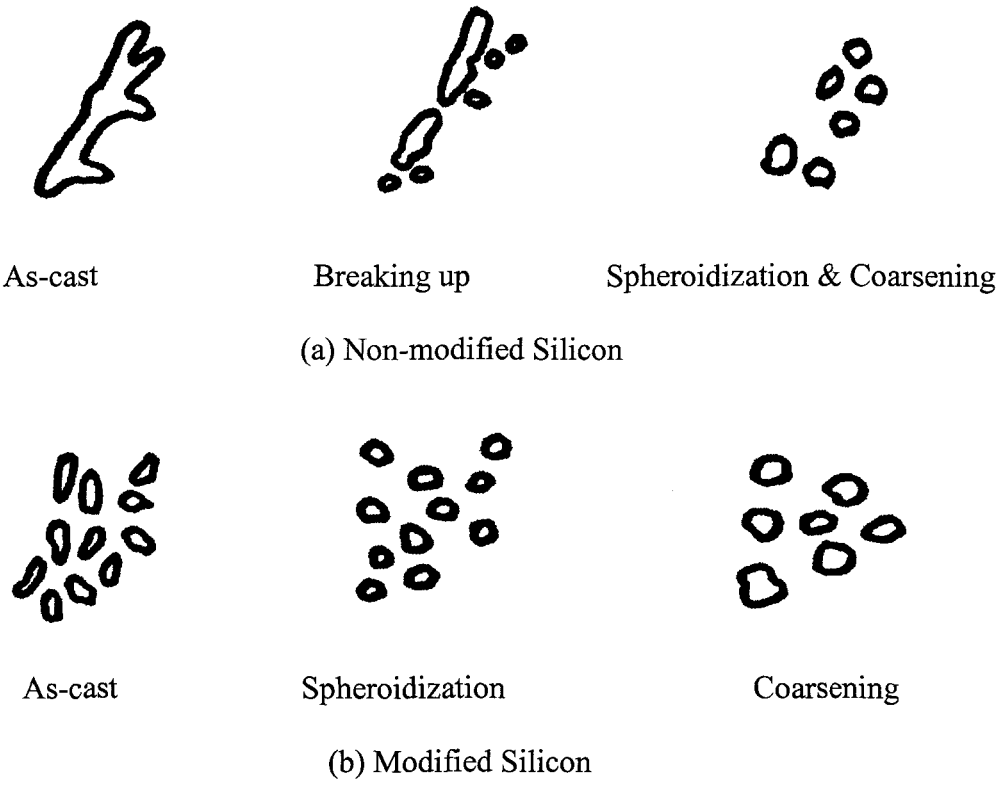

Figure 2.6 Schematic diagram showing modification of Si particles during solution heat treatment in the case of: (a) non-modified, and (b) modified Al-Si alloys.[46]

The fragmentation and spheroidization stages are controlled by the instability of the interface between the two different phases and the driving force for this stage is the decrease in the total interfacial energy of the system.[1] Thus, the change in Si particle size and morphology is highly dependent on the surface energy. The average Si particles exhibit a decrease in size due to separation during the fragmentation and spheroidization stages. From the thermodynamic point of view, the instability of the interface between two faces is

a surface energy driven force. The driving force for spheroidizatin and coarsenimg of the Si particles is the reduction in surface energy. In the non-modified alloy, the eutectic Si possesses a plate-like structur (i.e., high surface energy) and hence, interfacial instabilities cannot easily occur. Consequently, the Si eutectic structure in the non-modified alloys is more resistant to spheroidization, whilst the fine fibrous Si eutectic structure in the modified alloys is susceptible to shape perturbations and the particles are readily fragmented. The rate of spheroidizaton, therefore, is much higher in the modified alloys.[47, 7]

To explain the coarsening of the Si particles with prolonged solution treatments in both non-modified and modified alloys, Ostwald [1, 48] proposed the following mechanism: the Si particles will coarsen and increase in size provided their size is greater than the critical volume, whereas smaller particles will dissolve in the larger particles, as shown in Figure 2.7. Therefore, the average size and the spacing of the Si particles will increase, while the particle density will decrease during the coarsening stage.

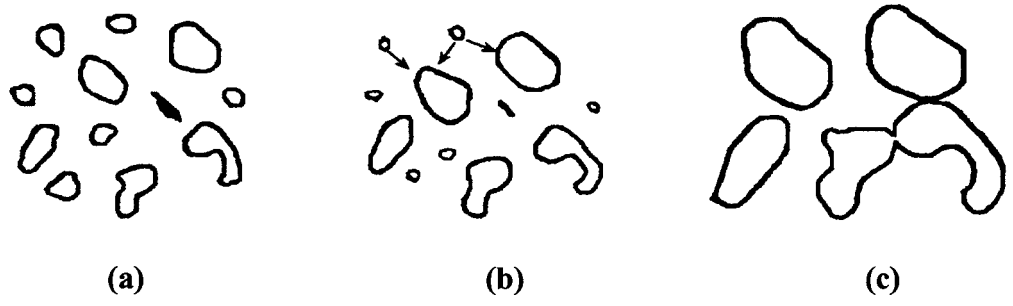

Figure 2.7 Schematic illustration of Ostwald ripening mechanism: (a) before solution heat treatment, (b) small particles dissolve in large particles, and (c) coarsening of large particles.[46]

In their study on the heat treatment of cast Al-Si Mg alloys, Apelian *et al.*[7] confirmed that the Si particles exhibit spheroidization and coarsening during solution treatment. The rate of spheroidization is found to be much faster in modified alloys than in the non-modified alloys as only a small fraction of Si particles are spherodized even after 10 to 15 h of solution treatment. The driving force for coarsening is greater in the non-modified alloys than in the modified alloys owing to the fact that the difference in particle size distribution in the non-modified alloys is high. Therefore, the unmodified alloys reveal a higher coarsening rate.

The structural changes in the Si particle morphology occurring during solution treatment result in an appreciable improvement in the mechanical properties. The tensile strength, elongation and the quality index increase with the duration of the solution heat treatment. The ductility of the alloy and, to a lesser extent, the tensile strength are increased upon modification. The overall effect of modification is to reduce the time required to achieve the desired property level in the casting. A 2 h solution treatment in modified alloys gives properties equivalent to the properties obtained after a 12 h solution treatment in non-modified alloys. [47] In recent years, chemical modification in conjunction with thermal modification are being used in the industry in order to produce the desired properties of a casting.[49, 50]

Haque and Maleque [34] reported significant changes in the structure and properties of both non-modified and modified Al-Si piston alloys that were, subjected to full heat treatments (i.e., solution heat treatment at 520°C for 8h, quenching in hot water, then aging at 180°C for 8h). Due to heat treatment, both primary silicon and eutectic silicon particles

undergo partial spheroidization. The modified heat-treated alloys possess more uniform and refined structures owing to the combined influence of Sr-modification and heat treatment, resulting in a significant improvement in the tensile strength, hardness and ductility of the alloy, as shown in Figure 2.8.

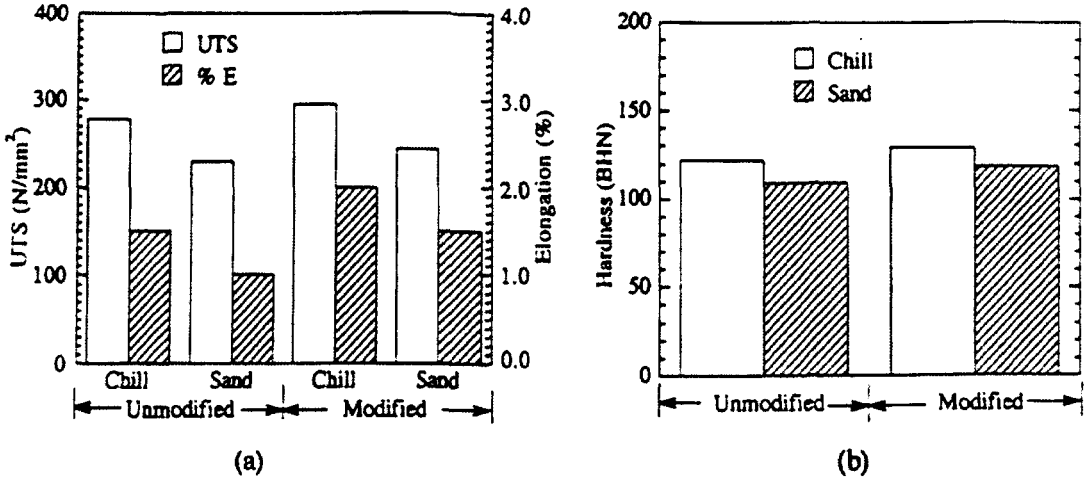

Figure 2.8 Graphical representation of Al-Si piston alloy in the heat-treated condition: (a) Tensile properties; (b) hardness values. [34]

2.6 HEAT TREATMENT OF ALUMINUM-SILICON CASTING ALLOYS

When applied to aluminum alloys, heat treatment refers to the specific operations carried out to improve the strength and the hardness of "heat-treatable" alloys or those whose properties can be enhanced through precipitation hardening. [37] Heat-treatable aluminum alloys gain strength from subjecting the material to a sequence of processing steps called solution heat treatment, quenching, and aging. The primary goal is to create

sub-micron sized particles in the aluminum matrix, called precipitates, during the aging stage (either natural or artificial aging), which improve the properties of the alloy.

Solution Heat Treatment aims to take into solid solution the maximum practical amounts of the soluble strengthening alloying elements (such as Cu and Mg) in the alloy. This process consists of heating the aluminum alloy to an elevated temperature, and soaking at this temperature for a sufficient time to obtain a nearly homogenous solid solution.[37, 51, 52] The alloying elements are able to dissolve into the aluminum matrix to form a supersaturated solid solution. Pure aluminum cannot be strengthened through thermal treatment as it contains no alloying elements.

Time and temperature control are important aspects of solution heat treatment. The solution temperature should be lower than the solidus temperature, otherwise it can cause a harmful effect on the grain boundary regions and, hence, adversely affect the mechanical properties.

Quenching is the second stage of heat treatment. In this stage, a maximum amount of solute (alloying elements) are available for the formation of the fine scale hardening precipitates during subsequent ageing. The main purpose of the quenching before ageing is to have a supersaturated solid solution (which contains more solute atoms than its equilibrium level), and to prevent the formation of equilibrium second phase precipitates (i.e., Mg_2Si or $CuAl_2$).

The effectiveness of the quenching stage strongly depends on the quench medium used and the quench interval. The quench medium should have sufficient volume/heat extracting capacity to produce a high cooling rate. A rapid quench ensures that all

precipitates are retained in solid solution. Highest strength can be achieved using a fast quench rate (normally in water). Thin sections require a small quench rate as they are more likely to undergo distortion, and are quenched in oil or other polymer based media.

Aging is the final stage in the heat treatment of cast aluminum alloys. After solution treatment and quenching, strengthening can be obtained either at room temperature (natural aging) or with a precipitation heat treatment (artificial aging). In some Al alloys, sufficient precipitation occurs in a few days at room temperature to produce stable products with properties that are satisfactory for many applications. These alloys sometimes are precipitation heat-treated to provide increased strength and hardness in wrought or cast products. Other alloys with slow precipitation reactions at room temperature are always precipitation heat-treated before being used.

Natural aging refers to the room temperature aging that occurs in the quenched alloy before it is subjected to artificial aging at higher temperatures. During natural ageing, factors considered are: (i) Formation of clusters, and (ii) Superstauration of the matrix. When the clusters become stable (possess a critical radius) that formed during natural ageing process, they can act as nuclei for the formation of GP zones in the artificial aging at high temperatures, leading to an increase in both nucleation density and strength properties. The effect of natural aging is more intensified in the presence of excess Si due to the high rates of clustering. This could be attributed to the fact that the rate of clustering increases as the amount of Mg in the matrix increases, resulting in a considerable improvement in the strength properties. [51, 53]

In the artificial aging process, precipitation strengthening is achieved when the alloying elements that are soluble at elevated temperature undergo a significant decrease in solid solubility with decreasing temperature. The precipitation hardening of aluminum copper alloys takes place in a number of steps. Regions of solute segregation or clustering (GP zones) were first detected by Guinier and Preston, [51, 54] in these alloys after quenching from solid solution, localized in specific planes in the matrix lattice. In some alloy systems, these GP zones are disk-shaped, while in others they can be rods or spheres. The GP (1) zones have higher hardness values than the solid solution. With increasing ageing temperature or time, GP (2) zones are formed which are metastable precipitates and semi-coherent with the matrix. The general precipitation sequence of GP zones is:

$$\alpha_{sss} \rightarrow \text{ GP zones} \rightarrow \text{ GP(1) zones } (\theta'') \rightarrow \text{ GP(2) zones } (\theta') \rightarrow \theta \text{ (equilibrium phase)}$$

During the ageing process, it is normal to form a coherent precipitate and lose coherency when the particles grow to a critical size. GP zones are considered to be powerful obstacles for the motion of the dislocations, and provide maximum impedance to dislocation movement when the distance between these particles is smaller or equal to the curvature radius of the moving dislocation line. [51]

2.6.1 Mechanism of Precipitation Hardening

The precipitation hardening process obtained during aging treatment implies the formation of fine dispersed precipitates from the supersaturated solid solution. The aging is often carried out not only below the equilibrium solvus temperature, but also below a

metastable miscibility gap called the Guinier-Preston (GP) zone solvus line. The high concentration of of vacancies in solid solution allows diffusion (and thus zone formation) to occur much faster than expected from the equilibrium diffusion coefficients.

The mechanism of precipitation hardening entails the formation of coherent clusters of solute atoms (having the same crystal structure as the solvent matrix). This results in a great coherency strain in the matrix around the particles owing to the mismatch in size between the solvent and the solute atoms. The strain fields in the matrix surrounding the coherent particles interact strongly with the stress field of the dislocations, which hinders and retards the movement of the dislocations, providing higher strength. The exact size, shape, and distribution of the GP zones are dependent on the chemical composition of the alloy, and on the thermal and mechanical history of the specimen, as well. [37]

The dominant precipitate is the coherent GP zones, and these precipitates are sheared by the moving dislocation as they glide on the slip plane at small interparticle spacing, giving maximum strength to the alloy. Once the GP zones are cut, the dislocations continue to pass through the particles and the rate of work hardening is comparatively small. As the aging time increases, the precipitate particles become larger and wide enough, to lose their coherency (i.e., have a different crystal structure from the matrix). At this point, the dislocation can move by by-passing (cross slip) or bending (looping) around the precipitates and rejoin again, leaving a small dislocation loop behind, according to the mechanism proposed by Orawan. [54] This is the case when time and temperature are increased sufficiently to form a high proportion of the final equilibrium incoherent precipitates; the alloy softens and is said to be overaged, where the strength increases

(peak-aged condition), and then decreases with longer aging time (overaged condition).

This may be attributed to the transition of the dislocation movements from cutting the precipitates (i.e., high strength) to by-passing the precipitates which are much easier (i.e., low strength). [51] The various mechanisms of strengthening during solution and aging treatment are summarized and illustrated in the schematic plot of Figure 2.9. [55]

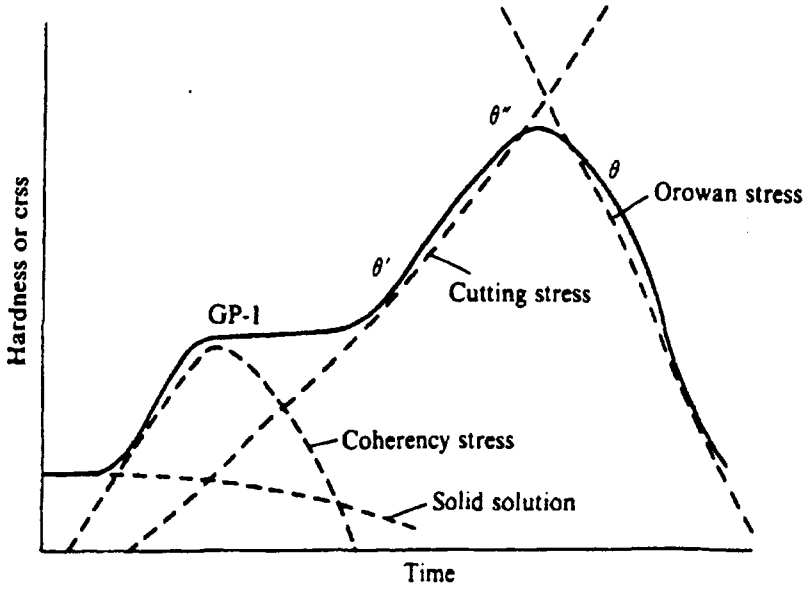

Figure 2.9 Interplay of various precipitation hardening mechanisms at successive stages in the hardness-time curve. [55]

2.6.2 Precipitation Hardening in Al-Si-Cu and Al-Si-Cu-Mg Alloys

Al-Si-Cu alloys, generally belonging to the 319 family of alloys, are used extensively in many automotive applications. Al-Si-Cu alloys are heat treated to achieve an optimum combination of strength and ductility. The heat treatment consists of solutionizing at a temperature close to, but below, the eutectic temperature, quenching, and a

combination of natural and artificial aging. Under practical heat treatment conditions for alloys such as 319, the solutionizing temperature is often selected below 495°C, to overcome the problem of localized melting in the grain boundaries regions. [36] It is well accepted that the precipitation sequence:

$$\alpha_{sss} \rightarrow \text{GP zones} \rightarrow \theta'' \rightarrow \theta' \rightarrow \theta \text{ (equilibrium phase)}$$

is mainly responsible for the hardening of Al-Cu and Al-Si-Cu alloys, as shown in Figure 2.10. Upon aging, the supersaturated solid solution tends to transform to the equilibrium structure through a number of intermediate stages. The first intermediate forms of the precipitates are regions of rich copper in the form of thin plates located in the {100} planes of the α-aluminum matrix, called GP (1) zones. Further aging results in an ordered coherent structure consists properly from two layer of copper separated by three layer of Al which are designated as GP(2) zones or θ''. By increasing the aging time, the semi-coherent precipitates θ' are formed on {100} planes in the α-aluminum lattice, assuming tetragonal plate-like forms. At the final stage, the alloy softens in the overaged condition due to formation of the non-coherent equilibrium precipitates θ ($CuAl_2$) having a body centered cubic structure. [52] It has been reported that the θ phase had been observed to nucleate on dislocations. [56, 57, 58] Therefore, these plate-like metastable phases nucleate and grown on dislocations at the expense of fine and uniform GP zones.

In Al-Si-Cu-Mg alloys, the GP zones and metastable phases formed during the precipitation hardening process effectively strengthen the alloy during aging, resulting in peak aging. Fine and profuse GP zones homogenously distribute in the matrix in the early stage of aging, leading to a significant hardening of the alloy. In the intermediate stage of

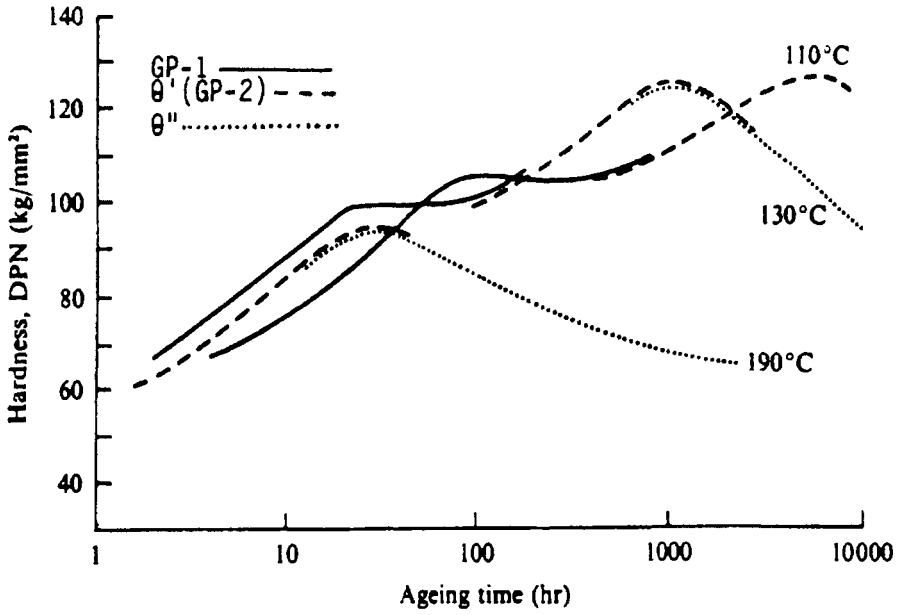

Figure 2.10 Precipitation hardening of Al-4Cu alloy: hardness and precipitate structure versus aging time at various temperatures (solution treated: 540°C for 2 days).[55]

aging, metastable phases are formed and remain semi-coherent with the matrix. Theses semi-coherent precipitates can effectively hinder and retard the motion of dislocations, thereby also providing a certain strengthening effect.[56, 59, 60]

In the transition stage from GP zones to metastable phases, the number of GP zones decreases significantly due to the dissolution, while the metastable precipitates have still not grown and their size is too small to effectively resist the movement of dislocations. Therefore, the age hardening effect in the alloy is low at this stage.

2.6.3 Precipitation Hardening in Al-Si-Mg Alloys

The prolonged aging treatment of cast Al-Si-Mg alloys aims to improve the strength properties in the casting. In most cases the casting are used in the underaged condition to obtain an acceptable combination of strength and ductility.

The precipitation of the metastable Mg_2Si phase from the supersaturated solution during the aging treatment of Al-Si-Mg alloys improves the alloy strength. This precipitation can occur very rapidly even at room temperatures within a short period of time. Due to the presence of excess silicon in solid solution after the formation of Mg_2Si precipitates, the precipitation process can be accelerated. The presence of excess silicon reduces the solid solubility of Mg_2Si in the α-aluminum matrix and increases the solvus temperature at a given Mg_2Si level as well. Thus, a finer dispersion of precipitates is obtained in the alloys containing excess silicon.

The main precipitation sequence in Al-Si-Mg alloys can be given as:

α_{sss} → GP Zones of needle-like or spherical morphology → rod like β' phase →

platelet equilibrium precipitates of the compound Mg_2Si

The precipitation process begins with the decomposition of the supersaturated solution by the clustering of silicon atoms. This clustering results in the formation of spherical Guinier-Preston (GP) zones which are coherent with the matrix. These zones are needle shaped in form, and extend in the {100} direction of the cubic aluminum matrix. During the early stages, the GP zones are disordered, with a high vacancy content, and as aging increases they acquire an ordered structure. GP zones are relatively stable and may

exist up to temperatures of about 260°C. With increasing aging treatment, the needle-like GP zones begin to grow and become rods of an intermediate phase (β') and then eventually platelets (β). The β' particles are semicoherent with the matrix phase, and the rod axes are parallel to the cube matrix directions to form cubic or hexagonal structures. The final equilibrium Mg_2Si (β) forms incoherent platelets with the aluminum matrix, and has an ordered face centered cubic structure, with the Mg atoms located at tetrahedral positions. The maximum hardness is obtained even before the platelets form. The maximum size of the Mg_2Si particles is found to be of the order of 0.03 μm, before the hardness begins to decrease in the overaged condition. [51, 53]

2.7 MISCHMETAL AS A MODIFIER IN AL-SI CASTING ALLOYS

In the last few decades, the use of rare earth metals, especially La, Ce, Nd, Sc, and mischmetal (MM, a mixture of rare earth elements) in aluminum alloys has been studied by many workers, [2, 11, 12, 61] where it has been reported that the microstructure of these alloys is modified, and the mechanical properties are improved as well.

The nature of rare earth (RE) elements determines their effect on aluminum alloys. Owing to their large atomic radii and tendency to lose the two outermost level s-electrons and a 5d or 4f electron to become trivalent ions, rare earth elements are chemically very active. They can react easily with the alloying elements and the Al matrix in aluminum alloys to form stable rare earth compounds which, with their high hardness values and melting points, tend to improve the alloy properties, particularly at high working temperature conditions. [61]

2.7.1 Effect of Mischmetal Addition on the Microstructure

The use of rare earth (RE) metals in cast aluminum alloys may be classified into three categories: (a) RE as a major constituent in alloys with high strength at elevated temperature; (b) small addition of RE to the alloys as an alloying element to improve technological and mechanical properties; (c) RE as a modifier for Al-Si alloys.[62] Owing to their very limited solubility in Al, only a very small fraction of the Ce and La contents of mischmetal (MM) dissolve in solution. [30, 63, 64]

Remarkable work has been carried out to explore the modification effect of RE metals in Al-Si alloys. [11, 62, 63, 64] Rare earth addition was found to alter the morphology of the eutectic silicon. It is reported that La is the most powerful among the RE elements, and that a small addition of mischmetal (0.03-0.09% RE content) can be enough to modify the eutectic Si provided a critical cooling rate is reached. The RE-treated alloy has a low fading effect compared to Na-modified alloys, as it maintains the modified structure much longer than the Na-treated alloys.

Sharan [13] reported that modification using rare earth metals can easily be explained by using the hypothesis of the critical growth temperature stated by Kim and Heine [10] i.e., the modifying element should have a chemical affinity to combine with the silicon phase at a temperature below the normal eutectic temperature in order to form compounds. However, this modifying element should display some tendency for compound formation with (and have low solubility in) the α-aluminum matrix (solvent phase). Lanthanum is reported to meet most of these requirements, but cerium (Ce) and neodymium (Nd) satisfy them only partially, as they have a limited solubility in aluminum and react with the

aluminum as well. Therefore, the influence of Ce and Nd as modifiers is less significant compared with that of La. [13] These rare earth metals have been reported to form many fine intermetallic compounds with aluminum and silicon (e.g., Al_4Ce, Al_2Ce, SiCe, $SiCe_2$, $SiCe_4$, etc.).[11]

Sharan and his co-workers extensively studied the modification effect of rare earth additions in hypoeutectic and hypereutectic Al-Si alloys.[12, 13, 14] They observed that the addition of rare earth metals in amounts of up to 0.2% to hypoeutectic Al-Si alloys led to the refinement of the primary α-aluminum and the eutectic structure.

The function of mischmetal was investigated primarily as a modifier, and secondly as a beneficial alloying addition. The structure was modified appreciably in both sand and metal mold castings by the addition of mischmetal in the range of 0.5 to 1% and led to the improvement of the tensile strength and elongation.[15, 16] In the case of hypereutectic Al-Si alloys,[14, 15, 16] mischmetal addition in the range of 1.0 to 1.5% refined both the primary and the eutectic silicon.

The modification effect by mischmetal can be easily explained. Ce, La and Nd react with Al and Si to form fine a dispersion of coherent intermediate phases like $CeAl_4$, $LaAl_3$, etc., providing heterogeneous nuclei during solidification for the refinement of the primary silicon.[14]

In this context, Agrawal and Menghani [65] have observed that, while several studies on rare earth additions to Al-Si alloys have been carried out, [14] these were carried out on non-heat treatable hypereutectic alloys.

An investigation by Sharan and coauthors reported rare earth additions to improve the machinability and mechanical properties and was found to act as a pronounced grain refiner and modifier for hypereutectic Al-Si alloys. However the effect of rare earth additions may not be restricted to modification only, as they need to be added in quantities much larger (0.5% to 1.5%) than conventional modifying agents such as Na or Sr. Rare earth additions also act as minor alloying elements and act as scavengers for interstitial impurities such as oxygen, nitrogen and carbon, contributing to improvement in the alloy strength and toughness. [65]

In Al-Si alloys, rare earths (RE) act in the following ways:

a) A 2% mischmetal addition increases the eutectic undercooling by about 25 $^{\circ}$K thus modifying the eutectic Si and the shapes of precipitates.

b) They form several fine and hard intermetallic compounds that suppress the growth of the eutectic silicon.[66]

c) They decrease the adverse effect of hydrogen in aluminum and its alloys by increasing its solid solubility and forming stable hydrides.

Ye *et al.* [11] have investigated the role of rare earth metals in the eutectic modification of cast Al-Si alloys. They reported that a reliable and persistent eutectic modification effect can be obtained with rare earth additions. The silicon phase modified by rare earths exhibits the same changes in crystallographic structure as achieved through modification with sodium. In both cases, the Si phase changes from growth in the < 211 > directions to growth in the < 100 > directions, where it develops a refined, rounded, and interconnected morphology. The eutectic modification achieved through the use of rare

earths is extremely resistant to fading and may persist up to several hours, as shown in Figure 2.11.

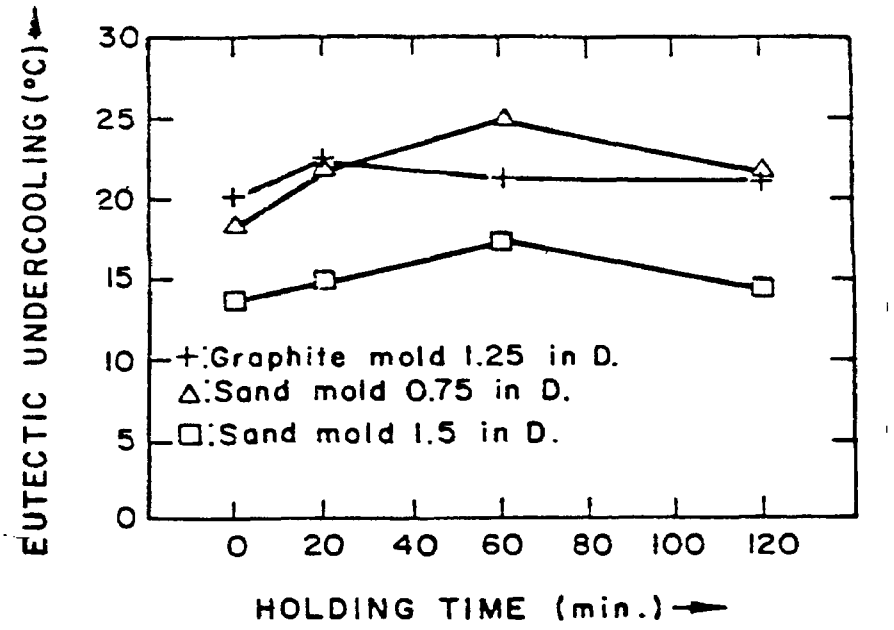

Figure 2.11 Fading effect of 0.2% mischmetal–modified 356 aluminum alloy as indicated by eutectic undercooling. [11]

In their study of the primary silicon in hypereutectic Al-Si casting alloys, Weiss and Loper [67] found that the refining of primary silicon by cerium addition was not significant compared to that achieved using phosphorus, however the influence of Ce on the modification of the eutectic silicon was moderately pronounced. In their investigation of the influence of rare earth addition in hypereutectic Al-20%Si alloy, Kowata *et al.* [68] concluded that the primary Si crystals were modified by rare earth metals.

Chang *et al.*[69] investigated the refinement of the cast microstructure of hypereutectic Al-Si alloys by the addition of rare earth metals (added as mischmetal). They

reported that a simultaneous refinement of both primary silicon and eutectic silicon was obtained, where the morphology of the eutectic Si was altered from coarse acicular to fine fibrous form, and that of the primary silicon crystals from coarse star shape to polyhedral shape. Figure 2.12 shows how this refining effect increased with increasing addition of rare earth metals (1, 2 and 3 wt %) and cooling rate (33°C/s through 130°C/s). They proposed a different mechanism to explain the change in the silicon morphology in that rare earth-containing intermetallic compounds were not believed to act as nucleating agents for primary silicon and did not increase the twin density in eutectic silicon.

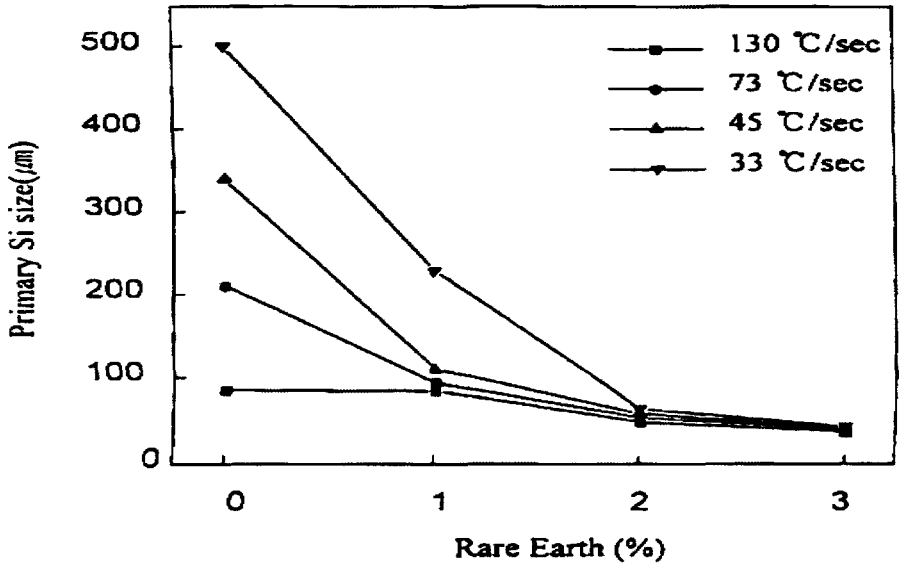

Figure 2.12 Relation between primary silicon size and amount of RE addition at different cooling rates. [69]

The refinement of silicon with rare earth additions may be ascribed to the lowering of the nucleation temperature of the silicon phase, with depressions of 2-7°C as shown in

Figure 2.13, and limited growth due to the decrease in diffusion rate with the decrease in growth temperature.

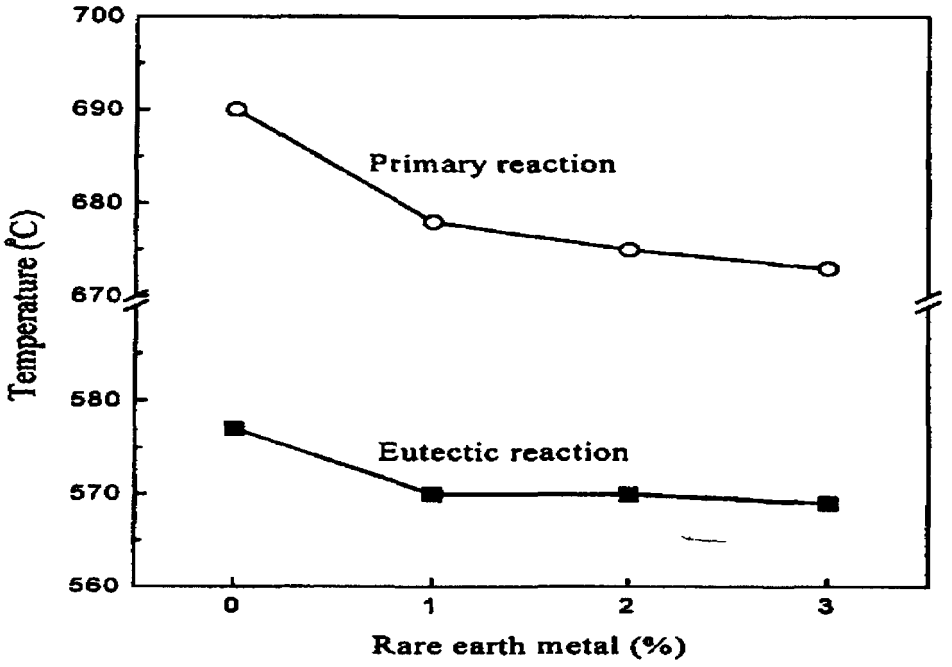

Figure 2.13 Change of primary reaction and eutectic reaction temperature in Al-12%Si alloy with the addition of rare earth metal. [69]

Ye *et al.*,[11] however, found that high levels of rare earth metals were detected at the interface between the Si and the aluminum in the eutectic, supporting the adsorption of rare earth on the growth front faces (111) and hence, poisoning the growth of the eutectic Si, leading to the change in its morphology. However, this mechanism has not been proven and cannot explain the weaker modification action of rare earth metals compared to other modifiers.

A study of the influence of mischmetal additions to Al-7Si-0.3Mg (LM25) alloy was made by Ravi and his co-workers.[63] They found that the dendrite arm spacing (DAS) decreased with the addition of mischmetal up to 1 wt% because of the increase in the eutectic undercooling, whereas beyond 1 wt% mischmetal addition, the DAS remained the same as in the base alloy.

In their investigation on the effects of rare earth addition on the eutectic modification of 356 alloy, Ye *et al.* [11] found that with up to 2% mischmetal addition some primary dendrite refinement (reduction in secondary dendrite arm spacing) became apparent as shown in Figure 2.14. Eutectic undercoolings of 15°C at 1 wt% mischmetal addition and 25°C at 2 wt% addition were also observed, as shown in Figure 2.15. As can be seen, this effect is highly dependent on the amount of rare earth addition and may be attributed to the alloying effect of rare earth metals. As the interdendritic regions restrict the growth of the eutectic silicon, the reduction in the dendrite arm spacing would slightly alter the eutectic silicon morphology. However, this would not be considered as a modification effect. [11]

Chen *et al.* [64] investigated the influence of cerium and mischmetal addition on the microstructure, hardness and brightness of Al-Mg-Si alloys. They reported that the microstructure was clearly modified by mischmetal addition and that the dendrite arm spacing decreased with increasing mischmetal concentration (up to 4 wt %). Due to the low solid solubility of Ce, and no measurable solubility of La in Al, a greater part of Ce and La would concentrate on the interface during solidification, providing constitutional undercooling, resulting in the refinement of the dendrite arm spacing.

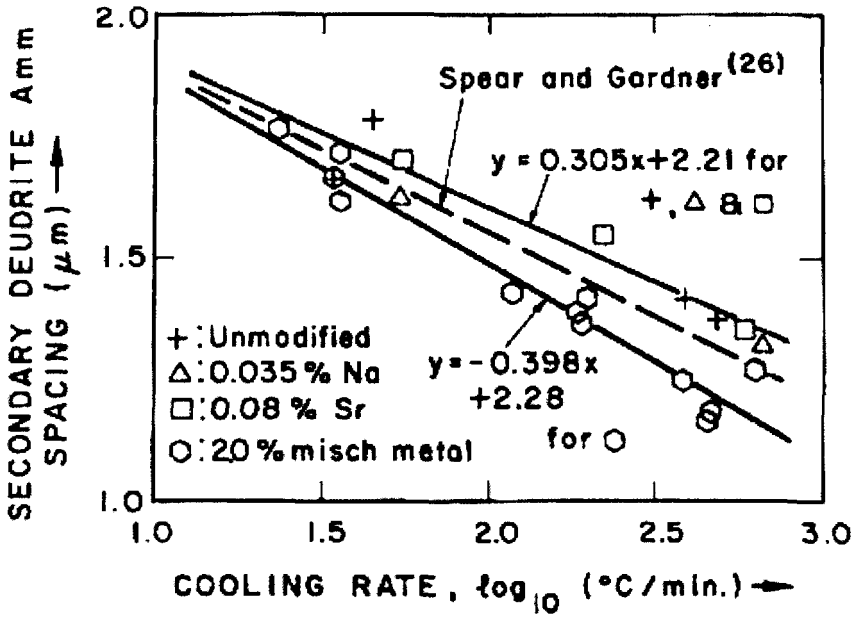

Figure 2.14 Effect of solidification cooling rate on the secondary dendrite arm spacing of 356 aluminum alloy. [11]

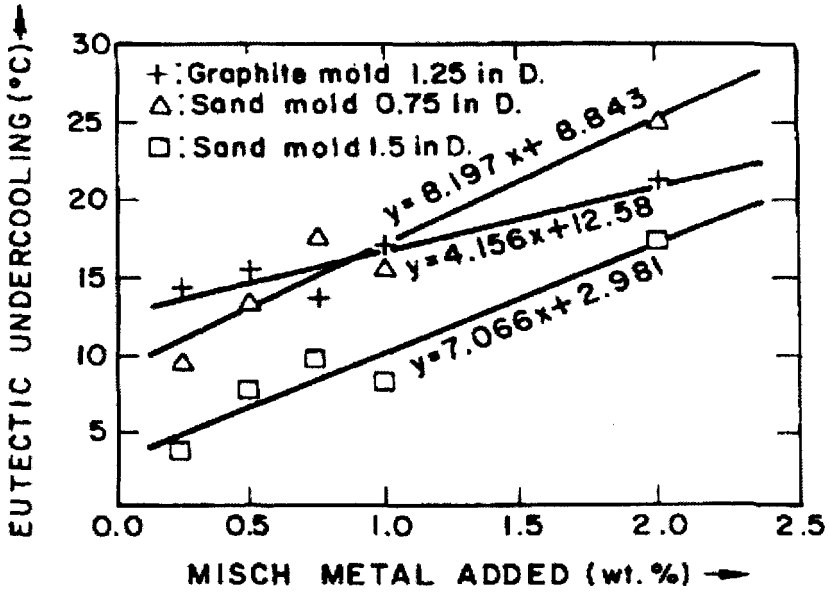

Figure 2.15 Influence of mischmetal addition on the amount of eutectic undercooling in 356 aluminum alloy. [11]

It was reported that the addition of 1 pct MM to Al-7%Si-0.3%Mg alloy (LM25 alloy) containing iron levels of 0.2 to 0.6 pct resulted in the grain refinement and partial modification of the eutectic silicon. With the addition of 1% MM to the same alloy containing 0.6% Fe, Ce, La, and Nd present in the Al matrix combined with Fe and Si to form fine and fibrous intermetallic compounds, which reduced the effective amount of Fe available for the formation of brittle β-Al_5FeSi plates and π-Al_8FeMg_3Si6 phase, as shown in Figure 2.16, therefore reducing the size and volume fraction of these phases, and resulting in improving the strength and ductility of the alloy. [2]

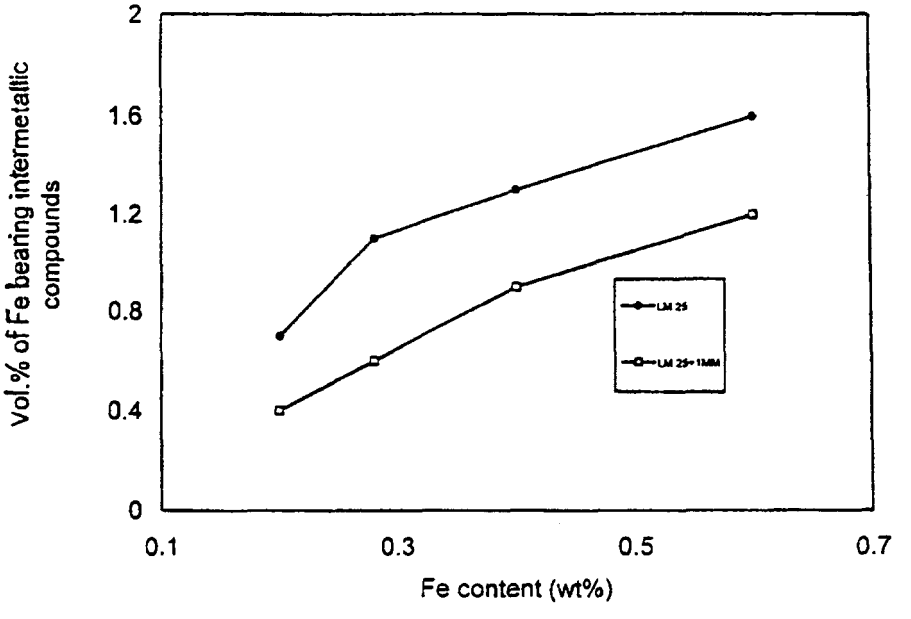

Figure 2.16 Effect of Fe content on the volume percent of Fe-bearing intermetallic compounds in LM25 and LM25+1 pct MM alloys. [2]

2.7.2 Effect of Mischmetal Addition on the Mechanical Properties

Rare earth metals in Al alloys interact preferentially with other elements to form intermetallic compounds which concentrate in the grain boundary regions and result in hindering grain boundary movement by slip. As a result, the strength of the alloy is improved at elevated temperature.

In the work of Sharan and Prasad [16] on the influence of rare earth fluorides in hypoeutectic Al-7.5%Si alloy, the tensile strength was reported to exhibit an increase by 36% and the percentage elongation by about 2 to 3 times its original value due to the addition of up to 0.2% rare earth fluorides to the alloy.

Agrawal and Menghani [65] studied the effect of rare earth addition on the age hardening behavior of A356 alloy, used as standard material for alloy wheels of quality cars. It was found that RE additions (0.25%, 0.5%, and 1%) affected the aging behavior of A356 alloy (aged at 160°C for 0h, 8h and 10h); it appeared that the rare earth addition modified the original precipitation sequence (with only Mg_2Si precipitation). It was also observed that with aging heat treatment not only the tensile strength of the alloy containing mischmetal increased, but the percentage elongation values obtained were also higher, compared to alloys free of mischmetal. In the case of alloys with 0.25% mischmetal addition, the highest combination of UTS (281.3MPa), hardness (80 BHN) and percent elongation (10%) was achieved after 8 h of aging. This improvement in mechanical properties, in particular, the UTS and elongation, may be ascribed to the refinement of the microstructure in terms of modification of the eutectic silicon, and partly to the hardening

effect obtained from the precipitation of fine, stable and hard precipitates during the aging treatment.

It has been reported by Ravi *et al.* [63] that the addition of mischmetal up to 1 wt% results in an increase in the tensile properties, and hardness by up to 20% in Al-7Si-0.3Mg alloy. This is attributed to the refinement of the microstructure and the formation of intermetallic compounds between Al and Si, Mg, Fe, Ce, and La. Mischmetal addition above 1 % was observed to decrease the tensile properties, but increased the hardness, as illustrated in Figure 2.17. Owing to the formation of Ce- and La-containing hard and stable intermetallic compounds in the aluminum matrix, a certain amount of Mg was consumed from the aluminum matrix in order to form these compounds. This reduced the amount of the precipitation hardening Mg_2Si phase, thus reducing the strength of the alloy. [63]

Ravi *et al.*[2] also investigated the behavior of Al-7Si-0.3Mg alloy containing different levels of Fe and mischmetal at elevated temperatures. They reported that the strength of alloys containing 0.2 % Fe (LM25 alloys) decreased and reached the same value as that of alloys containing 0.6% Fe at 200°C, as shown in Figure 2.18. The alloys containing 1% mischmetal exhibited higher levels of strength and percent elongation and become more stable beyond 150°C. The alloys with 1 % mischmetal and 0.6% Fe display a better compromise between the UTS and percent elongation at temperatures above 150°C. This is evident from comparing the UTS and percent elongation at 150°C (270 MPa and 3.8 %) with that at 200°C (260 MPa and 4.8%). This may be due to the formation of fine a dispersion of hard and stable mischmetal-containing intermetallic compounds with the

other alloying elements, which provide powerful obstacles to the movement of dislocations at high temperature, and prevent the coarsening of the precipitation hardening Mg_2Si phase.

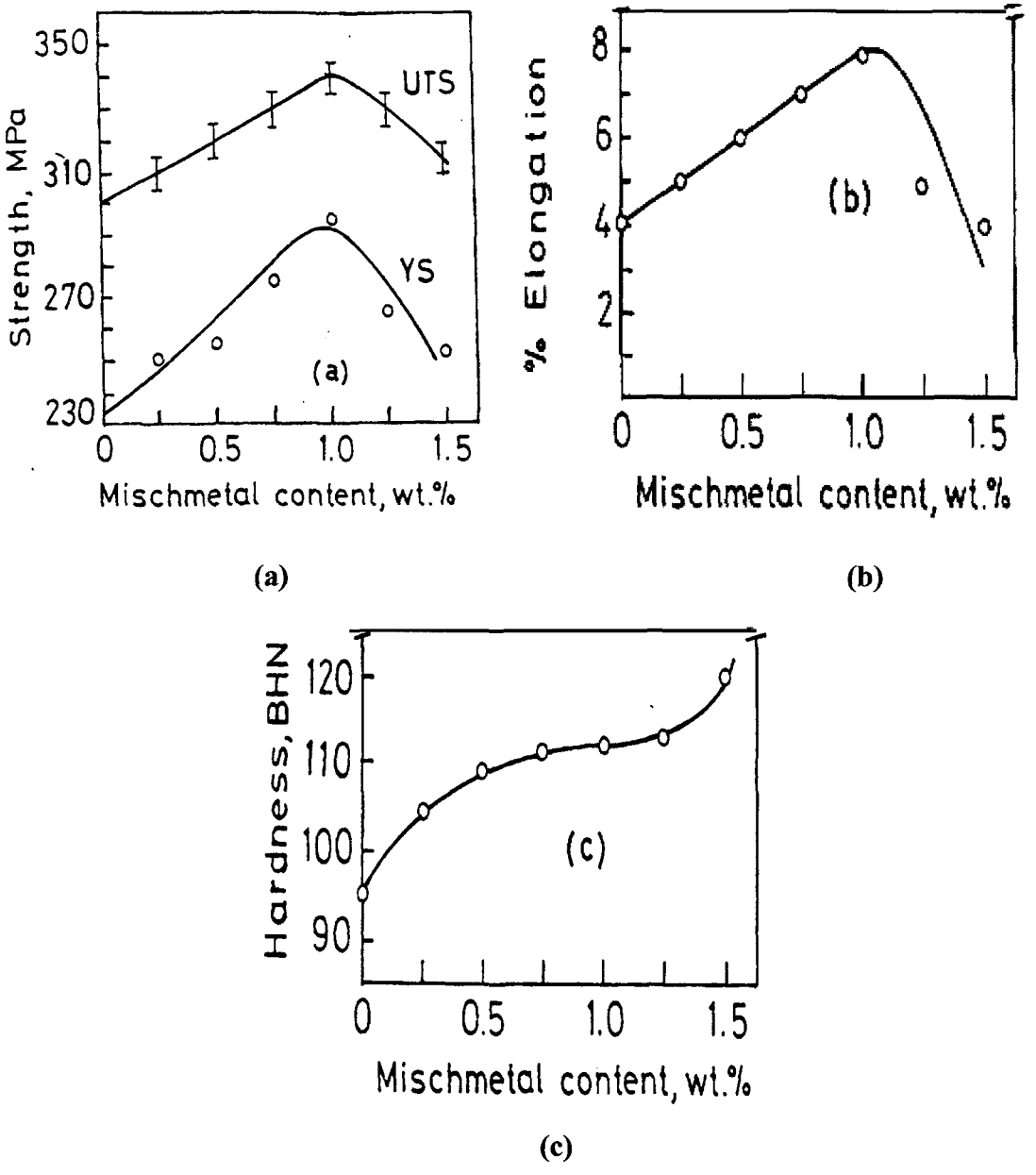

Figure 2.17 Effect of MM additions on (a) strength, (b) elongation, and (c) hardness of LM25 alloy. [63]

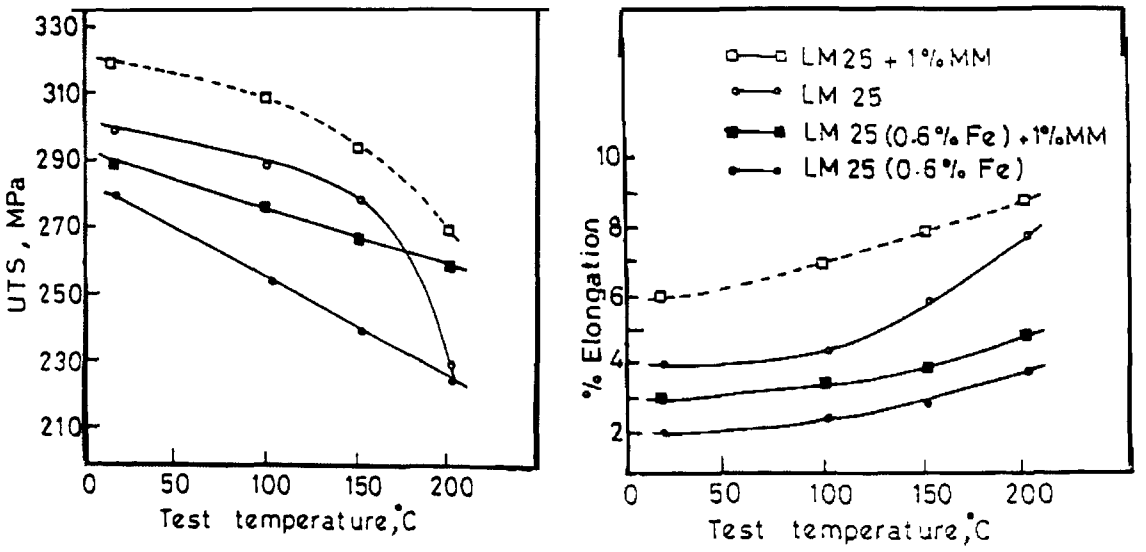

Figure 2.18 Tensile properties of Al-7Si-0.3Mg alloys (T6 condition) containing different amounts of Fe and mischmetal at elevated temperatures.[2]

Recent studies on rare earth metal additions to aluminum alloys were also carried out by Nie *et al.* [61] They reported that the addition of rare earth metals leads to the improvement in the hardness of aluminum alloys because the rare earth metals can react easily with Al to form high melting point and infusible dispersed intermetallic compounds, which leads to grain refining and the strengthening of the grain boundary regions. The change in the microstructure (such as grain refining, improved grain orientation and proper secondary phase distribution) results in an appreciable enhancement in the alloy properties.

CHAPTER 3

EXPERIMENTAL PROCEDURES

CHAPTER 3

EXPERIMENTAL PROCEDURES

3.1 ALLOYS, ADDITIVES AND MELTING PROCEDURES

Alloys A319.1, A356.2 and A413.1 were used in the present study. Their chemical compositions are shown are shown in Table 3.1

Table 3.1 Chemical compositions of commercial grade 319, 356 and 413 Al-Si casting alloys used in the present work

Alloy	Element (wt %)								
	Si	**Fe**	**Cu**	**Mg**	**Mn**	**Ti**	**Ni**	**Zn**	**Al**
A319.1	5.57	0.151	**3.45**	0.02	0.001	0.138	0.004	0.008	bal.
A356.2	6.99	0.139	0.071	**0.352**	<.0005	0.148	.0061	0.006	bal.
A413.1	12.36	**0.705**	0.276	0.074	**0.260**	0.127	.0877	0.11	bal.

The alloys were received in the form of 12.5 kg ingots. These ingots were cut into smaller pieces, cleaned, dried and melted in a silicon carbide crucible of 30-kg capacity, using an electrical resistance furnace. The melting temperature was held at 730 ± 5°C. The molten metal was degassed using pure dry argon injected into the molten metal (30 ft^3/h) by means of a graphite rotary degassing impeller. The degassing time/speed was kept constant at 30 min/150 rpm. Such a degassing process served two purposes: (a) to minimize

the hydrogen level of the melt, and (b) to eliminate inclusions and oxides via flotation. To these base alloys, mischmetal additions were made using Al-20% mischmetal master alloy with an average chemical composition as shown in Table 3.2. The additions were made to achieve mischmetal levels of 0%, 2%, 4%, and 6 wt%, in order to study the effect of the mischmetal additions on the morphology and size of the eutectic silicon particles, on the morphology of the intermetallic phases formed, as well as the hardness behavior. After degassing (hydrogen level ~0.1 mL/100g), all melts were grain refined using Al-5 wt% Ti-1 wt% B master alloy. The hydrogen level was checked using AlScan apparatus.

Four levels of mischmetal were added to both non-modified and Sr-modified alloys, to investigate the effect of mischmetal as a modifier as well as the combined modification effect of Sr and MM by comparing the microstructures observed in the two cases (non-modified vs. Sr-modified alloys). The Sr-modified alloys were obtained through the addition of an appropriate amount of Sr to the as-received (non-modified) alloys. The Sr was added in the form of rods of Al-10%Sr master alloy (200-250 ppm Sr) to the degassed melt prior to casting using a graphite bell immersed into the melt, following which degassing was carried out for 15 min before pouring. A sampling for chemical analysis was also made.

Table 3.2 Average chemical composition of the Al-20% mischmetal master alloy used in the present work

Element	Ce	La	Nd	Pr	Others	Al
wt%	10	7	1	1	1	bal.

3.2 CASTING PROCEDURES

Castings were carried out using a steel permanent mold. Figure 3.1(a) shows a schematic diagram of the mold and its dimensions, while Figure 3.1(b) shows an actual picture of the mold and the casting obtained from it.

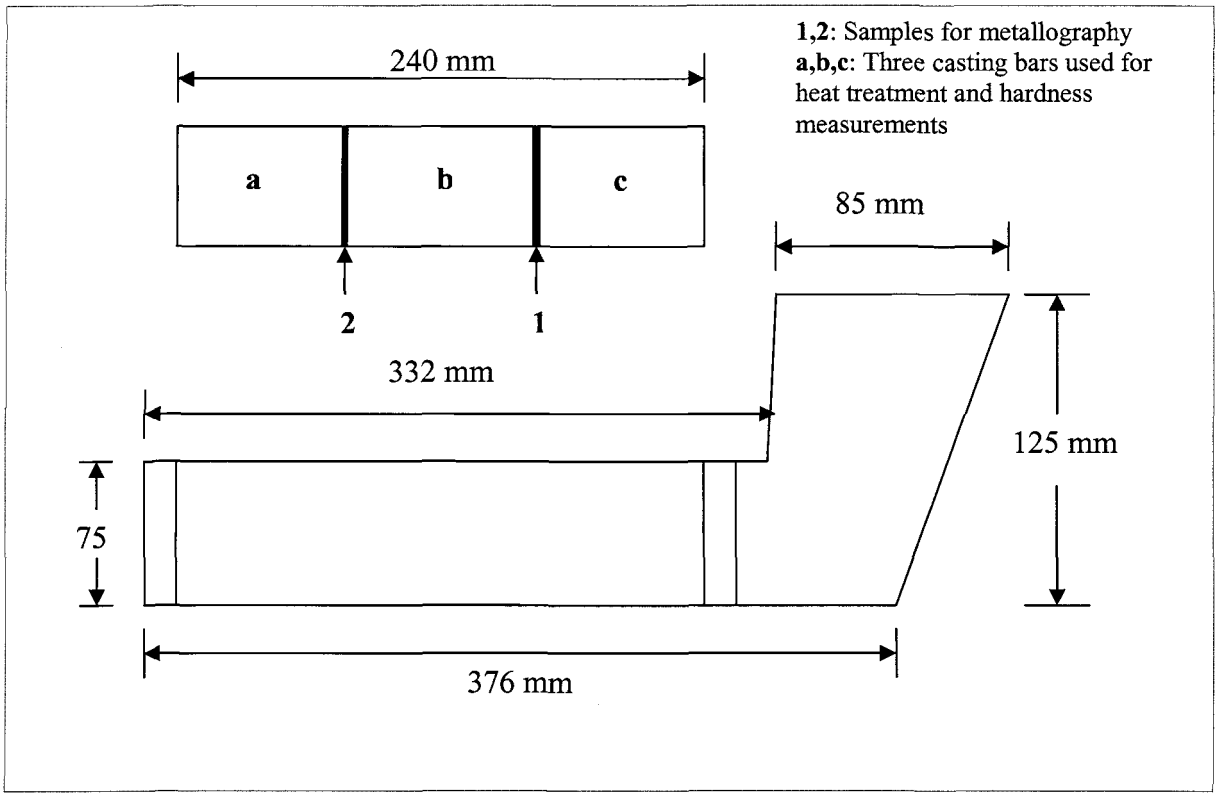

(a)

Figure 3.1 (a) Schematic diagram of the permanent mold used for casting.

contuined.....

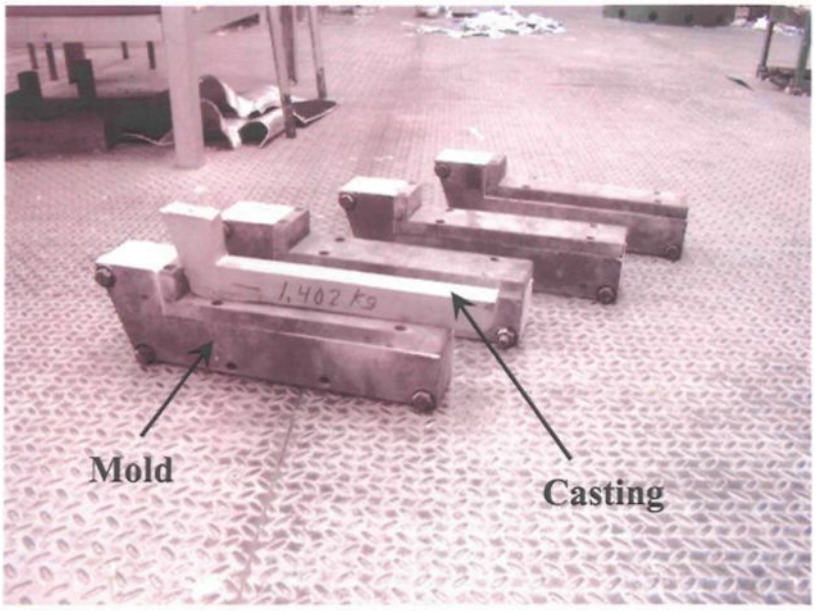

(b)

Figure 3.1 (a) Schematic diagram of the permanent mold used for casting, (b) actual mold and casting obtained from it

In order to obtain high and low cooling rates, the castings were carried out as follows. In the first case, the mold was preheated at 450°C, which was cooled after pouring in atmospheric air to provide a high cooling rate (low DAS), and (ii) a steel permanent mold preheated at 750°C, which was cooled after pouring to 450°C inside the furnace, to provide a low cooling rate (high DAS).

Table 3.3 and Table 3.4 show the chemical compositions of the various alloys that were prepared and their respective codes, cast at the tow cooling rates. With respect to the alloy codes, prefix A represents the A319.1 alloy, prefix B the A356.2 alloy, and prefix C the A413.1 alloy. The letter S represents Sr-modified alloys, while the numbers 0, 2, 4 and

6 correspond to mischmetal addition levels of 0 wt%, 2 wt%, 4 wt%, and 6 wt%, respectively.

Table 3.3 Chemical compositions of the alloys used in the present work (castings obtained under high cooling rate conditions)

Alloy Code	Element (wt %)									
	Si	**Fe**	**Cu**	**Mg**	**Ti**	**Sr**	**Ce**	**La**	**Nd**	**Al**
A0	5.58	.187	**3.661**	.007	.1221	.0001	<.0001	.0096	<.0001	90.4
A2	6.04	.2056	3.921	.0123	.1229	.0029	**.1744**	**.136**	**.0229**	89.2
A4	5.53	.1754	3.621	.0068	.1121	.0003	**.3618**	**.2394**	**.0502**	89.8
A6	6.11	.2307	4.035	.0149	.1248	.0007	**.613**	**.3825**	**.0844**	88.2
AS0	5.66	.2320	3.405	.0114	.1308	**.0137**	<.0001	.0133	<.0001	90.4
AS2	5.59	.2426	3.551	.0120	.1296	**.0138**	.1618	.1237	.0264	89.7
AS4	6.17	.2725	3.661	.0142	.128	**.0129**	.3655	.2447	.0609	88.9
AS6	5.5	.1272	3.396	.0091	.1159	**.0111**	.4815	.3104	.0764	89.7
B0	7.19	.159	.0796	**.377**	.1495	.0003	<.0001	.0126	<.0001	91.9
B2	6.65	.1204	.1097	.3682	.1124	.0004	**.1439**	**.1240**	**.0195**	92.2
B4	6.34	.117	.1463	.3742	.133	.0004	**.3486**	**.2327**	**.0475**	92.1
B6	6.25	.1084	.1776	.3673	.1361	.0005	**.523**	**.3331**	**.073**	91.8
BS0	6.33	.0795	.0598	.3649	.1367	**.0156**	<.0001	.0131	<.0001	93
BS2	6.38	.0941	.1084	.3706	.1373	**.0151**	.1584	.1231	.0252	92.5
BS4	6.51	.1409	.1483	.3682	.1340	**.015**	.3448	.2338	.0552	91.9
BS6	6.08	.0902	.1725	.3692	.1331	**.014**	.4754	.3086	.0795	92.1
C0	13.03	**.735**	**.3119**	.0953	.1438	.0004	<.0001	.0141	.0029	85
C2	12.03	.737	.3263	.0432	.0725	.0002	**.1639**	**.1242**	**.0222**	85.9
C4	12.15	.750	.3686	.0482	.07	.0005	**.3491**	**.2318**	**.0505**	85.3
C6	12.13	.788	.4102	.048	.077	.0007	**.545**	**.3423**	**.0842**	84.9
CS0	11.96	.678	.2850	.043	.077	.0180	<.0001	.013	<.0001	86.4
CS2	12.33	.705	.3393	.0493	.0875	.0202	.1616	.1241	.0293	85.5
CS4	11.65	.701	.3356	.0426	.0713	.0153	.3117	.2103	.0501	86
CS6	12.27	.819	.4528	.0552	.0743	.0149	.527	.3337	.0869	84.7

To distinguish the two cooling rate conditions used, the prefix H has been used in Table 3.4 for all alloys to indicate that these alloy castings were cooled at a low cooling rate, providing a high (H) dendrite arm spacing (DAS).

Table 3.4 Chemical composition of the alloys used in the present work (castings obtained under low cooling rate conditions)

Alloy Code	Element (wt %)									
	Si	**Fe**	**Cu**	**Mg**	**Ti**	**Sr**	**Ce**	**La**	**Nd**	**Al**
HA0	5.56	.1161	3.325	.0343	.154	.0000	<.0001	.0096	<.0001	90.7
HA2	5.55	.1174	3.277	.0349	.1477	.0001	.1463	.117	.0137	90.5
HA4	5.66	.1141	3.298	.0434	.1602	.0005	.3248	.2253	.0444	90
HA6	5.38	.1150	3.165	.0302	.1379	.0003	.4715	.3078	.0679	90.1
HAS0	5.9	.1216	3.266	.0362	.1513	.0218	<.0001	.0137	<.0001	90.4
HAS2	5.61	.1177	3.225	.0329	.1458	.0192	.1557	.1222	.0167	90.5
HAS4	5.42	.1238	3.044	.0353	.1597	.0260	.3084	.2146	.0410	90.5
HAS6	5.77	.1324	3.336	.0357	.1632	.0158	.517	.3350	.0755	89.4
HB0	6.79	.1207	.0628	.3272	.1482	<.000	<.0001	.0126	<.0001	92.5
HB2	6.49	.1394	.0728	.308	.1334	.0004	.1733	.1356	.0182	92.4
HB4	6.85	.1497	.1138	.3125	.1269	.0006	.3707	.2497	.0496	91.6
HB6	6.69	.1523	.1444	.3168	.1278	.001	.526	.3429	.0756	91.4
HBS0	6.19	.105	.1221	.309	.1376	.0201	<.0001	.0184	<.0001	93
HBS2	6.19	.1062	.1556	.3097	.1312	.0189	.1753	.1335	.0195	92.7
HBS4	6.06	.1084	.1845	.3042	.1304	.0149	.3429	.2325	.0462	92.4
HBS6	5.87	.1063	.2027	.3012	.1283	.0143	.4928	.3214	.0705	92.3
HC0	11.69	.675	.2410	.053	.1101	<.000	<.0001	.0131	<.0001	86.7
HC2	11.5	.708	.2715	.0552	.0875	.0001	.1505	.1167	.0177	86.5
HC4	11.8	.709	.3095	.073	.0787	.0004	.322	.2202	.0459	85.8
HC6	11.37	.731	.3224	.041	.0692	.0003	.4655	.3017	.0659	86.0
HCS0	11.68	.671	.2406	.0464	.0731	.0182	<.0001	.0176	<.0001	86.7
HCS2	11.52	.668	.2584	.0512	.0815	.0199	.1753	.1388	.0234	86.5
HCS4	10.91	.684	.2845	.0442	.0713	.0114	.3311	.2239	.0459	86.8
HCS6	11.32	.703	.3259	.0455	.0688	.0100	.518	.3330	.0737	86.0

3.3 METALLOGRAPHY

For microstructural examination purposes, samples were prepared from the different castings and examined using various metallographic techniques.

3.3.1 Sample Preparation

Samples for metallographic examination were sectioned from each casting, as shown in Figure 3.1(a). The sectioned pieces were mounted in bakelite, then polished to a

fine finish (1 μm diamond paste) using a Buehler Variable Speed Grinder-Polisher. Details of the grinding and polishing stages that were employed are shown in Table 3.5.

Table 3.5 Grinding and polishing procedure used for metallography samples

Stage	Abrasive	Speed (rpm)	Time (min)	Lubricant	Force (lb)
1	120	120	Until flat	Running water	30
2	240	120	1	Running water	30
3	320	120	1	Running water	30
4	400	120	1	Running water	30
5	600	120	1	Running water	30
6	800	120	1	Running water	30
7	Diamond (6 μm)	120	6	Metadi fluid	30
8	Diamond (1 μm)	120	6	Metadi fluid	30
9	Buehler Matsermet	90	4	Water droplets	30

After every stage of polishing, the samples were washed using a soap-alcohol mixture, then dried by forced air to avoid carry over of any contamination to the next step. The polished samples were then used for microstructural examination.

3.3.2 Microstructure Examination Using Optical Microscopy and Image Analysis

Quantitative measurements of the dendrite arm spacing (DAS) and the eutectic Si particle characteristics (area, length, roundness, aspect ratio and density) was made for as-cast and solution heat-treated samples obtained at the two cooling rates, using a Leco 2001 image analyzer in conjunction with an Olympus BH2-UMA optical microscope. The optical microscope and image analysis set-up is shown in Figure 3.2.

Figure 3.2 Optical microscope-image analysis system used for microstructural analysis.

For each sample, fifty fields were examined over the entire surface of the sample, by traversing the sample in a regular, systematic manner and the Si particle characteristics noted for each field. Measurements were carried out at magnifications of 500X and 1000X for the non-modified alloys and the Sr-modified alloy samples, respectively. From these, the following parameters were determined:

- Average Si particle area (μm^2) and standard deviation;
- Average Si particle length (μm) and standard deviation;
- Roundness ratio of Si particles (%);
- Aspect ratio; ratio of maximum to minimum dimensions of the Si particle ; and
- Density of the Si particles in counts per unit area (number of particles/mm^2).

With respect to the average and standard deviation values, it should be noted that, owing to the wide range of Si particle sizes of the Si particle observed - as will be seen from all the microstructures presented in chapter 4, it is expected that the standard deviation will be of the order of, or higher than, the average value. The particle size distribution plotted by the image analyzer system in the execution of "Feature" measurements (of individual Si particles) provides a range of particle sizes, and the corresponding counts, as shown in Figure 3.3. It is found that the maximum particle count generally corresponds to the particle size range which includes or lies close to the average value calculated by the system. In other words, the average values *do* reflect the overall modification effect obtained from one casting type/condition to another.

For the dendrite arm spacing measurements, at least 30 measurements were taken per sample, over a number of dendrites for each measurement. From these, the average dendrite arm spacing or DAS value was calculated. In general, the castings obtained at low cooling rate exhibited an average DAS of ~120 μm, while those obtained at the high cooling rate exhibited a finer average DAS value of ~ 40 μm.

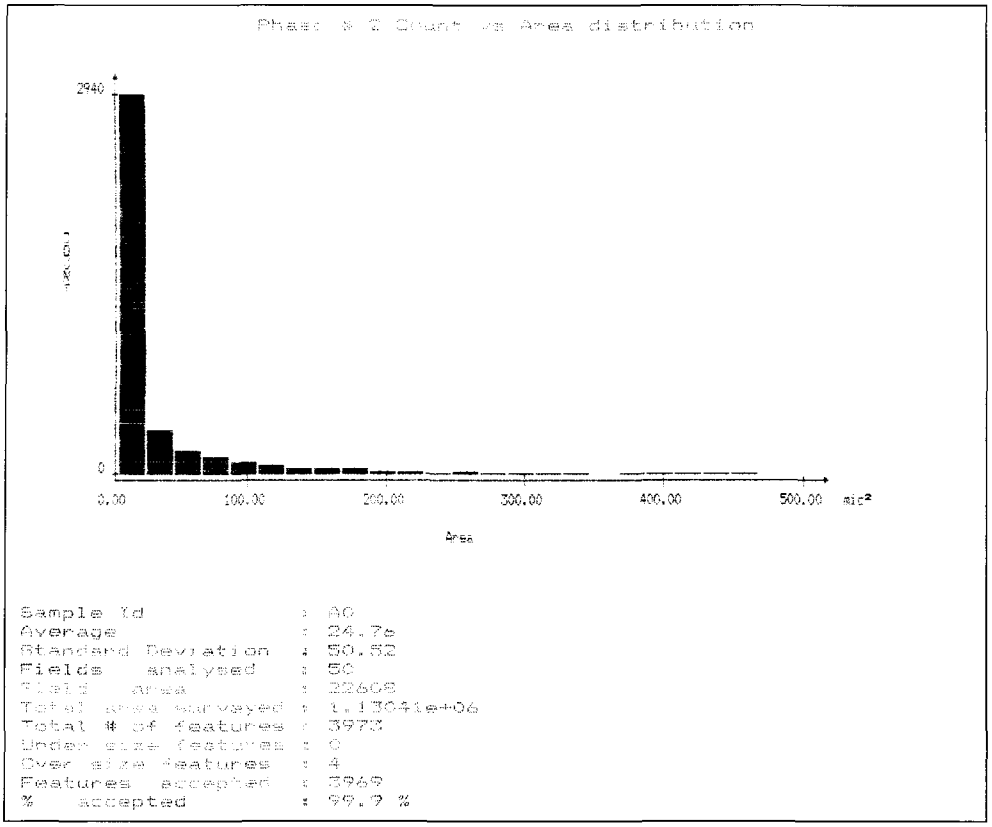

Figure3.3 Example of an image analyzer prints out shows the number of counted Si particles versus the area distribution and the corresponding standard deviation in A319.1 alloy.

3.3.3 Phase Identification Using SEM and EPMA Analysis

Measurements of the surface fraction of intermetallics and their identification were carried out on the as-cast and heat-treated samples obtained at the two cooling rate conditions, employing Electron Probe Microanalysis (EPMA) and scanning electron microscopy (SEM), coupled with energy dispersive X-ray (EDX) and wavelength dispersion spectroscopic (WDS) analyses. The WDS analysis provided the means to determine the chemical compositions and formule of the mischmetal-containing intermetallics.

Figure 3.4 shows the Jeol WD/ED Combined Microanalyzer (located at the McGill Microprobe Laboratory) that was employed for this purpose (model JXA-8900R, operating at 20 kV and 30 nA, with an electron beam size of ~ 1μm).

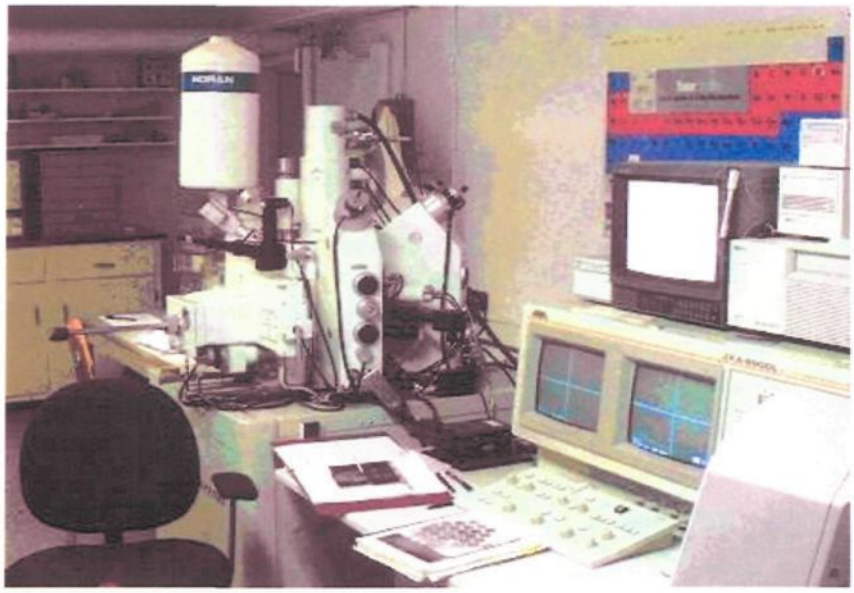

Figure 3.4 Electron probe microanalyzer (EPMA) used for identification and quantification of intermetallics.

3.4 HEAT TREATMENT PROCEDURES

Castings obtained from the various alloys were machined and milled, then cut into three pieces (rectangular bars) for different heat treatments. The bars were heat treated using the T6 regime. A Blue M forced air furnace (model SPX), was used for the heat treatment, as shown in Figure 3., where the temperature could be controlled to within ± 1°C. The T6 heat treatment details are summarized below.

- Solution heat treatment of the permanent mold test bars of A319.1 and A413.1 alloys at 495°C±1°C for 8 h, and those of A356.2 alloy at 540°C±1°C for 8 h.

- Quenching in warm water (60°C).
- Natural aging at room temperature of A356.2 alloy test bars for 24 h.
- Artificial aging of all three alloys for 5 h at aging temperatures of 155°C, 180°C, 200°C, 220°C and 240°C.

Figure 3.5 Blue M-forced air furnace used for heat treatment.

The quench interval was less than a few seconds. Heat-treated samples were analyzed to assess the microstructural changes occurring during heat treatment, in particular, those relating to Si particle size and morphology and the intermetallic phases.

3.5 HARDNESS MEASUREMENTS

Hardness testing, recognized as a semi-destructive method, is an attractive way of determining properties easily and in a short period of time. Hardness measurements can provide a good indication of the strength and ductility of alloys; since strength is related to

the number, type and spacing of second phase precipitates, hardness measurements can thus be used to monitor the precipitation hardening process.

In the present work, extensive Brinell hardness measurements were conducted to determine the precipitation characteristics in each alloy. The hardness test specimens were lightly polished using SiC paper. A Brinell hardness tester with a 10 mm steel ball indentor and a load of 500 Kgf (applied for a dwell time of 30 sec) was used to determine the hardness measurements in the as-cast and aged conditions. Figure 3. shows the Brinell hardness tester that was used.

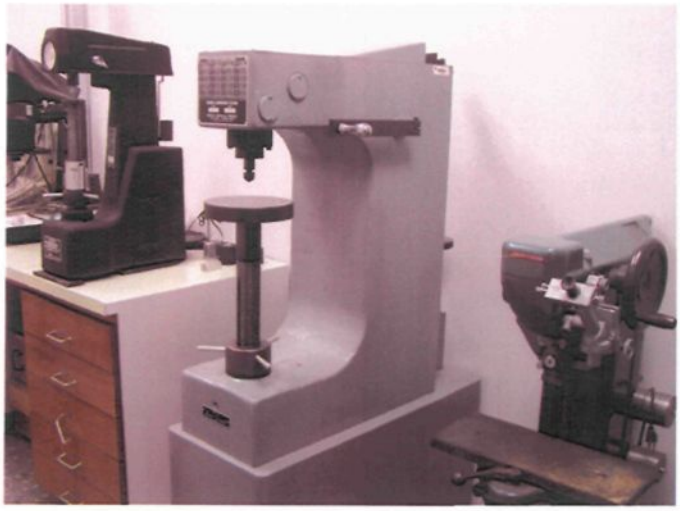

Figure 3.6 The Brinell hardness tester.

Each Brinell hardness value (BHN) obtained was taken as the average of at least eight readings taken from two adjacent faces of each tested specimen bar. The large indentation of the steel ball of the Brinell hardness tester ensured that the whole matrix (i.e., containing the α-aluminum phase, eutectic Si particles and intermetallic phases) was covered in each measurement.

CHAPTER 4

SI PARTICLE CHARACTERIZATION

CHAPTER 4

SI PARTICLE CHARACTERIZATION

4.1 INTRODUCTION

The microstructural features exhibited by an alloy after solidification are determined by the alloy chemistry and solidification conditions. The microstructural features, excluding casting defects (i.e., porosity and inclusions) that most strongly control the mechanical properties are the fineness of the microstructure as measured by the dendrite arm spacing, the grain size and morphology, as well as the size, form, and presence of other microconstituents in the solidified structure.

In Al-Si alloys, the eutectic silicon morphology plays a vital role in determining the mechanical properties. Particle size, shape, and spacing are the main factors that characterize the silicon particle morphology. Under normal cooling conditions, the Si particles are present as coarse acicular needles. These needles act as crack initiators and lower the mechanical properties appreciably. Small amounts of Sr are added to the melt to chemically modify the morphology of the Si particles to a fibrous form, providing a well modified eutectic structure and enhancement of the alloy properties. The Si particle characteristics can also be altered by subjecting the casting to a high temperature treatment for a specified length of time. In recent years, both chemical and thermal modification are being used in conjunction to produce the desired properties in a casting.

4.2 SILICON PARTICLE CHARACTERIZATION

In the present study the silicon particle characteristics were measured in both as-cast and solution heat-treated conditions, for samples obtained from A319.1, A356.2, and A413.1 alloys in the non-modified and Sr-modified conditions at the two cooling rates studied (DASs of 40 μm and 120 μm), and with 0, 2, 4, and 6 wt% mischmetal additions. These measurements were carried out in order to investigate the effect of mischmetal as a modifier, the combined effect of Sr and mischmetal, and also the effect of solution heat treatment on the morphology and size of the eutectic Si particles.

To separate the effect of solidification conditions from those of alloy chemistry and additives, the results of the Si particle characteristics for each alloy have been presented in two sections, corresponding to the two cooling rates (high and low, DASs of 40 μm and 120 μm).

4.2.1 A319.1 Alloy

4.2.1.1 Effect of high cooling rate

Table 4.1 shows the Si particle characteristics observed for the various A319.1 alloy samples solidified under high cooling rate conditions (i.e. DAS ~ 40 μm), in the as-cast condition and after solution heat treatment.

With respect to the alloy code in the first column, the A319.1 alloy is coded A, the Sr-modified version is coded AS, and the suffix T in the AT and AST alloys distinguishes

the solution heat-treated samples from the as-cast A and AS alloy samples. Similar coding systems were adopted for the A356.2 alloy (coded B) and A413.1 alloy (coded C).

Table 4.1 Silicon particle characteristics of various A319.1 alloy samples obtained at high cooling rate (DAS ~ 40 μm)

Alloy Code	Misch Metal wt.%	Particle Area (μm^2)		Particle Length (μm)		Roundness Ratio (%)		Aspect Ratio (%)		Density (particles/ mm^2)
		Av.	SD	Av.	SD	Av.	SD	Av.	SD	
A*	0%	24.7	50.5	9.5	14.0	58.7	32.5	2.5	1.5	3514
	2%	18.9	34.9	8.0	9.9	55.6	30.4	2.3	1.2	4526
	4%	15.1	27.3	7.2	8.4	55.6	28.9	2.4	1.2	4955
	6%	15.2	28.1	7.4	8.8	56.0	29.5	2.4	1.3	5005
AS	0%	4.2	3.7	3.3	3.1	65.7	25.8	2.0	0.9	32548
	2%	3.1	4.6	2.8	2.6	68.6	24.9	1.9	0.8	50640
	4%	3.4	6.6	2.8	3.0	71.3	23.9	1.8	0.7	44807
	6%	2.3	4.2	2.5	2.4	68.3	24.7	2.0	0.8	42717
AT	0%	31.1	51.8	10.9	13.7	59.7	30.0	2.5	1.4	2775
	2%	29.9	45.9	9.6	10.4	61.6	28.5	2.2	1.1	3352
	4%	25.1	42.0	8.9	10.7	62.5	28.9	2.2	1.2	3613
	6%	21.9	35.5	8.2	8.9	63.7	27.3	2.3	1.2	3849
AST	0%	8.1	10.2	4.5	4.0	71.3	22.9	1.9	0.8	19116
	2%	6.8	8.3	3.9	3.3	74.9	20.5	1.8	0.7	19067
	4%	6.7	8.67	3.9	3.5	74.0	21.0	1.8	0.7	20355
	6%	7.1	10.8	4.4	4.4	68.6	24.2	2.1	0.9	15967

*A= A319.1 alloy, S= Strontium modified, and T= solution heat-treated

As can be seen from Table 4.1, the non-modified A alloy displays the largest particle sizes (area and length) and the roundness and aspect ratio values indicate the acicular nature of the particles (keeping in mind that a spherical particle would exhibit an aspect ratio of 1 and a roundness of ~99%).

With the addition of mischmetal, a slight change in the Si particle size and density is observed, the maximum change being obtained for 4-6 wt% mischmetal addition. The roundness and aspect ratio, however, apparently remain the same.

The significant modification effect of Sr addition is evident from the Si particle characteristics exhibited by the AS alloy samples. While Sr addition alone reduces the average particle area from 24.7 μm^2 to 4.2 μm^2, addition of mischmetal is found to decrease the particle size further. The best results are obtained with 6 wt% mischmetal addition, where both the particle size and morphology characteristics are ameliorated. The Si particle density values shown in the last column underline the considerably stronger modification effect of a combined Sr and MM addition, and even more so compared to the non-Sr containing A alloys.

Figure 4.1(a) to (d) compares the optical microstructures of non-modified, MM-modified, Sr-modified and Sr-MM modified A319.1 alloy samples, respectively. As can be seen, the acicular Si particles in (a) are refined to a certain extent in (b). Addition of Sr to the non-modified alloy produces a well modified eutectic structure, Figure 4.1(c). Again, addition of MM to the Sr-modified alloy further refines the Si particles. As Figure 4.1(b) shows, the modification due to MM addition is non-homogenous and tends to be localized around the mischmetal-containing intermetallics (lighter grey needles in the micrograph).

Figure 4.2 displays the microstructures of the same samples shown in Figure 4.1 after solution heat treatment (at 495°C for 8 h). As Table 4.1 reveals, the eutectic Si particles coarsen and the average particle area increases by about 26%. The particle length also increases by about 14%. This indicates the coarsening of the Si particles with solution

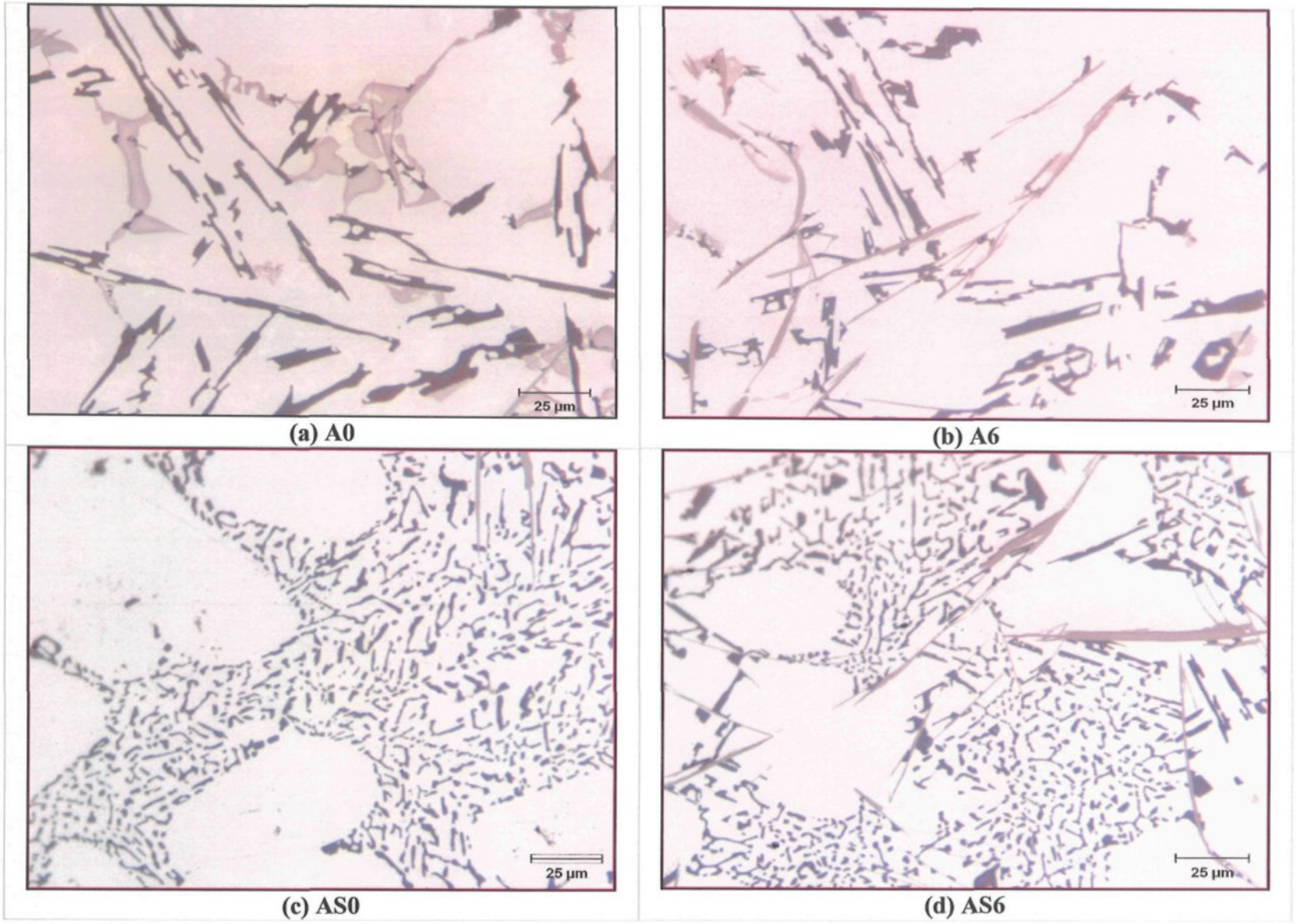

Figure 4.1 Effect of mischmetal (MM) and Sr additions on the Si particle morphology in as-cast A319.1 alloy samples obtained at high cooling rate : (a) 0% MM, (b) 6%MM, (c) Sr-modified, and (d) Sr-modified + 6 wt %MM.

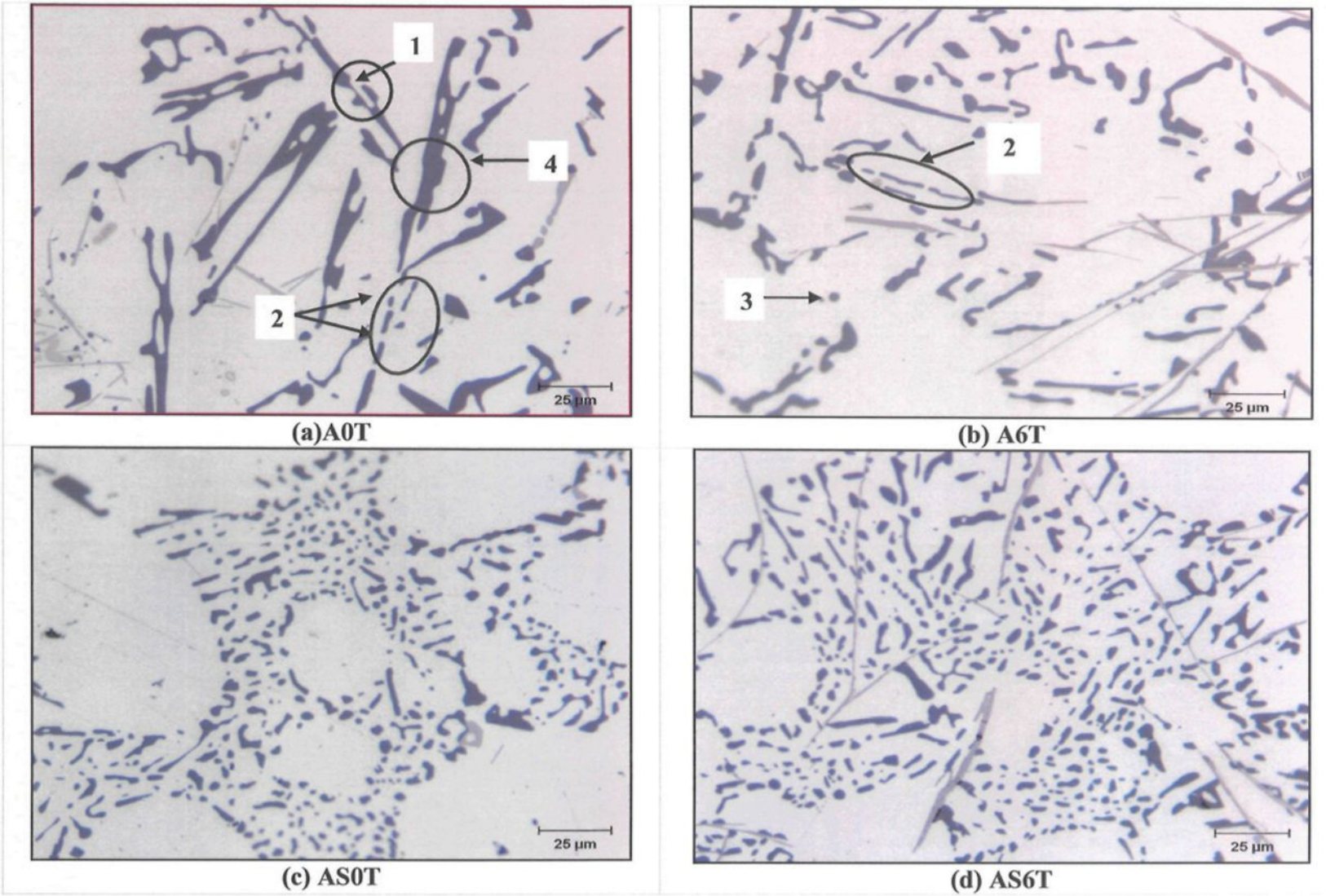

Figure 4.2 Effect of solution heat treatment on the Si particle morphology in the A319.1 alloy samples shown in Figure 4.1 at high cooling rate: (a) 0 wt% MM, (b) 6 wt% MM, (c) Sr-modified, and (d) Sr-modified + 6 wt% MM. Arrows represent: 1-necking, 2- fragmentation, 3- spheroidization, and 4- thickening of Si particles.

heat treatment, as expected. During solution heat treatment, the Si particles undergo necking, fragmentation, spheroidization and coarsening. Figure 4.2(a), corresponding to the non-modified alloy sample A0 of Figure 4.1(a), shows examples of these stages in the same microstructure, marked 1 through 4 in the micrograph.

Although the Si particles were subjected to necking, then fragmentation and spheroidization, the decrease in the eutectic Si particle density from 3514 to 2775 particles/mm^2 supports the suggestion that in the non-modified alloy, the small Si particles dissolved in the large Si particles, i.e., they coarsened in accordance with the phenomenon of ostwald ripening. Meyers [70] observed this phenomenon in the solution heat treatment of A357 alloys. The mechanism of Ostwald ripening [71] involves the separation of smaller particles (mass transfer), followed by the diffusion of these particles through the matrix to attach themselves to the surfaces of larger particles.

In other words the smaller particles ripens by losing atoms to the larger particles, leading to the dissolution of small particles and the growth of the large particles. From the physical point of view the driving force for the coarsening of large particle is that the system tends to decrease or release the excess of its overall surface energy through the dissolution (increases solubility) of small particles (assume high ratio of surface energy to volume) in the matrix. This would result in a higher coarsening rate than the rate of fragmentation and spheroidization. Also, the plate-shaped Si particles in the non-modified alloy would tend to be more easily coarsened than spheroidized. [7]

For the non-modified A alloy modified with mischmetal then solution heat-treated, the Si particles are observed to exhibit a slight modification behavior in that the particle

area, length, and aspect ratio decrease gradually as the mischmetal level increases from 0 to 6 wt%. However, the coarsening of the Si particles during solution treatment offsets the benefits achieved due to the MM addition, resulting in particle size that are larger than those exhibited by the non-modified A alloys in the as-cast condition. This is easily seen by comparing Figure 4.1(b) with Figure 4.2(b). However, on the other hand, the spheroidization of the Si particles with solution heat treatment improves the roundness and aspect ratio values of the AT alloys. Also, the increase in the Si particle density from 2775 to 3849 particles/mm^2 with increasing MM addition reflects modification effect of the latter.

In the case of the Sr-modified AS alloys, solution heat treatment increases (coarsens) the Si particle size (area and length) of the as-cast alloy. Both roundness and aspect ratio are considerably improved, as well.

With MM addition, the particle size decreases somewhat, while the roundness and aspect ratio improve, correspondingly, for the solution heat-treated AST alloy. Overall, the much smaller particle densities, as well as the larger standard deviation values with respect to the particle areas observed for the AST alloys compared to the AS alloys, suggest the occurrence of Ostwald ripening and consequent coarsening of larger Si particles at the expense of much smaller ones.

4.2.1.2 Effect of low cooling rate

Table 4.2 lists the Si particle characteristics observed for the various A319.1 alloy

samples solidified under low cooling rate conditions (DAS ~120 μm), in the as-cast and after solution heat treatment conditions.

Table 4.2 Si particle characteristics of various A319.1 alloy samples obtained at low cooling rate (DAS ~ 120μm)

Alloy Code	Misch Metal wt.%	Particle Area (μm^2)		Particle Length (μm)		Roundness Ratio (%)		Aspect Ratio (%)		Density (particles/ mm^2)
		Av.	SD	Av.	SD	Av.	SD	Av.	SD	
HA*	0%	42.8	120.7	9.8	19.2	66.2	29.1	2.2	1.3	1859
	2%	34.8	67.8	11.1	15.3	55.9	31.7	2.5	1.3	2790
	4%	33.4	100	7.7	17.0	73.8	30.2	2.1	1.2	3279
	6%	31.4	52.6	9.8	10.9	58.5	27.2	2.3	1.1	2032
HAS	0%	8.6	11.5	4.8	4.5	64.5	25.1	2.1	1.02	19413
	2%	6.7	8.6	4.2	3.67	70.9	22.8	1.9	0.8	25256
	4%	12.2	24.1	5.3	7.9	73.1	27.8	1.9	1.0	11352
	6%	22.1	43.1	7.1	10.5	67.8	30.4	2.0	1.0	6394
HAT	0%	50.9	108	12.8	19.3	63.3	29.4	2.4	1.3	1726
	2%	43.1	74.7	12.6	15.9	56.7	32.2	2.6	1.6	2911
	4%	33.3	48.2	10.7	10.5	59.4	28.3	2.4	1.2	3449
	6%	29.2	39.2	10.2	10.0	57.9	27.2	2.4	1.2	3777
HAST	0%	9.1	10.9	4.6	3.4	69.8	21.8	1.9	0.9	17880
	2%	8.8	11.7	4.7	4.5	65.3	24.2	2.3	1.4	17015
	4%	10.4	18.2	4.9	5.7	68.6	24.8	2.0	0.9	13022
	6%	16.0	17.4	8.4	8.4	60.6	27.4	2.3	1.2	6027

*A= A319.1 alloy, S= Strontium modified, T= solution heat-treated, and H= slowly cooled inside the furnace.

With respect to the alloy codes, the prefix H represents the low cooling rate condition that provided a high DAS value. The low cooling rate condition was achieved by allowing the casting to cool slowly inside the furnace. The other letters A, S and T represent the same alloy, strontium and solution treatment conditions as in Table 4.1.

Figure 4.3 displays the microstructures of the same alloys as those shown in Figure 4.1, obtained under low cooling rate conditions. Comparing the two figures, as also Tables 4.2 and 4.1 the Si particles sizes are seen to be much larger in this case. The addition of 4-6 wt% MM to the non-modified HA alloys decreases the particle size by about 10-12 μm, i.e., by ~ 25%. The same tendency is observed in the solution heat-treated non-modified HAT alloys, viz., the addition of MM decreases the particle size - in this case to a somewhat larger extent, due to the effect of solution heat treatment, as well.

In the Sr-modified HAS alloys, the combined effect of MM and Sr apparently has a beneficial effect at 2 wt% MM addition, but a detrimental effect is observed at higher MM additions. A slight amount of coarsening of the Si particles is observed after solution heat treatment of the HAS alloy (*cf.* the particle areas of HAS-0 and HAST-0 samples). As before, a 2 wt% MM addition is beneficial, but higher additions negate the beneficial effect of Sr modification. As will be seen in Chapter 5, the Sr and MM interact to form intermetallic phases. This leads to a decrease in the amount of Sr available in the melt to modify the eutectic Si particles and, hence, a loss in the level of modification achieved.

The variations in the particle density and roundness observed in the solution heat treated samples listed in Table 4.2 give an indication of the fragmentation and spheroidization taking place along with the coarsening of the Si particles.

Figure 4.4 through Figure 4.6 summarize the Si particle sizes (area and length) and densities exhibited by the various A319.1 (A) alloy samples for the two cooling rates and in the as-cast and heat treated conditions, providing at a glance, the results listed in Tables 4.1 and 4.2.

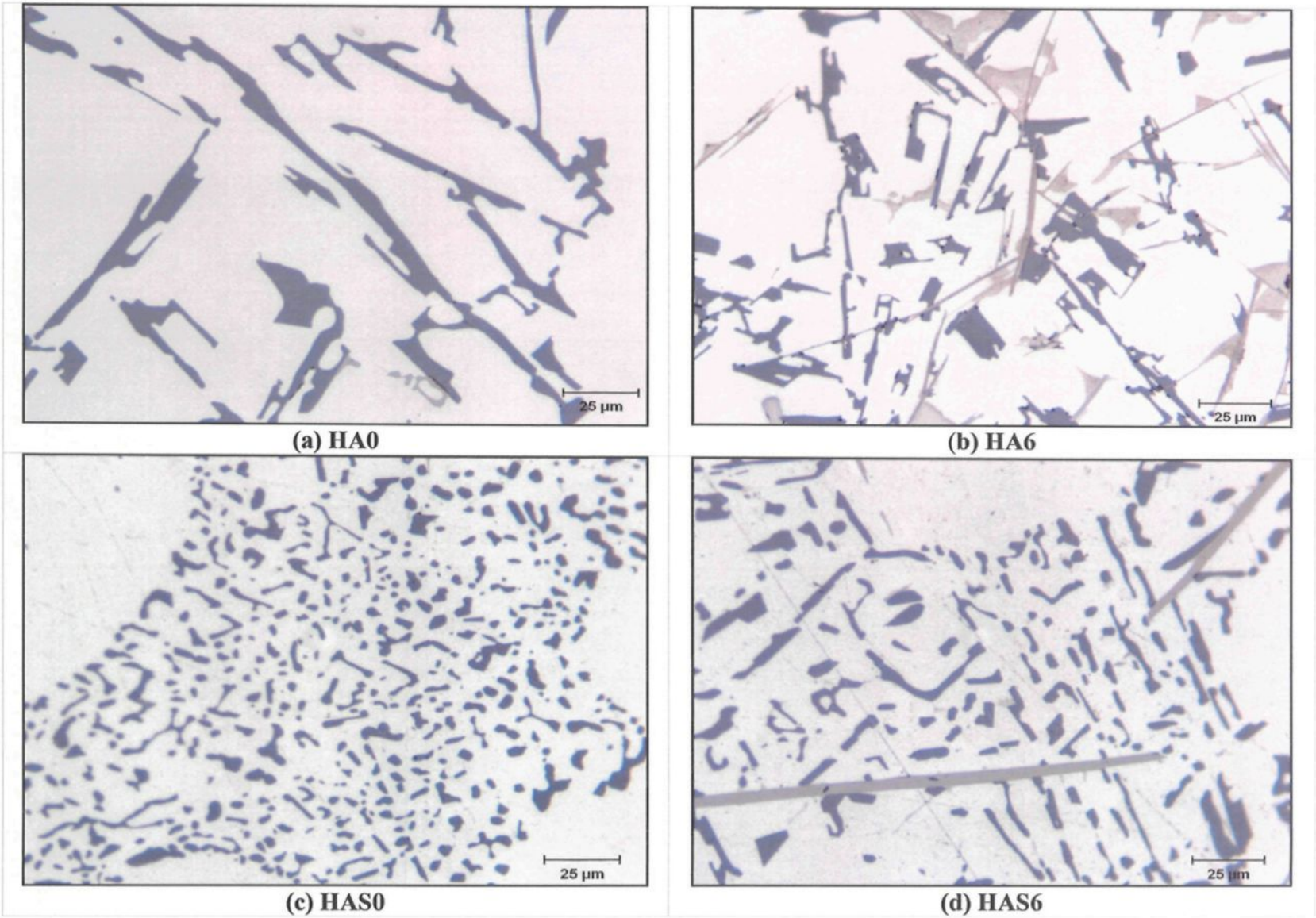

Figure 4.3 Effect of mischmetal addition (MM) on the morphology of the eutectic silicon in the as-cast A319.1 alloy samples obtained at low cooling rate: (a) 0 wt% MM, (b) 6 wt% MM, (c) Sr-modified with 0 wt % MM and (d) Sr-modified with 6 wt% MM.

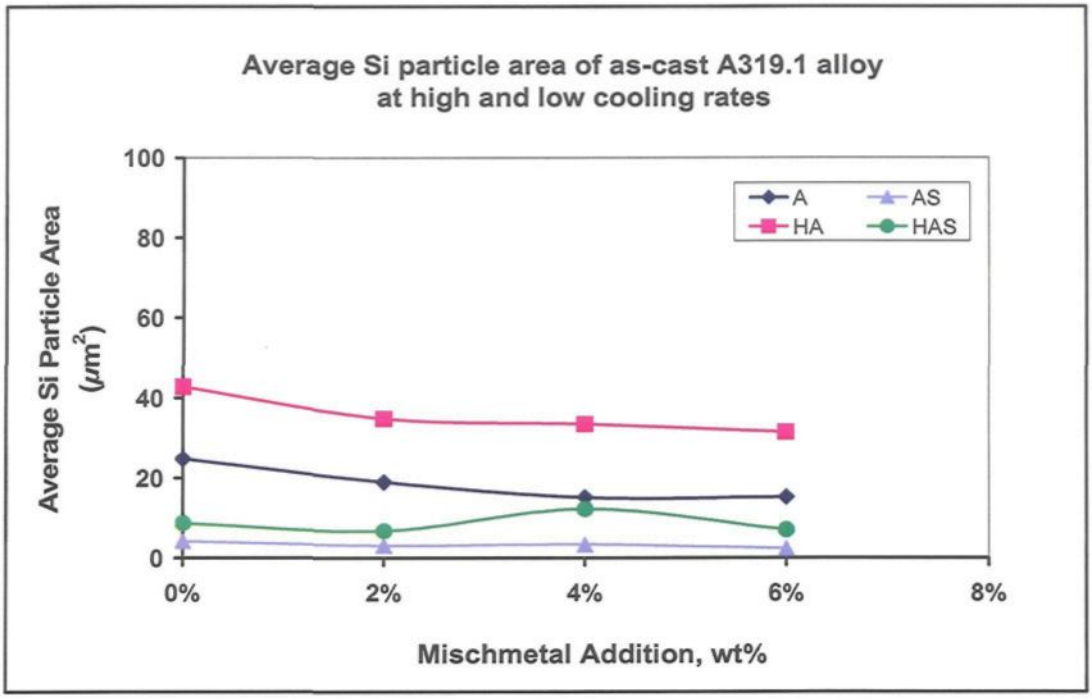

(a)

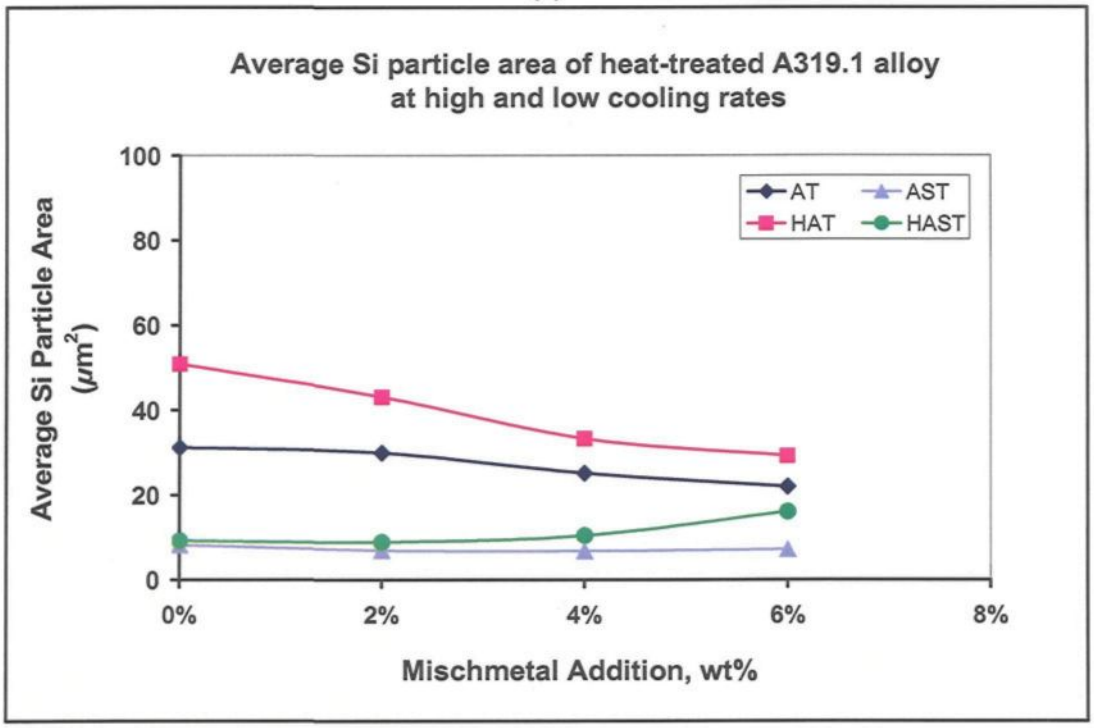

(b)

Figure 4.4 Average Si particle area values obtained in various A319.1 alloys at the two cooling rates: (a) as-cast, and (b) heat-treated samples.

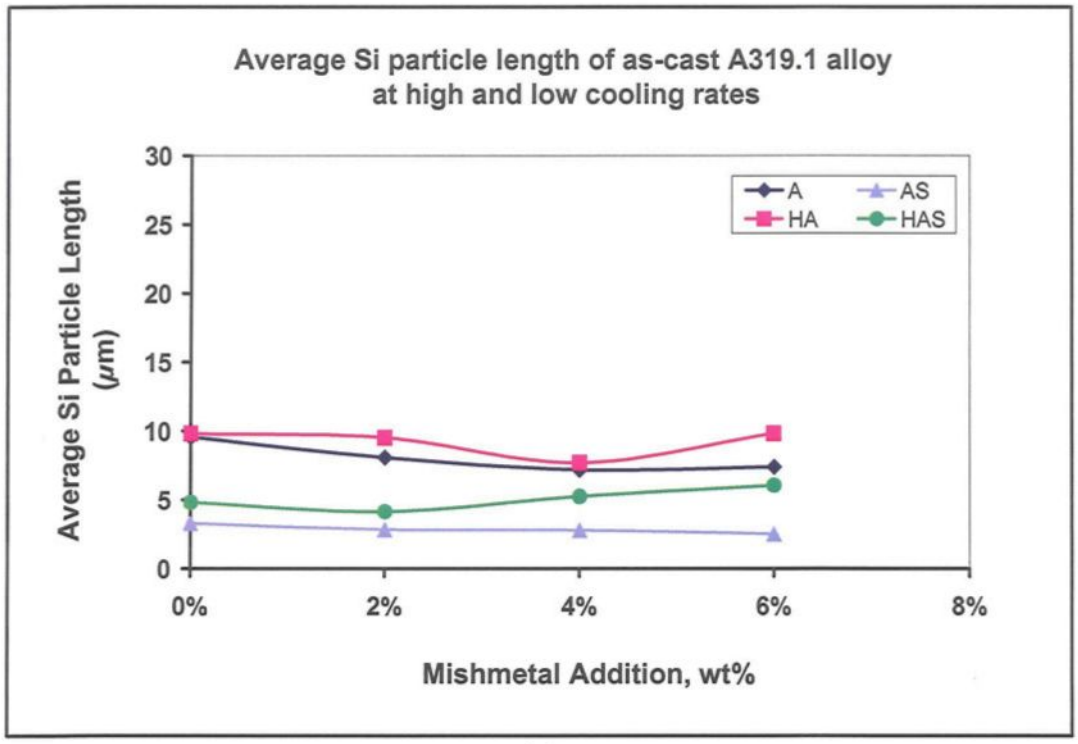

(a)

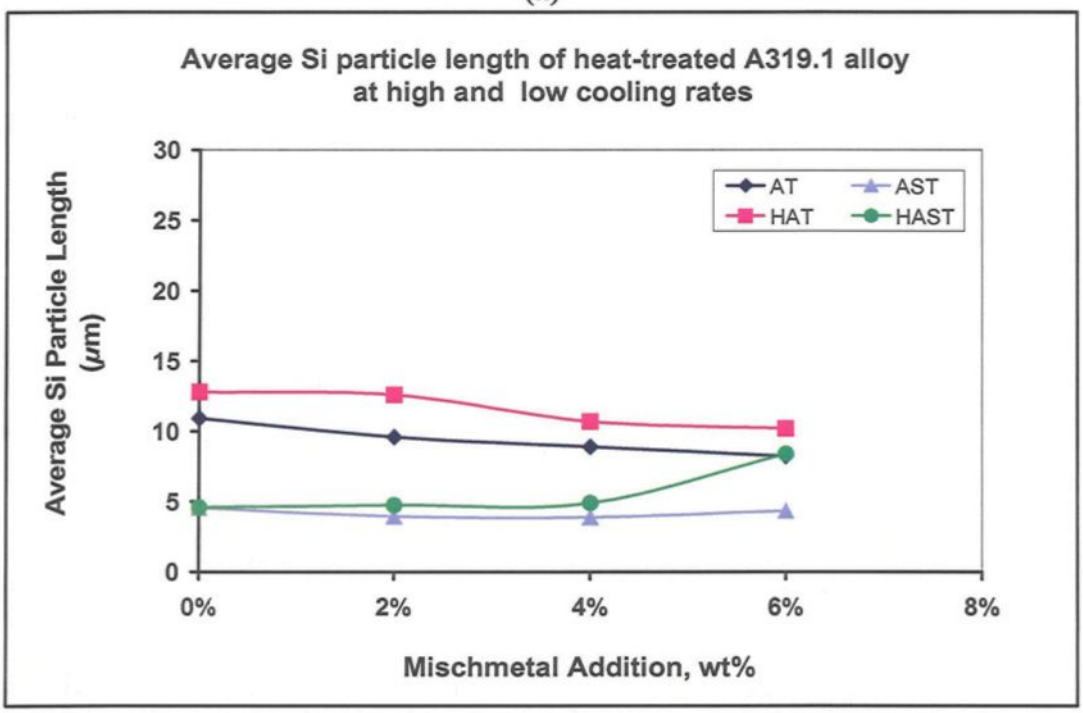

(b)

Figure 4.5 Average Si particle length values obtained in various A319.1 alloys at the two cooling rates: (a) as-cast, and (b) heat-treated samples.

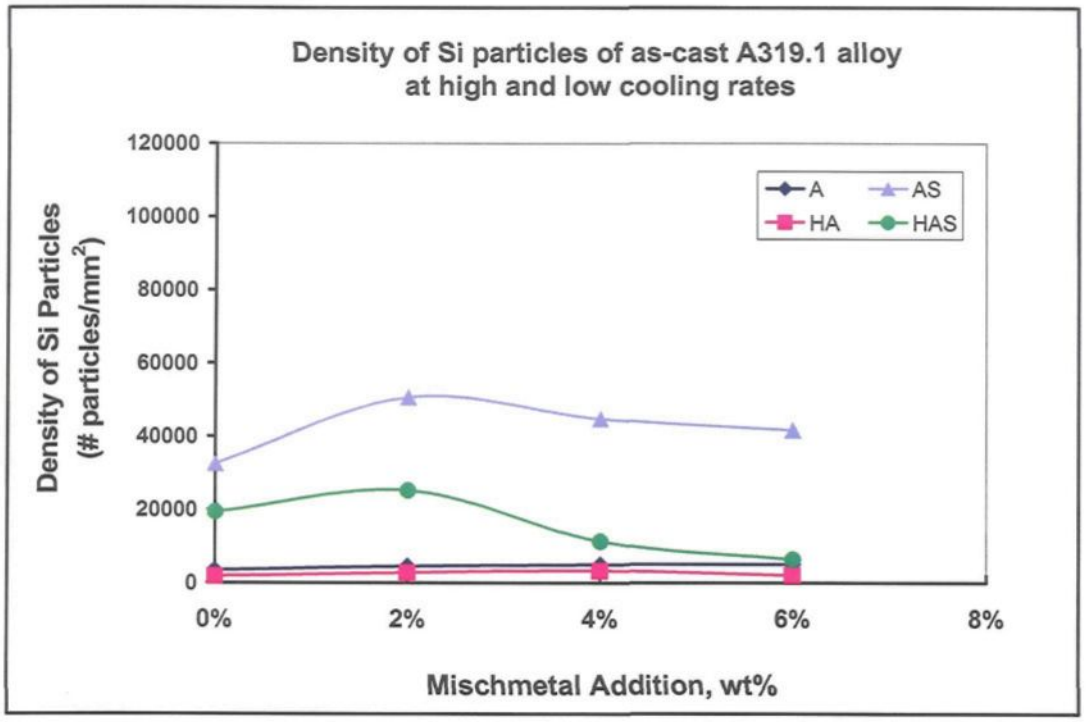

(a)

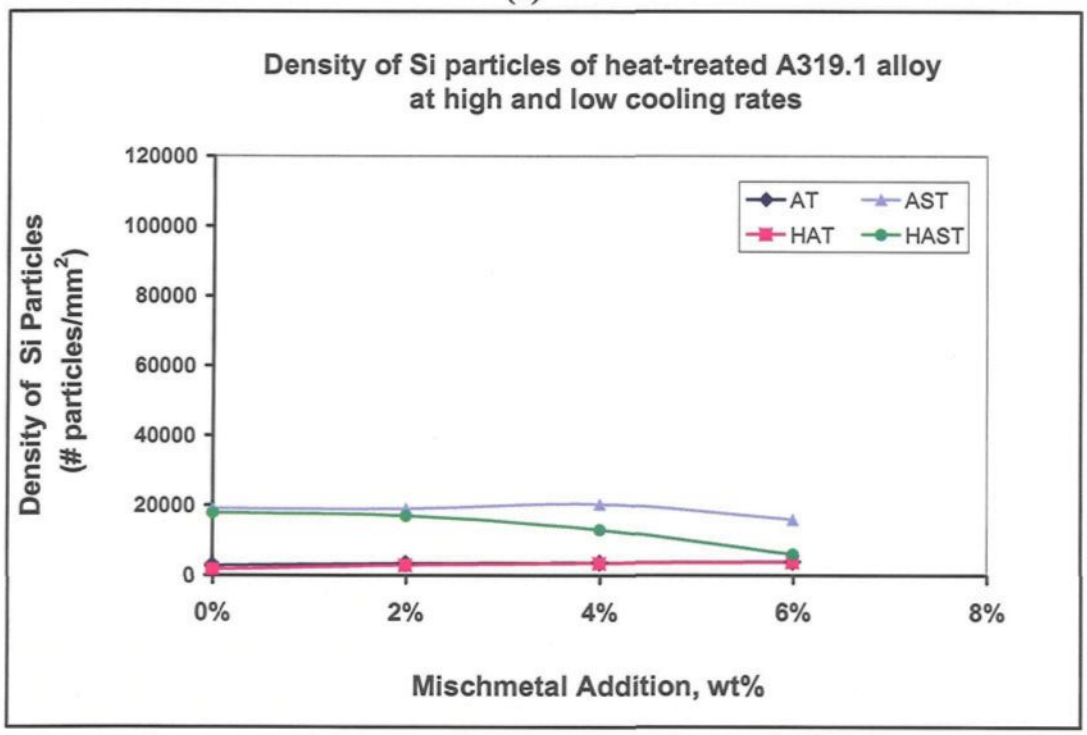

(b)

Figure 4.6 Silicon particle density of various A319.1 alloy samples obtained at the two cooling rates: (a) as-cast, and (b) heat-treated conditions.

4.2.2 A356.2 Alloy

4.2.2.1 Effect of high cooling rate

Table 4.3 reveals the Si particle characteristics observed for the various A356.2 alloy samples solidified under high cooling rate conditions (i.e., DAS ~ 40 μm), in the as-cast condition and after solution heat treatment.

Table 4.3 Si particle characteristics of various A356.2 alloy samples obtained at high cooling rate (DAS ~ 40μm)

Alloy Code	Misch Metal wt.%	Particle Area (μm^2)		Particle Length (μm)		Roundness Ratio (%)		Aspect Ratio (%)		Density (particles/ mm^2)
		Av.	SD	Av.	SD	Av.	SD	Av.	SD	
B*	0%	15.4	30.3	7.7	10.3	57.1	31.8	2.6	1.6	3916
	2%	17.5	30.7	7.6	8.5	58.2	28.1	2.4	1.2	4178
	4%	13.5	29.3	6.0	8.32	64.8	30.4	2.2	1.1	3579
	6%	11.2	27.2	5.5	7.87	65.3	30.1	2.2	1.2	4659
BS	0%	3.1	4.7	3.0	3.3	67.7	25.4	2.0	0.9	52469
	2%	1.7	2.9	2.0	1.8	71.9	22.6	1.9	0.8	69456
	4%	1.2	3.4	1.7	1.8	74.5	22.9	1.9	0.8	81094
	6%	2.6	4.7	2.3	2.7	69.6	25.6	1.9	0.8	47384
BT	0%	22.2	27.0	8.4	10.2	69.9	28.6	2.5	1.5	2724.6
	2%	24.8	38.9	8.3	9.5	65.4	27.1	2.2	1.2	2493
	4%	20.3	38.6	6.9	8.7	67.2	28.2	2.2	1.1	3069
	6%	20.2	37.5	6.9	8.9	68.8	27.6	2.2	1.2	3449
BST	0%	9.1	9.8	4.3	3.6	78.8	18.0	1.7	0.7	15603
	2%	9.5	11	4.1	3.3	81.5	16.1	1.6	0.5	15225
	4%	7.2	8.1	3.6	2.8	83.6	15.6	1.6	0.5	19046
	6%	12.8	15	5.3	4.7	75.0	21.9	1.8	0.9	10946

*B= A356.2 alloy, S= Strontium modified, and T= solution heat-treated.

It can be observed from Table 4.3 that in the non-modified as-cast B alloy, the eutectic Si particles are large in size (large particle area, length), assuming acicular plate-like forms (low roundness and high aspect ratio).

With the introduction of mischmetal to the B alloy melt, a slight increase can be observed in the Si particle area for the 2 wt% mischmetal-containing alloy. Increasing the mischmetal addition (4-6 wt%), results in a slight decrease in the Si particle size and aspect ratio, while the roundness displays some improvement. The Si particle density increases slightly (i.e., by ~19%), indicating the partial modification effect of the mischmetal additions.

The fine Si particle characteristics exhibited by the BS alloy samples is a strong evidence of the considerable modification effect of Sr addition. While Sr addition alone reduces the average particle area from 15.4 μm^2 to 3.1 μm^2, addition of mischmetal is observed to decrease the particle size further. The best results are achieved with 4 wt% mischmetal addition, where both the particle size and morphology are improved. The increase in the Si particle density of the BS alloys by 10-23 times compared to the non-Sr containing B alloys, confirms the strong modification effect of a combined Sr and mischmetal addition. At 6 wt% mischmetal addition, however, the Si particle size exhibits a slight increase, indicating the possibility of an interaction between mischmetal and Sr which, reduces the effectiveness of their combined modification effect. A corresponding decrease in the particle density by about ~ 42% supports this suggestion.

Figure 4.7(b) depicts the effect of solution heat treatment (at 540°C/8h) on the morphology of the eutectic Si particles in the non-modified B alloy at high cooling rate.

The eutectic Si particles seem to be relatively unaffected by solution heat treatment and retain their large sizes. In spite of the fact that the Si particles are liable to undergo partial fragmentation and spheroidization, the eutectic Si particle coarsen. This increase in the average Si particle area by about 44% seems to be as a result of the thickening of the Si particles (increase in the width), as is evident from a comparison of the morphology of Si particles in Figure 4.7(a) with those in Figure 4.7(b). This observation is even more apparent in the samples obtained at low cooling rate, as shown in Figure 4.7(c) and (d).

Figure 4.8 represents the average thickness of the eutectic Si particles observed in the as-cast and solution heat-treated non-modified B alloys, at the two cooling rate conditions. It is apparent that the average thickness of the Si particles increases after solution heat treatment from 1.9 μm to 4.2 μm. The fact that the as-cast Si particles are in the non-modified alloy samples are in the form of acicular plates in a large variety of sizes would indicate a greater driving force for the coarsening of the particles. [7] At the same time, the interface instabilities (caused by shape perturbations in a fibrous eutectic structure during thermal treatment at elevated temperatures) require for fragmentation and spheroidzation would not occur readily in such an acicular plate-like (non-modified) eutectic structure, making it resistant to spherodization. Both these factors would lead to the thickening of the Si particles in this case. [7, 71] As reported by Apelian *et al.*, [7] the small radius found at the tip of the Si plate-like particles (needles) prefers to grow at the corners, giving rise to an increase in the width of the Si particle, while smaller particles dissolve due to the Ostwald ripening effect. The overall effect is therefore a coarsening (increase in

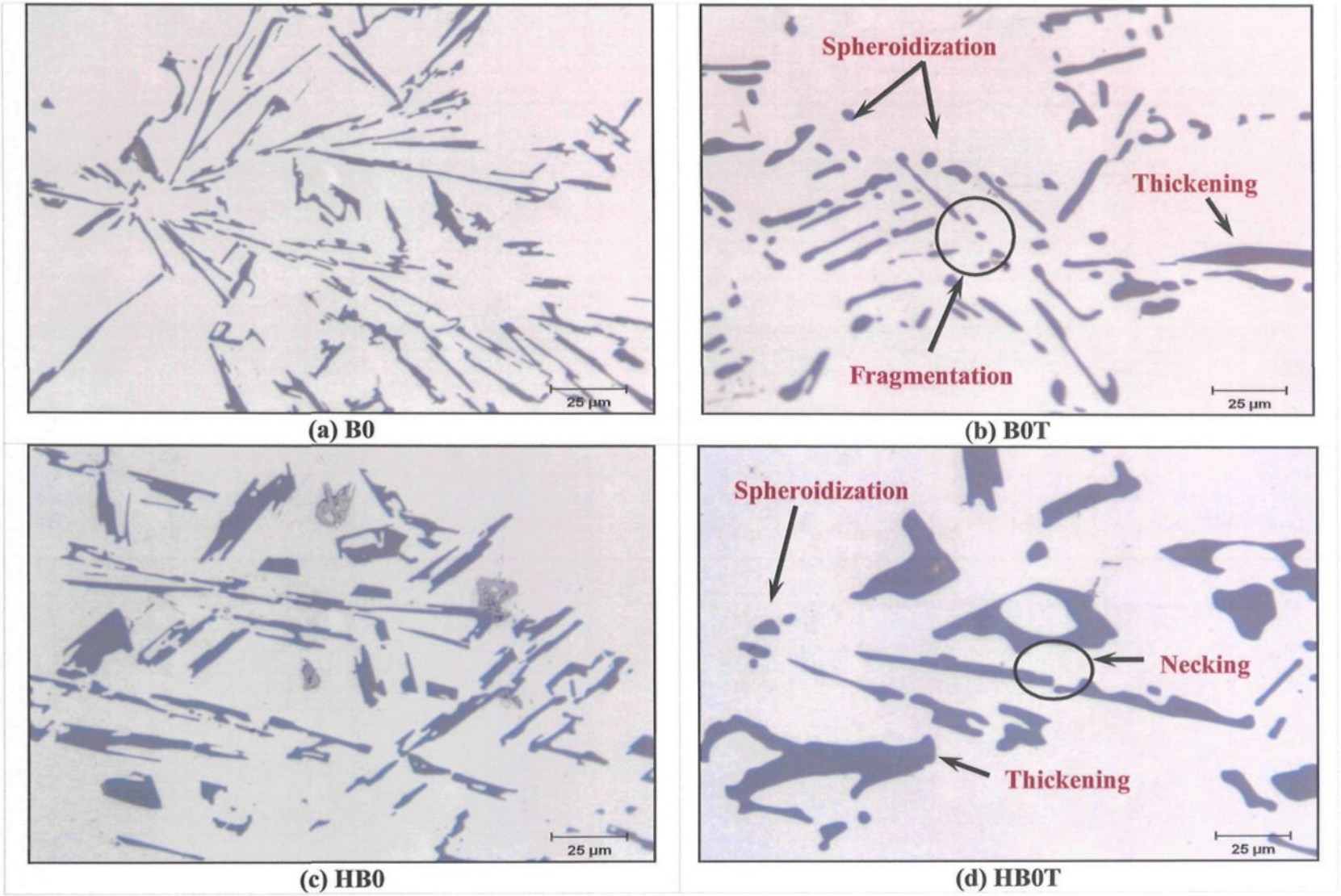

Figure 4.7 Effect of solution heat treatment on the Si particle morphology in non-modified A356.2 alloy: (a) as-cast and (b) heat-treated at high cooling rate; (c) as-cast and (d) heat-treated at low cooling rate.

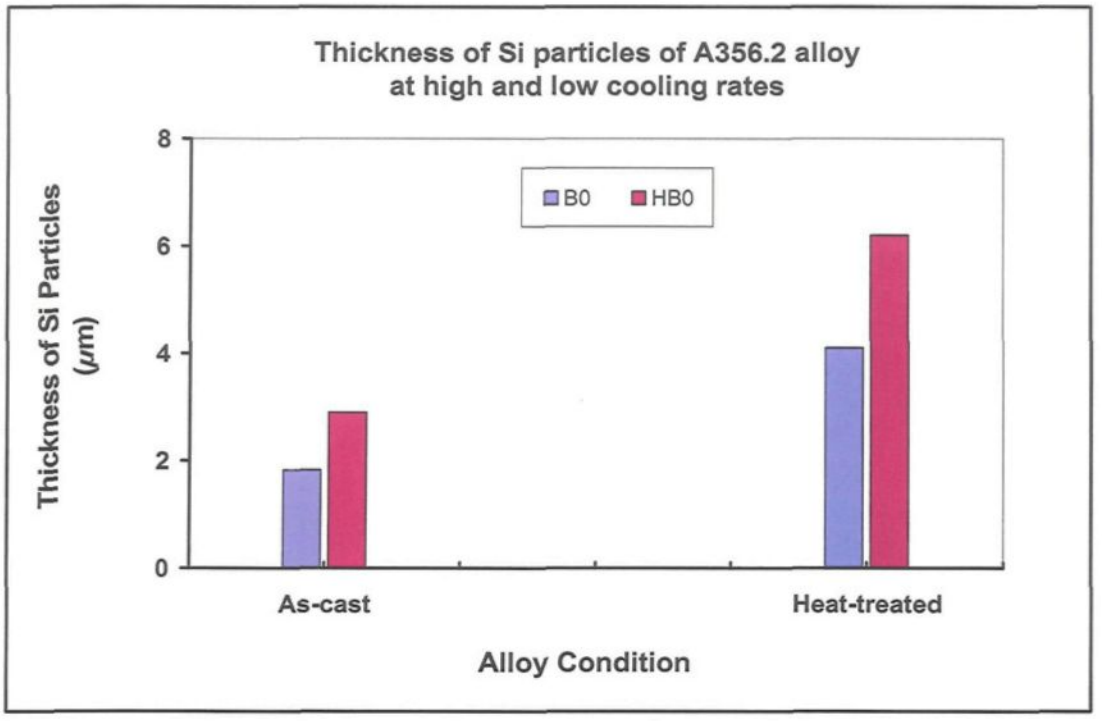

Figure 4.8 Average Si particle thickness of as-cast and heat-treated A356.2 alloy samples obtained at the two cooling rate conditions.

thickness) of the Si particles. The drastic decrease in particle density by ~30% as can be seen in Table 4.3 supports the suggestion that the non-modified B alloys display higher coarsening rates. The very small decrease in aspect ratio (~ 4%) reflects the persistence of the Si particle as platelets, as is also seen clearly in Figure 4.7(b).

For the B alloy samples modified with mischmetal, after solution heat treatment at 540°C/8h, the average Si particle area, length and aspect ratio display a slight decrease indicating that the eutectic Si particles are somewhat modified, whereas the particle density increases by about 26%, as shown in Table 4.3. However, the coarsening of the Si particles size during solution heat treatment weakens the modification benefits obtained due to MM

addition, leading to larger Si particles than those observed in both the as-cast non-modified and mischmetal modified B alloys. On the other hand, the spheroidization of the Si particles during solution heat treatment improves the roundness values of the BT alloys, and their aspect ratios to a certain extent.

In the case of the Sr-modified BS alloys, solution heat treatment increases (coarsens) the Si particle size and decreases the particle density of the as-cast alloy. Both roundness and aspect ratio are significantly improved as well. With MM addition, the particle size decreases somewhat, while the roundness and aspect ratio improve for 2-4 wt% mischmetal addition, correspondingly, for the solution heat-treated BST alloys. Also, the maximum combined modification effect of MM and Sr is achieved at 4 wt% mischmetal addition. With further increase of mischmetal addition to 6 wt%, it is observed that the Si particles lose their modification as a result of the interaction between MM and Sr which decreases the amount of Sr available in the melt to achieve an acceptable degree of Si particle modification. Overall, the much smaller particle densities, as well as the larger standard deviation values with respect to the particle areas observed for the BST alloys compared to the BS alloys suggest the occurrence of Ostwald ripening and the consequent coarsening of larger Si particles at the expense of much smaller ones.

4.2.2.2 Effect of low cooling rate

Table 4.4 lists the Si particle characteristics observed for the various A356.2 alloy samples solidified under low cooling rate conditions (DAS ~120 μm), in the as-cast condition and after solution heat treatment.

With respect to the alloy codes, the prefix H represents the low cooling rate condition that provided a high DAS value. The low cooling rate condition was obtained by allowing the casting to cool slowly inside the furnace. The other letters B, S and T represent the same alloy, strontium and solution treatment conditions as in Table 4.3.

Table 4.4 Si particle characteristics of various A356.2 alloy samples obtained at low cooling rate (DAS ~ 120μm)

Alloy Code	Misch Metal wt.%	Particle Area (μm^2)		Particle Length (μm)		Roundness Ratio (%)		Aspect Ratio (%)		Density (particles/ mm^2)
		Av.	SD	Av.	SD	Av.	SD	Av.	SD	
HB	0%	37.2	100	9.6	19.7	67.4	33.2	2.3	1.4	2780
	2%	36.0	108	8.5	18.9	71.3	30.1	2.0	1.1	2426
	4%	37.9	122	8.8	20.3	71.4	30.2	2.0	1.1	2111
	6%	36.3	115	7.7	17.2	71.5	30.2	1.9	1.0	2756
HBS	0%	3.7	4.7	3.3	3.0	67.8	23.6	2.1	0.9	36092
	2%	4.2	5.4	3.3	3.1	71.3	22.8	2.0	0.9	30705
	4%	14.3	16.9	8.2	8.5	57.3	28.2	2.2	1.1	6857
	6%	16.0	22.8	7.5	7.6	56.3	27.6	2.4	1.2	8859
HBT	0%	79.1	108	19.4	20.0	50.5	29.1	2.8	1.6	1391
	2%	76.3	125	18.4	25.7	60.2	32.0	2.4	1.4	968.
	4%	67.9	134	13.6	21.7	67.1	32.5	2.1	1.1	1521
	6%	48.6	115	10.7	20.7	69.4	30.7	2.2	1.2	2027
HBST	0%	5.1	5.6	2.9	1.8	79.6	16.9	1.6	0.9	32449
	2%	6.9	8.3	3.6	2.9	71.3	20.2	1.6	0.7	22407
	4%	14.0	14.6	9.0	8.5	63.3	27.3	2.2	0.9	3986
	6%	9.2	15.6	4.3	6.5	78.7	25.7	1.8	0.9	13848

*B= A356.2 alloy, S= Strontium modified, T= solution heat-treated, and H= slowly cooled inside the furnace

As can be seen from Table 4.4, in the non-modified as-cast HB alloys (solidified slowly inside the furnace), the eutectic Si particles are coarse with an average particle area

of ~37.2 μm^2 compared with those of the B alloys (~ 15 μm^2) in Table 4.3, where the low cooling rate conditions provide more time for the Si particles to coarsen.

With the addition of mischmetal to the non-modified HB alloys, the Si particles become slightly modified as evidenced by the slight decrease in the average particle length and aspect ratio values and a slight improvement in the roundness ratio.

Figure 4.9(a) to (d) shows the effects of Sr and MM addition on the size and morphology of the eutectic Si particles in both the as-cast and solution heat-treated conditions. Addition of Sr to the non-modified HB alloys results in full modification of the Si particles as shown in Figure 4.9(a), and the Si particle characteristics for the HBS alloys listed in Table 4.4, where the average Si particle area is seen to decrease from 37.2 μm^2 to 3.7 μm^2 for the Sr-modified HBS-0 MM alloy and 4.2 μm^2 for the HBS alloy containing 2 wt% mischmetal.

The addition of 6 wt% mischmetal increases the average particles size to 16 μm and alters the particle morphology as can be seen clearly in Figure 4.9(b). The drastic decrease in roundness and particle density (~75%) as seen in Table 4.4 would suggest that the addition of mischmetal to the Sr-modified HBS alloys consumes Sr and weakens its effectiveness as a Si particle modifier.

For the non-modified HB alloy during solution heat treatment at 540°C for 8h, it can be observed from Table 4.4 that the Si particles are coarsened to about twice their size. Therefore, the initial Si particle size is an important factor and plays a significant role in determining the change in the Si particle size and morphology during solution heat treatment. This increase in the Si particle size can be ascribed to the increase in the Si

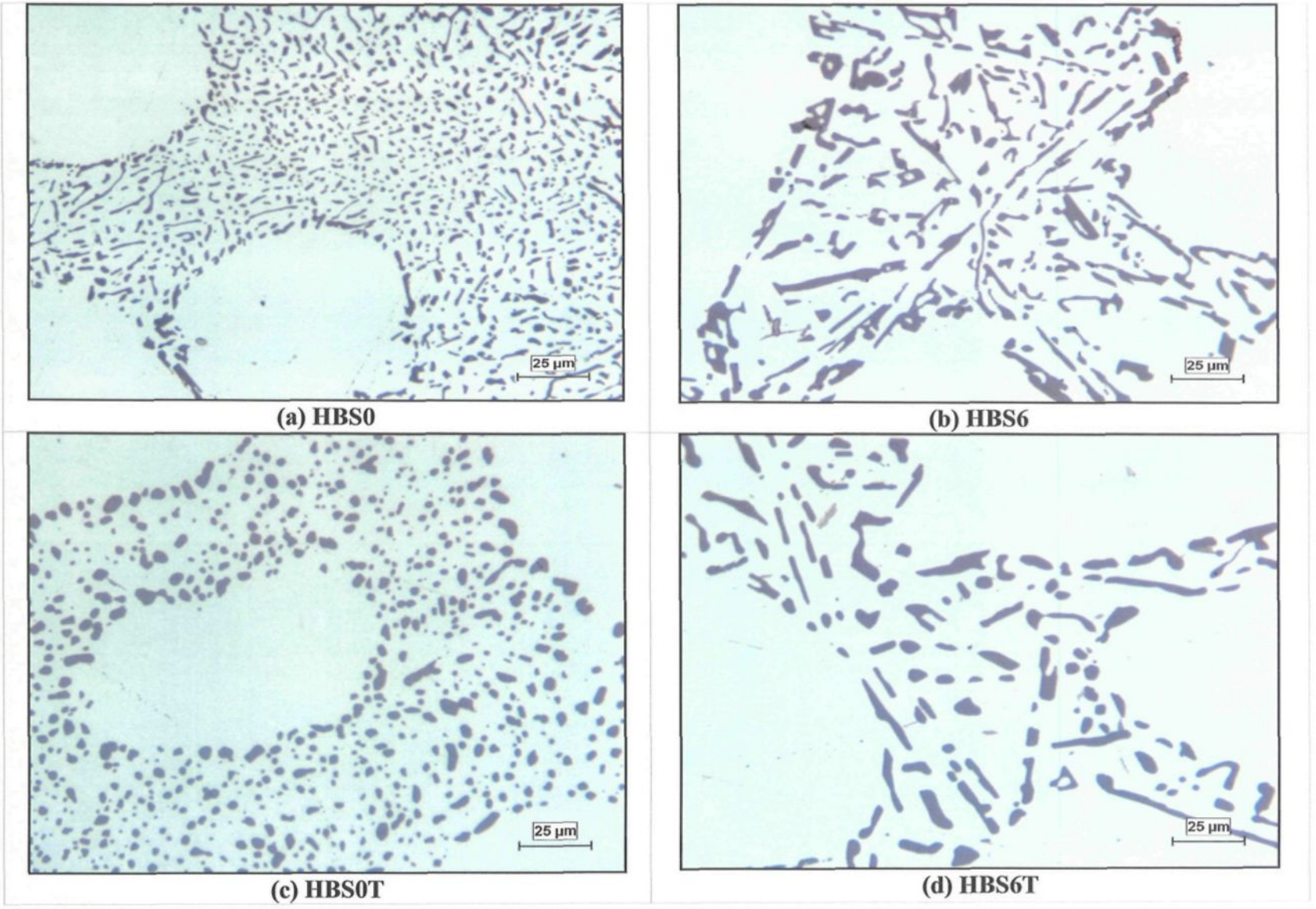

Figure 4.9 Effect of solution heat treatment on the Si particle morphology in the Sr-modified A356.2 alloy samples obtained at low cooling rate: (a) 0 wt% MM (b) 6 wt% MM as-cast, and (c) 0wt%, (d) 6 wt% MM heat-treated condition.

particle thickness, as was shown in Figure 4.8 where, after solution heat treatment, the average Si particle thickness increased from 3.8 μm to 6.2 μm, in spite of the fact that the Si particles were subject to slightly partial fragmentation and spheroidization during the solution heat treatment. The solution temperature of 540°C is sufficient for assisting the coarsening stage of the Si particles (diffusion), which have already undergone a certain amount of coarsening due to Ostwald ripening

These observations at the two cooling rate conditions are in agreement with the findings of Apelain *et al.*,[7] who reported that the driving force for coarsening of the Si particles during solution heat treatment is greater in the non-modified A356 alloys than that in the Sr-modified ones and thus, the former display higher coarsening rates. This may be attributed to the fact that in the non-modified alloy, the eutectic Si possess plate-like shaped particles and thus, the interfacial instabilities is difficult to take place, therefore the non-modified alloy is more resistant to spherodization.[71]

For the solution heat-treated HBT alloys containing up to 6 wt% mischmetal, the Si particles were considerably modified with respect to those of the HBT alloy free of mischmetal. As can be seen from Table 4.4, a significant decrease was observed in the Si particle characteristics (area, length, and aspect ratio), while the roundness and particle density revealed a significant increase. Due to the coarsening of the Si particles during solution heat treatment, however, the modification effect of the mischmetal is reduced. From this it could be reasonable to conclude that the MM-modified HB alloys display a smaller coarsening rate during solution heat treatment than that non-MM-modified HB alloy.

During solution heat treatment of the Sr-modified HBS alloys, the morphology of the Si particles were altered from fibrous form to rounded form, as shown in Figure 4.9(a) and (c). As Table 4.4 shows the roundness was ameliorated from 68 to 80%, with a low aspect ratio of 1.57, although the average Si particle area showed a slight increase (coarsening), decreasing particle density by about 10%. It is worthwhile to note that, in the Sr-modified HBS alloys, the solution heat treatment process further improves the Si particle characteristic. Thus, a combination of Sr-modification and solution heat treatment modification is more effective for improving the eutectic Si particles characteristics.

Figure 4.9(c) and (d) show the microstructures of the Sr-modified heat-treated HBST alloys with 0 and 6 wt% mischmetal additions. Comparing the two microstructures and also from Table 4.4, it can be seen that the modification effect of Sr decreases with increasing mischmetal addition: the average Si particle area, length, and aspect ratio increase, while the particle density and roundness decrease. This can be ascribed to the interaction between mischmetal and Sr (which is clearer at 4 wt% mischmetal addition), leading to form complex intermetallic compounds and hence, a decrease in the degree of modification obtained. This effect is more pronounced at the low cooling rate conditions where enough time is available for this interaction to take place and reduce the level of modification.

Figures 4.10 through 4.12 summarize the Si particle sizes (area and length) and densities exhibited by the various A356.2 (B) alloy samples for the two cooling rates and in the as-cast and heat treated conditions providing at a galnce, the results listed in Table 4.3 andTable 4.4.

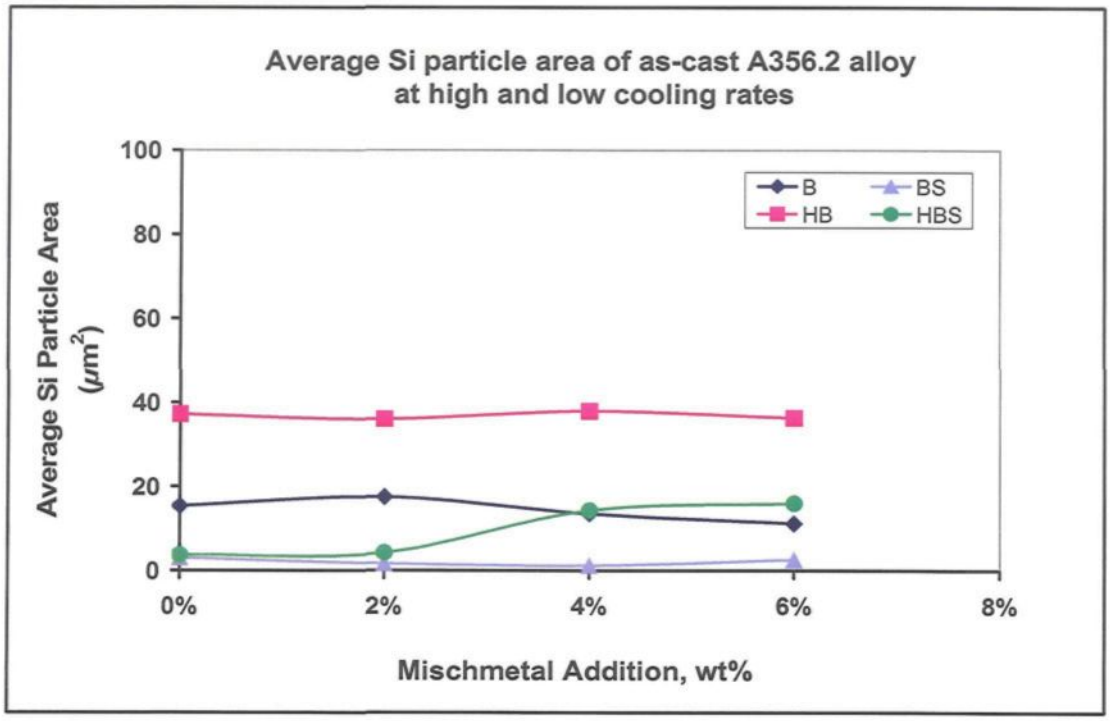

(a)

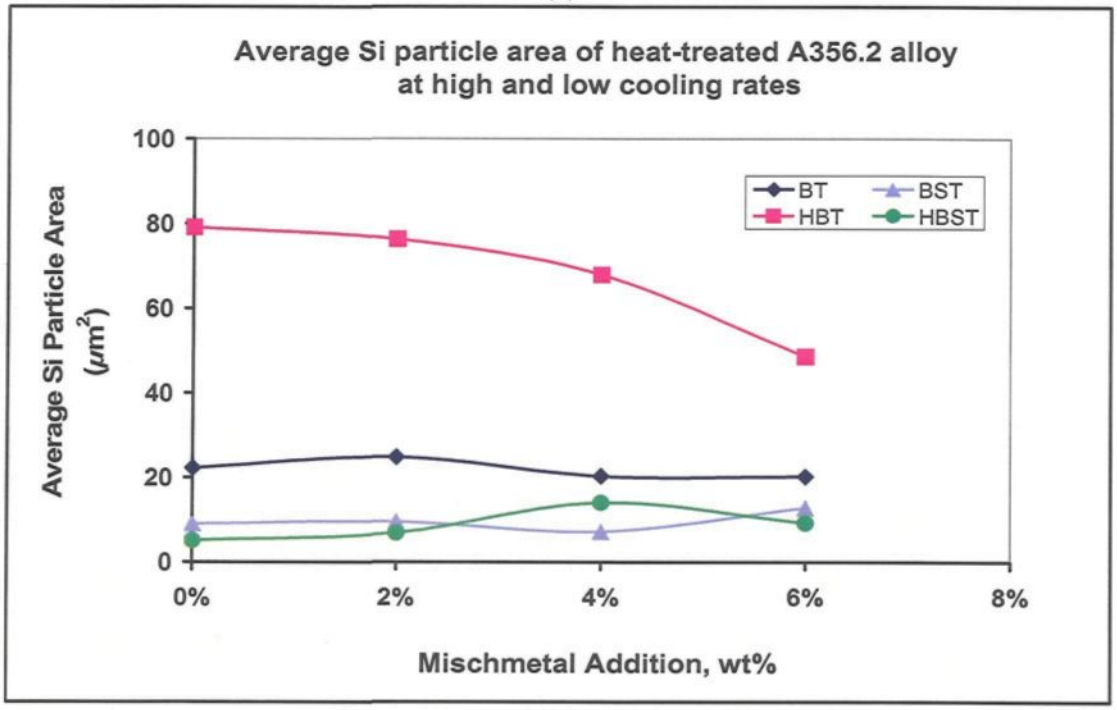

(b)

Figure 4.10 Average Si particle area obtained in various A356.2 alloys at the two cooling rates: (a) as-cast, and (b) heat-treated conditions.

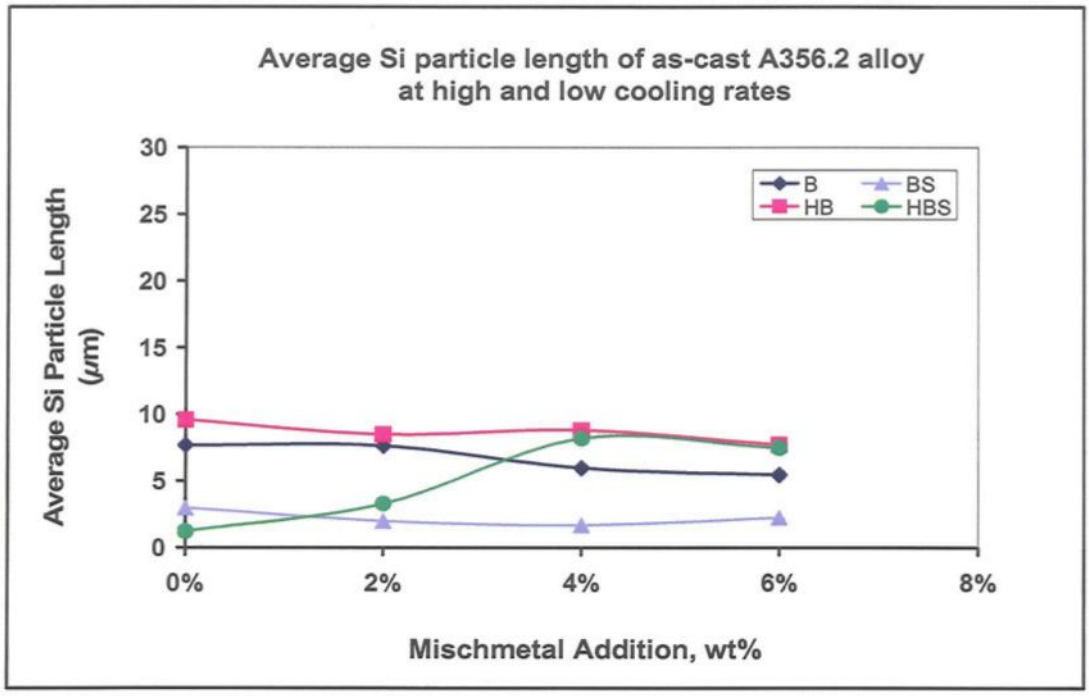

(a)

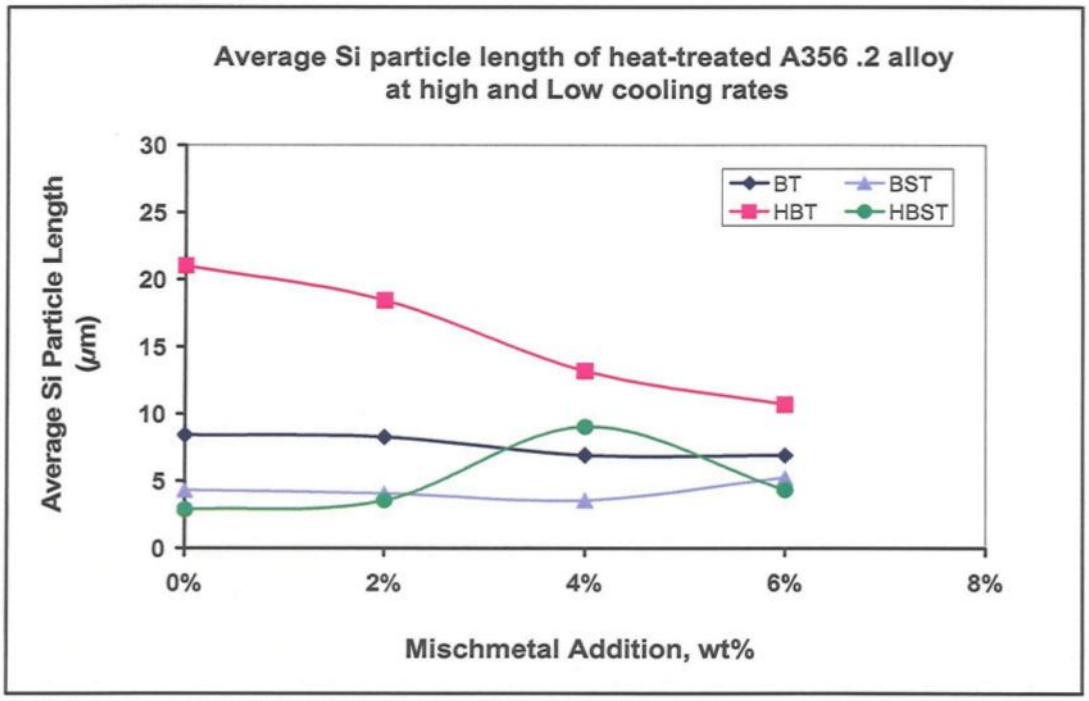

(b)

Figure 4.11 Average Si particle length obtained in various A356.2 alloys at the two cooling rates: (a) as-cast, and (b) heat-treated conditions.

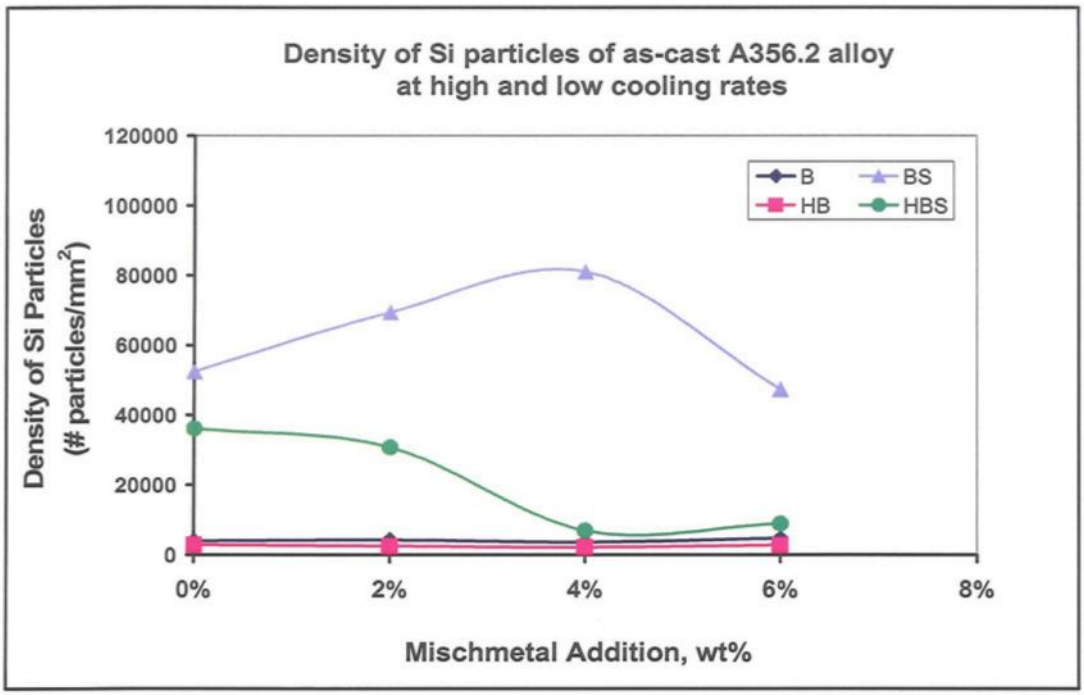

(a)

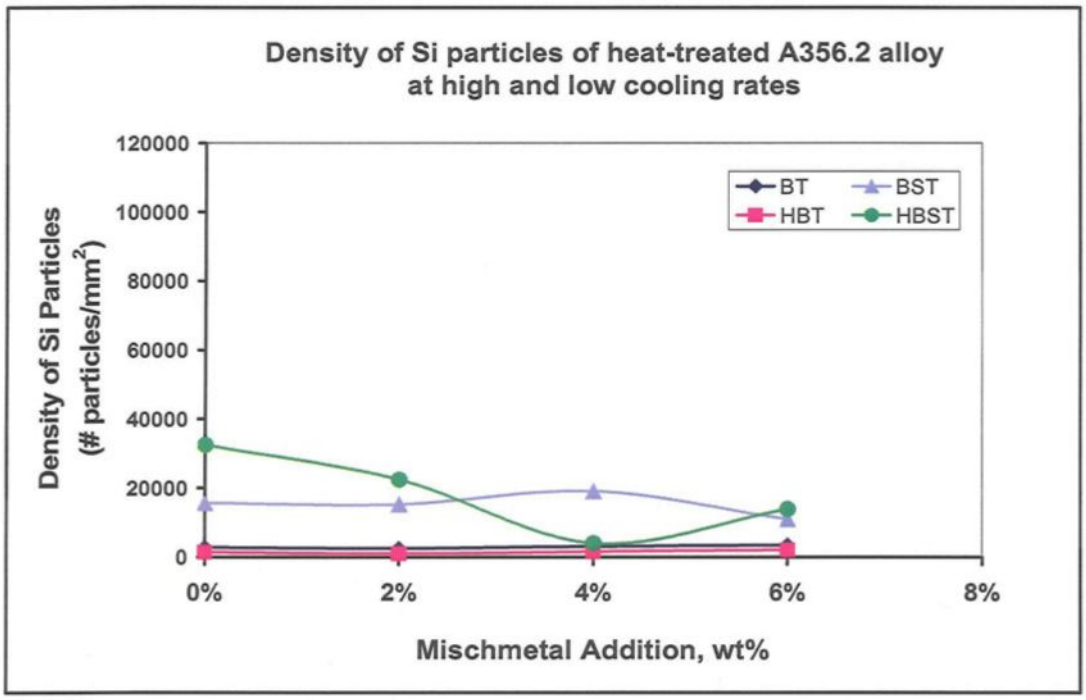

(b)

Figure 4.12 Si particle density of various A356.2 alloy samples obtained at the two cooling rates: (a) as-cast, and (b) heat-treated conditions.

4.2.3 A413.1 Alloy

4.2.3.1 Effect of high cooling rate

Table 4.5 represents the Si particle characteristics observed in the as-cast condition and after solution heat treatment.for the various A413.1 alloy samples solidified under high cooling rate conditions (i.e. DAS ~ 40 μm).

Table 4.5 Si particle characteristics of various A413.1 alloy samples obtained at high cooling rate (DAS~ 40μm)

Alloy Code	Misch Metal wt.%	Particle Area (μm^2)		Particle Length (μm)		Roundness Ratio (%)		Aspect Ratio (%)		Density (particles/ mm^2)
		Av.	SD	Av.	SD	Av.	SD	Av.	SD	
C*	0%	15.7	34.2	7.4	10.9	54.2	31.4	3.1	1.9	6007
	2%	14.8	32.7	7.3	10.2	57.5	30.8	2.6	1.5	6123
	4%	11.4	28.5	5.5	8.7	64.4	30.5	2.2	1.1	9594
	6%	7.8	19.6	4.5	6.0	67.5	27.3	2.0	0.9	16929
CS	0%	1.1	1.3	1.5	1.0	80.4	18.0	1.7	0.7	107279
	2%	1.6	1.7	2.0	1.5	74.0	21.2	1.8	0.7	81299
	4%	2.1	2.4	2.4	1.9	69.9	23.7	1.9	0.8	71596
	6%	1.5	1.6	1.8	1.9	82.4	15.8	1.7	0.7	67620
CT	0%	20.1	40.9	9.3	11.1	53.2	29.6	3.2	1.9	4648
	2%	19.6	39.6	8.5	1.6	59.5	29.9	2.6	1.6	5153
	4%	19.3	39.1	7.9	10.6	63.6	27.9	2.3	1.3	5412
	6%	16.3	34.0	6.9	9.2	66.4	27.0	2.2	1.2	6885
CST	0%	1.81	2.4	2.8	1.8	69.4	23.4	1.9	0.8	67444
	2%	2.8	21.8	2.4	1.8	79.0	17.0	1.7	0.6	47109
	4%	3.0	3.0	2.5	1.8	79.2	16.9	1.7	0.6	40919
	6%	3.8	4.1	2.9	2.3	74.3	19.4	1.8	0.7	31421

*C=A413.1 alloy, S= Strontium modified, and T= solution heat-treat

As can be observed from Table 4.5, in the non-modified as-cast C alloys the eutectic Si particles possess large sizes with an average particle area of 15.7 μm^2. With the addition of mischmetal, the Si particles begin to undergo modification. This is clearly seen at 4 and 6 wt% mischmetal additions, where the the Si particles size is reduced considerably, with a corresponding increase in the particle density by about 1.8 to 2.5 times, respectively.

With the addition of Sr to the C alloy, the Si particles become well modified, the average particle area and aspect ratio being reduced from size 15.7μm^2 and 3.07 to fine 1.05μm^2 and 1.75, as seen in Table 4.5 and Figure 4.13(a). The roundness ratio increases by about 48% and the particle density reaches its maximum - almost 18 times that observed in the non-modified C0 alloys, showing that the Sr-modified C alloys exhibit the highest level of Si particle modification compared with A and B alloys.

Comparing the Si particle size in Figure 4.13(a) with that in (b), it can be observed that the addition of mischmetal up to 6 wt % to the Sr-modified CS alloys decreases the effect of Sr modification. In Table 4.5, this is most clear at 4 wt% mischmetal, but the Si particles retain their improved morphology (roundness and aspect ratio). Due to the interaction between mischmetal and Sr to form a variety of intermetallic phases (i.e., Al_4Sr and Al_2Si_2Sr),[27] the amount of Sr available for achieving an acceptable degree of modification is reduced.

From Table 4.5, it can observed that after subjecting the non-modified C alloy to solution heat treatment process at 495°C for 8h, the Si particles coarsen (increase in area and length), but it maintain the same morphology (same roundness and aspect ratio).

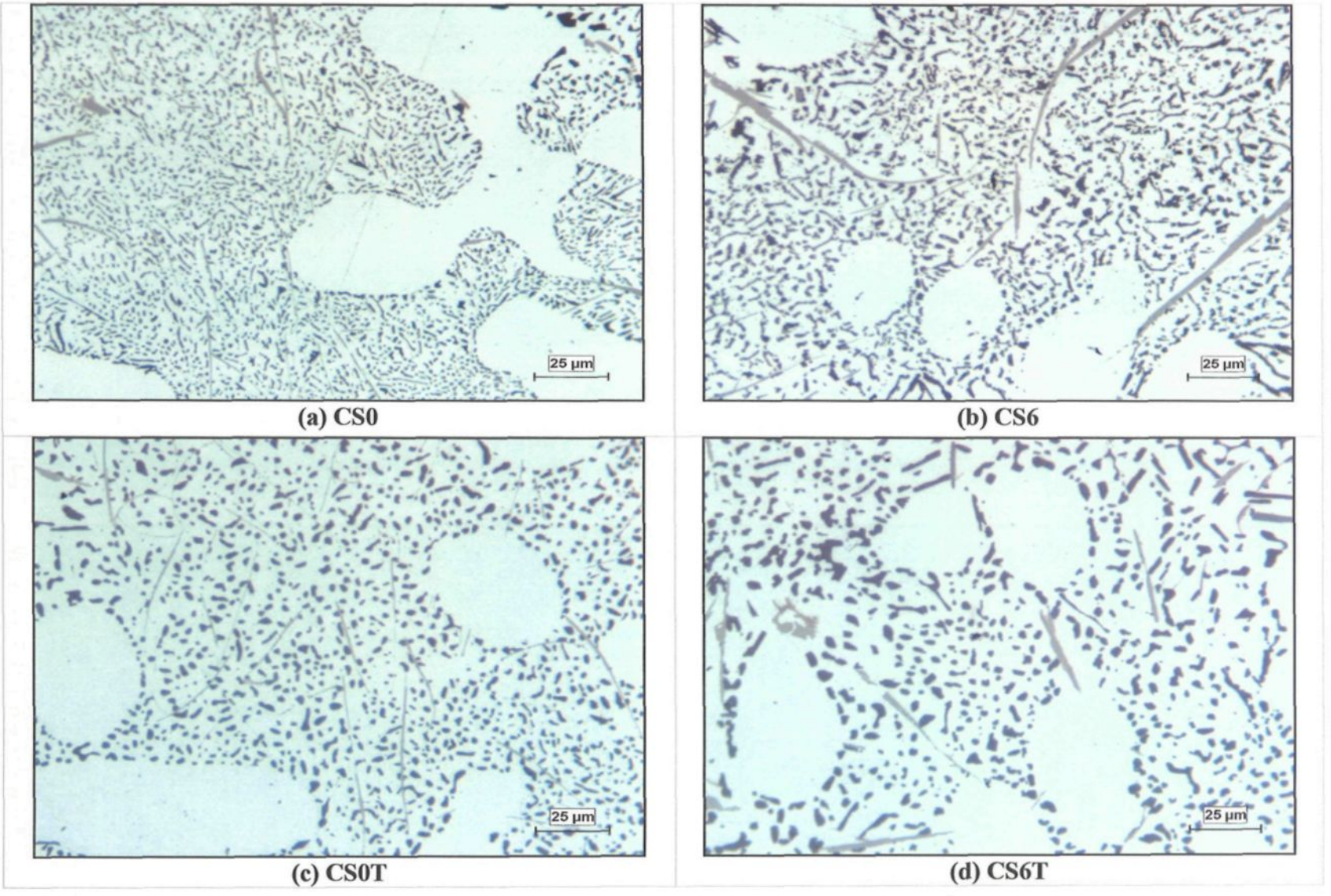

Figure 4.13 Effect of solution heat treatment and mischmetal (MM) on the Si particle morphology of Sr-modified A413.1 alloy samples obtained at high cooling rate: (a) 0 wt% MM and (b) 6 wt% MM as-cast, and (c) 0 wt% and (d) 6 wt% MM heat-treated samples.

The decrease in the particle density (by about 22 %), indicates that the coarsening rate is more dominant than the spheroidization rate in the non-modified CT alloys, in agreement with the theoretical and experimental investigations that carried out by Apelian *et al.* [7] and Zhu *et al.*[72] on the effect of heat treatment on the Si particles morphology.

For the CT alloy containing up to 6 wt% mischmetal, a slight degree of modification is observed, compared to the CT alloy free of mischmetal, as seen in Table 4.5. The decrease in the particle length and aspect ratio, as well as the increase in the particle density and roundness supports this. As the coarsening of the Si particles during solution treatment is quite pronounced, the modification due to mischmetal addition is not that apparent.

The response of the Sr-modified CST alloys to solution heat treatment is different than that of the non-modified CT alloys. Due to the fact that the Si particles in the as-cast CS alloy are already fine and rounded (see Table 4.5), they begin to coarsen rapidly during solution heat treatment, with the average area increasing from 1.05 μm^2 to 1.8 μm^2 and the average length from 1.55 μm to 2.17 μm, as can also be seen from a comparison of Figure 4.13(a) and (c). The decrease in the particle density (by about 38%) indicates the commencement of the coarsening stage. These results reveal the fact that the initial eutectic silicon structure controls the response of the non-modified and Sr-modified C alloys to solution heat treatment process.

Again during solution heat treatment and as it is observed in the as-cast Sr-modified CS alloy with further mischmetal addition, the Si particles coarsen and their area increases from 1.8 μm^2 to 3.8 μm^2 as shown in Table 4.5, while the particle density decreases by about 53%. The roundness and aspect ratio, however, are only affected slightly. This is due

to the effect of heat treatment, as well as the interaction between Sr and mischmetal. As in the case of the other alloys, the combined effect of Sr and mischmetal in the Sr-modified C alloys negates the degree of Si particle modification achieved in both as-cast and solution heat-treated conditions.

4.2.3.2 Effect of low cooling rate

Table 4.6 lists the Si particle characteristics observed for the various A413.1 alloy samples in the as-cast condition and after solution heat treatment and solidified under low cooling rate conditions (DAS ~120 μm).

With respect to the alloy codes, the prefix H represents the low cooling rate condition that provided a high DAS value. The low cooling rate condition was obtained by allowing the casting to cool slowly inside the furnace. The other letters C, S and T represent the same alloy, strontium and solution treatment conditions as those shown in Table 4.5

In general, the effect of cooling rate is not so significant on the morphology as on the size of the eutectic silicon particles, where the Si particle size increases as the cooling rate decreases.

As can be seen in Table 4.6, the eutectic Si particles are large (average particle area 19.7 μm^2) in the non-modified HC alloy, owing to the low cooling rate provided high dendrite arm spacing (DAS of ~120 μm). With the addition of 6 wt% mischmetal, the non-modified HC alloys display some change in the Si particle characteristics

Table 4.6 Si particle characteristics of various A413.1 alloy samples obtained at low cooling rate (DAS ~ 120μm)

Alloy Code	Misch Metal wt.%	Particle Area (μm^2)		Particle Length (μm)		Roundness Ratio (%)		Aspect Ratio (%)		Density (particles/ mm^2)
		Av.	SD	Av.	SD	Av.	SD	Av.	SD	
HC*	0%	19.7	35.1	11.7	16.0	49.2	33.5	3.5	2.4	5790
	2%	19.5	48.9	7.5	13.1	63.4	33.3	2.7	1.7	6704
	4%	19.7	57.9	6.6	13.7	68.6	13.7	2.4	1.6	6468
	6%	26.1	68.2	7.7	15.2	69.4	31.4	2.1	1.2	4945
HCS	0%	4.3	4.1	3.1	2.3	76.1	19.1	1.8	0.7	28459
	2%	3.7	3.8	2.9	2.3	71.5	20.5	1.9	0.8	31011
	4%	12.8	22.6	9.3	13.2	62.5	30.9	2.1	0.9	3270
	6%	10.1	21.1	6.3	10.0	70.1	30.1	1.9	0.9	4538
HCT	0%	43.3	89	12.7	19.1	60.7	30.8	2.7	1.6	2708
	2%	32.2	53	12.3	15.5	56.3	33.1	2.9	1.9	3645
	4%	41.7	101	10.9	21.2	67.4	33.4	2.5	1.8	2752
	6%	35.8	83	9.5	17.4	70.6	31.9	2.2	1.4	3604
HCST	0%	2.1	2.0	2.0	1.4	81.2	16.0	1.6	0.6	68217
	2%	5.1	5.4	3.2	2.6	77.7	18.5	1.7	0.7	29999
	4%	8.2	9.6	4.7	4.4	70.1	22.5	2.0	0.9	16040
	6%	6.9	15.5	4.9	8.5	74.1	28.3	1.9	0.9	4949

*C= A413.1 alloy, S= Strontium modified, T= solution heat-treated, and H= slowly cooled inside the furnace

Figure 4.14(a) depicts the microstructure of the as-cast Sr-modified HCS alloy. With the addition of Sr, the average Si particle area is reduced from 19.7μm^2 in the non-Sr-modified HC alloy to 4.26 μm^2.

The change in morphology is reflected by the corresponding changes in the aspect ratio and roundness values, which decrease from 3.5 to 1.8, and increase from 49% to 76%,

respectively, as shown in Table 4.6. Obviously, the modification effect of Sr is higher at high cooling rate conditions than that obtained at low cooling rate conditions.

As seen from Table 4.6, the addition of 2 wt% mischmetal to the Sr-modified HCS alloy appears to ameliorate the modification effect, judging mostly from the increase in the Si particle density, and the slight changes observed in the particle size. Increasing the amount of mischmetal addition to 4 and 6 wt% leads to coarsening of the Si particles, instead. A comparison of the Si particles size and morphology shown in Figures 4.14(a) and 4.14(b) shows this effect clearly. As seen from Table 4.6, a greater amount of coarsening is observed in the 4 wt% MM-containing alloy. This is attributed to the interaction between Sr and mischmetal which weakens the modification effect of Sr.

With solution heat treatment (495°C/8h), the Si particles coarsen considerably in the non-modified HCT alloy (*cf.* 43 μm^2 with 19.7μm^2 for the HC alloy). As the average length is increased only slightly, this indicates that the increase in the particle size (area) may be the result of an increase in the width of the Si particles. The coarsening rate of the silicon particles is higher than the spheroidization rate for the non-modified HCT alloys. In spite of the fact that the solution heat treatment temperature (495°C) is not so high as that used for A356.2 alloy (540°C) to promote Si particle coarsening, however, the high content of Si in the A413.1 alloy provides many more smaller particle that can dissolve into the large particles. This explains the large decrease in the particle density i.e., by about 53%, of HCT alloy compared to the HC alloy (Table 4.6). Thus, the initial as-cast eutectic Si structure governs the behavior of non-modified A413.1 alloys during solution heat treatment.

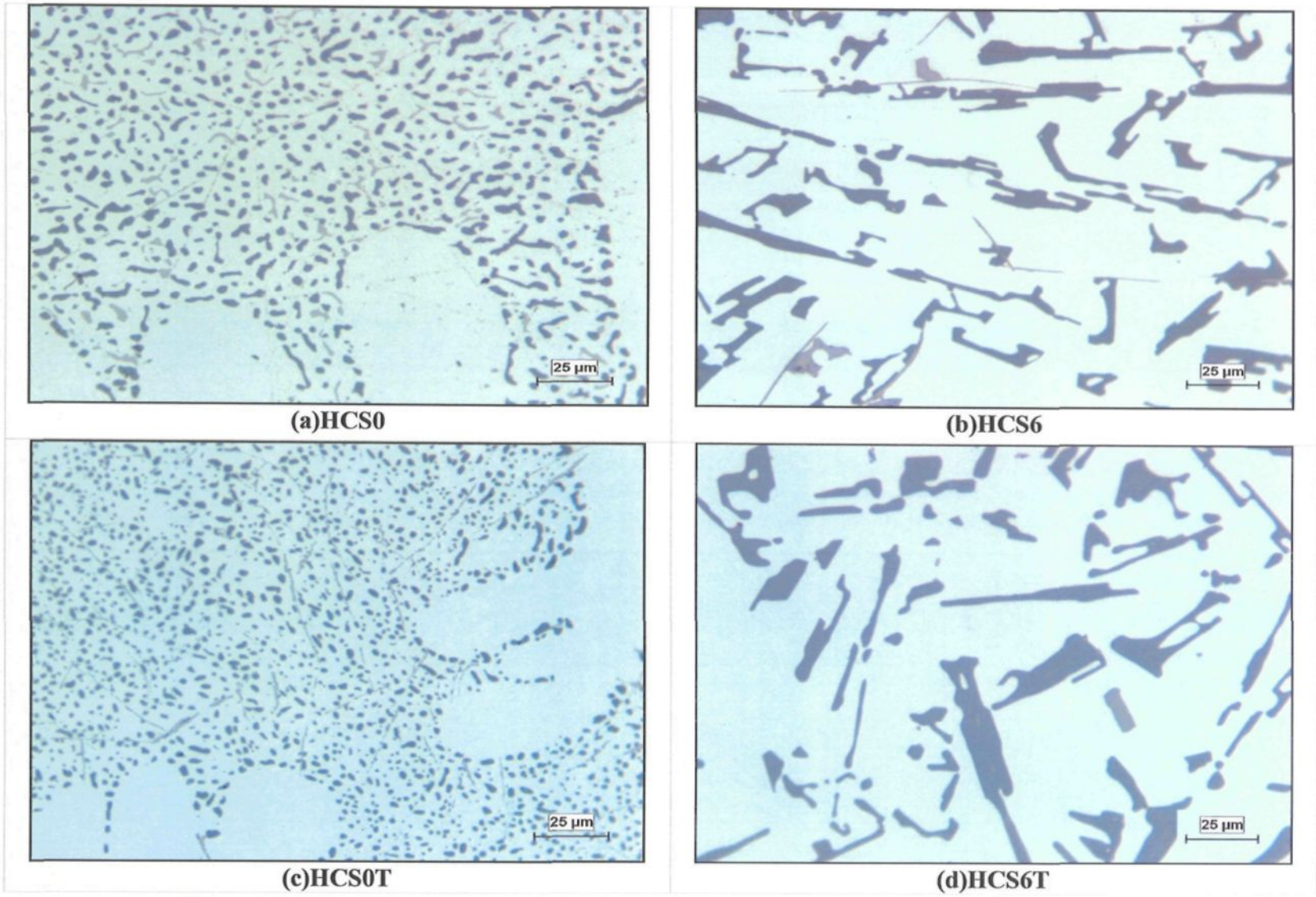

Figure 4.14 Effect of solution heat treatment and mischmetal (MM) on the Si particle morphology in the Sr-modified A413.1 alloy samples obtained at low cooling rate: (a) 0 wt% (b) 6 wt% MM as-cast, and (c) 0 wt %, (d) 6 wt % MM heat-treated conditions.

In the Sr-modified HCS alloys, during solution heat treatment, the Si particles undergo fragmentation and spheroidization, resulting in more rounded Si particles with a roundness of 81% and a low aspect ratio of 1.6 (see Table 4.6). A comparison of Figure 4.14(a) with 4.14(c) also makes this clear. The increase in particle density by about 1.5 times as a result of the decrease in the average Si particles area by 51% is a clear evidence that the solution heat-treated Sr-modified HCST alloy exhibits a higher spheroidization rate.

For the same HCST alloys containing mischmetal, in comparing the optical micrographs of Figures 4.14(c) and (d), it can be observed that the Si particles coarsen during solution heat treatment for 6 wt% mischmetal addition. Although the addition of mischmetal partially improves the eutectic Si particle characteristics, at the same time, the solution heat treatment process offsets and weakens the effect.

It is interesting to note, however, that for 4 and 6wt% mischmetal additions to A413.1 alloy, solution heat treatment provides better Si particle characteristics, i.e., smaller particle sizes to the HCST alloys than the HCS alloys in the as-cast condition. Figures 4.15 through 4.17 summarize the results shown in Tables 4.5 and 4.6 for the Si particle area, length and density values exhibited by the various A413.1 (C) alloy samples for the two cooling rates studied in both the as-cast and heat treated conditions.

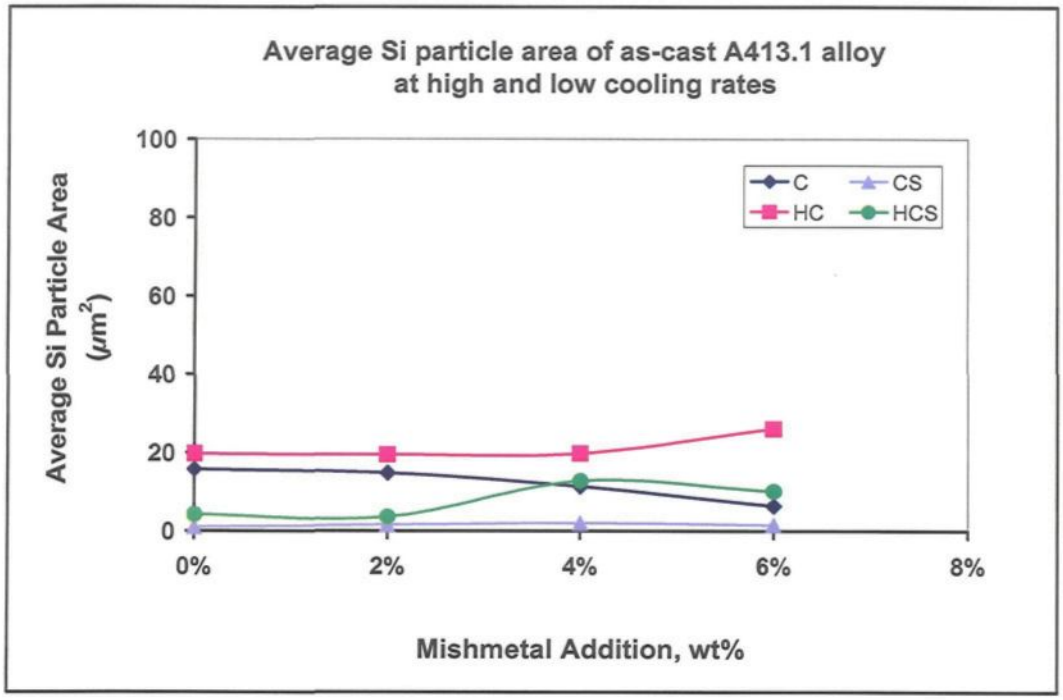

(a)

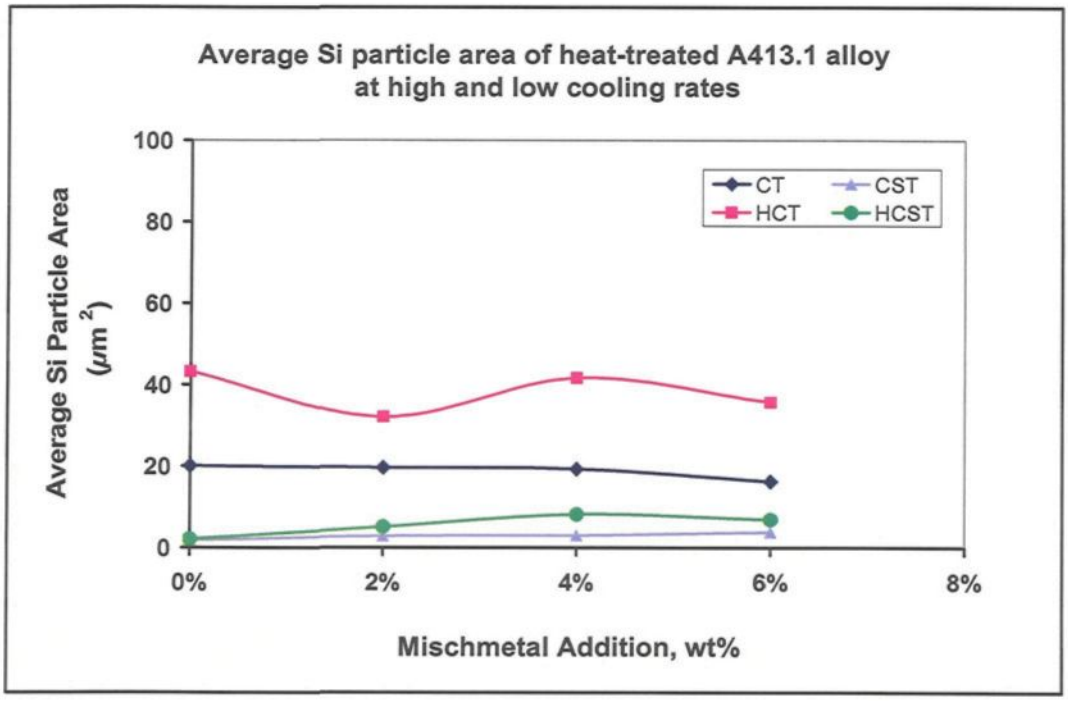

(b)

Figure 4.15 Average Si particle area in various A413.1 alloys obtained at the two cooling rates: (a) as-cast, and (b) heat-treated conditions.

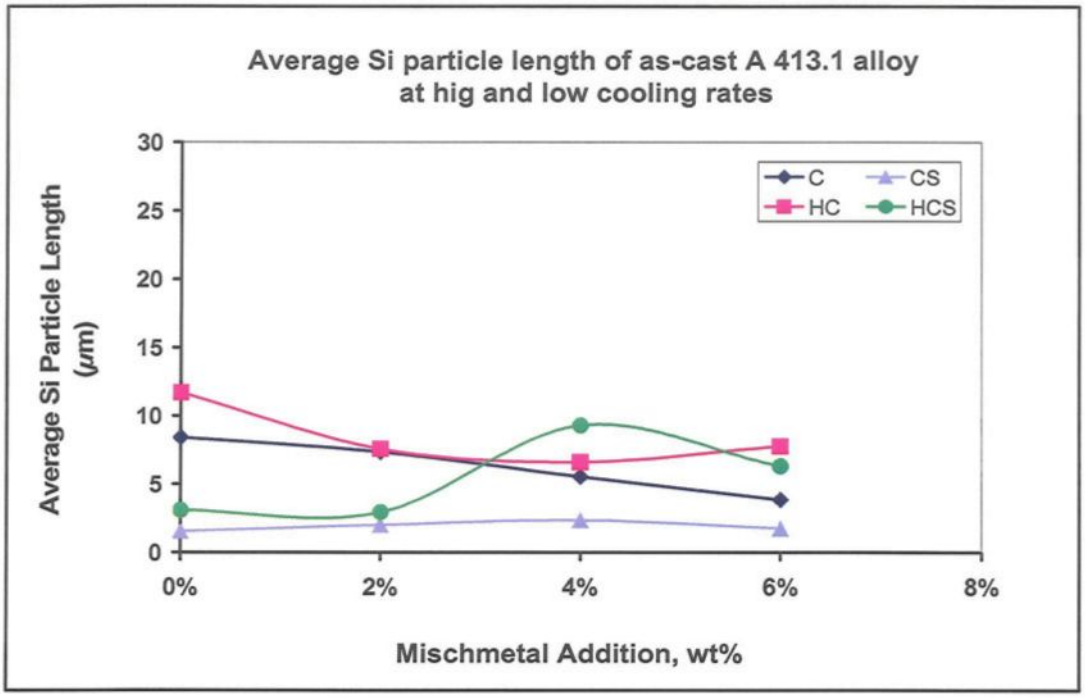

(a)

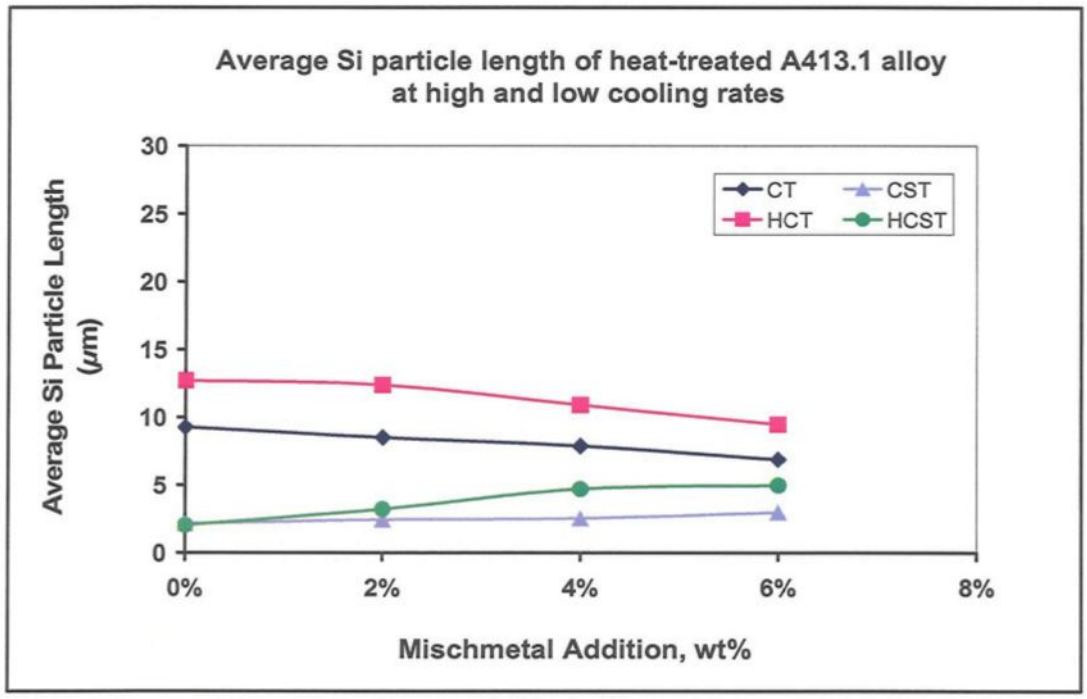

(b)

Figure 4.16 Average Si particle length in various A413.1 alloys obtained at the two cooling rates: (a) as-cast, and (b) heat-treated conditions.

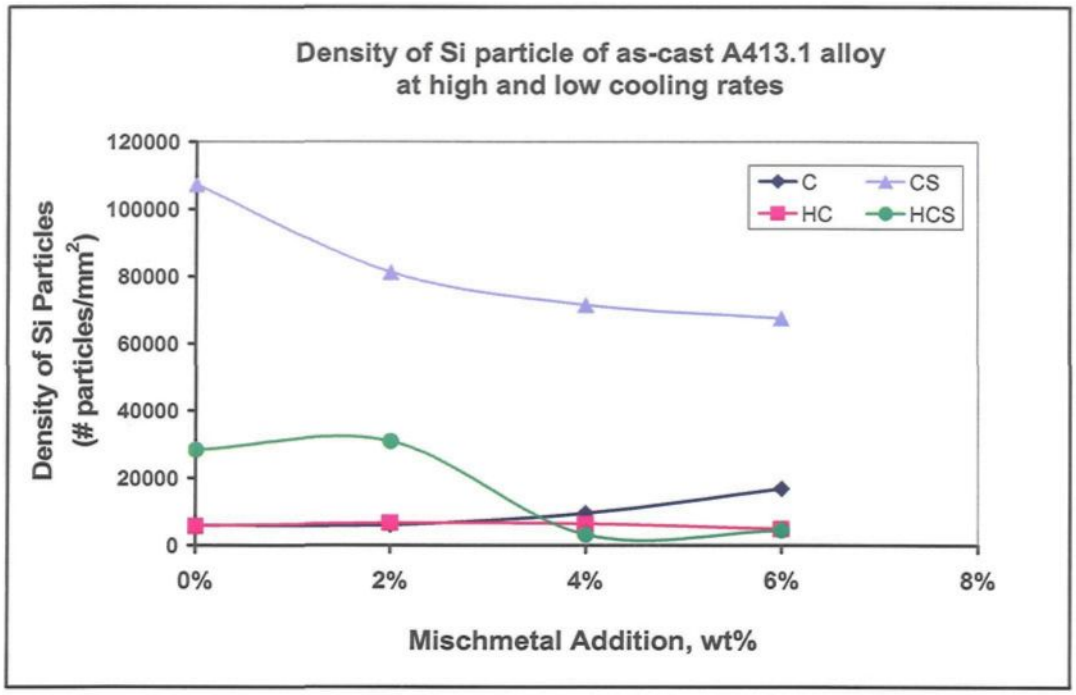

(a)

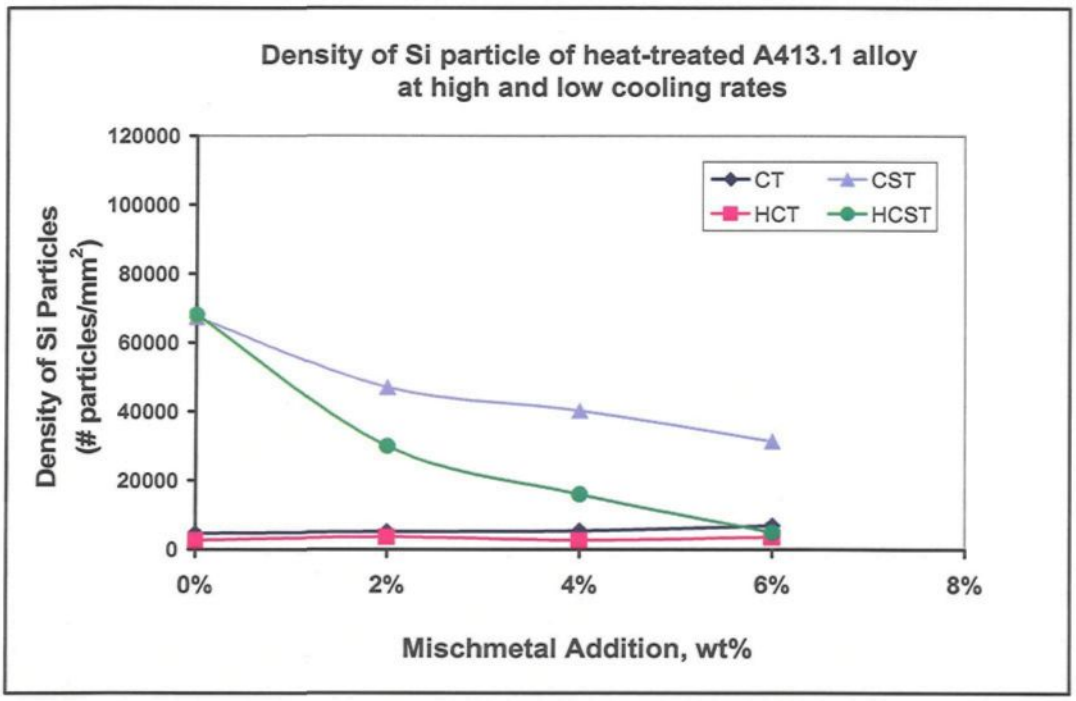

(b)

Figure 4.17 Si particle density of various A413.1 alloy samples obtained at the two cooling rates: (a) as-cast, and (b) heat-treated conditions.

CHAPTER 5

CHARACTERIZATION OF INTERMETALLICS

CHAPTER 5

CHARACTERIZATION OF INTERMETALLICS

5.1 INTRODUCTION

In aluminum alloys, the aluminum can form different types of intermetallic phases with the alloying elements present in the alloy (such as Si, Mg, Fe, Cu, and Mn). In fact these intermetallic phases are solid solutions that usually possess a range of compositions and are observed to precipitate at different temperatures. [73] However, they can be expressed by definite chemical formulae. [73, 74] They also have a tendency for dissolving other alloying elements. [75]

In the present study, it was expected that the addition of mischmetal to the Al-Si alloys investigated would results on the precipitation of mischmetal-containing intermetallics, in addition to those already expected to occur on account of the alloying elements contained in these alloys. To characterize and quantify intermetallics, the surface area fraction of all intermetallics was measured using Electron Probe Microanalysis (EPMA). As it was difficult to separate the different intermetallics, the *total* surface fraction was measured. The identification of intermetallics was carried out using wavelength dispersive spectroscopy (WDS) and X-ray imaging. These results are presented in this chapter.

5.2 SURFACE FRACTION OF INTERMETALLICS

In order to determine the total surface fraction of all intermetallic phases observed, quantitative measurements were carried out on samples obtained from the three alloys under both high and low cooling rate conditions. By comparing the amounts obtained for each MM addition level with that observed in the samples with no mischmetal addition, the effect of mischmetal addition as well as that of the alloying elements (chemical composition) on the amount of intermetallics obtained in the three alloys could be determined.

5.2.1 Effect of High Cooling Rate

In general, the surface fraction of intermetallic phases in the unmodified and Sr-modified alloys increases with increasing mischmetal addition, in both as-cast and heat-treated conditions, as shown in Figure 5.1. This is attributed to the high chemical affinity of mischmetal, which leads to the formation of intermetallic phases containing mischmetal and other alloying elements (i.e., Cu, Mg, Si, Ti, and Sr).

In the A319.1 alloy, it is clear that the surface fraction of intermetallics in the as-cast condition is a little bit higher than that in heat-treated condition for both non-modified and Sr-modified alloys taking into consideration the standard deviation. Figure 5.1(a) reveals that the as-cast Sr-modified alloys exhibit higher surface fractions of intermetallics. This is attributed to the formation of the Al_2Cu copper intermetallic phase and to the reaction of mischmetal with Al, Si, Sr and Cu to form different intermetallics.

At the 6 wt% level of mischmetal addition, the surface fraction of intermetallics in the non-modified and Sr-modified A319.1 heat-treated alloys display the same level as in the as-cast Sr-modified condition (Figure 5.1(a)). This is ascribed to the fact that in the as-cast alloy (6 wt%), mischmetal combines with all the copper in the melt during solidification, resulting in a low amount of copper available to form the Al_2Cu intermetallic phase.

Figure 5.1(b) depicts the total surface fraction of intermetallics observed in A356.2 alloy. Again it is found that as the addition of mischmetal is increased, the total surface fraction of intermetallics also increases, with the as-cast alloys showing higher levels of intermetallics compared to the heat-treated alloys. This is owing to the fact that the Mg_2Si phase in the heat-treated alloys is completely dissolved during solution heat treatment (at 540°C for 8h), reducing the total surface fraction of intermetallics in the heat-treated alloys.

In the A413.1 alloy, as can be seen from Figure 5.1(c), the same observations are noted as in the A356.2 alloys; however, compared to A319.1 and A356.21 alloys, the A413.1 alloy exhibits much higher levels of intermetallics.

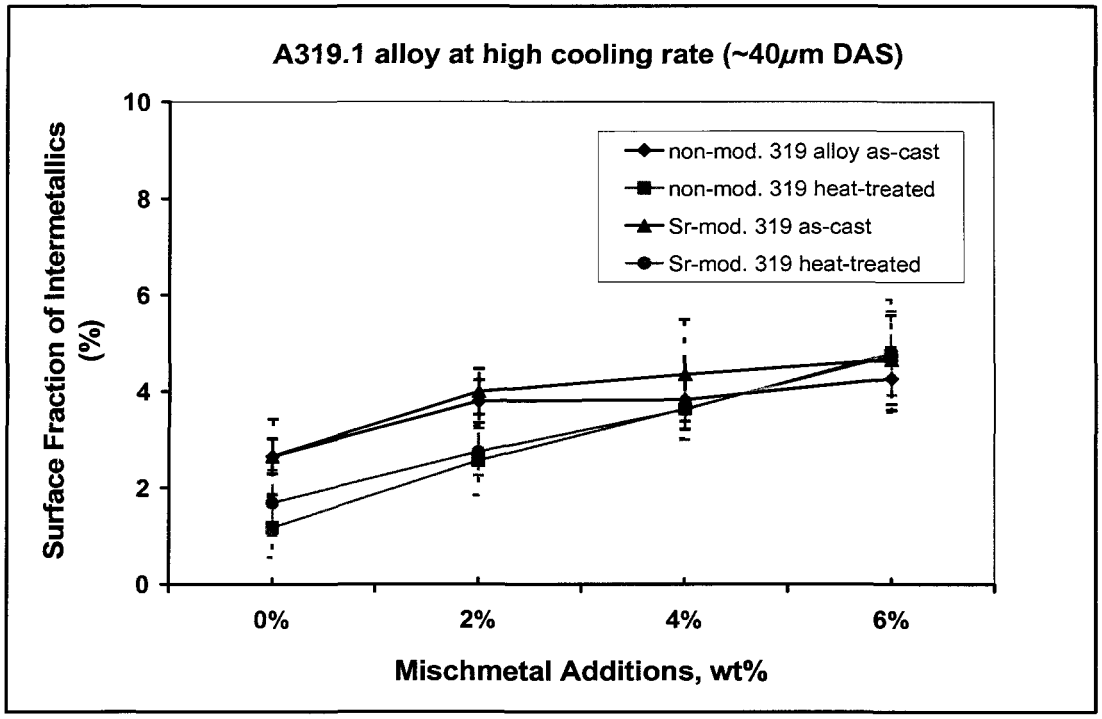
A319.1 alloy at high cooling rate (~40μm DAS)
Surface Fraction of Intermetallics (%)
10
8
6
4
2
0
non-mod. 319 alloy as-cast
non-mod. 319 heat-treated
Sr-mod. 319 as-cast
Sr-mod. 319 heat-treated
0%
2%
4%
6%
Mischmetal Additions, wt%

(a)

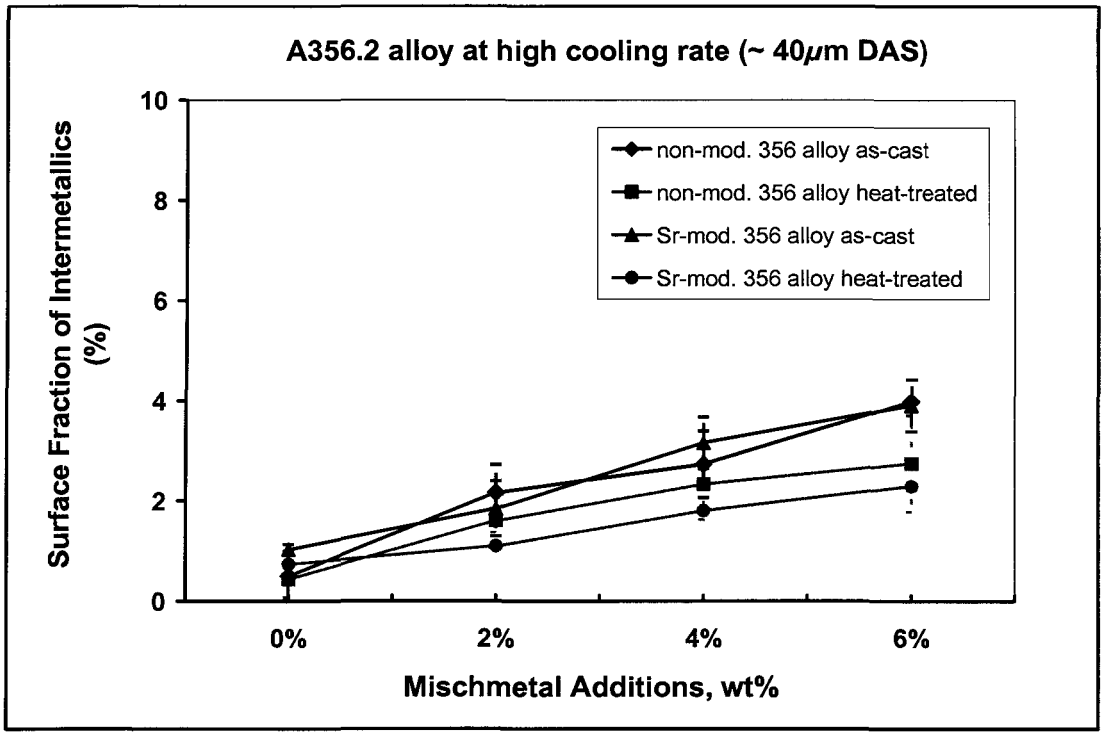
A356.2 alloy at high cooling rate (~ 40μm DAS)
Surface Fraction of Intermetallics (%)
10
8
6
4
2
0
non-mod. 356 alloy as-cast
non-mod. 356 alloy heat-treated
Sr-mod. 356 alloy as-cast
Sr-mod. 356 alloy heat-treated
0%
2%
4%
6%
Mischmetal Additions, wt%

(b)

Figure 5.1

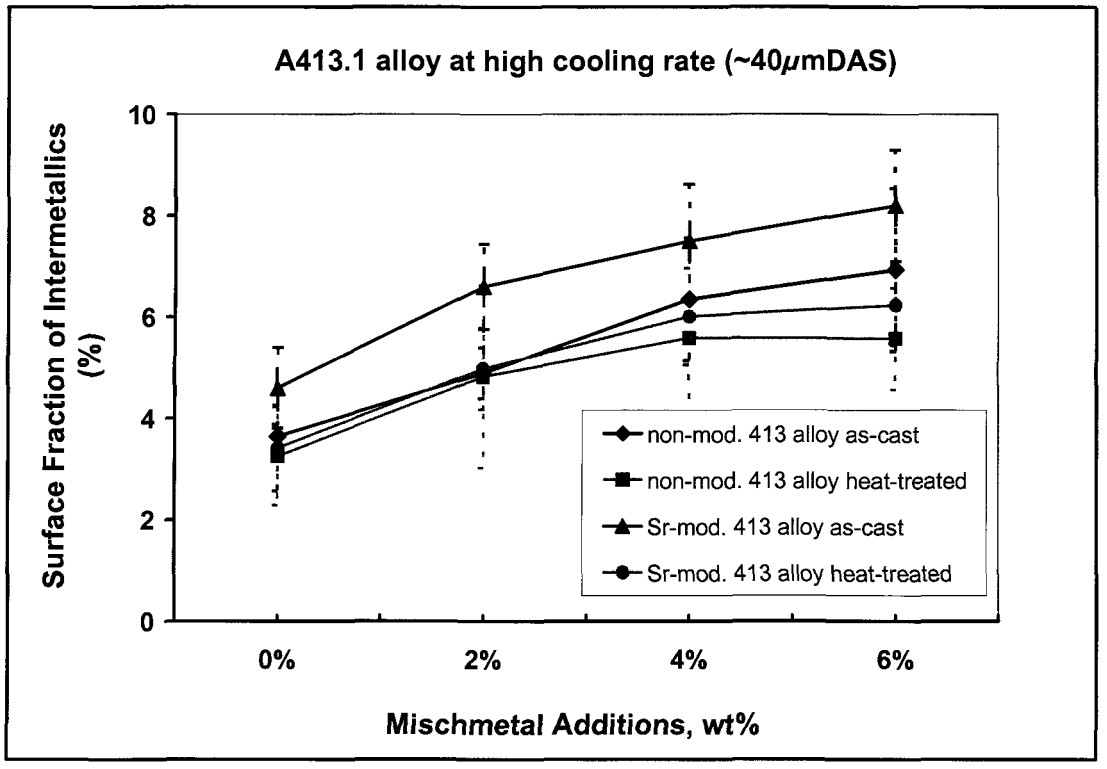

(c)

Figure 5.1 Effect of mischmetal addition, heat treatment and Sr-modification on the total surface fraction of intermetallic phases obtained in (a) A319.1, (b) A356.2, and (c) A413.1 alloys solidified under high cooling rate conditions.

5.2.2 Effect of Low Cooling Rate

Similar to the samples obtained under high cooling rate conditions, the surface fraction of intermetallic phases also increases with increasing mischmetal addition up to 6 wt% in the non-modified and Sr-modified alloy samples obtained at low cooling rates, in both as-cast and heat-treated conditions, as shown in Figure 5.2. However, the total surface fraction of intermetallics obtained is higher in this case, particularly so for the A319.1 alloy (*cf.* Figure 5.2(a) with Figure 5.1(a)). This is expected, due to the longer solidification times involved, allowing the intermetallic phases to grow/coarsen.

It is also clear that the surface fraction of intermetallics is higher in the A319.1 as-cast samples than in the heat-treated samples. At the 6 wt% level of mischmetal addition, the Sr-modified as-cast A319.1 alloy exhibits the highest surface fraction of intermetallics than at all other conditions. This is attributed to the interaction between mischmetal, Al, Si, Cu, and Sr to form varieties of intermetallics, besides the formation of the intermetallic Al_2Cu phase.

In the A356.2 alloy, as can be seen from Figure 5.2(b), all the alloy samples possess approximately the same amount of intermetallics at each level of mischmetal addition. Compared to Figure 5.1(b), the as-cast A356.2 alloy samples show somewhat lower amounts of intermetallics in spite of the slower cooling rate conditions. This could be due the low content of Mg in the A356.2 alloy, as well as, the higher interaction between mischmetal and Mg and thus, leads to reduce the available amount of Mg to form the Mg_2Si intermetallic phase.

In the case of A413.1 alloy, the Sr-modified as-cast samples exhibit the lowest surface fractions of intermetallics at low level of mischmetal (0, 2 wt%) addition, Figure 5.2(c), in contrast to what is observed under the high cooling rate conditions (Figure 5.1(c)). At 6 wt % mischmetal addition, the surface fraction of intermetallics in the A413.1 alloys is more or less the same, irrespective of the alloy conditions, as shown in Figure 5.2(c).

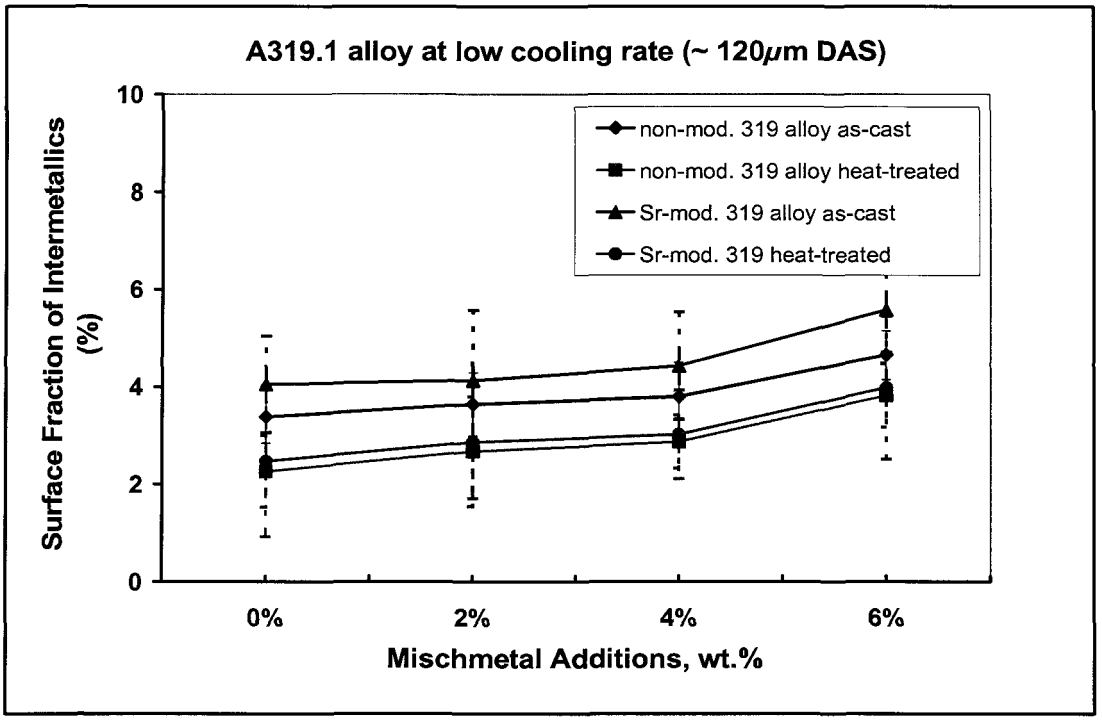
A319.1 alloy at low cooling rate (~ 120μm DAS)
Surface Fraction of Intermetallics (%)
10
8
6
4
2
0
non-mod. 319 alloy as-cast
non-mod. 319 alloy heat-treated
Sr-mod. 319 alloy as-cast
Sr-mod. 319 heat-treated
0%
2%
4%
6%
Mischmetal Additions, wt.%

(a)

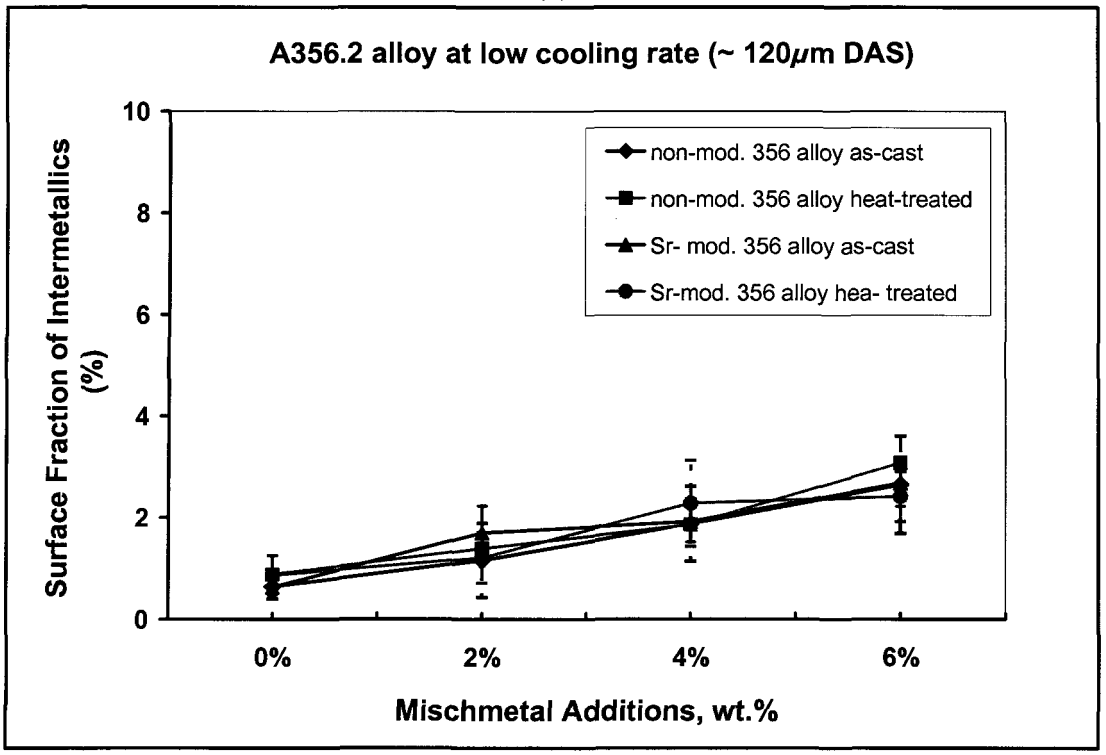
A356.2 alloy at low cooling rate (~ 120μm DAS)
Surface Fraction of Intermetallics (%)
10
8
6
4
2
0
non-mod. 356 alloy as-cast
non-mod. 356 alloy heat-treated
Sr- mod. 356 alloy as-cast
Sr-mod. 356 alloy hea- treated
0%
2%
4%
6%
Mischmetal Additions, wt.%

(b)

Figure 5.2

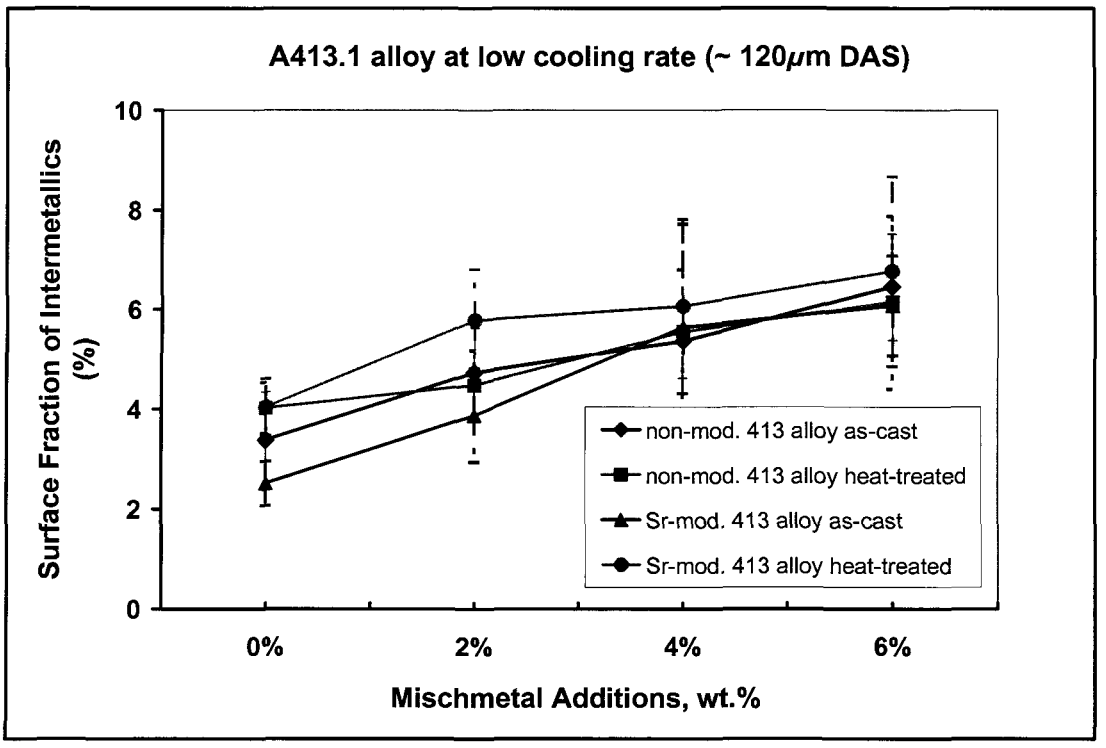

(c)

Figure 5.2 Effect of mischmetal addition, heat treatment and Sr-modification on the total surface fraction of intermetallic phases obtained in (a) A319.1, (b) A356.2, and (c) A413.1 alloys solidified under low cooling rate conditions.

5.3 IDENTIFICATION OF INTERMETALLICS

Quantitative measurements (based on the average of at least 5 points for each phase) were carried out using wavelength dispersion spectroscopic (WDS) analysis to determine the chemical compositions of the various intermetallic phases observed in the A319.1, A356.2 and A413.1 alloy samples, obtained under both high and low cooling rate conditions. The effect of mischmetal addition on the morphology and type of precipitated intermetallics and the effect of cooling rate were investigated, as well as the influence of

chemical composition of the alloy on the mischmetal-containing intermetallics. The results are presented according to alloy type and cooling rate condition in the following sections.

5.3.1 A319.1 Alloy

A319 alloy essentially belongs to the hypoeutectic Al-Si alloy system which has two main solidification stages: formation of the aluminum-rich α-Al dendrites, followed by development of the Al-Si eutectic. However, the presence of additional alloying elements such as Cu and Mg, as well as impurities such as Fe and Mn, leads to the formation of more complex intermetallic phases. Accordingly, the as-cast microstructure of A319 alloy presents many intermetallic phases in addition to the Al and Si phases. The formation of these phases implies that successive reactions occur during solidification (as the temperature decreases), resulting in the precipitation of these phases. [35]

The addition of mischmetal (MM) to the A319.1 alloy (viz., Ce, La, Nd and Pr) results in the formation of several intermetallics by the reaction of these rare earth metals with Al, Si, Cu and Ti. This is attributed to the high chemical affinity of mischmetal. [61]

5.3.1.1 Intermetallics Observed Under High Cooling Rate Conditions

The various intermetallics that were observed in the A319.1 alloy samples obtained under high cooling rate conditions were identified using WDS analysis. Figure 5.3 presents some interesting examples of these intermetallics, while Table 5.1 lists the average chemical compositions of the intermetallics identified by numbers in the figure.

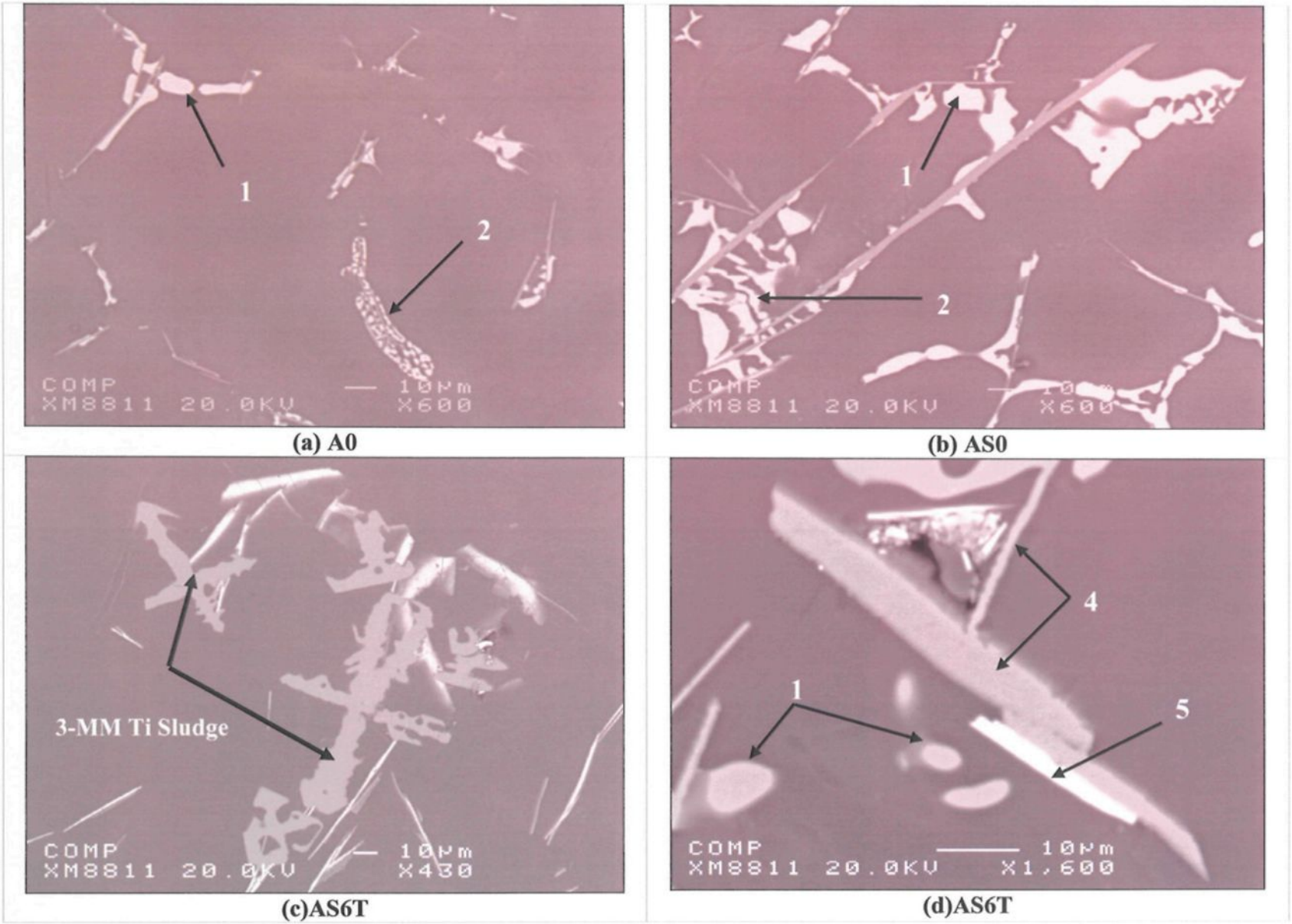

Figure 5.3 Backscattered images of A319.1 alloy samples containing (a, b) 0 wt % and (c, d) 6wt % mischmetal, depicting the intermetallic phases observed at the high cooling rate conditions (T: heat-treated samples).

Table 5.1 Chemical compositions of the intermetallic phases observed in A319.1 alloy containing 0 wt% and 6 wt% mischmetal (WDS analysis, Figure 5.3)

Phase #	Element	wt.% Av.	at.% Av.	Calculated formula	Shape & Colour	Suggested Formula
1	Al	57.65	71.67	Al_3Cu	Block-like	Al_2Cu
	Cu	45.43	24.07			
	Si	2.24	2.66			+ excess of Al
	Total	105.2	98.4		Pink	
2	Al	48.61	66.89	Al_2Cu	Eutectic-like	Al_2Cu
	Cu	51.1	29.86			
	Si	0.77	1.02			
	Total	100.4	97.77		Pink	
3	Al	65.65	83.8	$Al_{40}(CeLaPrNd)_2Ti_4CuSi$	MM-Ti sludge	$Al_{40}MM^*{}_2Ti4CuSi^{**}$
	Si	1.18	2.12			
	Ti	10.21	7.41			
	Cu	3.23	1.89	**(Ce:La=4.1:1)**	grey	
	Ce	12.07	2.87			
	La	2.44	0.7			
	Pr	1.87	0.5			
	Nd	0.61	0.16			
	Total	97.26	99.45			
4	Al	52.2	70.45	Al_8FeCu_2	Platelet	Al_7FeCu_2
	Cu	34.84	19.96			
	Fe	13.36	8.71		grey	
	Total	100.4	99.12			
5	Al	34.8	56.96	$Al_{10}(CeLaPrNd)_2Cu_4Si_2$	Plate-like	Al5MM*Cu2Si**
	Si	7.18	11.28			
	Cu	30.46	21.17			+
	Ce	13.6	4.28	**(Ce:La=1.8 :1)**	white	**0.45wt% Sr**
	La	7.43	2.36			
	Pr	3.17	0.99			
	Nd	1.25	0.38			
	Sr	**0.45**	**0.25**			
	Total	98.34	97.67			

*MM:mischmetal, **Al could be higher than the actual content due to the small size of the examined particles

Copper intermetallic phases

Copper has a limited solid solubility in aluminum, where it can reach to maximum value of ~ 0.01wt% at room temperature. This solubility can be increased to 5.7% by

increasing the temperature to 540°C. During solidification of A319.1 alloy, copper forms the Al_2Cu intermetallic, which can precipitate in block-like form, or as the ($Al+Al_2Cu$) eutectic, or a mixture of both. The eutectic form is finer in nature.

Samuel *et al.* [76, 77] reported that the shape of the intermetallic Al_2Cu phase depends mainly on the cooling rate and the modification conditions. Owing to the low melting point of the Al_2Cu phase (495°C), localized incipient melting can occur at the grain boundaries when the solution temperature exceeds 495°C, leading to the formation of shrinkage cavities during the quenching step, following solution treatment. To avoid such incipient melting, the solution temperature should be maintained at a temperature lower than that of the melting point of Al_2Cu phase (495°C).

Sokolowski *et al.* [78] suggested a two-stage solution heat treatment process to overcome the problem of localized melting, where the alloy is subjected to a second solution treatment at a temperature above 495°C, following the conventional solution treatment.

As can be seen from the backscattered images in Figure 5.3(a) and (b) and Table 5.1, the Al_2Cu intermetallic phase is observed to precipitate in the form of both block-like and eutectic-like forms at the high cooling rate conditions (~40μm DAS) with approximately the same chemical composition. The Al_2Cu phase is observed to nucleate on the coarse Si platelets in the non-modified alloys, as can be seen clearly in the optical micrograph of Figure 4.1(a).

In the Sr-modified alloy, the Al_2Cu phase is observed to mostly precipitate in the block-like form due to the effect of strontium in causing segregation of the copper phase

away from the Al-Si eutectic areas. The modified Si particles also act as nucleation sites for the precipitation of the block-like Al_2Cu phase. These observations confirm the findings of Samuel *et al.*,[76] who studied the factors controlling the type and morphology of the copper phase in 319 aluminum alloy. They also reported that the copper phase precipitates mostly in the form of the fine eutectic phase ($Al+Al_2Cu$) at high cooling rates.

Due to the presence of a low Fe content (0.12-0.2%) in the alloy, the iron reacts with aluminum and copper to form a Cu-Fe intermetallic (Al_7CuFe). The Al_7CuFe phase is observed to precipitate in the form of grey plate-like particles (phase #4), as shown in Figure 5.3(d).

Mischmetal-containing intermetallic phases

The combination of rare earth elements such as Ce, La, Pr, and Nd in mischmetal leads to the formation of many intermetallic phases with Al, Si and Cu in 319 type alloys. These intermetallics are very hard and highly stable, which makes them hard to dissolve in the aluminum matrix during solution heat treatment.[79]

As Table 5.1 shows, for a high Ce/La ratio of 4.1:1, and due to the high melting point of mischmetal, a grey sludge type of intermetallic $Al_4MM_2Ti_4Cu$ is formed (phase # 3), as shown in Figure 5.3(c). This grey intermetallic sludge settles to the bottom of the melt on account of its high specific gravity.

As the Ce/La ratio decreases, another intermetallic is observed to form (marked phase #5 in Figure 5.3(d)). This intermetallic possesses a shiny white plate-like appearance, with a suggested chemical formula of $Al_5(CeLaPrNd)Cu_2Si$ at a Ce/La ratio of 1.8:1. Due to the interaction of Sr with mischmetal, the presence of Sr in this intermetallic (0.45 wt%,

(which is different than the actual added amount of Sr, 250 ppm, used in the present work) and, hence, its depletion from the Al matrix would leave less Sr in the melt to act as a modifier of the eutectic silicon phase in the alloys containing mischmetal (up to 6 wt%). These observations were substantiated by the measurements of the Si particle characteristics of these samples (reported in Chapter 4).

5.3.1.2 Intermetallics Observed Under Low Cooling Rate Conditions

As mentioned previously, the solidification time has a significance influence on the size and morphology of the copper-containing Al_2Cu intermetallic where, at the low cooling rate condition (~120 μm DAS), the Al_2Cu intermetallic phase tends to precipitate mostly in the form of block-like rather than in the fine eutectic form ($Al+Al_2Cu$), as can be seen in Figure 5.4 which shows the backscattered images of the slowly cooled samples of as-cast and heat-treated AS6 alloy (A319.1 alloy containing 6 wt% mischmetal). Table 5.2 lists the average chemical compositions of the two intermetallic phases observed in this alloy.

Mischmetal Intermetallics

As can be seen from Table 5.2, mischmetal combines with Al, Cu, and Si to form a shiny white plate-like intermetallic phase with a low Ce/La ratio of 1.43:1, marked phase #2 in Figure 5.4. This intermetallic is also observed at high cooling rate (phase #5 in and Table 5.1 and Figure 5.3(d)).

Table 5.2 Chemical compositions of the intermetallic phases observed in A319.1 alloy containing 6wt% mischmetal (WDS analysis, Figure 5.4)

Phase #	Element	wt.% (Av)	at. % (Av)	Calculated formula	Shape&Colour	Suggested Formula
1	Al	48.46	67.1	Al_2Cu	Block-like	Al_2Cu
	Cu	51.49	30.2			
	Si	0.77	1.03		pink	
	Total	100.7	98.33			
2	Al	32.55	50.01	$Al_{10}(CeLaPrNd)_2Cu_4Si_3$	Plate-like	$Al_5MM^*Cu_2Si^{**}$
	Si	8.96	15.38			
	Cu	22.95	19.35			+
	Ce	14.97	5.94	**(Ce : La = 1.43 :1)**	white	**0.3 wt %Sr**
	La	10.71	4.15			
	Pr	4.15	1.53			
	Nd	1.47	0.53			
	Sr	**0.30**	**0.16**			
	Total	96.06	97.05			

*MM:mischmetal, **Al could be higher than the actual content due to the small size of the examined particles

The backscattered image and corresponding X-ray images shown in Figure 5.5 of such a white plate-like particle reveal the presence of Ce, Sr and Cu. The presence of Sr in this intermetallic decreases the amount of Sr available to obtain a full modification effect of the eutectic Si particles in the Al matrix, accounting for the reduced effect of Sr as a modifier in the alloys containing mischmetal. This supports the conclusion that the addition of mischmetal to Sr-modified alloys has a negative effect on the Si particle characteristics. These observations support the eutectic Si particle measurements obtained for these alloys under low cooling rate conditions.

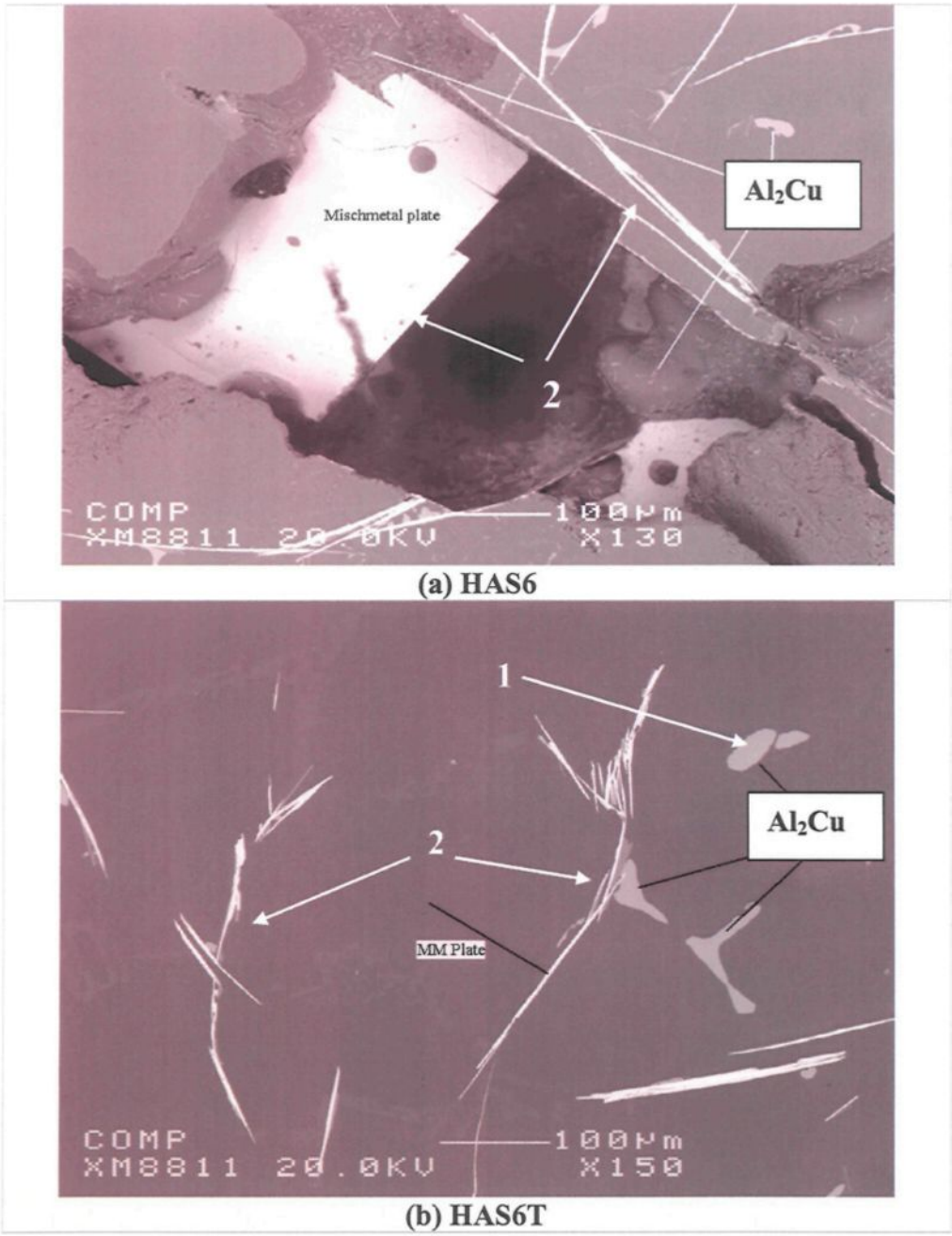

Figure 5.4 Backscattered images of A319.1 alloy with 6 wt% mischmetal depicting the intermetallics observed at low cooling rate.

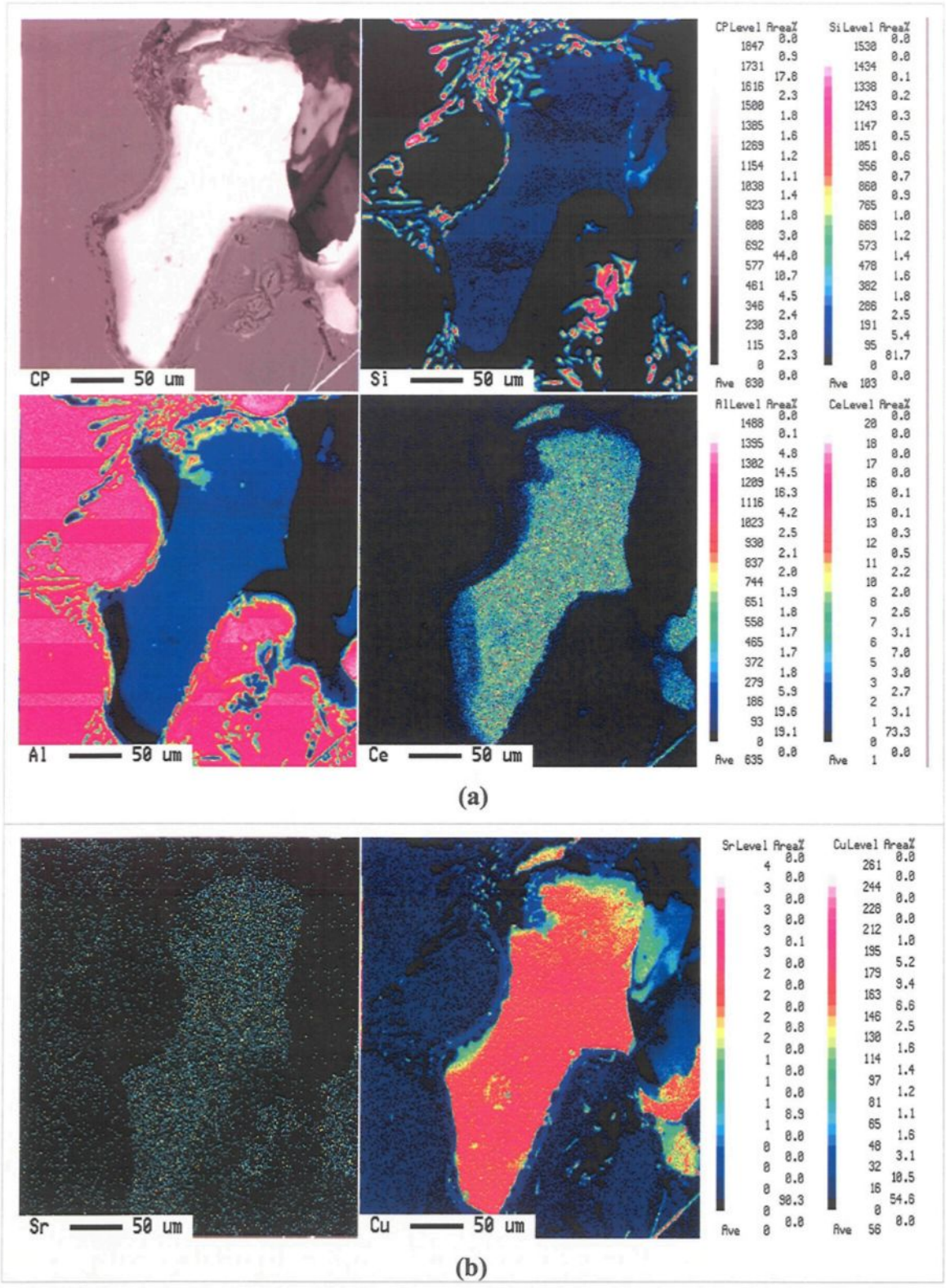

Figure 5.5 Backscattered image (CP), and X-ray images of (a) Al, Si, and mischmetal (Ce), and (b) Sr and Cu obtained from Sr-modified A319.1 alloy containing 6 wt% mischmetal, obtained at low cooling rate, as-cast condition.

5.3.2 A356.2 Alloy

A356.2 alloy belongs to the Al-Si-Mg system and is a heat-treatable alloy owing to the presence of magnesium (Mg) which combines with Si to form the Mg_2Si precipitation hardening phase. Such alloys are subjected to solution heat treatment at a temperature close to the eutectic temperature, in order to obtain the maximum amount of Mg and Si in solid solution and to avoid localized melting at the grain boundaries, as well. The second phase Mg_2Si precipitates out during aging (at 155°C), when the solubility decreases with temperature.[1, 7]

5.3.2.1 Intermetallics Observed Under High Cooling Rate Conditions

The solubility of Mg in Al increases with temperature and at a solution temperature of 540°C, the maximum amount of Mg in Al-Si alloy is found to be 0.6%.[7] In the non-modified alloy, the Mg_2Si intermetallic phase appears in the form of black Chinese script particles, as shown Figure 5.6(a). After solution heat treatment at 540°C for 8h, the Mg_2Si phase is completely dissolved in the Al-matrix (Figure 5.6(b)).

Mischmetal-containing intermetallic phases

Table 5.3 lists the chemical compositions of the mischmetal-containing intermetallics observed in A356.2 alloy. A mischmetal intermetallic containing Ti is formed under high cooling rate conditions, in the form of grey sludge particles (marked phase #1) with a formula of Al_4MMTi_2Si + 0.26 wt %Mg, as shown in Figure 5.7(a). The

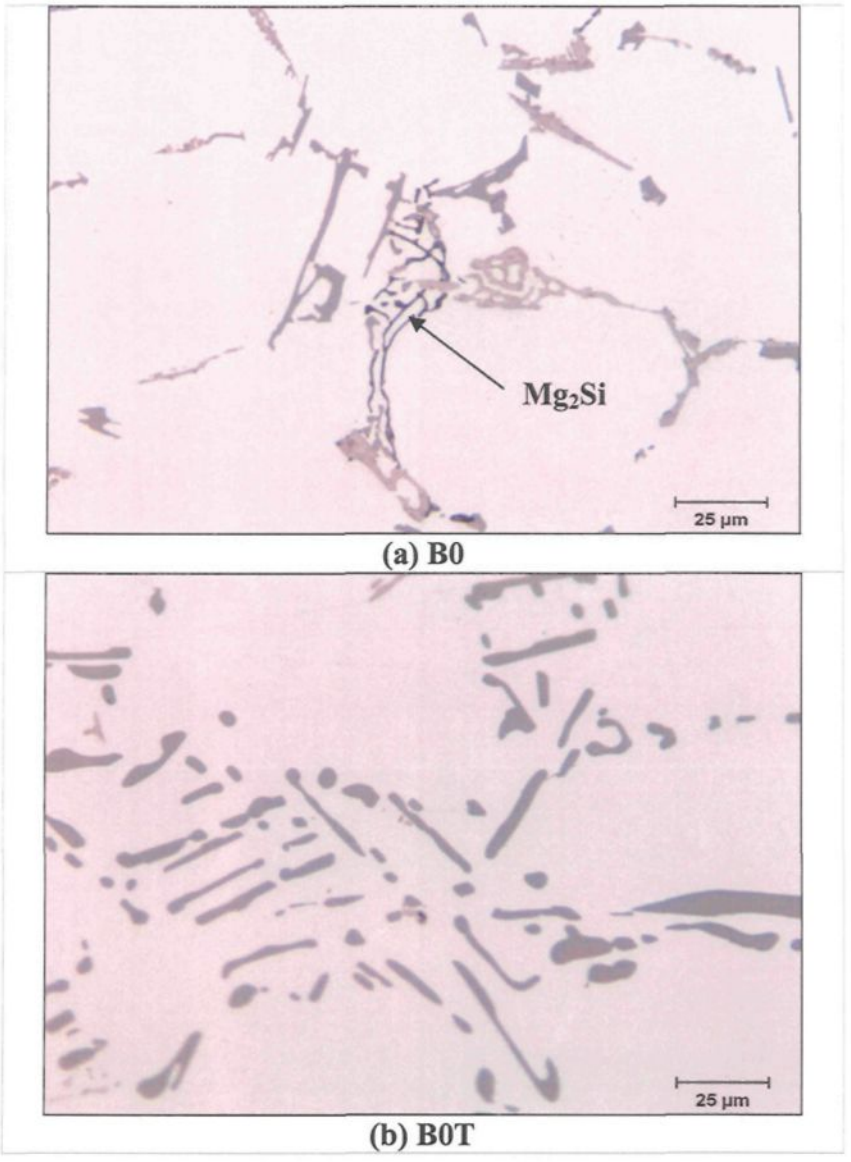

Figure 5.6 Optical micrographs showing: (a) the presence of a large black Chinese script Mg_2Si particle in A356.2 alloy in the as-cast condition, and (b) dissolution of Mg_2Si after solution treatment (540°C/8h).

association/interaction of Mg with the mischmetal means that there is a decrease in the amount of Mg available to form the precipitation hardening phase Mg_2Si. This would

Table 5.3 Chemical compositions of the intermetallic phases observed in Sr-modified as-cast A356.2 alloy containing 6 wt% mischmetal (WDS analysis, Figure 5.7)

Phase #	Element	wt.% Av	at. % Av.	Calculated formula	Shape&Colour	Suggested Formula
	Al	69.61	85.045	$Al_{60}(CeLaPr)_3Ti_5Si$	MM-Ti sludge	$Al_{20}MM^{*}Ti_2Si^{**}$
	Si	1.22	1.432			
	Ti	11.5	7.9			+
1	Ce	11.24	2.64	**(Ce: La =3.4:1)**	grey	**0.26 wt% Mg**
	La	3.23	.766			
	Pr	2.22	.517			
	Mg	**0.26**	**0.36**			
	Total	99.28	98.65			
	Al	22.85	40.45	$Al_{10}(Ce\ La\ PrNd)_4Si_{10}$	Round-type	$Al_2MM^{*}Si_2^{**}$
	Si	21.68	38.54			
	Ce	24.4	8.7			**+ 1.6 wt% Sr**
2	La	18.22	6.55	**(Ce: La =1.32:1)**	white	**+ 0.6 wt% Mg**
	Pr	7.29	2.36			
	Nd	2.49	0.86			
	Sr	**1.67**	**0.95**			
	Mg	**0.62**	**1.3**			
	Total	99.22	99.7			

*MM:mischmetal, **Al could be higher than the actual content due to the small size of the examined particles

explain the continuous decrease in the hardness value of these alloys with increasing mischmetal addition (to be discussed in Chapter 6).

At a lower Ce/La ratio (1.32:1), the mischmetal-intermetallic appears in the form of white particles that are more rounded than plate-like, as shown in Figure 5.7(b), associated with Sr and Mg, and with a formula corresponding to Al_2MMSi_2 + 1.6 wt% Sr + 0.6 wt% Mg, as listed in Table 5.3. The interaction of Sr and Mg with the mischmetal would explain the corresponding decrease in the level of Si particle modification observed in Table 4.3 and Table 4.4 in Chapter 4, as well as the decrease in the hardness with further mischmetal

addition (to be discussed in Chapter6). The presence of magnesium oxide (MgO) particles on the surface of this phase suggests that MgO particles (i.e., inclusion in the A356.2 alloy) act as nucleation sites for the precipitation of the mischmetal intermetalllic.

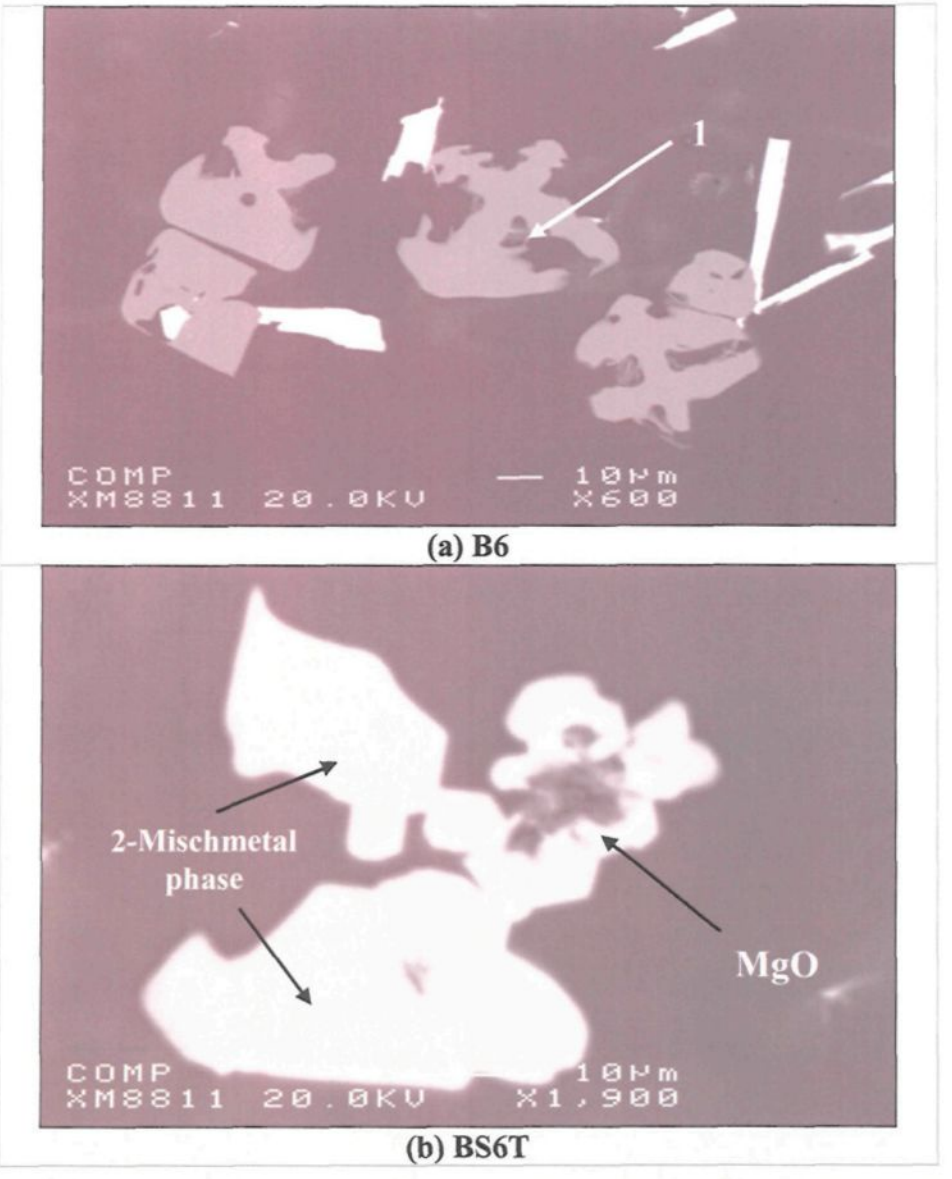

Figure 5.7 Backscattered images obtained from A356.2 alloy containing 0.35% Mg and 6 wt% mischmetal showing the mischmetal intermetallics in the (a) non-modified, as-cast, (b) Sr-modified, heat-treated conditions.

5.3.2.2 Intermetallics Observed Under Low Cooling Rate Conditions

Mischmetal combines with Al and Si to form different kinds of intermetallics observed under low cooling rate conditions. At a Ce/La ratio of 1.5:1, the mischmetal intermetallic phase appears in the form of long, white Chinese script particles (phase #4) observed to precipitate within the α-Al dendrites, as shown in Figure 5.8(a). The suggested chemical formula obtained from WDS analysis is Al_2MMSi_2 associated with 0.25 wt% Mg (see Table 5.4).

Mischmetal forms another type of intermetallic phase which precipitates in the form of rounded white particles (phase # 2) with a low Ce/La ratio (1.23:1), as shown in Figure 5.8(b). The suggested chemical formula is also Al_2MMSi_2 + 1.4 wt% Sr + 0.36 wt% Mg, as shown in Table 5.4.

The backscattered image and corresponding X-ray images shown in Figure 5.9 of the rounded white mischmetal phase confirm the interaction between mischmetal and Sr and Mg. This implies the weakening of both the modification action of Sr and the precipitation hardening effect of the Mg_2Si phase. Interestingly, the presence of SrO, MgO and P_2O_5 oxides on the surface of this mischmetal phase strengthens the hypothesis that these oxides act as preferred nucleation sites for the formation of mischmetal-containing intermetallics.

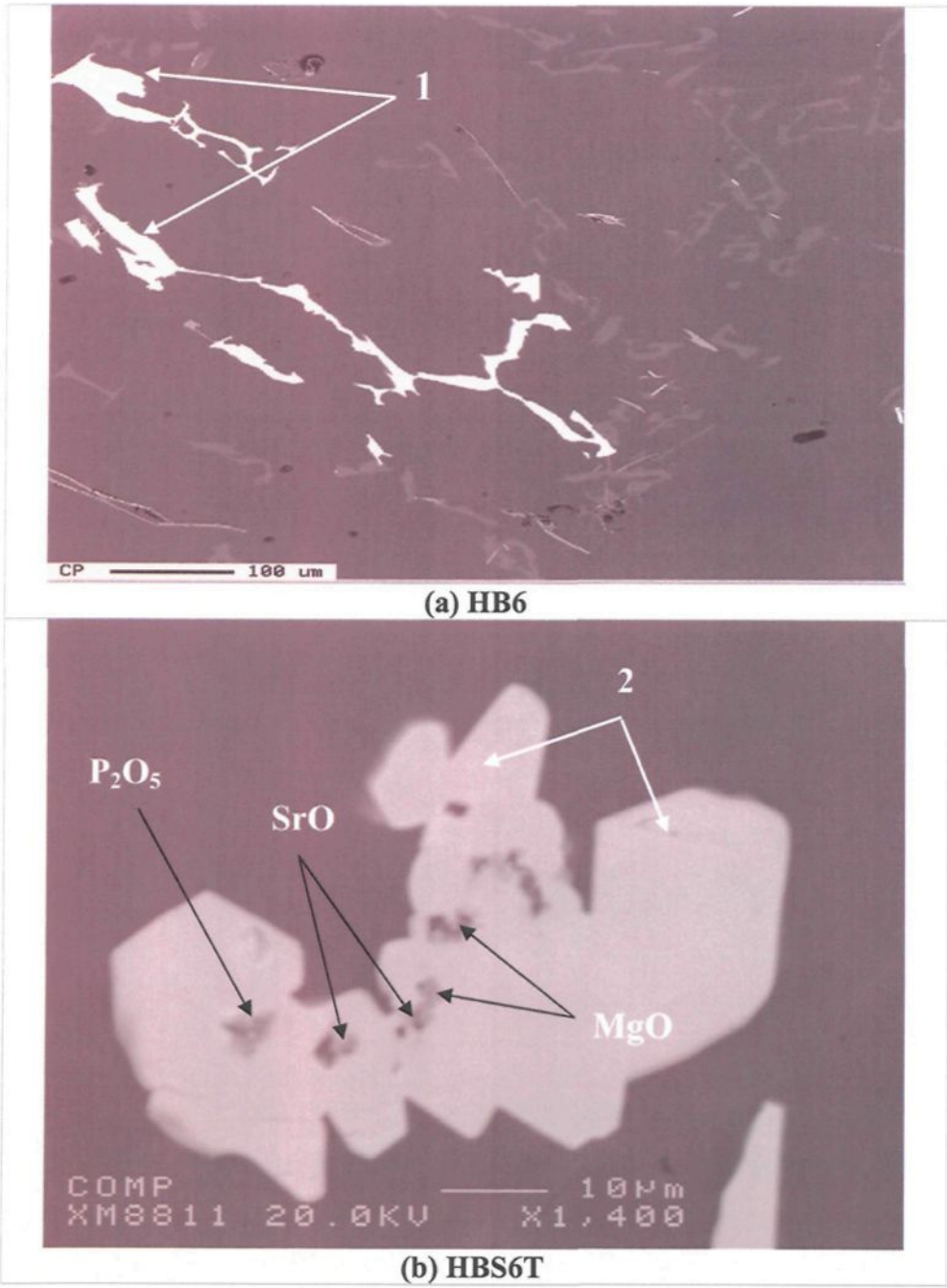

Figure 5.8 Backscattered images of the MM intermetallics obtained from A356.2 alloy containing 6 wt% mischmetal addition: (a) non-modified as-cast, and (b) Sr-modified heat-treated conditions.

Table 5.4 Chemical compositions of the intermetallic phases observed in A356.2 alloy containing 6 wt% mischmetal (WDS analysis, Figure 5.8)

Phase #	Element	wt.% Av.	at. % Av.	Calculated formula	Shape&Colour	Suggested Formula
1	Al	21.82	39.8	$Al_6(CeLaPrNd)_3Si_6$ **(Ce : La = 1.5 :1)**	Chinese script white	$Al_2MM^*Si_2^{**}$ + **0.25 wt % Mg**
	Si	22.51	39.4			
	Ce	28.26	9.58			
	La	16.95	6.31			
	Pr	7.06	2.42			
	Nd	2.63	0.89			
	Mg	**0.25**	**0.5**			
	Total	99.48	98.9			
2	Al	22.5	40.8	$Al_6(CeLaPrNd)_3Si_6$ **(Ce : La = 1.23 :1)**	Rounded particle white	$Al_2MM^*Si_2^{**}$ + **1.4 wt% Sr** **0.36 wt% Mg**
	Si	22.66	38.85			
	Ce	23.54	8.21			
	La	19.84	6.68			
	Pr	6.12	2.18			
	Nd	2.29	0.82			
	Sr	**1.4**	0.78			
	Mg	**0.36**	0.73			
	Total	98.71	99.05			

*MM:mischmetal, **Al could be higher than the actual content due to the small size of the examined particles

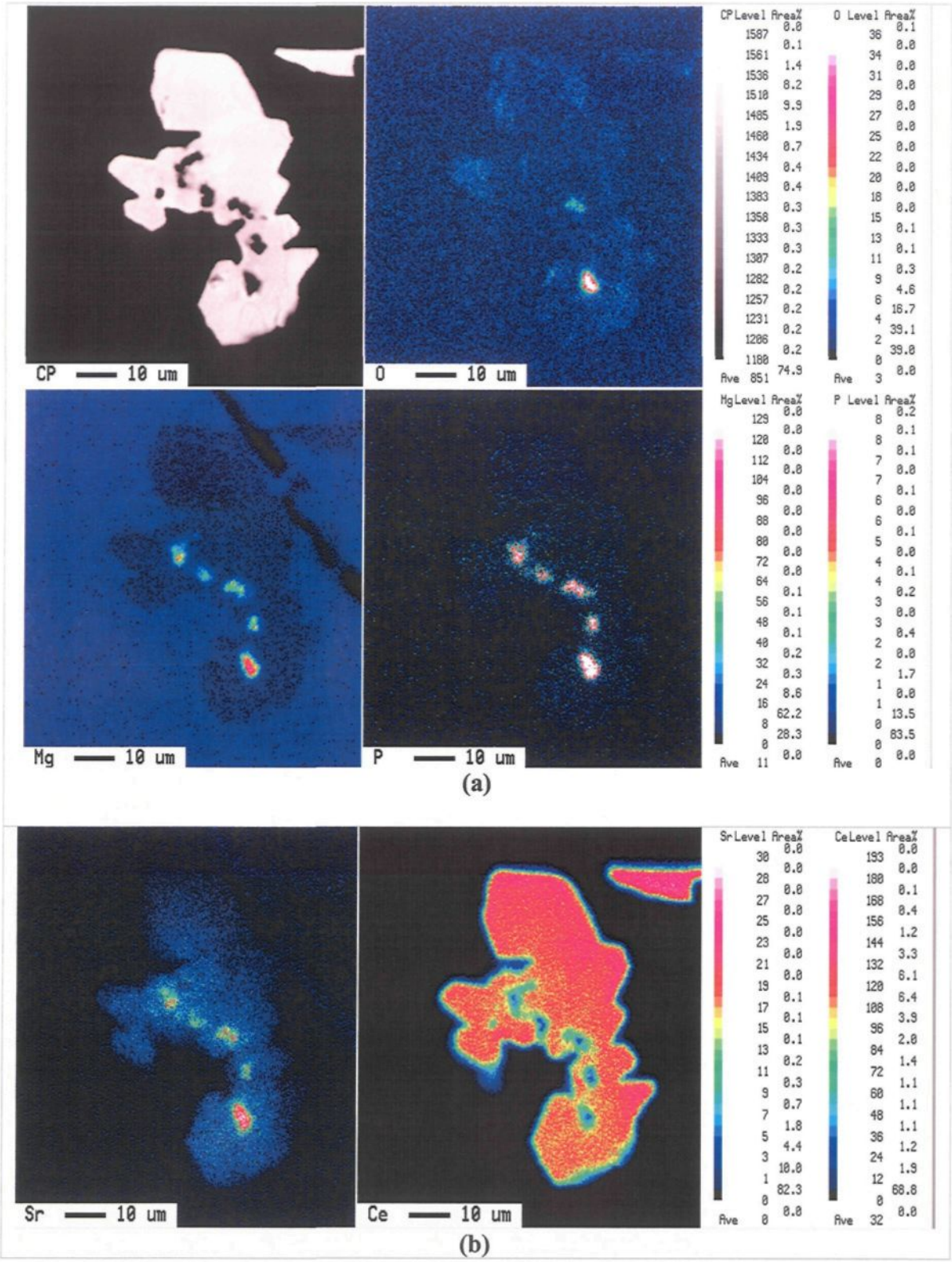

Figure 5.9 Backscattered image (CP), and X-ray images of (a) Mg, O and P, and (b) Sr, and mischmetal (Ce) obtained from Sr-modified A356.2 heat-treated alloy containing 6 wt% mischmetal, obtained at the low cooling rate.

5.3.3 A413.1 Alloy

The A413.1 alloy contains 11.7% Si and a small level of alloying elements and impurities, such as Cu, Ni and Fe. With the addition of mischmetal to the alloy, these alloying elements/impurities and the mischmetal can form different intermetallic phases.

5.3.3.1 Intermetallics Observed Under High Cooling Rate Conditions

Figure 5.10 and 5.11 show examples of the intermetallic phases observed in the non-modified and Sr-modified alloys with no mischmetal addition, obtained at the high cooling rate condition. Table 5.5 lists the chemical compositions of these intermetallics as obtained from WDS analysis.

Copper intermetallic phases

The low content of copper in A413.1 alloy (0.35%) is not enough to form the Al_2Cu intermetallic phase. The presence of Ni, also in low amount, results in the combination of Cu and Ni with Al to form a new phase, Al_3NiCu, observed in the as-cast non-modified alloys, as shown in Figure 5.10(a) and Table 5.5. This phase precipitates as block-like particles on the surface of the β-Al_5FeSi iron intermetallic platelets.

Iron intermetallic phases

Iron as an impurity at a level of 0.7% to 0.8% is considered to be relatively high in A413.1 alloy. This leads to the formation of different iron intermetallics which possess a variety of morphologies. As summarized in Table 5.5, the main iron intermetallics observed

in the A413.1 alloys are the α-Fe phase with a chemical composition of $Al_{11}(MnFeNiCu)_4Si$, and the β-Fe phase, Al_5FeSi. Under high cooling rate conditions, the

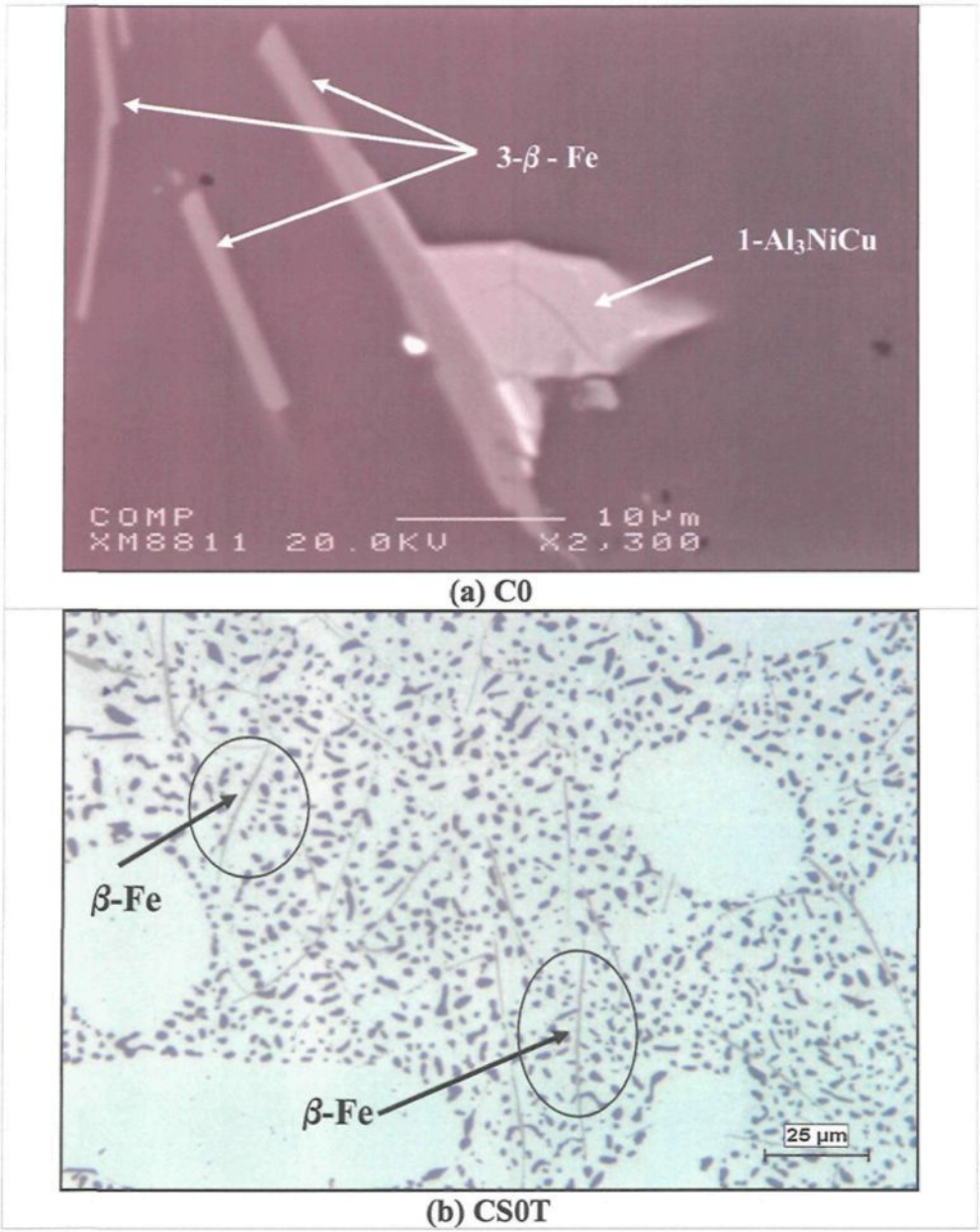

Figure 5.10 Morphology of the intermetallics observed in the A413.1 alloy showing: (a) Al_3NiCu phase and β-Fe intermetallics in the as-cast non-modified alloy-BS image, and (b) β-Fe phase (see circled areas) in the Sr-modified heat-treated alloy optical micrograph.

α-Fe phase is observed to precipitate in the interdendritic regions along with the eutectic Si, in the form of light grey Chinese script particles with a high level of Ni and at an Fe/Mn ratio of 2.8:1, as shown in Figure 5.11(a) (circled area) and (c). The size and the distribution of this phase are highly dependent on the amount of Sr addition. With the addition of Sr to the non-modified A413.1 alloy, the α-Fe phase tends to precipitate within the α–Al dendrites. In other words, it precipitates prior to the formation of the α–Al dendrites (i.e., in a predendritic reaction), as denoted clearly by the arrow in the optical micrograph of Figure 5.11(b) and in the backscattered image of Figure 5.11(d). This would result in the strengthening of the α-aluminum matrix and, hence, improving the alloy properties.

Figure 5.11(b) depicts the presence of the α-Fe phase in the as-cast and heat-treated alloy, where it appears to remain unchanged and its solubility relatively unaffected after solution treatment. These observations are consistent with the findings of Moustafa *et al.* [80] on the effect of additives and solution treatment on the microstructural characteristics of Sr-modified A413 alloy. They have also reported that the α-iron phase is observed to precipitate within the α–aluminum dendrites when Sr is added to the alloy to modify the eutectic Si particles.

Generally, the β-Al_5FeSi intermetallic phase is brittle and has a low coherence with the Al matrix, leading to a decrease in the alloy ductility. In the as-cast non-modified alloys, the β-phase precipitates in the form of plates which appear as needles in the microstructure, as depicted in Figure 5.10(a).

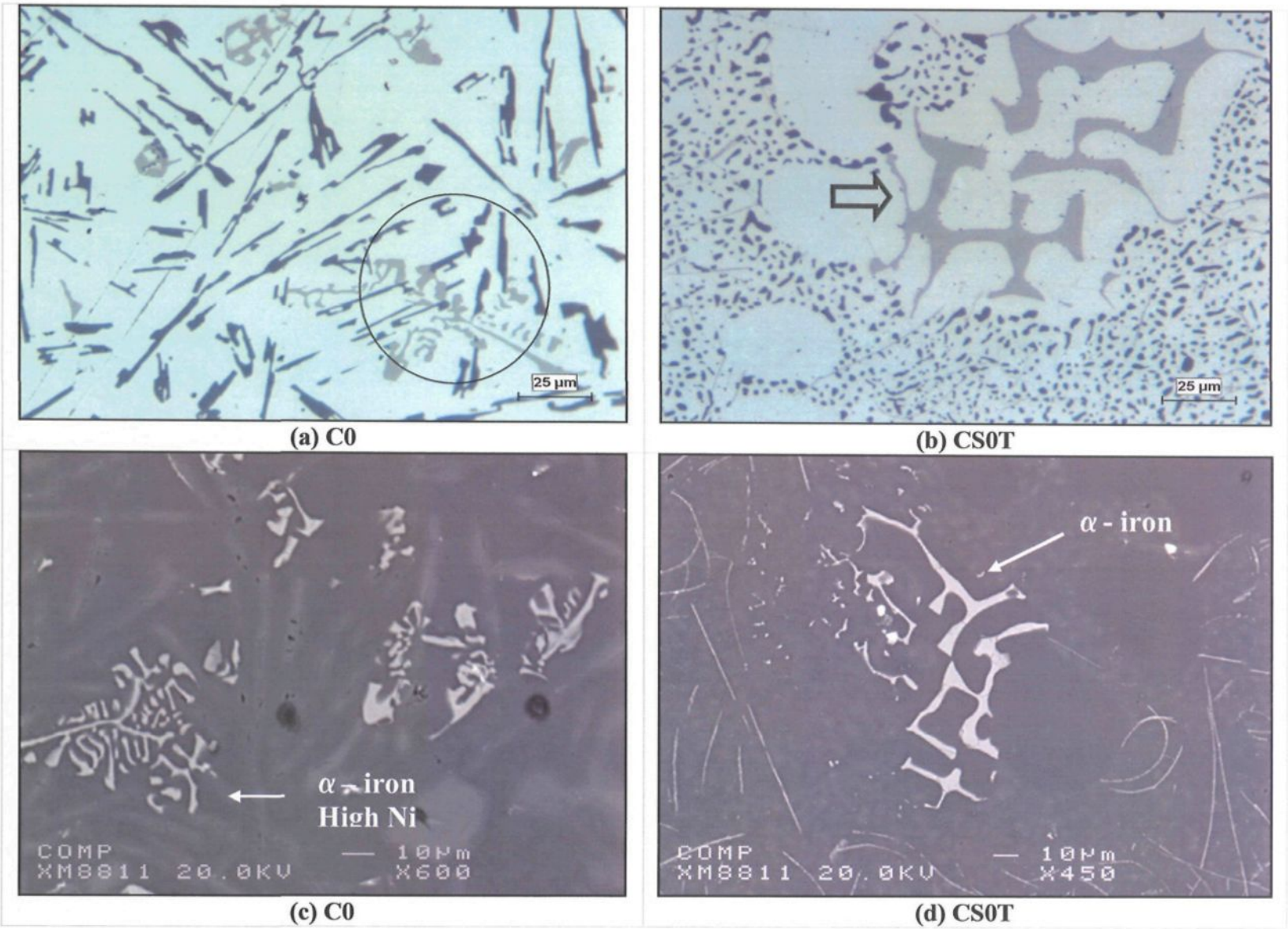

Figure 5.11 Morphology of the α-Fe intermetallic phase observed in A413.1 alloy free of mischmetal: (a), (c) optical (a) and BS image (c) of as-cast non-modified alloy; (b), (d) optical (b) and BS image (d) of solution heat-treated Sr-modified alloy.

Table 5.5 Chemical compositions of the intermetallic phases observed in A413.1 alloy containing 0 wt% mischmetal (WDS analysis, Figures 5.10 and 5.11)

Phase #	Element	wt.% Av.	at. % Av.	Calculated formula	Shape& Colour	Suggested Formula
1	Al	42.84	62.86	$Al_{10}Ni_3Cu_2$	block-like	Al_3NiCu
	Ni	32.04	22.61			
	Cu	21.01	12.7		grey	
	Total	95.89	98.17			
2	Al	55.08	70.31	$Al_{11}(MnFeNiCu)_4Si$	Chinese script	$Al_{11}(MnFeNiCu)_4Si$
	Si	4.89	6.00			
	Cu	5.68	3.07		Light grey	α-iron (high Ni)
	Fe	4.96	3.05			
	Ni	26.83	15.73			
	Mn	1.76	1.10			
	Total	99.2	99.26			
3	Al	57.03	67.14	$Al_{11}Fe_3Si_2$	plate-like	Al_5FeSi
	Si	15.44	17.46			
	Fe	26.83	15.26		dark grey	β-iron
	Total	99.3	99.86			

In Al-Si alloys, the presence of Sr is known to poison and reduce the preferred nucleation sites of the β-Fe intermetallic phase. Fragmentations and dissolution of the β-Fe needles is also observed with the addition of Sr. [81] Thus, the Sr-modified alloys exhibit somewhat lower levels of the β-Fe phase compared with non-modified alloys. After solution heat treatment of the Sr-modified A413.1 alloy, the β-Fe phase undergoes partial dissolution through the rejection of Si ahead of the β-platelets. [82] The circled areas in Figure 5.10(b) depicts fine needles of the β-iron phase observed interspersed with the modified Si particles in the heat-treated Sr-modified A413.1 alloy.

Mischmetal-containing intermetallic phases

Figure 5.12 depicts the morphologies of the mischmetal-containing intermetallics

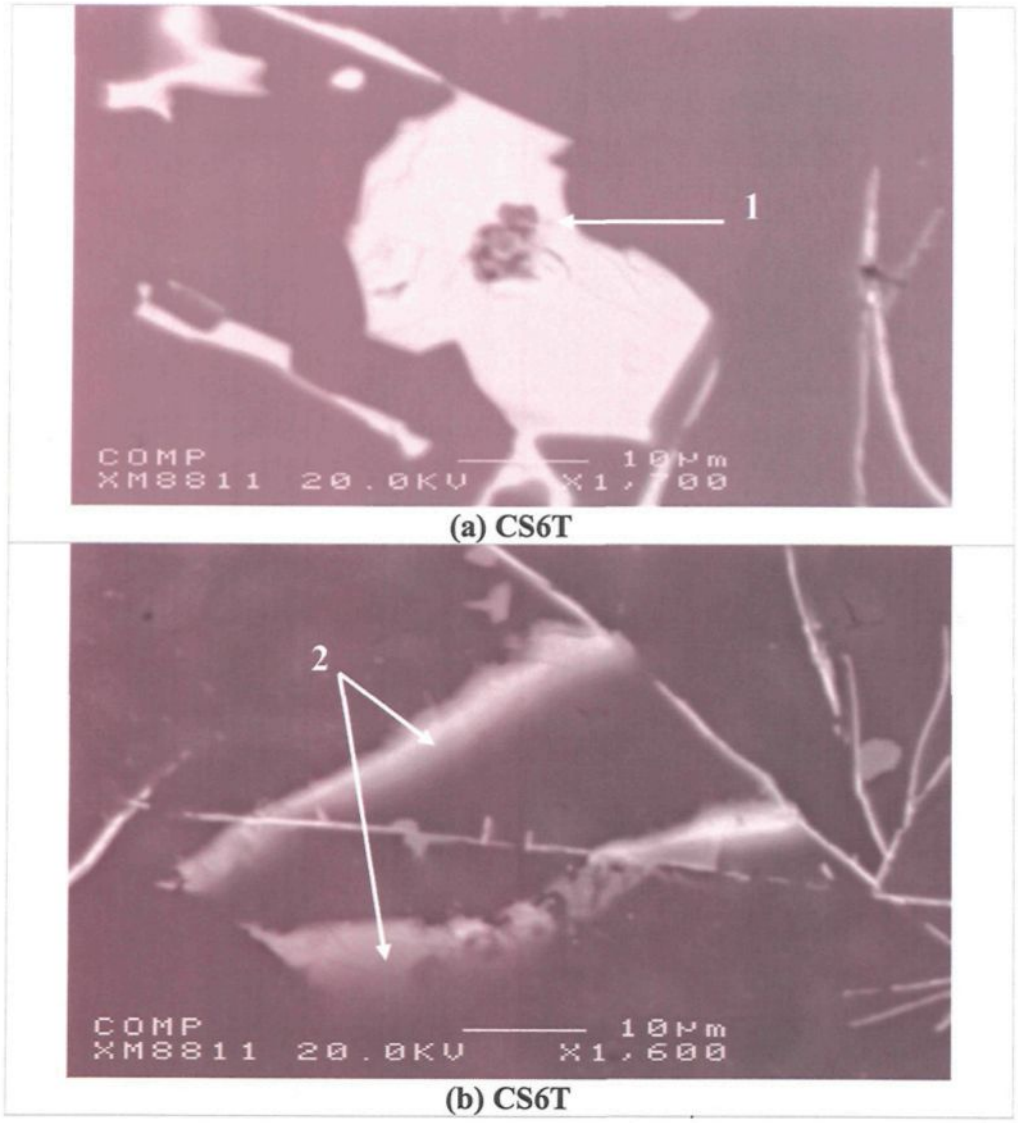

Figure 5.12 Backscattered images of mischmetal intermetallics obtained from Sr-modified heat-treated A413.1 alloy containing 6 wt% mischmetal showing: (a) the white block-like Al_2MMSi_2 mischmetal phase, (b) the rod-like $Al_5MM(CuNi)Si_2$ mischmetal phase.

observed in the Sr-modified heat-treated A413.1 alloy under high cooling rate conditions. The chemical compositions of these intermetallics as obtained from WDS analysis are

Table 5.6 Chemical compositions of the intermetallic phases observed in Sr-modified heat-treated A413.1 alloy containing 6 wt% mischmetal (WDS analysis, Figure 5.12)

Phase #	Element	wt.%	at. %	Calculated formula	Shape & Colour	Suggested Formula
	Al	22.33	41.75	$Al_7(CeLaPrNd)_3Si_6$	Block-like	$Al_2MM^*Si_2^{**}$
	Si	21.15	37.98			
1	Ce	23.22	8.36			
	La	19.5	7.08	**(Ce:La=1.18 :1)**	white	
	Pr	5.65	2.02			**+ 2.7wt%Sr**
	Nd	2.01	0.70			
	Sr	2.77	1.59			
	Total	96.63	99.48			
	Al	55.35	74.8	$Al_{13}(CeLaPrNd)(CuNi)Si_2$	Rod-like	$Al_6MM^*(CuNi)Si^{**}$
	Si	8.16	10.6			
2	Cu	8.72	5.07			
	Ni	3.09	1.93	**(Ce:La = 2 :1)**	Light grey	
	Ce	11.45	3.00			
	La	5.65	1.5			
	Pr	2.75	.72			
	Nd	1.11	.28			
	Total	96.28	97.9			

*MM:mischmetal, **Al could be higher than the actual content due to the small size of the examined particles.

shown in Table 5.6. Mischmetal (up to 6 wt %) combines with Al and Si to form an intermetallic compound that precipitates in the form of white block-like particles at a low Ce/La ratio of 1.18:1, marked phase #1 in Figure 5.12(a) and Table 5.6. The chemical composition of this phase as obtained from WDS analysis shows it corresponds to AL_2MMSi_2.

It is worth noting that this white phase contains 2.7 wt% Sr (which is different than the actual added amount of Sr, 250 ppm, used in the present work) which reveals the interaction between mischmetal and Sr to form complex intermetallic compounds. Therefore, there is less Sr available to obtain the same level of Si particle modification as

when only Sr is added to the alloy. Thus, it can be said that the addition of mischmetal reduces the "effectiveness" of the Sr-modification. These observations substantiate the results of the Si particle characteristics reported in Table 4.5

At a moderate Ce/La ratio (2:1), mischmetal is found to react with Si, Cu and Ni to form another type of intermetallic phase. The suggested chemical formula of this phase is Al_2MMSi_2, as shown in Table 5.6. This phase precipitates in the form of light grey rods, as shown in Figure 5.12(b), marked as phase #2.

5.3.3.2 Intermetallics Observed Under Low Cooling Rate Conditions

Figure 5.13 shows examples of the α-Fe intermetallic phase observed in A413.1 alloy containing 6 wt% mischmetal, btained under low cooling rate conditions. In the case when no Sr is added, the α-$Al_{15}(MnFe)_3Si_2$ phase is observed to precipitate without Ni at an Fe/Mn ratio of 2.4:1, in the form of large branched medium grey Chinese script particles in Figure 5.13(a). As was observed under high cooling rate conditions, in this case also, the α-Fe phase precipitates within the α-Al dendrites in the as-cast Sr-modified alloy, as depicted by the BS image of Figure 5.13(c). The α–Fe intermetallic is marked phase #1 in both figures.

Mischmetal-containing intermetallics

At the low cooling rate, mischmetal (MM) forms a different type of intermetallic in the as-cast non-modified alloy containing 6 wt% mischmetal. This intermetallic has the same chemical composition as the white plate-like mischmetal intermetallic Al_2MMSi_2 observed under the high cooling rate conditions, but precipitates in the form of large white

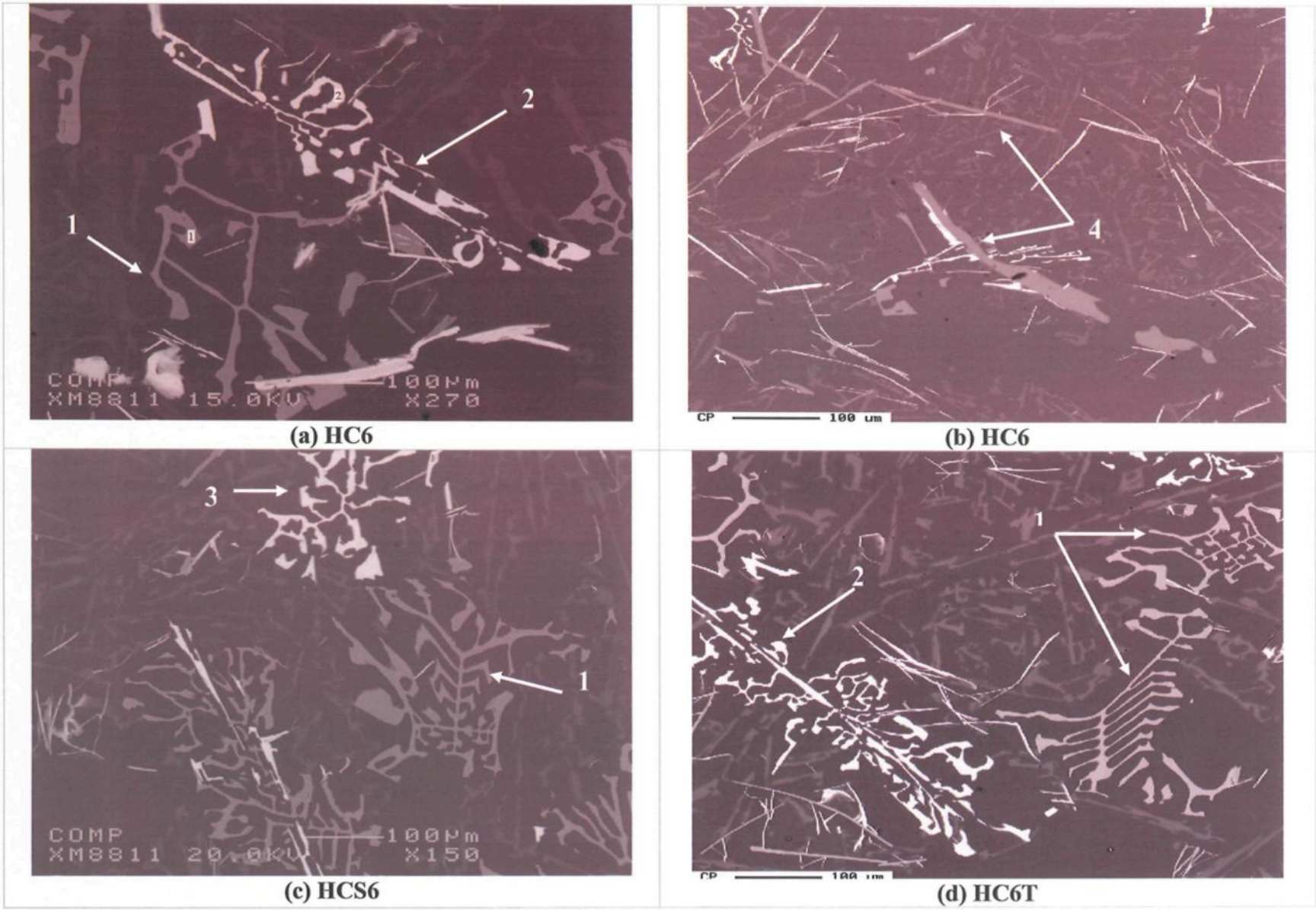

Figure 5.13 Backscattered images of the intermetallics obtained from A413.1 alloy containing 6wt% mischmetal showing: (a),(b) in the as-cast, (c) Sr-modified as-cast, and (d) in the heat-treated conditions.

Table 5.7 Chemical compositions of the intermetallic phases observed in the as-cast A413.1 alloy containing 6 wt% mischmetal (WDS analysis, Figure 5.13)

Phase #	Element	wt.%	at. %	Calculated formula	Shape& Colour	Suggested Formula
	Al	59.76	70.74	$Al_{16}(MnFe)_4Si_3$	Chinese script	$Al_{15}(MnFe)_3Si_2$
1	Si	10.07	11.44			
	Fe	20.3	11.6		meduim grey	α-Iron
	Mn	8.31	4.83			
	Total	98.44	98.61			
	Al	23.21	41.32	$Al_{10}(CeLaPrNd)_4Si_9$	Chinese script	$Al_2MM^*Si_2^{**}$
	Si	21.99	38.77			
2	Ce	26.93	9.47			
	La	17.05	6.03	**(Ce : La = 1.57 :1)**	white	
	Pr	6.83	2.31			
	Nd	2.66	0.9			
	Total	98.67	98.8			
	Al	22.7	41.06	$Al_{10}(CeLaPrNd)_4Si_9$	Chinese script	$Al_2MM^*Si_2^{**}$
	Si	22.5	39.11			
	Ce	26.65	9.28			
3	La	17.78	6.24	**(Ce : La = 1.48 :1)**	white	**+ 0.48wt% Sr**
	Pr	6.53	2.26			
	Nd	2.39	0.8			
	Sr	**0.48**	**0.26**			
	Total	99.03	99.01			
	Al	31.02	52.6	$Al_{10}(CeLaPrNd)_2(CuNi)_3Si_3$	Plate-like	$Al_5MM^*(CuNi)Si^{**}$
	Si	10.92	18.58			
	Cu	14.02	9.03			+
4	Ni	6.05	5.40	**(Ce:La= 2.1 :1)**	Medium-light	excess of Al
	Ce	21.78	7.05		grey	
	La	10.41	3.36			
	Pr	5.12	1.57			
	Nd	1.91	0.57			
	Total	101.2	98.16			

*MM:mischmetal, **Al could be higher than the actual content due to the small size of the examined particles

Chinese script particles (marked phase #2 in Figure 5.13(a)), with a Ce/La ratio of 1.5:1. This phase is also observed in the non-modified heat-treated A413.1 alloy containing 6 wt% mischmetal, see phase # 2 in Figure 5.13(d). While the same white Chinese script Al_2MMSi_2 phase is also observed in the as-cast Sr-modified alloy (marked phase #3 in

Figure 5.13(c), it contains 0.48 wt% Sr, as confirmed by the X-ray image of Sr corresponding to the backscattered image of such particles, shown in Figure 5.14(b). This confirms the interaction between mischmetal and Sr. The effect of this interaction is quite apparent at the low cooling rate condition, where an increase in the Si particle characteristics is observed (see Table 4.6 in Chapter 4). Thus, the addition of mischmetal to the Sr-modified A413 alloy at low cooling rate negates the influence of Sr as a modifying agent of the eutectic Si to a considerable extent.

As mentioned previously in the section 5.3.3.1 on the intermetallics observed under high cooling rate conditions, mischmetal forms another type of intermetallic phase at a moderate Ce/La ratio (2.1:1), but in this case, the phase precipitates in the form of medium light grey plate-like particles marked phase #4 in Figure 5.13(b), possessing the same chemical formula (Al_2MMSi_2) as obtained under high cooling rate. Table 5.7 summarizes the various intermetallics obtained under low cooling rate conditions in A413.1 alloys containing 6 wt% mischmetal.

Figure 5.14 displays the backscattered image and corresponding X-ray images for Fe, Si, Cu, Ce and Sr obtained from the as-cast Sr-modified A413.1 alloy containing 6 wt% mischmetal showing the presence of two types of Chinese script phases. The first Chinese script phase represents the α-Fe intermetallic phase observed in Figure 5.14(a) (marked phase #1 in Table 5.7). The second white Chinese script phase represents the mischmetal intermetallic Al_2MMSi_2 phase marked phase #3 in Table 5.7 and Figure 5.13(c). The X-ray images of Fe and Si and Ce (mischmetal) and Sr corresponding to the two script phases shown in Figure 5.14 confirm their respective identities.

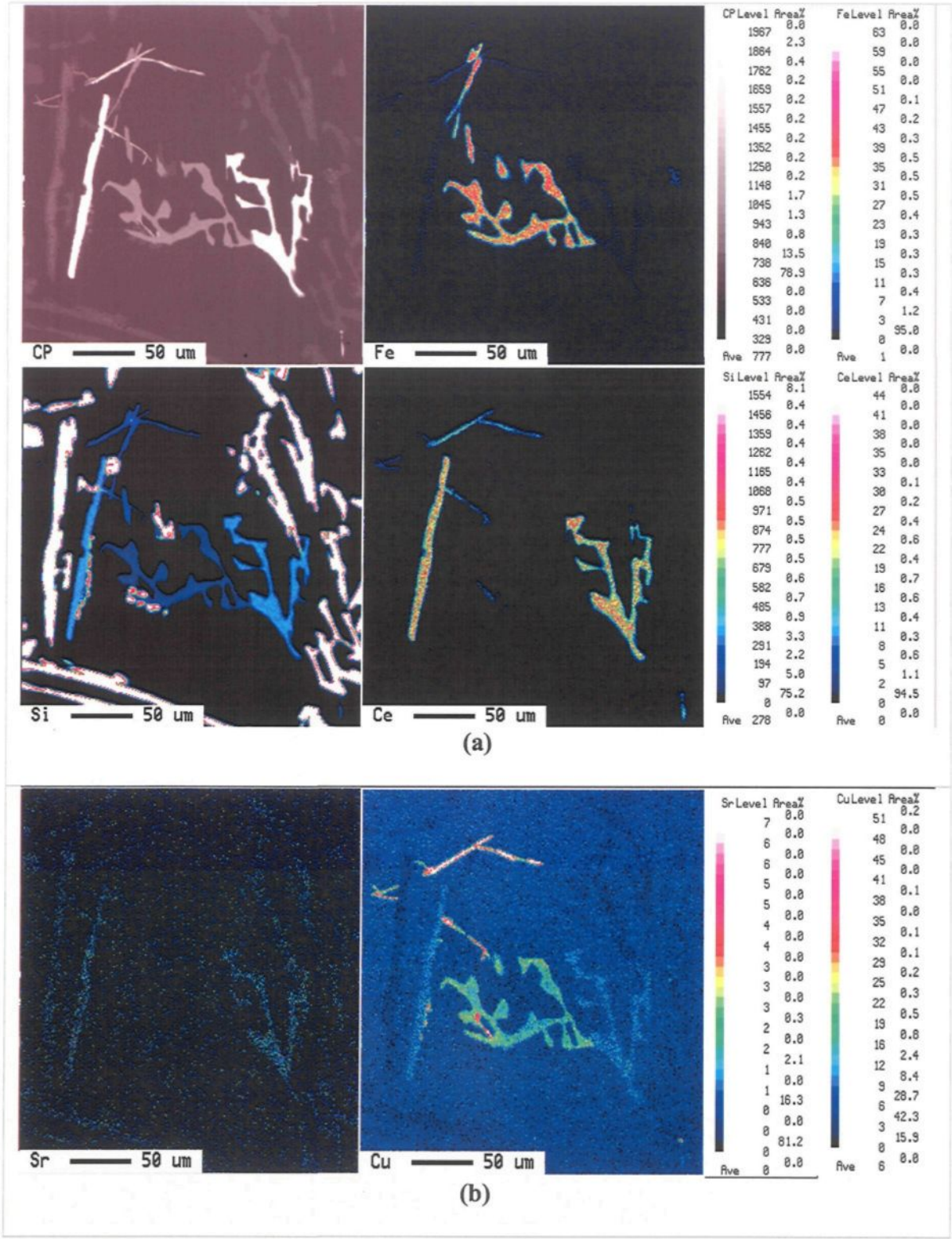

Figure 5.14 Backscattered image (CP) and corresponding X-ray images obtained from Sr-modified as-cast A413.1 alloy containing 6 wt% mischmetal showing the presence of : (a) Fe, Si and mischmetal (Ce), and (b) Sr and Cu in the two intermetallic types observed in the BS image.

CHAPTER 6

HARDNESS

CHAPTER 6

HARDNESS

6.1 INTRODUCTION

Hardness testing is an attractive way to measure the resistance of a material to permanent indentation and is performed in a quick and easy manner. Hardness measurements can provide a good indication of the strength and ductility of alloys, since strength is related to the number, type and spacing of second phase precipitates in the matrix. Thus, hardness measurements were used in the present work to monitor the precipitation hardening process in the two alloy systems studied, namely Al-Si-Cu (A319.1) and Al-Si-Mg (A356.2) alloys, as well as determine the effect of mischmetal addition in terms of eutectic Si modification and the formation of mischmetal-containing intermetallics, and that of cooling rate and heat treatment on the hardness of the investigated alloys.

There are three main types of tests that are used to determine the hardness of alloys.

1. The Rockwell hardness test is the most popular hardness test because it is fast and easy to perform. It carried out by pressing a steel or diamond hemisphere-conical penetrator against a test specimen and measures the resulting indentation depth as a gage of the specimen hardness. In the test, a minor load (10 kgf) is first applied, and

the test dial (measuring the indention depth) is reset to zero. Then a major load (60, 100, or 150 kgf) is applied to create the full indention. The major load is reduced back to the minor load, and the indention depth measurement is taken. The hardness number may then be read directly from the scale.

2. The Brinell hardness test is carried out by applying a constant load (500 to 3000 Kgf) for a specified time (10 to 30 s) using a ball indenter on the flat surface of the test specimen and measuring the diameter of the impression in the material. The hardness value is obtained by dividing the applied load (in kg) by the spherical area of the impression (in mm^2). In testing aluminum alloys, a load of 500 kg is applied to a ball 10 mm in diameter for a specific dwell time, normally 30 sec.

3. The Vickers hardness test is applied to different materials across a very wide range of hardness values. The vickers test uses a square-based diamond pyramid with a 136° point angle. The load (which is usually 50 kgf, but could also be 5, 10, 20, 30, or 120 kgf) is applied via the pyramid against the smooth, firmly supported, flat surface of the test specimen for 30 seconds. The resulting Vickers hardness value read from a conversion table depends on the load and the area of the permanent pyramid impression.[83]

In the present investigation hardness measurements were carried out using a Brinell hardness tester with a 500 kg force applied to a ball of 10 mm diameter for 30 sec, for the non-modified and Sr-modified A319.1, A356.2, and A413.1 alloys in the as-cast and solution heat-treated conditions, for samples obtained at the two cooling rates. The average

of eight readings taken from two adjacent surfaces was taken to represent the hardness value with standard deviation in the rang of ± 2.5%.

6.2 EFFECT OF HIGH COOLING RATE

6.2.1 A319.1 Alloy

In the as-cast non-modified alloy, the hardness is observed to increase slightly (~5 %) with 2 wt% mischmetal addition and then decrease with further mischmetal addition (~13%). The hardness of the Sr-modified alloy decreases by about 4 % with the addition of mischmetal, as shown in Figure 6.1, but remains the same, more or less, with increasing mischmetal addition.

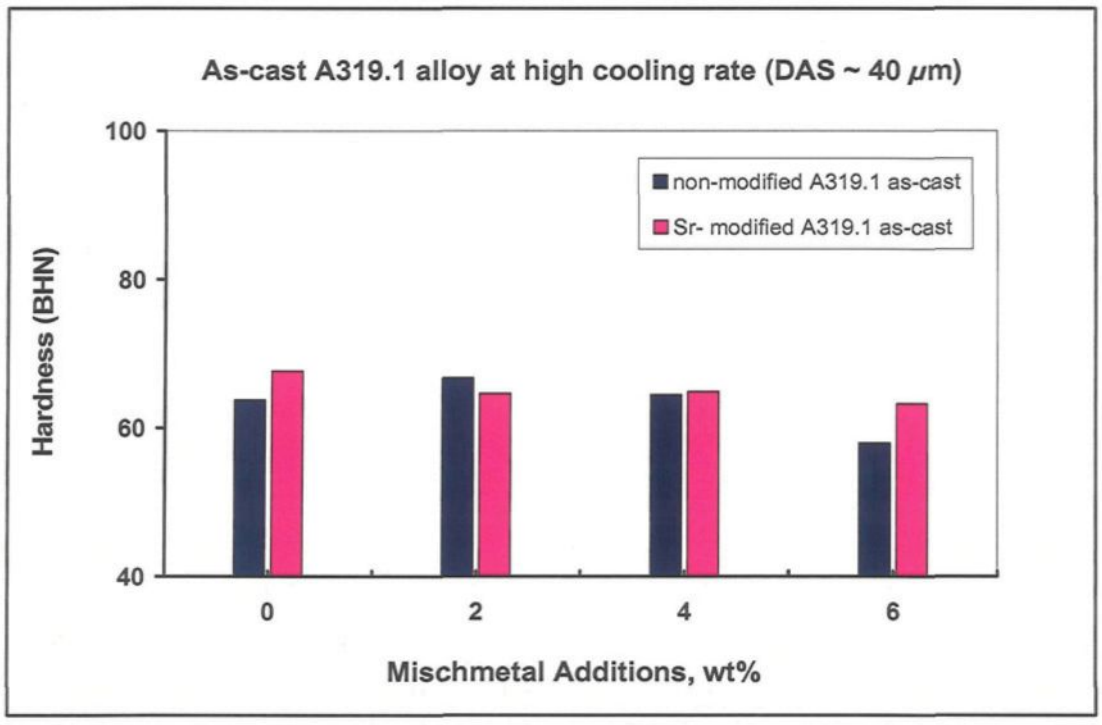

Figure 6.1 Effect of mischmetal addition and Sr-modification on the hardness of as-cast A319.1 alloy solidified at high cooling rate (DAS ~ 40μm).

The decrease in hardness in the as-cast alloys in both cases with mischmetal addition may be ascribed to the change of the Si particle morphology as a result of the modification effect of mischmetal (in the case of the non-modified alloys) and the combined effect of Sr and mischmetal (in the case of Sr-modified alloys).

It is well known that the addition of Sr results in the depression of the eutectic temperature. Similarly, mischmetal additions also depress the eutectic temperature, resulting in the shift of the eutectic point towards a higher Si content, leading to the increase of the amount of the soft α-Al matrix.

Two aging peaks are observed in the non-modified A319.1 alloy for mischmetal additions and after T6 treatment, as shown in Figure 6.2(a). The first peak occurs at 200°C/5h. The hardness is generally higher for the second peak condition (240°C/5h), except for the samples containing 2 wt% mischmetal. In general, the hardness of the non-modified A319.1 alloys decreases with the addition of mischmetal, except in the case of 2 wt % mischmetal addition where higher hardness values are observed at aging temperatures of 200°C and above. At this level, the amount of mischmetal added is apparently not enough to react with all the copper present in solid solution, leaving the rest available to form the precipitation hardening Al_2Cu phase. The mischmetal forms hard intermetallic compounds with other alloying elements, thus the modification effect (on the eutectic silicon) at 2 wt % mischmetal addition is not so pronounced. On the other hand, at mischmetal additions of 4 wt % and 6 wt %, the alloy hardness decreases due to further reaction of the mischmetal with copper preventing the formation of the Al_2Cu precipitation

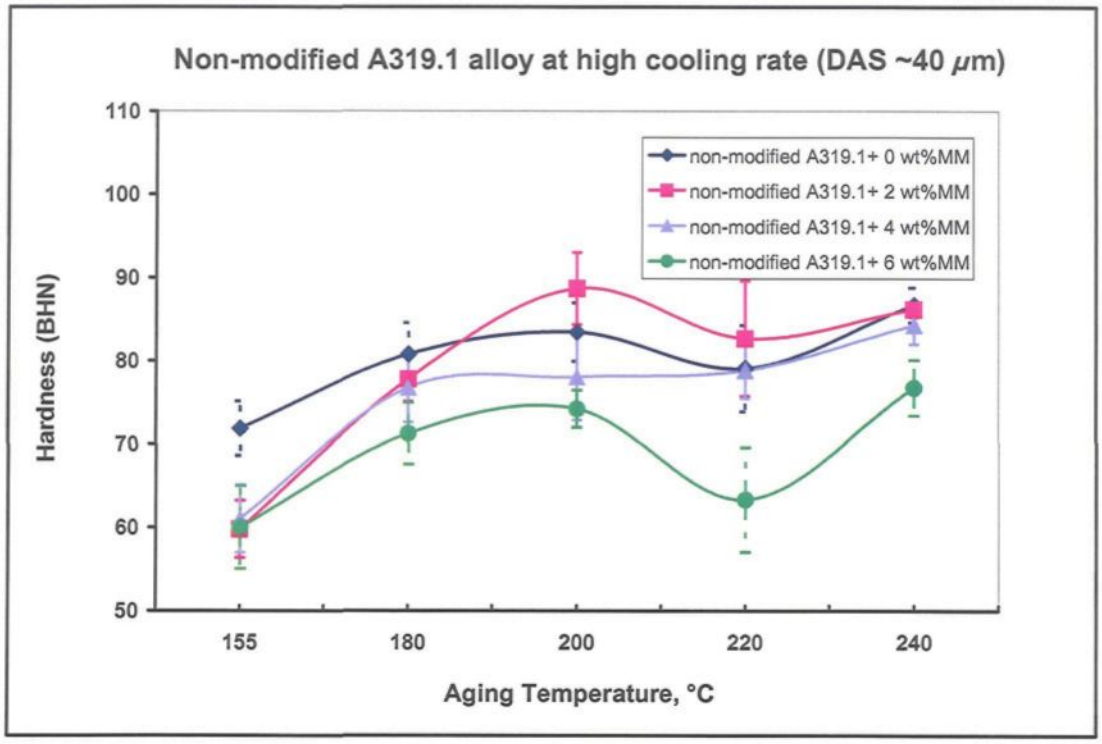

(a)

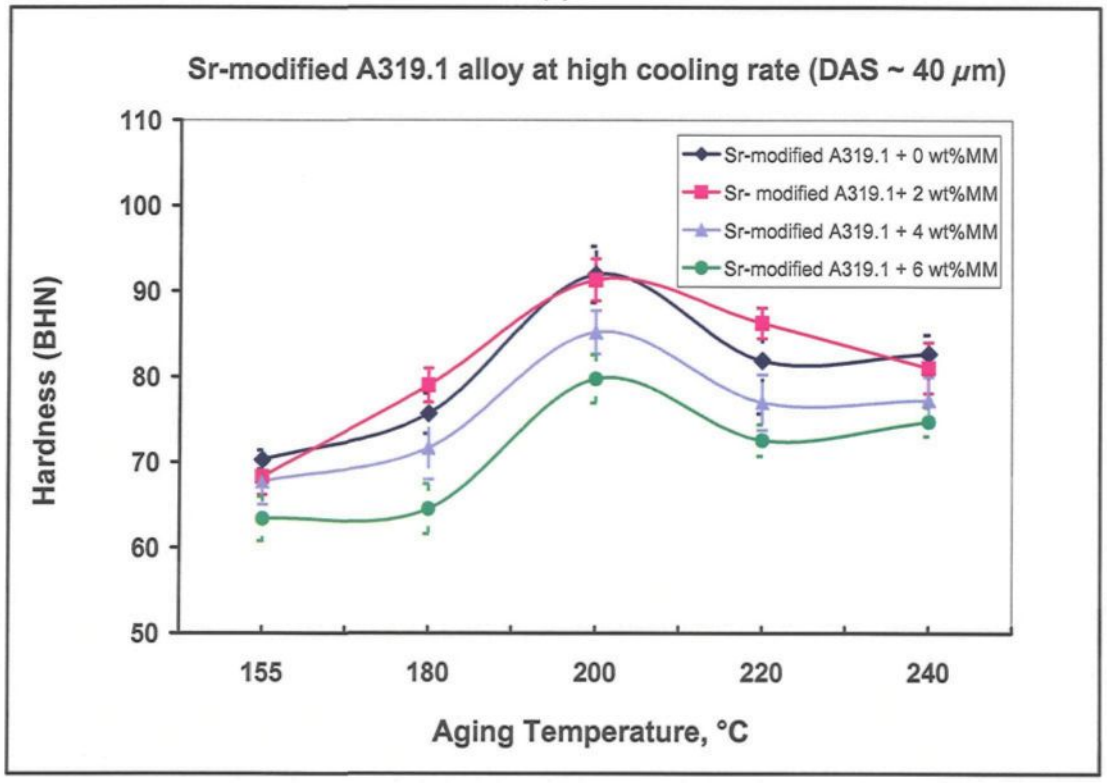

(b)

Figure 6.2 Effect of mischmetal additions and aging temperature on the hardness of A319.1 alloys solidified at a high cooling rate (DAS ~ 40μm): (a) non-modified, (b) Sr-modified conditions.

hardening phase, as well as further modification of the eutectic Si particles, and a corresponding increase in the amount of the α-Al matrix.

In the Sr-modified alloys, peak hardness is observed at 200/5h and the hardness is found to decrease with increasing mischmetal addition. The Sr-modified alloys with no and 2 wt% mischmetal additions display the highest hardness values (~92 and 91 BHN, respectively), as shown in Figure 6.2(b). As observed in the case of non-modified A319.1 alloys with 2 wt% mischmetal addition, the Sr-modified alloys with 2 wt% mischmetal also show the higher hardness values compared with the alloys containing 4 wt % and 6 wt% mischmetal (~85 and ~ 80 BHN, respectively), owing to the fact that the latter alloys provide a better combination of modified eutectic Si structure and soft α-aluminum matrix, and contain a considerable amount of the Al_2Cu precipitation hardening phase, as well as hard mischmetal-containing intermetallics.[11, 66, 63, 79]

It can also be noted that at the first peak aging condition (200°C/5h), the Sr-modified alloys exhibit somewhat higher hardness values (~ 3%) than the non-modified alloys. This may be explained as follows: during solution heat treatment, the Si particles coarsen, and the non-modified alloys display a higher coarsening rate than the Sr-modified alloys. In the non-modified alloys containing mischmetal, however, the Si particles exhibit somewhat smaller coarsening rates compared to the case with no mischmetal addition. Thus, the addition of mischmetal reduces the coarsening of the Si particles. In the Sr-modified alloys containing mischmetal, the decrease in the coarsening rate of the Si particles due to the presence of mischmetal is smaller than that observed in the non-modified MM-containing alloys. In other words, the modifying action of mischmetal on the

eutectic silicon particles is expected to be more effective in the non-modified than in the Sr-modified alloys. This effect is higher than the hardening effect caused by precipitation of the Al_2Cu hardening phase during aging. Hence, the non-modified alloys exhibit lower levels of hardness compared to the Sr-modified alloys.

6.2.2 A356.2 Alloy

In the as-cast non-modified alloy, the hardness changes slightly with mischmetal additions, while in the Sr-modified alloy the hardness is seen to decrease once the mischmetal is added, then remains the same (~ 55 BHN) at all addition levels, as shown in Figure 6.3. Owing to the fact that the modification of the eutectic Si particles by Sr is

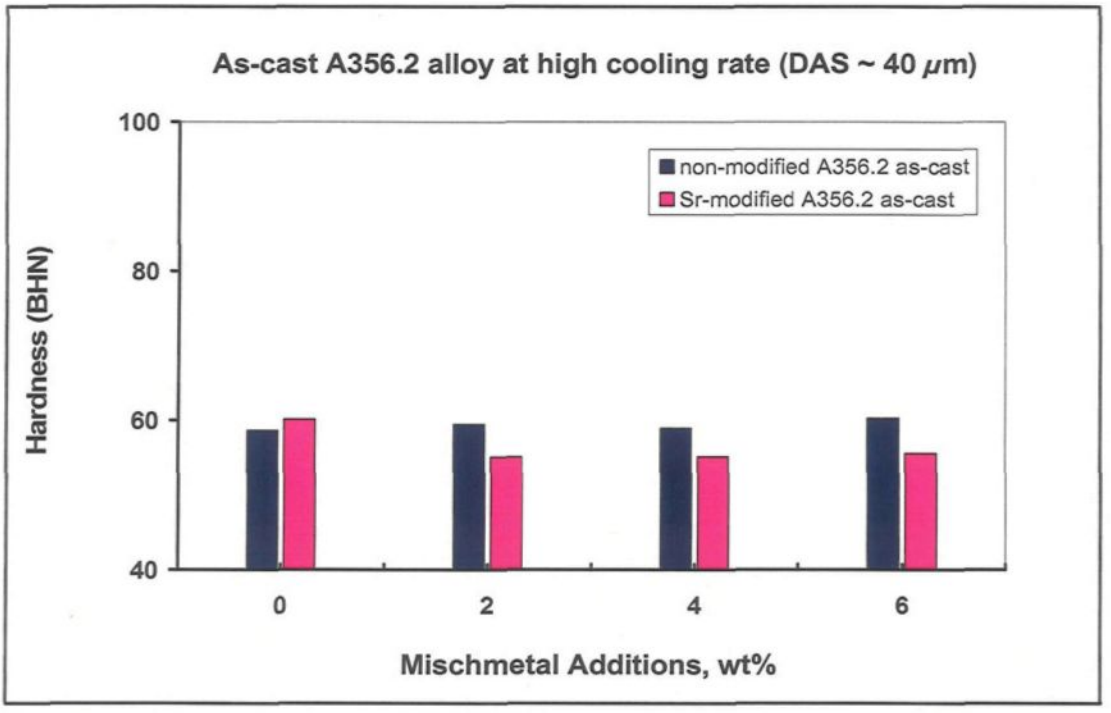

Figure 6.3 Effect of mischmetal addition and Sr-modification on the hardness of the as-cast A356.2 alloy solidified at a high cooling rate (DAS ~ 40μm).

greater than that obtained with mischmetal addition, the Sr-modified alloys containing up to 6 wt% mischmetal display lower levels of hardness than the non-modified alloys.

After aging for 5h at different temperatures (155°C-240°C), peak hardness is observed to occur at 180°C aging temperature, as can be seen in Figure 6.4.

Figure 6.4(a) reveals that the non-modified alloys free of mischmetal exhibit higher hardness values than those containing up to 6 wt% mischmetal. Comparing the hardness of the non-modified and Sr-modified alloys (see Figure 6.4(a) and (b)), it can be seen that all the non-modified alloys with and without mischmetal display higher levels of hardness than do the corresponding Sr-modified alloys. Also, the Sr-modified alloys show practically the same hardness levels irrespective of the mischmetal amount added, at aging temperatures of 180°C and above. This is in agreement with the findings of Ye *et al.*,[11] who reported that the influence of rare earth addition on the microhardness of the α-aluminum matrix is relatively small.

The decrease in hardness for the Sr-modified alloys can be attributed to the modification effect of Sr on both the eutectic Si particle morphology as well as the lowering of the eutectic temperature during solidification, both of which lead to an increase of the ductile α-Al matrix. This effect is greater than the hardening effect achieved through the precipitation of the Mg_2Si hardening phase.

The highest hardness values are exhibited by the alloys containing no mischmetal i.e., B0 and BS0 alloys, with maximum hardness being observed at 180°C aging temperature (B0:~104 BHN and BS0:~99 BHN). The decrease in hardness with increasing mischmetal addition could be due to the reaction of mischmetal with Mg to form complex

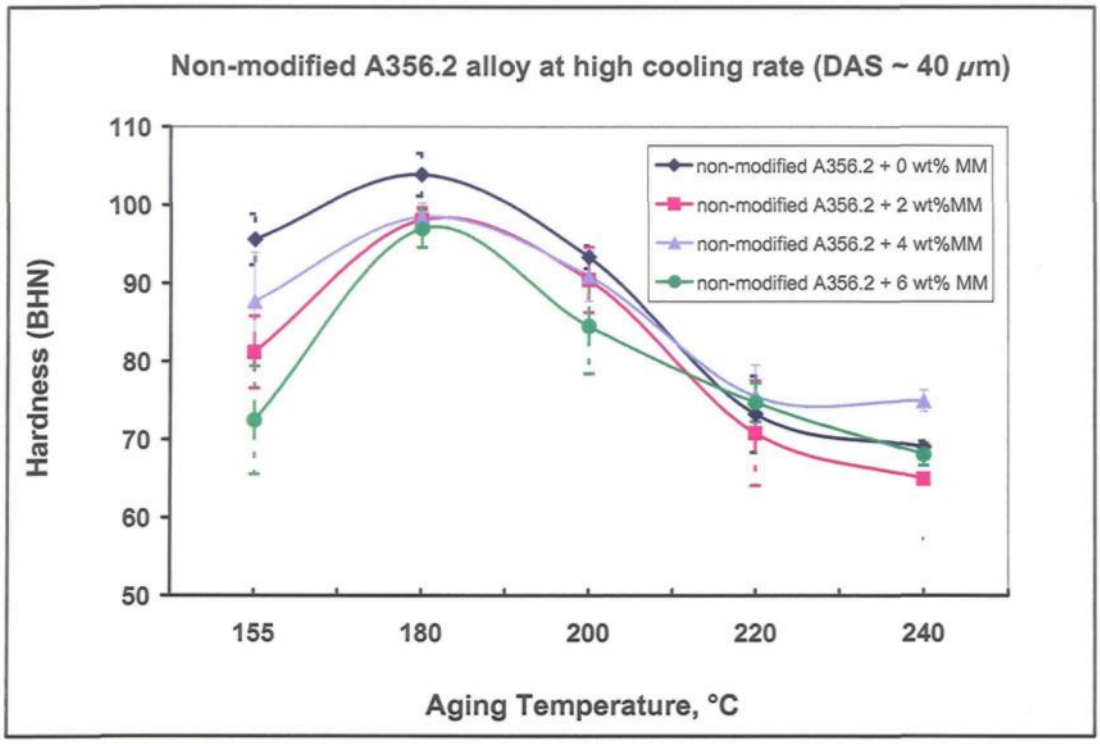

(a)

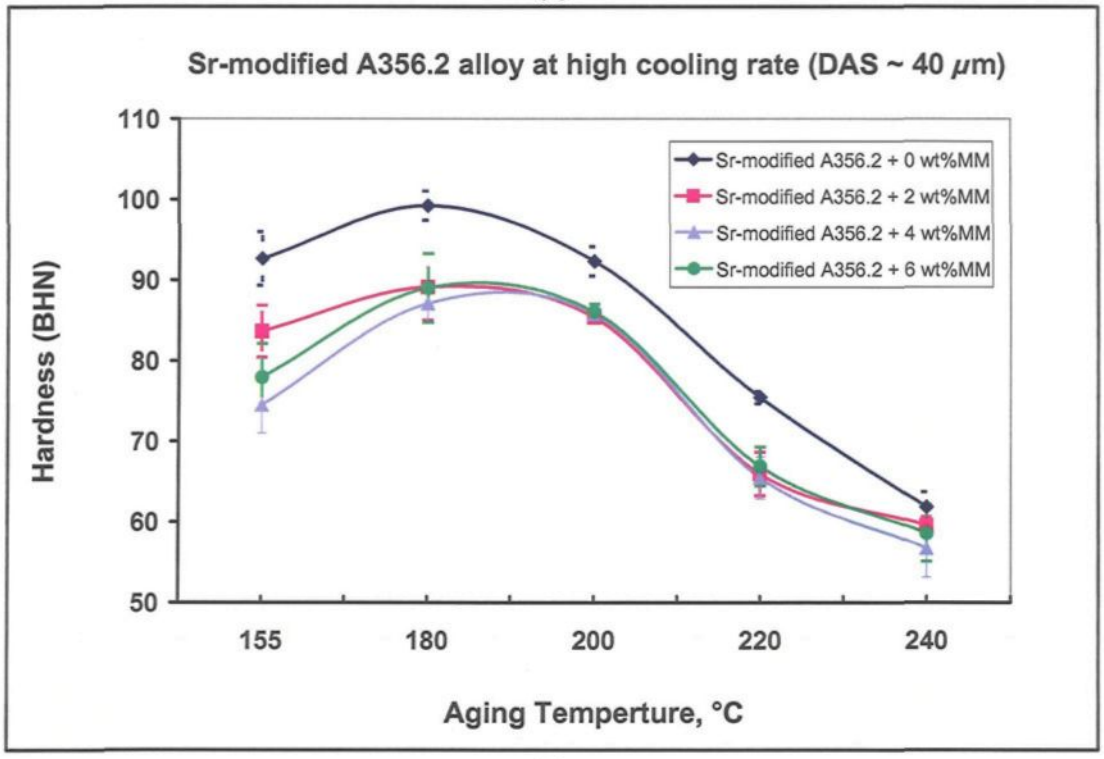

(b)

Figure 6.4 Effect of mischmetal additions and aging temperature on the hardness of A356.2 alloy solidified at a high cooling rate (DAS ~ 40μm): (a) non-modified, (b) Sr-modified conditions.

compounds, leading to a reduction in the amount of free Mg available to form the Mg_2Si phase.

In their investigation on the effect of rare earth addition on age-hardening behavior of 356 alloy, Agrawal and Menghani [65] reported that different additions of mischmetal cause different alterations in the sequence of the precipitation hardening reaction. This could also explain the present observations.

6.2.3 A413.1 Alloy

In the as-cast condition, the hardness changes very slightly with the amount of mischmetal added. A slight increase (~ 2%) is obtained in the case of the non-modified alloys, whereas the Sr-modified alloys display a slight decrease (~ 5%) with increasing mischmetal addition, as shown in Figure 6.5.

This may be explained on the basis of the fact that the degree of modification obtained by mischmetal addition is less than that achieved by Sr addition. Although the interaction between mischmetal and Sr lowers the modification effect of Sr, nevertheless the degree of Si particle modification obtained is greater than that obtained in the alloys modified only with mischmetal. The decrease in hardness for the Sr-modified alloys can also be attributed to the increase of ductile α-Al matrix resulting from the depression in the eutectic temperature and the corresponding shift in the eutectic point with the Sr addition.

No age hardening effect is observed in the A413.1 alloys, after aging for 5h at different temperatures (155°C-240°C), as can be seen in Figure 6.6. This is may be ascribed

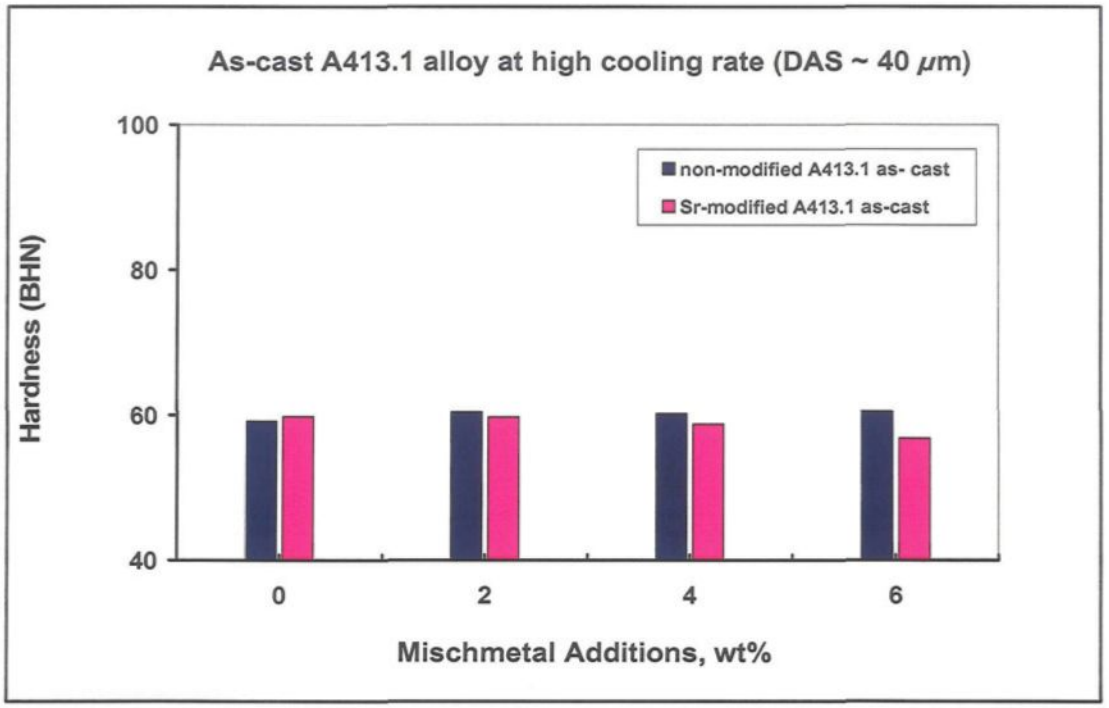

Figure 6.5 Effect of mischmetal addition and Sr-modification on the hardness of the as-cast A413.1 alloys solidified at a high cooling rate (DAS ~ 40μm).

to the low content of alloying elements in this alloy, leading to the lack of precipitation hardening phases. In addition, the interaction between mischmetal and copper (which is only ~ 0.3 % in the A413.1 alloy) to form intermetallic phases, prevents the formation of the Al_2Cu precipitation hardening phase. The non-modified alloys exhibit slightly higher levels of hardness than the Sr-modified alloys, again due to the partial modification of the Si particles with mischmetal addition versus full modification with Sr addition. The highest hardness values are obtained for the alloys free of mischmetal in both non-modified and Sr-modified cases, *viz.*, 65.1 BHN and 63.3 BHN, respectively, for the C0 and CS0 alloys aged at 200°C.

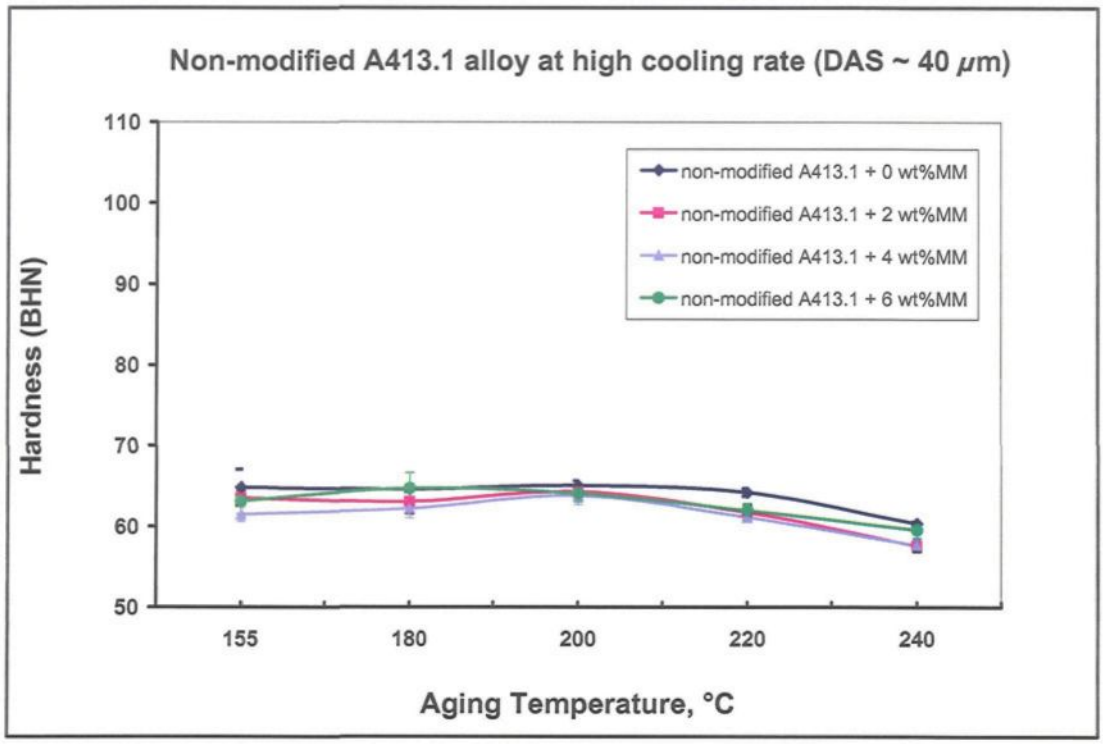

(a)

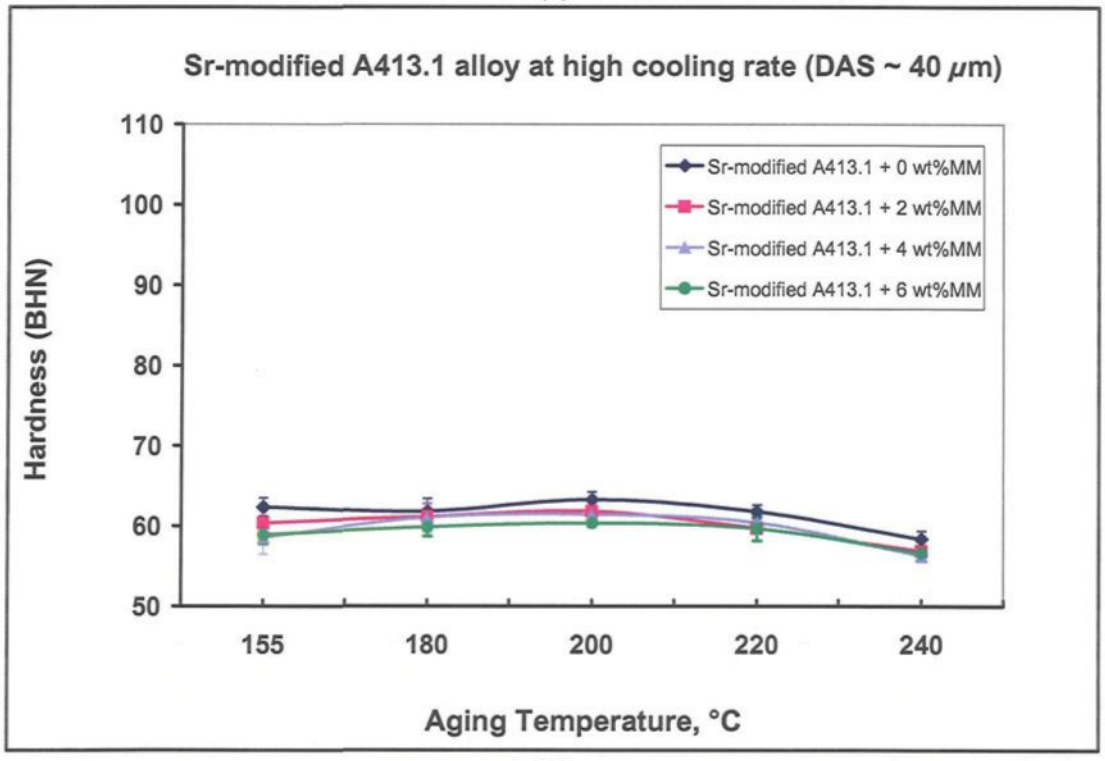

(b)

Figure 6.6 Effect of mischmetal additions and aging temperature on the hardness of A413.1 alloys solidified at a high cooling rate (DAS ~ 40μm): (a) non-modified, (b) Sr-modified conditions.

6.3 EFFECT OF LOW COOLING RATE

6.3.1 A319.1 Alloy

It is well known that as the cooling rate decreases, the size of the microconstituents present in the microstructure increases. Thus, dendrite arm spacing and the Si particles size show larger values compared to those observed at high cooling rate (cf. DAS of ~ 120 μm with ~ 40 μm in the present case).

In the as-cast non-modified alloy, the hardness is observed to decrease slightly (~ 4 %) with increasing mischmetal addition. On the other hand, the hardness of the Sr-modified alloys increases with 2 wt% mischmetal addition and then decreases with further addition of mischmetal, as shown in Figure 6.7.

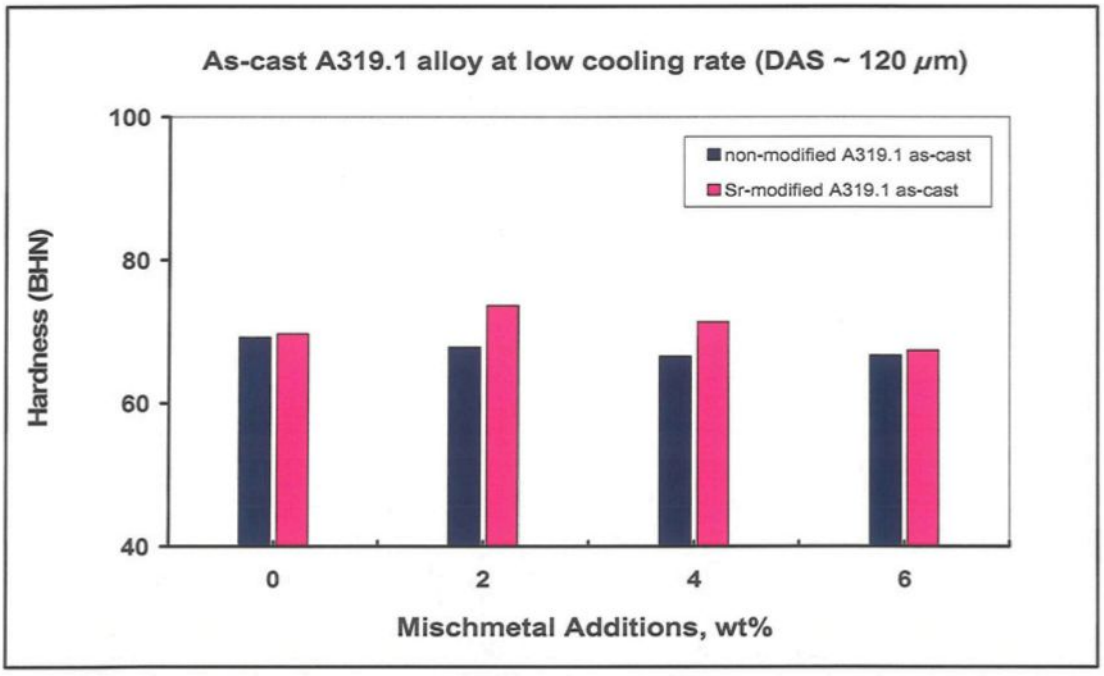

Figure 6.7 Effect of mischmetal addition and Sr-modification on the hardness of the as-cast A319.1 alloy solidified at a low cooling rate (DAS ~ 120μm).

At low cooling rate, the degree of modification obtained with mischmetal addition is somewhat greater in the as-cast non-modified alloys than that obtained in the Sr-modified alloys due to the interaction between Sr and mischmetal which reduces the effectiveness of Sr as a modifying agent. Thus, the non-modified alloys containing up to 6 wt% exhibit lower hardness levels than the corresponding Sr-modified alloys.

After aging the A319.1 alloys for 5h at different aging temperatures (155-240°C), it is observed that the non-modified alloys free of mischmetal exhibit two maximum hardness values were observed at 155°C and 180°C. At 155°C the alloy assumes slightly higher hardness values (~ 85 BHN) than at 180°C (~ 84 BHN), as shown in Figure 6.8(a). It can also be seen that the alloy hardness decreases with the addition of 2 wt% mischmetal. No pronounced difference in the hardness values of the alloy with further mischmetal additions (4 wt% and 6 wt%) are observed, owing to the interaction between mischmetal and copper, leading to a decrease in the amount of Al_2Cu phase formed during aging.

Figure 6.8(b) depicts the behavior of the Sr-modified alloys with aging treatment. The maximum hardness values can also be observed in the Sr-modified alloy free of mishcmetal at 155°C and 180°C assuming almost the same higher hardness values (~ 82 BHN). The addition of mischmetal has a slight effect on the alloy hardness and maximum hardness value at 220°C (~ 81 BHN) is observed in the alloy with 2 wt% mischmetal addition. In general, the hardness values of the non-modified alloys are higher than those of the alloys modified by Sr addition. This may be attributed to the fact that during solution heat treatment, the non-modified alloys containing mischmetal exhibit a low coarsening

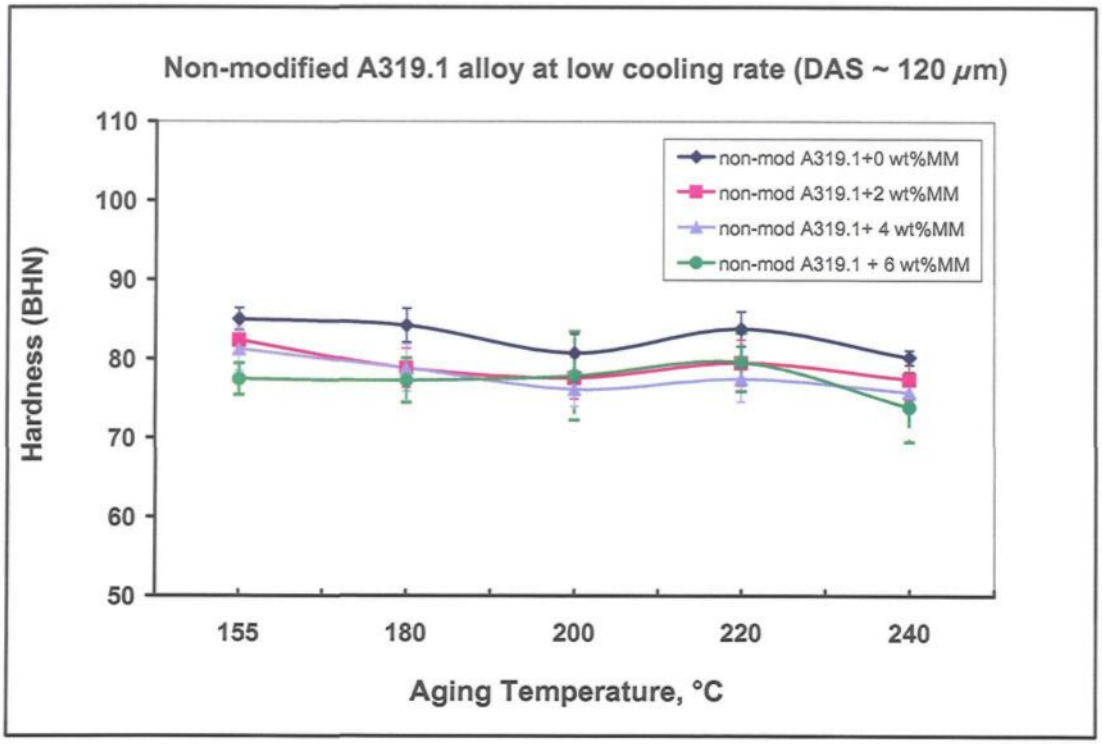

(a)

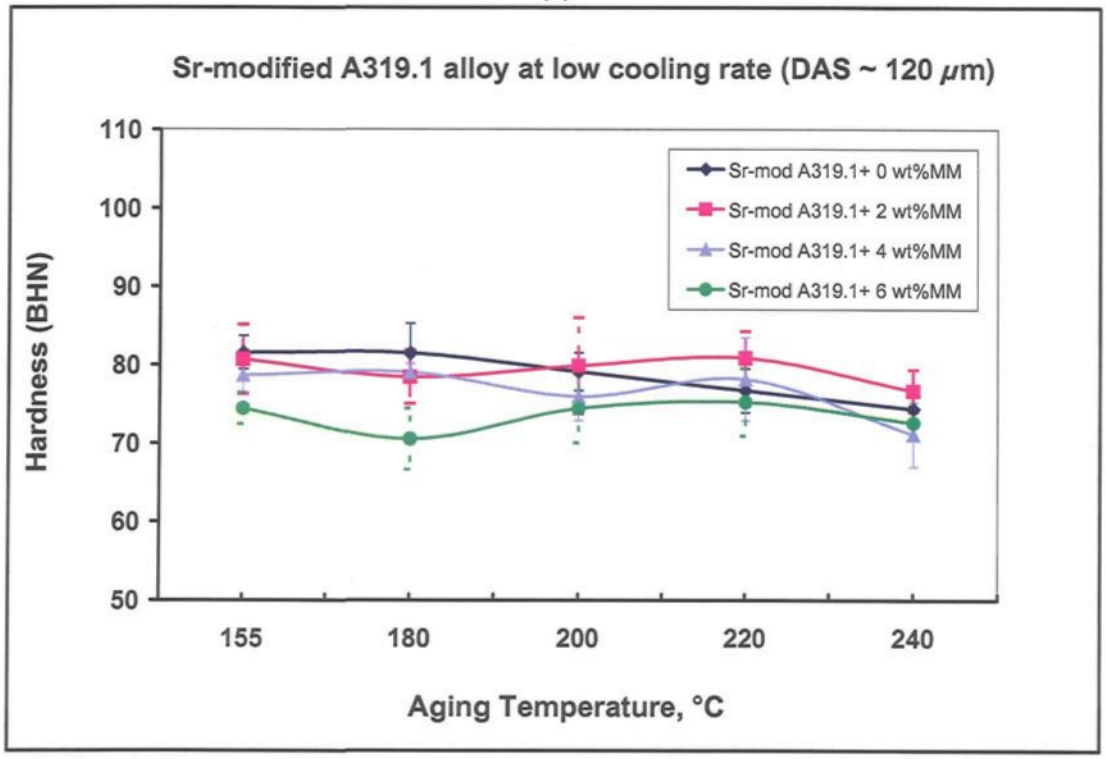

(b)

Figure 6.8 Effect of mischmetal additions and aging temperature on the hardness of A319.1 alloys solidified at a low cooling rate (DAS ~ 120μm): (a) non-modified, (b) Sr-modified conditions.

rate of the Si particles (due to Ostwald ripening mechanism [48, 71]). In the case of Sr-modified alloys which already contain modified Si particles, the eutectic Si particles in the mischmetal-containing alloys also exhibit a low coarsening rate, but these Si particles are finer than those in the corresponding non-modified alloys. It worth mentioning here that these observations were distinguished in spite of the interaction between mischmetal and Sr, which reduced the modifying action of Sr.

6.3.2 A356.2 Alloy

The hardness of the non-modified alloys increases slightly (~ 9%) with addition of mischmetal up to 4 wt % then decreases at 6 wt% mischmetal addition (by ~ 13% with respect to the maximum hardness value observed at 4 wt% MM), as shown in Figure 6.9. On the other hand, the hardness of the Sr-modified alloy is considerably lowered with mischmetal addition, particularly at the 4 and 6 wt% addition. Again this may be explained in terms of the good modification achieved with Sr addition, the related increase of the α-Al matrix, as well as the interaction between Sr and mischmetal. Apparently, the modification of the eutectic Si particles is the dominant factor, resulting in the decrease in hardness values observed.

After subjecting the A356.2 alloy to aging treatment for 5h at different temperatures, as shown in Figure 6.10(a). It can be observed that, in the non-modified alloy, peak hardness occurs at 180°C due to the precipitation of the Mg_2Si hardening phase. Addition of mischmetal causes slight variations in the hardness value, a maximum variation

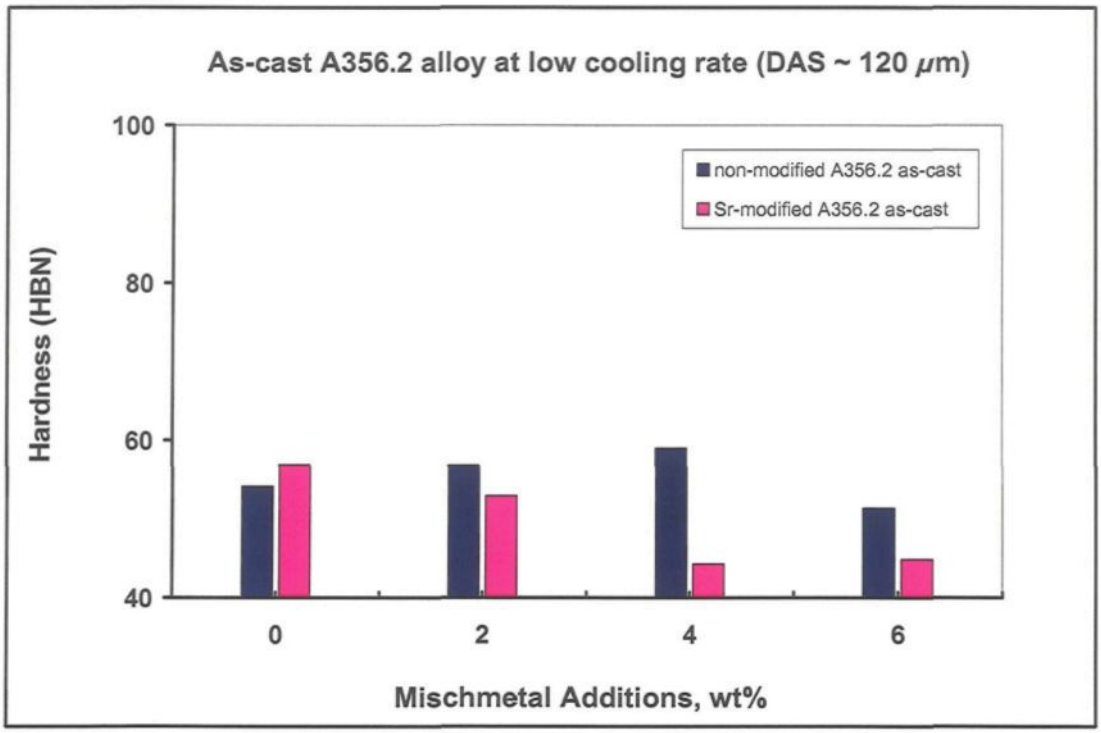

Figure 6.9 Effect of mischmetal addition and Sr-modification on the hardness of the as-cast A356.2 alloys solidified at a low cooling rate (DAS ~ 120μm).

of ~ 10 BHN being observed at 155°C aging temperature, for the 2 wt% mischmetal-containing alloy. The increase in the amount of mischmetal-containing intermetallics at higher additions contributes to the increase in hardness at this temperature. The high hardness values obtained at the peak aging temperature are controlled by the greater amount of Mg_2Si precipitation in the 2 wt% mischmetal-containing alloy, and by the increase in the amount of mischmetal intermetallics and modification effect at the higher mischmetal levels.

In the Sr-modified alloy, peak hardness is also observed at 180°C (see Figure 6.10(b)). The Sr-modified alloy free of mischmetal shows the highest hardness (~ 104

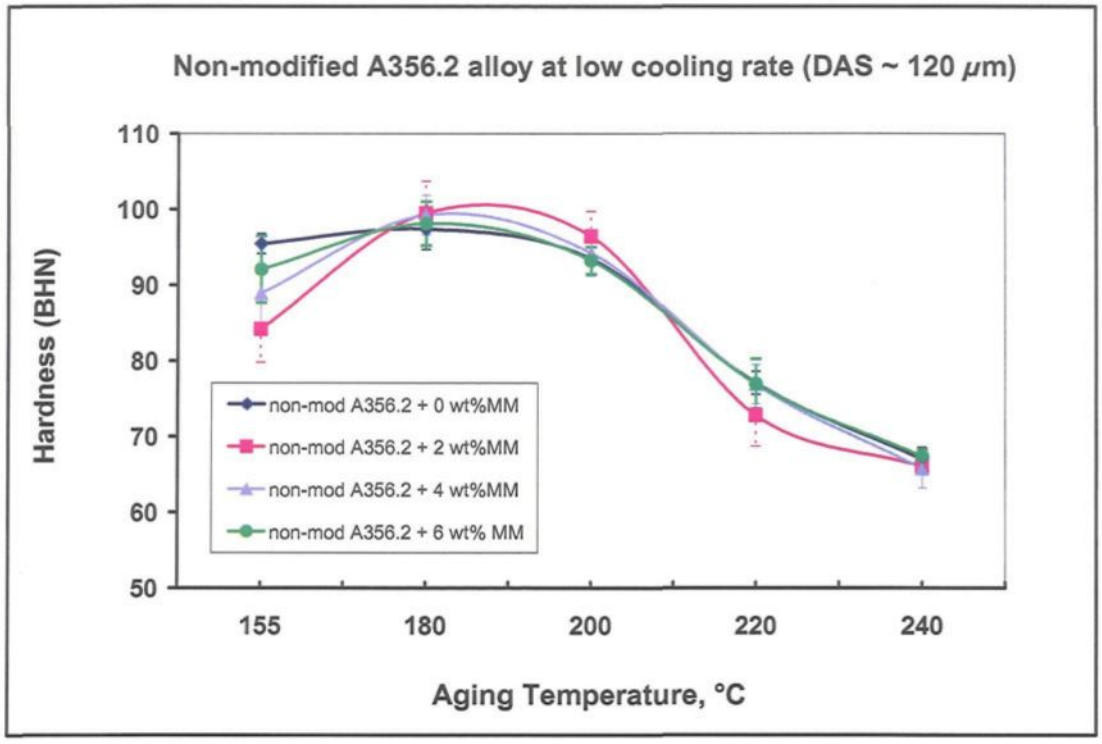

(a)

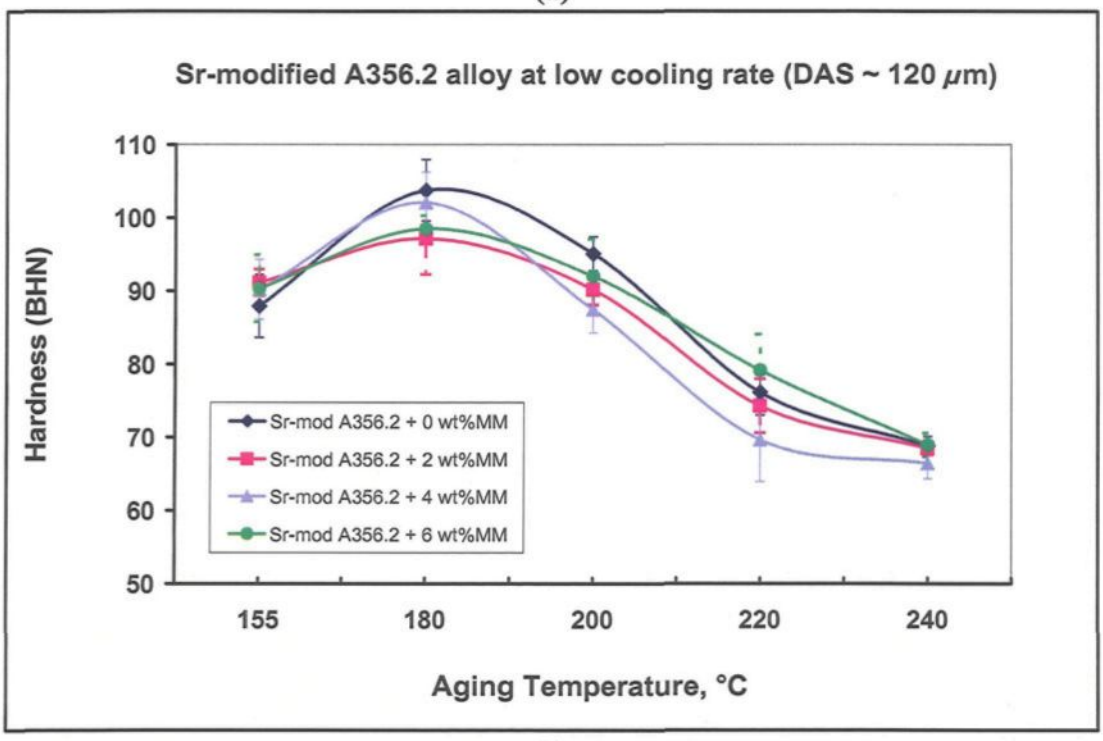

(b)

Figure 6.10 Effect of mischmetal additions and aging temperature on the hardness of A356.2 alloys solidified at a low cooling rate (DAS ~ 120μm): (a) non-modified, (b) Sr-modified conditions.

BHN) and the hardness decreases with mischmetal addition owing to the interaction between mischmetal and Mg. This implies a reduction in the amount of Mg available in solid solution to precipitate the Mg_2Si phase during aging, which causes the hardening of the alloy. As mentioned previously, mischmetal addition is reported to change the sequence is reported to change the sequence of the precipitation hardening reaction.[65]

The Sr-modified alloys exhibit slightly higher hardness values than the non-modified alloys as the hardening effect resulting from the precipitation of the Mg_2Si phase is greater in the Sr-modified alloys than the effect of a lower coarsening rate of the eutectic Si particles during solution heat treatment. In the non-modified alloys, the hardening effect caused by precipitation of the Mg_2Si phase is compromised by the high coarsening rate of the Si particles. This is in contrast to what is observed under the high cooling rate conditions, where the non-modified alloys exhibit a low degree of modification with mischmetal addition, so that the hardening effect caused by Mg_2Si precipitation is higher than the softening effect due to modification. In the Sr-modified alloys, the softening effect caused by full modification obtained with Sr addition and the related increase in the amount of soft α-aluminum matrix is greater than the hardening effect due to Mg_2Si precipitation. That is why the non-modified alloys exhibit higher hardness values than the Sr-modified alloys at high cooling rate.

6.3.3 A413.1 Alloy

Figure 6.11 shows the effect of mischmetal addition and Sr-modification on the as-cast A413.1 alloy hardness at low cooling rate (corresponding to DAS ~ 120 μm). It can

be seen that with increasing addition of mischmetal, the alloy hardness decreases in both the non-modified and Sr-modified alloys. The non-modified alloys display slight higher hardness values than the Sr-modified alloys except at 2 wt% mischmetal addition, where the Sr-modified alloy show a marginal increase in the hardness (by ~ 2%) compared with the non-modified alloy. The low levels of hardness in the Sr-modified alloys may be explained on the basis of full modification of the eutectic Si particles achieved with Sr addition versus the low modification degree achieved by mischmetal additions.

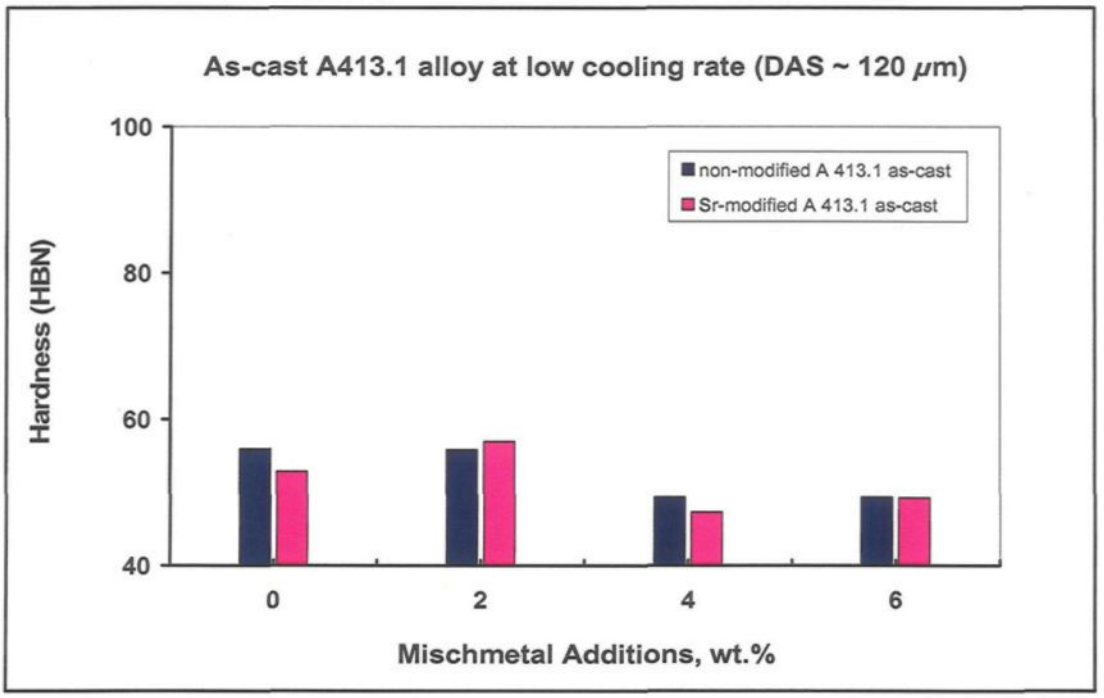

Figure 6.11 Effect of mischmetal addition and Sr-modification on the hardness of the as-cast A413.1 alloys solidified at a low cooling rate (DAS ~ 120μm).

After aging for 5h at different aging temperatures, it can be observed from Figure 6.12 that, the alloy hardness appears to be relatively unaffected by aging, due to the low

content of alloying elements in the A413.1 alloy. No peak hardness is distinguished for both non-modified and Sr-modified alloys.

Figure 6.12(a) shows the response of the non-modified alloys to the aging treatment. As can be seen, the alloy hardness decreases by ~ 5% with increasing addition of mischmetal. This is attributed to the partial modification of the eutectic Si particles with mischmetal. The alloy with 2 wt% mischmetal possesses the highest hardness value at 180°C aging temperature (~ 64 BHN). The effect of mischmetal addition level is relatively more sensitive at this aging temperature, then decreases as the aging temperature is increased to 200°C, until no distinction in the hardness values is observed at higher aging temperatures. In comparison, the non-modified alloy containing no mischmetal displays practically uniform hardness at all aging temperatures.

As Figure 6.12(b) shows, the Sr-modified alloys (free of mischmetal) exhibit somewhat lower levels of hardness than the non-modified alloys. The highest hardness (~ 64 BHN) being observed at 220°C aging temperature. As before, the addition of mischmetal is found to decrease the alloy hardness. The Sr-modified alloy containing 2 wt% mischmetal shows better hardness levels compared with those containing 4 wt% and 6 wt% mischmetal. The interaction between Sr and mischmetal lessens the effectiveness of Sr as a Si particle modifier. Judging by the hardness value obtained, it may be reasonably assumed that the softening effect due to Ostwald ripening in the 2 wt% mischmetal-containing alloy is lower than that in those containing 4 wt% and 6 wt% mischmetal. Compared to the case of the non-modified alloys, for the Sr-modified alloys, the 2 wt% MM-containing alloy shows a relatively uniform hardness at all aging temperatures.

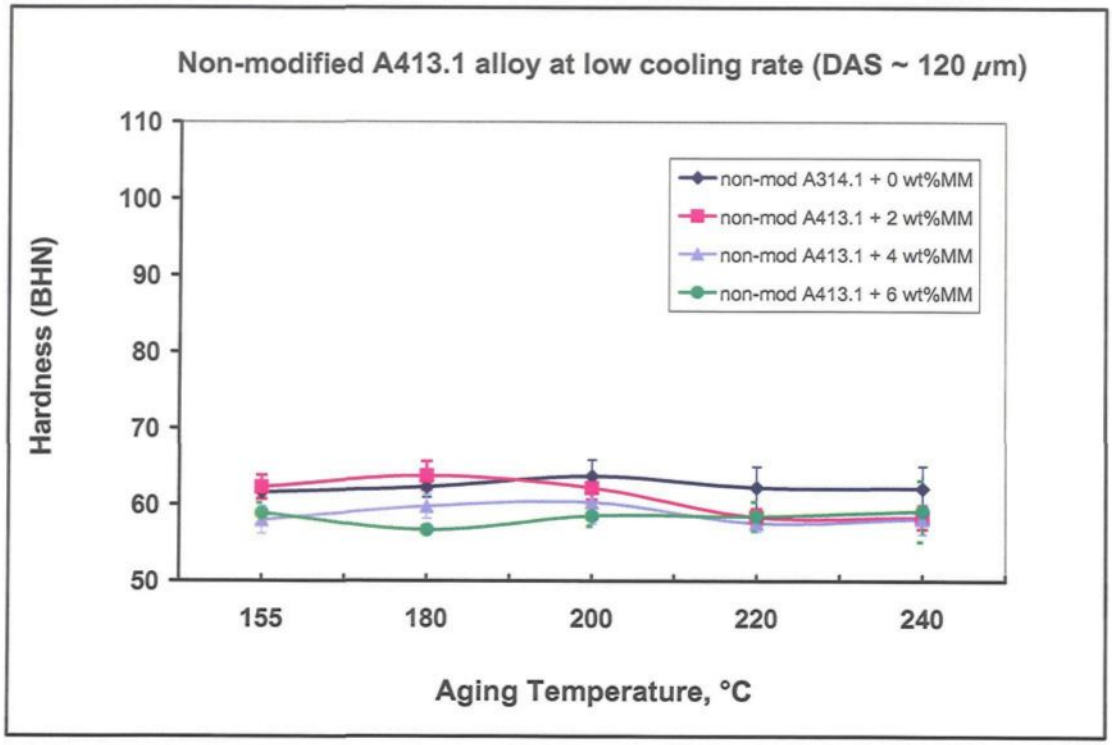

(a)

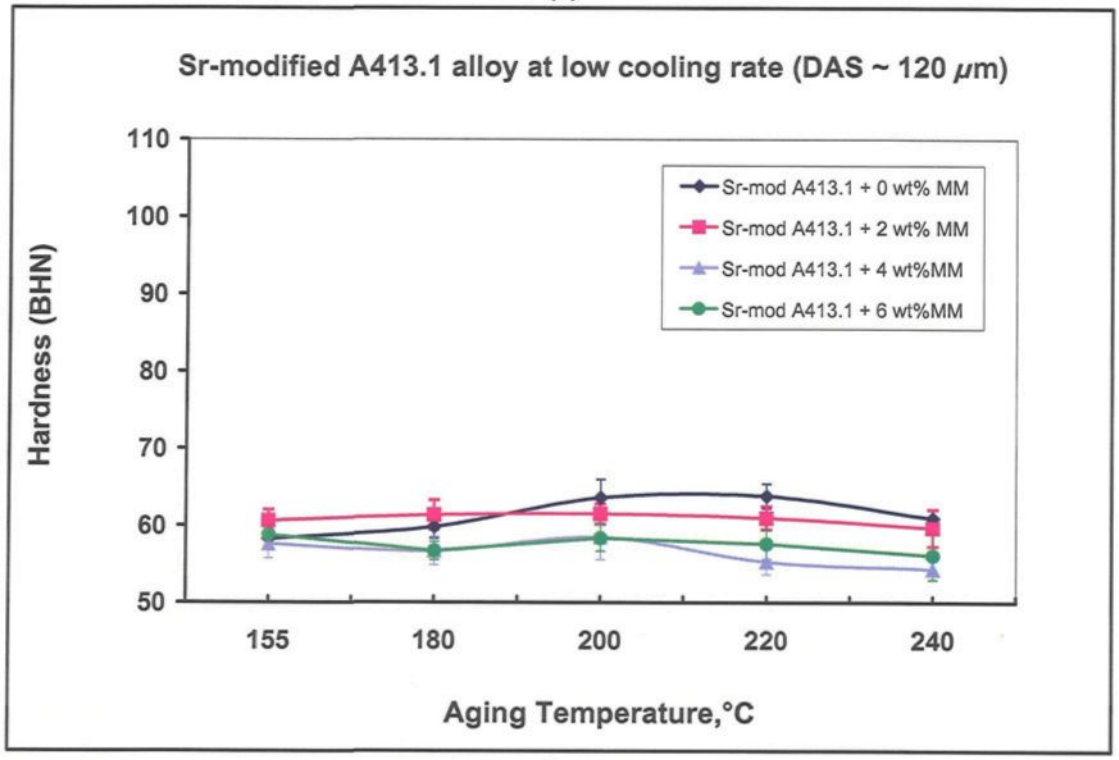

(b)

Figure 6.12 Effect of mischmetal additions and aging temperature on the hardness of A413.1 alloys solidified at a low cooling rate (DAS ~ 120μm): (a) non-modified, (b) Sr-modified conditions.

CHAPTER 7

CONCLUSIONS

CHAPTER 7

CONCLUSIONS

A study was carried out to determine the effect of mischmetal additions on the microstructural characteristics and hardness properties of non-modified and Sr-modified A319.1, A356.2 and A413.1 type Al-Si alloys, obtained under high and low cooling rate conditions (i.e., exhibiting dendrite arm spacing of 40 μm and 120 μm, respectively). Based on the results obtained and their analysis, the following conclusions can be drawn.

Microstructure

1. The addition of mischmetal to the non-modified as-cast alloys partially modifies the eutectic silicon particles. This effect is more pronounced in the A413.1 and A319.1 alloys than in A356.2 alloy.
2. The effect of mischmetal as a modifier is more effective at high cooling rate (corresponding to DAS ~ 40 μm) than at the low cooling rate (DAS ~ 120 μm) for all the as-cast non-modified alloys. However, at low cooling rate, the presence of mischmetal reduces the coarsening of the Si particles during solution heat treatment, i.e., a better modification effect is achieved in the heat treated samples.
3. The interaction between mischmetal and Sr is more evident at low cooling rate in both as-cast and heat-treated alloys.
4. During solution heat treatment and in samples obtained at low cooling rates, the coarsening rate (due to Ostwald ripening) is higher than the fragmentation and

spheroidization in the non-modified A356.2 and A413.1alloys, whereas in the case of Sr-modified A413.1 alloys, the spheroidization rate is higher.

5. The Al_2Cu phase is observed to precipitate in the block-like, eutectic-like or both forms in A319.1 alloy at high cooling rate, while it is found to occur mostly in the block-like forms at low cooling rate. The low Fe content (0.15%) of the A319.1 alloy results in the formation of the Al_7FeCu phase in the form of grey plate-like particles observed at the high cooling rate.

6. Addition of mischmetal up to 6 wt% to A391.1 alloy produces two different intermetallic compounds:

   (i) a mischmetal-Ti-Cu phase ($Al_4MM_2Ti_4CuSi$) with a high Ce/La ratio (4.1:1), which precipitates in the form of grey sludge particles under high cooling rate conditions.

   (ii) a mischmetal-Cu phase (Al_5MMCu_2Si) with a low Ce/La ratio (1.8:1), which precipitates as white plates at both cooling rates.

   The low Sr content (0.4 wt%) in the mischmetal plate-like phase confirms the interaction between mischmetal and Sr, which is also reflected in the results of the Si particle characteristics measured for these alloy samples.

7. In the as-cast non-modified A356.2 alloy, Mg_2Si is observed in the form of large black Chinese script particles. After solution heat treatment (540°C/8h), the Mg_2Si is completely dissolved.

8. The addition of up to 6 wt% mischmetal to A356.2 alloy produces two distinct mischmetal intermetallic phases at high cooling rate :

(i) a grey mischmetal phase containing Ti with a high Ce/La ratio (3.4:1), observed to precipitate in the form of sludge particles. The low Mg content (0.26 wt%) of this phase can lead to a decrease in the alloy hardness.

(ii) a white spherical mischmetal phase with a low Ce/La ratio (1.32:1), containing low amounts of Sr (1.5 wt%) and Mg (0.4 wt%). The presence of Sr and Mg would indicate a decrease in the effect of Sr as a modifier and that of Mg_2Si as a precipitation hardening phase.

(iii) This phase can also be observed at low cooling rate, having the same chemical composition, but exhibiting larger sized particles.

9. Addition of mischmetal up to 6 wt% to the A356.2 alloy at low cooling rate leads to the formation of a new phase, Al_2MMSi_2. This new phase precipitates in the form of white Chinese script particles with a low Ce/La ratio (1.5:1) and a low Mg content (0.26 wt %).

10. Due to the relatively high level of iron in the A413.1 alloys (~ 0.7%), a variety of iron intermetallics are formed: the β-Al_5FeSi phase (in the form of platelets) and an α-$Al_{15}(MnFeNiCu)_3Si_2$ phase (light grey Chinese script containing high Ni) that are observed at high cooling rate, and the α-$Al_{15}(MnFe)_3Si_2$ phase (large branched meduim grey Chinese script particles) observed at low cooling rate. Due to the low copper content in the A413.1 alloy, a pink block-like Al_3NiCu is observed to precipitate on the β–Al_5FeSi platelets in the as-cast condition.

11. Addition of mischmetal up to 6 wt% to the A413.1 alloy produces many intermetallic phases:

(i) A mischmetal block-like phase with low Ce/La ratio (Al_2MMSi_2) observed at high cooling rate.

(ii) A light grey mischmetal-Cu-Ni plate-like phase ($Al_5MM(CuNi)Si$) with a moderate Ce/La ratio (2:1) observed at both high and low cooling rates.

(iii) A white Chinese script mischmetal phase (Al_2MMSi_2) observed in the non-modified alloys at low cooling rate. In the Sr-modified alloys, however, this phase is found to also contain 0.48 wt% Sr.

Hardness

12. In the case of as-cast condition:

(i) The hardness of the non-modified A319.1 alloys increases by about ~ 5% with the addition of 2 wt% mischmetal at the high cooling rate and decreased with further mischmetal addition. In Sr-modified alloys, however, the hardness decreases by ~ 4% with mischmetal additions while, the alloy hardness exhibit an opposite trend at low cooling rate.

(ii) In the A356.2 alloys, the hardness of the non-modified alloys changes slightly (~ 3%) with mischmetal additions, while in the Sr-modified alloys the hardness decreases with mischmetal additions at both cooling rates.

(iii) In the non-modified A413.1 alloys, the hardness marginally increases (~ 2%), while it decreases by about 5% in Sr-modified alloy at high cooling rate. At low cooling rate, both non-modified and Sr-modified alloys exhibit decrease in the hardness with mischmetal additions. Generally, the hardness of the as-cast alloy is higher at high cooling rate than at low cooling rate.

13. In the non-modified A319.1 alloy, two peak hardness values were observed (at 200°C/5h and 240°C/5h) at high cooling rate, while the Sr-modified A319.1 alloy showed only one peak (at 200°C/5h). At low cooling rate, two maximum hardness value are observed at 155°C/5h and 180°C/5h. The alloys contain 0 and with 2 wt% mischmetal addition display the highest hardness values at both cooling rates. In general, the Sr-modified alloys exhibit about ~ 6% higher hardness levels than the non-modified alloys at high cooling rate, but about 4% lower hardness levels of than non-modified alloys at low cooling rate.

14. In the A356.2 alloy, peak hardness is observed at 180°C/5h in the non-modified and Sr-modified alloys at both cooling rate conditions. The alloys free of mischmetal exhibit relatively higher levels of hardness than those containing mischmetal. The hardness decreases with increasing level of mischmetal addition.

15. In the A413.1 alloy, no age hardening effect can be observed after 5h aging at different temperatures (155°C-240°C) for the two cooling rate conditions. In general, the non-modified alloys display somewhat higher hardness values than the Sr-modified alloys. Also, both non-modified and Sr-modified alloys free of mischmetal exhibit relatively higher levels of hardness than those containing mischmetal (at the two cooling rates).

RECOMMENDATIONS FOR FUTURE WORK

On the basis of the results obtained from the study of the use of mischmetal as a modifier the in A319.1, A356.2, and A413.1 alloys and the effect of alloy composition, cooling rate, and heat treatment on the microstructure and hardness of these popular commercially alloys, this study can be further elaborated to cover:

1. Tensile testing to determine the effect of mischmetal on the performance of these alloys in terms of tensile strength and ductility.
2. Impact testing using Charpy unnotched specimens to measure the impact energy and investigate the correlation between the impact toughness and the metallurgical factors studied in this work (viz., mischmetal addition, Sr-modification, cooling rate, and heat treatment).

REFERENCES

1. M.A. Moustafa, F.H. Samuel and H.W. Doty, "Effect of solution heat treatment and additives on the microstructure of Al-Si A413.1 automotive alloys", *Journal of Material Science*, Vol. 38, 2003, pp. 4507-4522.

2. M. Ravi, U.T.S. Pillai, B.C. Pai, A.D. Damodaran and E.S. Dwarakadasa, "The effect of mischmetal addition on the structure and mechanical properties of a cast Al-7Si-0.3Mg alloy containing excess iron (up to 0.6 pct)", *Metallurgical and Materials Transactions A,.*Vol. 33(A), 2002, pp. 391-400.

3. N. Abu-Dheir, M. Khraisheh, K. Saito, A. Male, "Silicon morphology modification in the eutectic Al-Si alloy using mechanical mold vibration", *Materials Science and Engineering* A, Vol. 393, 2005, pp. 109-117.

4. H. de la Sablonniere and F.H. Samuel, "Solution heat treatment of 319 aluminum alloy containing ~ 0.5 wt% Mg. Part 1- Solidification and tensile properties", *International Journal of Cast Metals Research*, Vol. 9, 1996, pp. 195-211.

5. P. Ouellet, F.H. Samuel, D. Gloria and S. Valtierra, "Effect of Mg content on the dimensional stability and tensile properties of heat treated Al-Si-Cu (319) type alloys", *Ibid International Journal of Cast Metals Res.*, Vol. 10, 1997, pp. 67-78.

6. C.W. Meyers, K.H. Hinton and J.S. Chou, "Towards the optimization of heat treatment in aluminum alloys", *Materials. Science Forum.* Vol 102-104, 1992, pp. 75-84.

7. D. Apelian, S. Shivkumar and G. Sigworth, "Fundamental aspects of heat treatment of cast Al-Si-Mg alloys", *AFS Transactions*, Vol. 97, 1989, pp. 727-742.

8. S. Shivkumar, C. Keller, M. Trazzera and D. Apelian, "Precipitation hardening in A356 alloys", in *Proceedings. International Symposium on Production, Refining, Fabrication and Recycling of Light Metals*, Hamilton, Ontario, Aug. 26-30, M. Bouchard and P. Tremblay (Eds), Pergamon Press, New York, 1990, pp. 264-278.

9. L. Pedersen and L. Arnberg, "The effect of solution heat treatment and quenching rates on mechanical properties and microstructure in AlSiMg foundry alloys", *Metallurgical and Materials Transactions A*, Vol. 32A, 2001, pp. 525-532.

10. C.B. Kim and R.W. Heine, "Fundamentals of solidification in the Aluminum Silicon system", *Journal of the Institute of Metals,* Vol. 92, 1963-64, pp. 367-376.

11. J. Ye, C.R. Loper, Jr., D.Y. Lu and C.S. Kang, "An assessment of the role of rare earth in the eutectic modification of cast aluminum-silicon alloy", *AFS Transactions*, Vol. 39, 1989, pp. 533-544.

12. R. Sharan and N.P. Saksena, "Rare earth additions to aluminum silicon alloys", *Castings*, Jan.-Feb., 1978, pp. 37-41.
13. R. Sharan and N. P Saksena, "Rare earth additions as modifiers of aluminum silicon alloys", *AFS Transactions*, Vol. 3(1), 1978, pp. 29-33.

14. S.N. Prasad and R. Sharan, "Rare earth additions as modifiers to hypereutectic aluminum-silicon alloys", *Indian Foundry Journal*, June, 1985, pp. 15-18.

15. R. Sharan, "Influence of Rare Earth addition to Aluminium-Silicon Alloys and Aluminium Bronzes", in *New Frontiers in Rare Erath Science and Application, Proceedings of the International Conference on Rare Earth Development*, Beijing, China,10-14 Sept., 1985, pp. 1336-1339.

16. R. Sharan and S.N. Prasad, "Development of aluminum alloys with rare earth additions", *Light Metal Age*, Vol. 47, 1989, pp. 23-26.

17. F. Paray, B. Kulunk, J. E. Gruzleski, "Impact properties of Al-Si foundry alloys", *International Journal of Cast Metals Research*, Vol. 13, 2000, pp. 17-37.

18. B. Kulunk and D. J. Zulian, "Applications for the strontium treatment of wrought and die-cast Al", *Journal of Materials*, Vol. 48(10), 1996, pp. 60-63.

19. G. Chai and L. Bäckerud, "Factors affecting modification of Al-Si alloys by adding Sr-containing master alloys", *AFS Transactions*, Vol. 100, 1992, pp. 847-854.

20. H.C. Liao, Y. Ding and G. X. Sun, "Effect of strontium on crystallization of Mg_2Si phase in Al-Si-Mg casting alloys", *Transactions of Nonferrous Metals Society of China* (English Edition) Vol. 12(3), 2002, pp. 409-415.

21. L. Liu, F. H. Samuel, A. M. Samuel, H. W. Doty and S. Valtierra, "Role of iron in relation to silicon modification in Sr-treated 319 and 356 alloys", *International Journal of Cast Metals Research,* Vol. 16 (4), 2003, pp. 397-408.
22. Leonhard Heusler and Wolfgang Schneider, "Influence of alloying elements on the thermal analysis results of Al-Si cast alloys", *Journal of Light Metal*s, Vol. 2, 2002, pp. 17-26.

23. John. E. Hatch, *Aluminum: Properties and Physical Metallurgy*, 2nd Edition, American Society for Metals, Metals Park, OH, 1984, pp.338-347.

24. M.M. Makhlouf and H.V. Guthy, "The aluminum-silicon eutectic reaction: mechanism and crystallography", *Journal of Light Metals*, Vol. 1, 2001, pp. 199-218.

25. M.M. Makhlouf, S. Shankar and Y.W. Riddle, "Mechanism of formation and chemical modification of the morphology of the eutectic phase in hypoeutectic aluminum silicon alloys", *AFS Transactions*, paper No. 05-88; 2005, 18 p.

26. J.L. Jorstad, W.M. Rasmussen and D.L. Zalensas, *Aluminum Casting Technology*, 2nd Edition, *American Foundrymen's Society*, Des Plaines, Illinois, 2001, pp. 35-53.

27. J.E. Gruzleski, B.M. Closset, *The Treatment of Liquid Aluminum–Silicon Alloys*, American Foundrymen's Society, Des Plaines, IL, 1990, pp. 12-21.

28. L. Bäckerud, G. Chai, J. Tamminen, *Solidifcation Characteristics of Aluminum Alloys, Vol. 2: Foundry Alloys*, AFS/Skanaluminium, Des Plaines, IL, 1990, pp. 71-229.

29. Z. Li, A.M. Samuel, F.H. Samuel, "Effect of alloying elements on the segregation and dissolution of $CuAl_2$ phase in Al-Si-Cu 319 alloys", *Journal of Material Science*, Vol. 38, 2003, pp. 1203-1218.

30. M. Hansen, *Constitution of Binary Alloys*, 2nd Edition, McGraw-Hill, New York, 1958, pp. 84-89

31. L.F. Mondolfo, *Aluminum Alloys: Structure and Properties*, Butterworths, London-Boston, 1976, pp. 760-774.

32. J.G. Kaufman, E.L. Rooy, "Aluminum Alloy Castings", 1st edition, *AFS Transaction*, Schaumburg, Illinois, 2004, pp. 17-20.

33. Metals Handbook, *Properties and Selection: Nonferrous alloys*, Tenth Edition, American Society for Metals, Materials Park, OH, Vol. 2, 1990, pp. 152-172.

34. M.M. Haque and M.A. Maleque, "Effect of process variables on structure and properties of aluminum-silicon piston alloy", *Journal of Materials Processing Technology*, Vol. 77, 1998, pp. 122-128.

35. E.J. Martinez D, M.A. Cisneros G., S. Valtierra and J. Lacaze, "Effect of strontium and cooling rate upon eutectic temperatures of A319 aluminum alloy" *Scripta Materialia* Vol. 52, 2005, pp. 439-443.

36. J.H. Sokolowski, X.C. Sun, G. Byczynski, D.O. Northwood, D.E. Penrod, R. Thomas and A. Esseltine, "The removal of copper-phase segregation and the subsequent improvement in mechanical properties of cast 319 aluminum alloys by a two-stage

solution heat treatment", *Journal of Materials Processing Technology*, Vol. 53, 1995, pp. 385-392.

37. Metals Handbook, *Casting*, Ninth Edition, American Society for Metals, Metals Park, OH, Vol. 15, 1988, pp. 290-295.

38. A. Pacz. US Patent No. 1387900, (Feb. 1920); British Patent No. 158827, Jan., 1921.

39. L. Grand, "The Modification of Aluminum-Silicon Alloys" *Revue de l'Aluminum*, Vol. 29, 1952, pp. 5-15.

40. P.D. Hess, E.V. Blackmun, "Strontium as a Modifying Agent for Hypoeutectic Aluminum-Silicon Alloys" A*FS Transactions*, Vol. 83, 1975, pp. 87-90.

41. M.M. Haque, "Effects of strontium on the structure and properties of aluminum-silicon alloys", *Journal of Materials Processing. Technology*, Vol. 55, 1995, pp. 193-198.

42. L.M. Leandro and F.R. Serafin, *4rd International Foundary Conference* (CIF-5), Budapest, 1976, pp. 7-.

43. P.C. Van Wiggen, B.V. Kbm Affilips, P. Huysmans and N.V. Affilips, "Modification by aluminum-strontium continuous evolution", *Fonderie Fondeur d'Aujourd'hui*, Vol. 225, 2003, pp. 10-19.

44. S. Shivumar, "The interactive effects of Sr modification and heat treatment on the mechanical properties of cast aluminum alloys" *17th ASM Heat Treating Society Proceedings including the 1st International Iinduction Heat Treating Symposium*, 15-18 Sep, Indianapolis, Indiana, 1997, pp. 265-269.

45. S. Shivkumar, S. Ricci, Jr., B. Steenhoff, D. Apelian and G. Sigworth, "An Experimental study to optimize the heat treatment of A356 alloy", *AFS Transactions*, Vol. 97, 1989, pp. 791-810.

46. F. Paray and J.E. Gruzleski, "Microstructure-mechanical property relationship in a 356 alloy. Part1: Microstructure", *Cast Metals*, Vol. 7(1), 1994, pp. 29-40.

47. H. Li, S. Shivkumar, S. Luo and D. Apelian, "Influence of modification on the solution heat treatment response of cast Al-Si-Mg alloys", *Cast Metals*, Vol. 1(4), 1989, pp. 227-234.

48. C.L. MacAdam and D.C. Jenkinson," The stability of silicon fibres in aluminium-silicon alloys and their influence on mechanical propertiers", *in Porc. 27th Annual*

Congress of the Australian Institute of Metals, 20-24 May 1974, Christchurch, N.Z., Vol. 27, 1974, pp. 58-63

49. P.S. Wang, S.L. Lee, J.C. Lin and M.T. Jahn, "Effects of solution temperature on mechanical properties of 319.0 aluminum casting alloys containing trace beryllium", *Journal of Materials Research*, Vol. 15, 2000, pp. 2027-2035.

50. Q.G. Wang and C.H. Caceres, "Mg effects on the eutectic structure and tensile properties of Al-Si-Mg alloys", *Material Science Forum*, Vol. 242, 1997, pp. 159-164.

51. G.V.R. Ragavan, K. Raghukandan, U.T.S. Pillai, K. Sukumaran and B.C. Pai, "General aspects of heat treatment processes on Al-Si-Mg alloys", *Indian Foundry Journal*, Vol. 50(4), 2004, pp. 28-34.

52. I.J. Polmear, *Light Alloys*, Edward Arnold Publisher, London, 1981, pp. 147-157.

53. S. Shivkumar, C. Keller and D. Apelian, "Aging behavior in cast Al-Si-Mg alloys", *AFS Transactions*, Vol. 98, 1990, pp. 905-911.

54. G.E. Dieter, *Mechanical Metallurgy*, 3rd Edition, McGraw Hill, UK, 1986, pp. 212-219.

55. O.H. Wyatt and D.Dew-Hughes, *Metals, Ceramics and Polymers*, Cambridge University Press, Bentley House, London, 1974, pp. 444-452.

56. R.X. Li, R.D. Li, Y.H. Zhao, L.Z. He, C.X. Li, H.R. Guan and Z.Q. Hu, "Age hardening behavior of cast Al-Si base alloy", *Material Letters*, Vol. 58, 2004, pp. 2096-2101.

57. H.K. Kang, M. Kida and H. Miyahara, "Age hardening characteristics of Al-Si-Cu-Base cast alloys", *AFS Transactions,* Vol. 107, 1999, pp. 507-515.

58. C.P. Dutta and H.G. Dutta, "Role of Al_2O_3 particule renforcement on precipitation in 2014 Al- matrix composites", *Metallurgical and Materials Transactions A*, Vol. 25A, 1994, pp. 1591-1602.

59. K.T. Kashyap, S.Murali, K.S. Raman and K.S.S. Murthy, "Casting and heat treatment variables of Al-7Si-Mg alloy", *Materials Science and Technology,* Vol. 9, 1993, pp. 189-203.

60. R.M. Gomes and T. Sato, "precipitation strengthening and mechanical properties of hypereutectic P/M Al-SiCu-Mg alloys containng Fe and Ni", *Material Science Forum*, Vols 217-222, 1996, pp. 789-794.

61. Z. Nie, T. Jin, J. Fu, G. Xu, J. Yang, J. Zhou and T. Zuo, "Research on rare earth in aluminum", *Materials Science Forum,* Vols 396-402, 2002, pp. 1731-1736.

62. T. Linghuan, "Application of rare earths in cast alloys in China", *New Frontiers in Rare Erath Science and Application, Proceedings of the International Conference on Rare Earth Development*, Beijing, China, 10-14 Sept, 1985, pp. 1425-1440.

63. M. Ravi, U.T.S. Pillai, B.C. Pai, A.D. Damodaran and E.S. Dwarakadasa, "A study of the influence of mischmetal additions to Al-7Si-0.3Mg (LM 25/356) alloy", *Metallurgical and Materials Transactions A,* Vol. 27(A), 1996, pp. 1283-1292.

64. Chen Yu Young, Li Qingchaun and Jiang Zhuling, "Influence of cerium and mischmetal on the hardness and brightness of Al-Mg-Si alloys", *Journal of the Less Common Metals*, Vol. 110, 1985, pp.175-178.

65. S. K. Agrawal and J. Menghani, "Effect of rare earth additions on age hardened behavior of LM 25 alloy", *Indian Foundry Journal*, Vol. 48, 2002, pp. 27-31.

66. A. D. Damodaran, "Rare earth additions in aluminum alloys", *Proceedings of the Second International Conference on Aluminium: INCAL-91,* 31 July-2 Aug. 1991, The Aluminium Association Of India, Bangalore, India, Vol. 1, 1991, pp. 211-219.

67. J.C. Weiss and C.R. Loper Jr, "Primary silicon in hypereutectic aluminum silicon casting alloys", *AFS Transactions*, Vol. 32, 1987, pp. 51-62.

68. T. Kowata, H. Hoire, S. Hiratsuka and A. Chida, "Influence of Rare-earth elements on refinement of primary silicon crystals in a hypereutectic Al-Si alloy", *Imono*, Vol. 66, 1994, pp. 803-808.

69. J. Chang, I. Moon and C. Choi, " Refinement of cast microstructure of hypereutectic Al-Si alloys through the addition of rare earth metals" *Journal of Materials Science*, Vol. 33, 1998, pp. 5015-5023.

70. C.W. Meyers, "Solution heat treatment effects in A357 alloys", *AFS Transactions*, Vol. 93, 1985, pp. 741-750.

71. J.W. Martin and R.D. Doherty, *Stability of Microstructure in Metallic Systems*, 2nd Edition, Cambridge University Press, Cambridge, U.K., 1997, pp. 239-251.

72. P.Y. Zhu, Q.Y. Liu and T.X. Hou, "Spheroidization of eutectic silicon in Al-Si alloys", *AFS Transactions*, Vol. 93, 1985, pp. 609-614.

73. M.A. Moustafa, C. Lepage, F.H. Samuel, and H.W. Doty, "Metallographic observations on phase precipitation in strontium-modified Al-11.7%Si alloys: Role of alloying elements", *International Journal of Cast Metals Research*, Vol. 15, 2003, pp. 609-626.

74. J.G. Barlock and L.F. Mondolfo, "Structure of some Aluminum-Iron-Magnesuim-Manganese-Silicon alloys", *Zeitschrift Für Metallkunde*, Vol. 60, 1975, pp. 605-611.

75. R.E Reed-Hill, *Physical Metallurgy Principles*, D. Van Nostrand Co., New York, 1973, pp. 220-236.

76. F.H. Samuel, A.M. Samuel, and H.W. Doty, "Factors controlling the type and morphology of copper-containing phases in 319 aluminum alloy", *AFS Transactions*, Vol. 104, 1996, pp. 893-901.

77. A.M. Samuel, J. Gauthier, and F.H. Samuel, "Microstructural aspects of the dissolution and melting of Al_2Cu phase in Al-Si alloys during solution heat treatment", *Metallurgical and Materials Transaction A*, Vol. 27A, 1996, pp. 1785-1798.

78. J.H. Sokolowski, M.B. Djurdjevic, C.A. Kierkus and D.O. Northwood, "Improvement of 319 aluminum alloy casting durability by high temperature solution treatment", *Journal of Materials Processing Techn*ology, Vol. 109, 2001, pp. 174-180.

79. Shkuka, B.J. Yang, R.W. Smith, M. Sadayappan and M. Sahoo, "Microstructure and mechanical properties of Al-Cu casting alloys-Effect of addition of mischmetal", *AFS Transactions*, Vol. 112, 2004, pp. 489-498.

80. A. Moustaf, F.H. Samuel, H.W. Doty and S. Valtierra, "Effect of Mg and Cu additions on the microstructural characteristics and tensile properties of Sr-modidifed Al-Si eutectic alloys", *International Journal of Cast Metals Res*earch, Vol. 14, 2002, pp. 235-253.

81. M. Samuel, F.H. Samuel, and H.W. Doty, "Observation on the formation of β-Al_5FeSi phase in 319 type Al-Si alloys", *Journal of Materials Science,* Vol. 31, 1996, pp. 5529-5539.

82. C. Villeneuve and F.H. Samuel, "Fragmentation and dissolution of β-Al_5FeSi phase during solution heat treatment of Al-13wt%Si-Fe alloys", *International Journal of Cast Metals Research,* Vol. 12, 1999, pp. 145-160.

83. Metals Handbook, *Mechanical Testing and Evaluation*, Tenth Edition, American Society for Metals, Materials Park, OH, Vol. 8, 1990, pp. 203-2225.